

Naturally Occurring Canine Osteosarcoma In The Dog  
Animal Model For Research Of Targeted Radiotherapy Using  
Beta-Emitting Radioisotopes With Various Ligands.

Rowan James Milner  
BVSc (Hons) MMedVet (Internal Medicine)

Submitted in fulfilment of the requirements for the degree Philosophiae Doctors  
in the Faculty of Health Sciences

University of Pretoria  
PRETORIA  
2013

Promoter: Professor Irene Dormehl

Co-Promoter: Dr Werner Louw

## TABLE OF CONTENTS

Chapter 1. Introduction and Literature Study .....	31
1.1 Overview .....	31
1.2 Bone Physiology .....	33
1.3 Human Bone cancer .....	35
1.4 Human Osteosarcoma .....	38
1.5 Human Metastatic Bone Cancer.....	40
1.6 Radiopharmaceuticals .....	42
1.7 Radiobiology.....	67
1.8 Tumour Vasculature.....	76
1.9 Scintigraphic Technique and Equipment .....	78
Chapter 2. Experimental Design.....	85
2.1 Animal Model .....	85
Chapter 3. Characterization of Canine Osteosarcoma as a Translational Model for Human Bone Cancer Using the Radiopharmaceuticals: $^{153}\text{Sm-EDTMP}$ , $^{188}\text{Re-HEDP}$ and $^{186}\text{Re-HEDP}$ .....	104
3.1 Overview .....	104
3.2 Research Hypothesis .....	107
3.3 Specific Aims .....	107
3.4 Ethical approval.....	107
3.5 Materials and Methods for Scintigraphic Studies in Normal Dogs and a Dog with Osteosarcoma.....	108
3.6 Results for dogs receiving $^{153}\text{Sm-EDTMP}$ and uncomplexed $^{153}\text{Sm}^{+3}$ .....	118
3.7 Results for normal and osteosarcoma dogs receiving $^{188}\text{Re-HEDP}$ .....	133
3.8 Results for dogs receiving $^{186}\text{Re-HEDP}$ and uncomplexed $^{186}\text{Re}$ .....	146
3.9 Results comparing canine pharmacokinetics and biodistribution for $^{153}\text{Sm-EDTMP}$ , $^{188}\text{Re-HEDP}$ , and $^{186}\text{Re-HEDP}$ .....	151
3.10 Results from a comparison between canine and human data for $^{153}\text{Sm-EDTMP}$ , $^{188}\text{Re-HEDP}$ , and $^{186}\text{Re-HEDP}$ .....	155
3.11 Materials and methods for the therapy group of dogs with osteosarcoma and multilobular osteochondrosarcoma receiving $^{153}\text{Sm-EDTMP}$ .....	159
3.12 A Pilot study: Radiosensitization using $^{153}\text{Sm-EDTMP}$ and carboplatin.....	170

3.13	Materials and methods for the therapy group of dogs with osteosarcoma receiving $^{188}\text{Re}$ -HEDP .....	181
3.14	Results from the therapy group of dogs with osteosarcoma receiving $^{188}\text{Re}$ -HEDP 183	
3.15	Survival comparison between dogs receiving $^{153}\text{Sm}$ -EDTMP and $^{188}\text{Re}$ -HEDP	191
3.16	Materials and Methods for $^{153}\text{Sm}$ -EDTMP autoradiography in the dog with osteosarcoma and the rat.....	194
3.17	Section Discussion.....	211
Chapter 4.	Radiolabelled Polyethyleneiminomethyl Phosphonic Acid (PEI-MP) Therapy ... .....	213
4.1	Introduction .....	213
4.2	Aims and objectives for the canine PEI-MP studies .....	215
4.3	Ethical Approval .....	215
4.4	Materials and methods for dynamic studies in normal dogs using variously sized MW-fractions of $^{99\text{m}}\text{Tc}$ -PEI-MP .....	216
4.5	Materials methods for a dynamic scintigraphic $^{99\text{m}}\text{Tc}$ -PEI-MP (10-30 kDa) study in a dog with osteosarcoma.....	234
4.6	Materials and methods for MW-fraction 10-30 kDa complexed to $^{153}\text{Sm}$ .....	238
4.7	Statistical comparison of biodistribution and pharmacokinetic data between normal dogs receiving $^{99\text{m}}\text{Tc}$ -PEI-MP (10-30 kDa) and $^{153}\text{Sm}$ -PEI-MP (10-30 kDa).....	249
4.8	Section Discussion .....	251
Chapter 5.	Comparative Dosimetry of Normal Dogs and Dogs with Osteosarcoma. ....	256
Chapter 6.	Discussion .....	260
Chapter 7.	Conclusions.....	270
Chapter 8.	Appendices.....	272
8.1	Client consent form .....	272
8.2	Study information pamphlet.....	273
8.3	Data analysis calculations used for all radiopharmaceuticals .....	274
8.4	Biodistribution and pharmacokinetic tables for dogs receiving various radiopharmaceuticals .....	283
8.5	Clinical cases receiving $^{153}\text{Sm}$ -EDTMP and $^{188}\text{Re}$ -HEDP.....	287
8.6	Biodistribution and pharmacokinetic tables for dogs receiving $^{153}\text{Sm}$ -PEI-MP MW- fraction 10-30 kDa .....	315

8.7	Combined pharmacokinetic data for dogs receiving PEI-MP and other radiopharmaceuticals .....	317
8.8	Dosimetry results for various radiopharmaceuticals .....	324
Chapter 9.	References.....	327

## DEDICATION

I would like to dedicate this dissertation to my family. To my wife Diane and my children Andrea, Sandra, Stephen, and Gregory for their love, patience, and understanding while they put up with a studying dad. To the memory of my parents, Donald and Jenny Milner, may they rest in peace. To my brother Donald John Milner who never had the opportunities I had. To my grandparents Jack and Sally Milner whose faith in Christ will always serve as a beacon of hope in my life.

## ACKNOWLEDGEMENTS

Words cannot describe my gratitude to my mentors Professor Irene Dormehl and Dr. Werner Louw. Without their guidance, and dedication the research would not have been possible. I will forever remain in their debt. Most importantly, I want to thank the Nuclear Energy Corporation of South Africa Ltd (NECSA) for supplying, producing and sponsoring the radioisotopes and the radiopharmaceuticals used in this research. The work was also in part funded by the VolkswagenStiftung of Germany\*. I would also like to thank Elmare Killian for all hard work and dedication she put in and the excellent tea we drank together during those long research days. The research would also not have been possible without support from the staff from the Pretoria Biomedical Research Centre and the Police Dog Training School, Roodeplaat. Thank you for making the facilities available to me. Lastly, I wish to thank my research colleagues at the University of Florida, Dr Jim Farese from the College of Veterinary Medicine and Dr. Wes Bolch and Laura Padilla from Radiological Engineering, where results from our collaborative research have benefitted my dissertation enormously.

---

\* VolkswagenStiftung (Foundation), Germany. Kastanienallee 35 30519 Hannover, Germany.

Tel: +49.511.83.810

Fax: +49.511.83.81344

Email: infoatvolkswagenstiftung.de

[www.volkswagenstiftung.de](http://www.volkswagenstiftung.de)

## ABBREVIATIONS

% ID	The percentage of the injected dose	$T_{1/2}$	compartment ratio Time for concentration/activity of the radiopharmaceutical to diminish by one-half.
% OD	The percentage organ distribution		
95% Conf	95 % confidence interval	$t_{1/2-\beta}$	Half-life beta = elimination phase of the radiopharmaceutical in blood
99% Conf	99 % confidence interval		
ANOVA (RM)	Analysis of Variance (Repeated Measures)	$T_b$	Biological half-life of the radiopharmaceutical
$AUC_{(0-t)}$	Cumulative area under curve for experimental time points only: 0-t	$T_e$	Effective half-life of the radiopharmaceutical
$AUC_{\infty}$	Cumulative area under the curve to infinity.	$T_{max}$	Time at maximum observed concentration / activity of the radiopharmaceutical at ROI.
BED	Biologically Effective Dose in radiation biology	$T_p$	Physical half-life of the radioisotope
BV	Canine blood volume (89-90ml /kg)		
CF	Conversion factor		
Corr. F	Correction factor		
CORTB	Cortical bone		
cts	counts		
Cumul.Amt.	Cumulative Amount		
D.corr.cts	Decay corrected counts		
DF	Decay factor		
Gy	Gray - absorbed dose		
IQR	Interquartile Range (25 <sup>th</sup> – 75 <sup>th</sup> percentile)		
Max	Maximum		
MBq	Megabecquerel		
mCi	Millicurie		
Min	Minimum		
MW	Molecular weight. The sum of the atomic weights of all the atoms in a molecule. Expressed in Daltons (Da)		
NTC	Non-tumour compartment		
OPG	osteoprotegerin		
PBPC	Peripheral-blood progenitor cells		
PTH	Parathyroid hormone		
PTHrP	Parathyroid related peptide		
RANK / L	Receptor activator of nuclear factor $\kappa$ -B / ligand		
RES TIME	Residence time		
ROI	Region of Interest		
SD	Standard Deviation		
SE	Standard Error		
T	Tumour		
$t_{1/2-\alpha}$	Half-life alpha = distribution phase of the radiopharmaceutical from blood to the rest of the body		
T/NTC	Tumour / Non-Tumour		

## LIST OF FIGURES

Figure 1-1 The development of bisphosphonates from pyrophosphate.....	49
Figure 2-1 A longitudinal section through the canine humerus showing the contribution of trabecular and cortical bone to the proximal and mid-shaft ROI.....	103
Figure 3-1 Positioning of dogs for dynamic scintigraphy. ....	113
Figure 3-2: $^{153}\text{Sm}$ -EDTMP scintigraphic image showing areas selected as regions of interest (ROI) for normal and osteosarcoma dogs.....	117
Figure 3-3 Decay corrected time-activity curves for uncomplexed $^{153}\text{Sm}^{+3}$ .....	118
Figure 3-4 Time-activity curves showing $^{153}\text{Sm}^{+3}$ clearance in blood and (cumulative) urine clearance .....	119
Figure 3-5 Time-activity curves for the cardiac ROI in normal and osteosarcoma dogs receiving $^{153}\text{Sm}$ -EDTMP .....	121
Figure 3-6 Time-activity curves for the lung ROI in dogs receiving $^{153}\text{Sm}$ -EDTMP .....	122
Figure 3-7 Time-activity curves for the liver ROI in dogs receiving $^{153}\text{Sm}$ -EDTMP .....	123
Figure 3-8 Time-activity curves for the left kidney ROI in dogs receiving $^{153}\text{Sm}$ -EDTMP .	124
Figure 3-9 Time-activity curves for the right kidney ROI in dogs receiving $^{153}\text{Sm}$ -EDTMP .....	125
Figure 3-10 Time-activity curves for trabecular bone ROI in dogs receiving $^{153}\text{Sm}$ -EDTMP .....	126
Figure 3-11 Time-activity curves for cortical bone ROI in dogs receiving $^{153}\text{Sm}$ -EDTMP .	127
Figure 3-12 Time-activity curves for background (soft-tissue) ROI in dogs receiving $^{153}\text{Sm}$ -EDTMP .....	128
Figure 3-13 Time-activity curves for the tumour ROI in a dog receiving $^{153}\text{Sm}$ -EDTMP....	129
Figure 3-14 Time-activity curves for blood in normal and osteosarcoma dogs receiving $^{153}\text{Sm}$ -EDTMP .....	130
Figure 3-15 Time-activity curves showing (cumulative) urine clearance as a percentage of ID in dogs receiving $^{153}\text{Sm}$ -EDTMP.....	132
Figure 3-16: Time-activity curves for the cardiac ROI in normal and osteosarcoma dogs receiving $^{188}\text{Re}$ -HEDP .....	134
Figure 3-17 Time-activity curves for the lung ROI in normal and osteosarcoma dogs receiving $^{188}\text{Re}$ -HEDP .....	135



Figure 3-18 Time-activity curves for the liver ROI in normal and osteosarcoma dogs receiving $^{188}\text{Re}$ -HEDP .....	136
Figure 3-19 Time-activity curves for the left kidney ROI in normal and osteosarcoma dogs receiving $^{188}\text{Re}$ -HEDP .....	137
Figure 3-20 Time-activity curves for the right kidney ROI in normal and osteosarcoma dogs receiving $^{188}\text{Re}$ -HEDP .....	138
Figure 3-21 Time-activity curves for the trabecular bone ROI in normal and osteosarcoma dogs receiving $^{188}\text{Re}$ -HEDP .....	139
Figure 3-22 Time-activity curves for the cortical bone ROI in normal and osteosarcoma dogs receiving $^{188}\text{Re}$ -HEDP .....	140
Figure 3-23 Time-activity curves for the background (soft-tissue) ROI in normal and osteosarcoma dogs receiving $^{188}\text{Re}$ -HEDP .....	141
Figure 3-24 Time-activity curves for the tumour in the osteosarcoma dog receiving $^{188}\text{Re}$ -HEDP .....	142
Figure 3-25: Time-activity curves for blood in normal and osteosarcoma dogs receiving $^{188}\text{Re}$ -HEDP. ....	143
Figure 3-26 Time-activity curves showing the cumulative dose in urine as a percentage of ID after renal clearance for dogs receiving $^{188}\text{Re}$ -HEDP .....	145
Figure 3-27 Time-activity curves for a normal dog receiving uncomplexed $^{186}\text{Re}$ .....	146
Figure 3-28 Blood clearance and cumulative dose in urine after renal clearance as a percentage of ID for a dog receiving uncomplexed $^{186}\text{Re}$ .....	147
Figure 3-29 Time-activity curves for a normal dog receiving $^{186}\text{Re}$ -HEDP .....	149
Figure 3-30 Blood clearance and urine clearance (cumulative) as a percentage of ID in a normal dog receiving $^{186}\text{Re}$ -HEDP .....	150
Figure 3-31 A comparison of whole body effective half-life ( $T_e$ ) for various radiopharmaceuticals in dogs .....	153
Figure 3-32: A histogram of osteosarcoma dogs (n=17) receiving $^{153}\text{Sm}$ -EDTMP showing the distribution of T/NTC uptake ratios .....	164
Figure 3-33 Graphs representing haemoglobin, haematocrit, white blood cell and platelets values for dogs (n=5) receiving $^{153}\text{Sm}$ -EDTMP .....	165
Figure 3-34 Plotted tumour volumes from baseline regressed over time for dogs (n=9) receiving $^{153}\text{Sm}$ -EDTMP .....	167

Figure 3-35 Platelet counts for dogs receiving $^{153}\text{Sm}$ -EDTMP (Group-1) and $^{153}\text{Sm}$ -EDTMP + carboplatin (Group-2).....	178
Figure 3-36 White blood cell count for dogs receiving $^{153}\text{Sm}$ -EDTMP (Group-1) and $^{153}\text{Sm}$ -EDTMP + carboplatin (Group-2).....	179
Figure 3-37 Haematology results for Group-1 (single-dose) and Group-2 (multiple-dose) $^{188}\text{Re}$ -HEDP dogs.....	186
Figure 3-38 Plotted tumour volumes from baseline regressed over time for dogs (n=5) receiving a single-dose of $^{188}\text{Re}$ -HEDP .....	188
Figure 3-39 Kaplan-Meier survival curve for dogs with osteosarcoma receiving $^{153}\text{Sm}$ -EDTMP (plus carboplatin) and $^{188}\text{Re}$ -HEDP.....	191
Figure 3-40 A lateral radiograph (A) and 24-hour scintigraphic ( $^{153}\text{Sm}$ -EDTMP) image (B) of the distal femur from Case-13.....	197
Figure 3-41: Transverse osteosarcoma sections taken from the distal femur from Case-13 .	198
Figure 3-42: Macro-autoradiography image of the proximal femur.....	198
Figure 3-43: Photomicrograph sections from the proximal rat femur showing areas of interest. These areas correspond to increased radioisotope uptake. Diff-Quik (X 40, I-bar = 50 $\mu\text{m}$ )	200
Figure 3-44: Photomicrograph sections selected from the diaphyseal region of bone. ....	201
Figure 3-45: Photomicrographs sections selected from the metaphyseal region of the bone. ....	202
Figure 3-46: A photomicrograph of an H&E from the metaphyseal region of the proximal femur. ....	203
Figure 3-47: Photomicrographs sections selected from the epiphyseal and joint region of the bone.....	204
Figure 3-48: Matching radiograph and macro autoradiograph images taken from the same area of the distal femur of the osteosarcoma dog (Case-13).....	205
Figure 3-49: Photomicrographs taken from areas (see Figure 3-48) of low (Images -1 and -2) and high (Image -3 and -4) radioisotope uptake. ....	206
Figure 3-50: Image-1 is a radiograph of the section (section-2 see Figure 3-40) taken from the diaphyseal area of the femur of Case-13.....	207
Figure 3-51: Photomicrograph images from stained sections taken from the diaphyseal area of the femur of Case-13.....	208
Figure 4-1 (a) Scintigraphic image and (b) time activity curves of a normal dog who received $^{99\text{m}}\text{Tc}$ -PEI-MP 50-100 kDa (-).....	222

Figure 4-2 (a) Scintigraphic image and (b) time activity curve of a normal dog who received $^{99m}\text{Tc}$ -PEI-MP 50-100 kDa (+) .....	222
Figure 4-3 (a) Scintigraphic image and (b) time activity curves of a normal dog who received $^{99m}\text{Tc}$ -PEI-MP MW-fraction 30-50 (-).....	223
Figure 4-4 (a) Scintigraphic image and (b) time activity curves of a normal dog who received $^{99m}\text{Tc}$ -PEI-MP MW-fraction 30-50 (+).....	224
Figure 4-5 Scintigraphic image showing biodistribution data from a normal dog (n=1) receiving $^{99m}\text{Tc}$ -PEI-MP MW-fraction 20-30 kDa .....	225
Figure 4-6 Time-activity curves for $^{99m}\text{Tc}$ -PEI-MP MW-fraction 20-30 kDa (n=1) .....	225
Figure 4-7 Scintigraphic image showing biodistribution data from a normal (n=1) dog receiving $^{99m}\text{Tc}$ -PEI-MP MW-fraction 10-30 kDa .....	227
Figure 4-8 Time-activity curve for $^{99m}\text{Tc}$ -PEI-MP 10-30 kDa (n=1) .....	227
Figure 4-9 Time-activity curves for $^{99m}\text{Tc}$ -PEI-MP 3-10 kDa (n=1).....	229
Figure 4-10 Static scan at 3-hours for Case-14 receiving $^{99m}\text{Tc}$ -PEI-MP MW-fraction 10-30 kDa.....	236
Figure 4-11 Time-activity curves for Case-14 receiving $^{99m}\text{Tc}$ -PEI-MP 10-30 kDa .....	236
Figure 4-12: Time-activity curves for the cardiac ROI in normal dogs $^{153}\text{Sm}$ -PEI-MP (10-30 kDa) (n=4).....	239
Figure 4-13 Time-activity curves for the lung ROI in normal dogs receiving $^{153}\text{Sm}$ -PEI-MP (10-30 kDa).....	240
Figure 4-14 Time-activity curves for the liver ROI in normal dogs receiving $^{153}\text{Sm}$ -PEI-MP (10-30 kDa).....	241
Figure 4-15 Time-activity curves for the left kidney ROI in normal dogs receiving $^{153}\text{Sm}$ -PEI-MP (10-30 kDa).....	242
Figure 4-16 Time-activity curves for the right kidney ROI in normal dogs receiving $^{153}\text{Sm}$ -PEI-MP (10-30 kDa).....	243
Figure 4-17 Time-activity curves for the trabecular bone ROI in normal dogs receiving $^{153}\text{Sm}$ -PEI-MP (10-30 kDa) .....	244
Figure 4-18 Time-activity curves for the cortical bone ROI in normal dogs receiving $^{153}\text{Sm}$ -PEI-MP (10-30 kDa).....	245
Figure 4-19 Time-activity curves for the background ROI in normal dogs receiving $^{153}\text{Sm}$ -PEI-MP (10-30 kDa).....	246

Figure 4-20 Time-activity curve for blood in normal dogs receiving  $^{153}\text{Sm}$ -PEI-MP (10-30 kDa).....247

Figure 4-21 Cumulative time-activity curve for urine in normal dogs receiving  $^{153}\text{Sm}$ -PEI-MP (10-30 kDa).....248

## LIST OF TABLES

Table 1-1 Bone-seeking radiopharmaceuticals .....	31
Table 1-2 Classification of human osteosarcoma .....	38
Table 1-3 Physical Characteristics of radionuclides used in radiotherapy .....	44
Table 1-4 Stopping powers and range tables for radionuclides in cortical bone (International Commission on Radiological Protection [ICRP]).....	45
Table 1-5 Stopping powers and range tables for radionuclides in soft-tissue (ICRP).....	46
Table 1-6 Bisphosphonates their uses, molecular weight (MW) and chemical structure.....	50
Table 1-7: Chemical structure of PEI-MP .....	65
Table 1-8 Canine Toxicity Grading Schemes .....	70
Table 2-1: Comparative clinical aspects of canine and human osteosarcoma.....	85
Table 2-2: A summary of the mutated oncogene and tumour suppressor genes found in humans and dogs with osteosarcoma. ....	86
Table 2-3 Histopathological classification of canine osteosarcoma .....	87
Table 2-4 Clinical staging of canine osteosarcoma .....	89
Table 2-5 A summary of the median survivals times of dogs with osteosarcoma receiving chemotherapy and surgery .....	91
Table 3-1 Data showing pharmacokinetics and bone localization of $^{153}\text{Sm}$ -EDTMP in humans and animals .....	105
Table 3-2 Data showing pharmacokinetics and bone localization of $^{186}\text{Re}$ -HEDP and $^{188}\text{Re}$ -HEDP in humans and animals .....	106
Table 3-3 Physical Characteristics of $^{153}\text{Sm}$ .....	108
Table 3-4: Physical characteristics of $^{188}\text{Re}$ .....	109
Table 3-5: Physical characteristics of $^{186}\text{Re}$ .....	111
Table 3-6 Population Characteristics of Normal and Osteosarcoma Dogs and Administered Radiopharmaceutical and Dose.....	112
Table 3-7 Pharmacokinetic data for all compartments in a normal dog receiving uncomplexed $^{153}\text{Sm}^{+3}$ .....	119
Table 3-8 Pharmacokinetic data for blood and cumulative urine clearance of uncomplexed $^{153}\text{Sm}^{+3}$ .....	120
Table 3-9 Pharmacokinetic data for the cardiac compartment in dogs receiving $^{153}\text{Sm}$ -EDTMP .....	121

Table 3-10 Pharmacokinetic data for the lung compartment in dogs receiving $^{153}\text{Sm}$ -EDTMP .....	123
Table 3-11 Pharmacokinetic data for the liver compartment in dogs receiving $^{153}\text{Sm}$ -EDTMP .....	124
Table 3-12 Pharmacokinetic data for the left kidney compartment in dogs receiving $^{153}\text{Sm}$ -EDTMP .....	125
Table 3-13 Pharmacokinetic data for the right kidney compartment in dogs receiving $^{153}\text{Sm}$ -EDTMP .....	126
Table 3-14 Pharmacokinetic data for trabecular bone compartment in dogs receiving $^{153}\text{Sm}$ -EDTMP .....	127
Table 3-15 Pharmacokinetic data for cortical bone compartment in dogs receiving $^{153}\text{Sm}$ -EDTMP .....	128
Table 3-16 Pharmacokinetic data for background (soft-tissue) compartment in dogs receiving $^{153}\text{Sm}$ -EDTMP .....	129
Table 3-17 Pharmacokinetic data for the tumour compartment in a dog receiving $^{153}\text{Sm}$ -EDTMP .....	130
Table 3-18 Pharmacokinetic data for blood clearance in dogs receiving $^{153}\text{Sm}$ -EDTMP .....	131
Table 3-19 Pharmacokinetic data for cumulative urine clearance in dogs receiving $^{153}\text{Sm}$ -EDTMP .....	132
Table 3-20 Pharmacokinetic data for the cardiac compartment in dogs receiving $^{188}\text{Re}$ -HEDP .....	134
Table 3-21 Pharmacokinetic data for the lung compartment in dogs receiving $^{188}\text{Re}$ -HEDP .....	136
Table 3-22 Pharmacokinetic data for the liver compartment in dogs receiving $^{188}\text{Re}$ -HEDP .....	137
Table 3-23 Pharmacokinetic data for the left kidney compartment in dogs receiving $^{188}\text{Re}$ -HEDP .....	138
Table 3-24 Pharmacokinetic data for the right kidney compartment in dogs receiving $^{188}\text{Re}$ -HEDP .....	139
Table 3-25 Pharmacokinetic data for trabecular bone compartment in dogs receiving $^{188}\text{Re}$ -HEDP .....	140
Table 3-26 Pharmacokinetic data for cortical bone compartment in dogs receiving $^{188}\text{Re}$ -HEDP .....	141

Table 3-27 Pharmacokinetic data for background (soft-tissue) compartment in dogs receiving $^{188}\text{Re}$ -HEDP .....	142
Table 3-28 Pharmacokinetic data for the tumour compartment in a dog receiving $^{188}\text{Re}$ -HEDP .....	143
Table 3-29 Pharmacokinetic data for blood clearance in dogs receiving $^{188}\text{Re}$ -HEDP.....	144
Table 3-30 Pharmacokinetic data for cumulative dose in urine after renal clearance for dogs receiving $^{188}\text{Re}$ -HEDP .....	145
Table 3-31 Pharmacokinetic data for all compartments in a normal dog given uncomplexed $^{186}\text{Re}$ .....	147
Table 3-32 Pharmacokinetic data for blood clearance and cumulative urine activity in receiving uncomplexed $^{186}\text{Re}$ .....	148
Table 3-33 Pharmacokinetic data for all compartments in a normal dog given $^{186}\text{Re}$ -HEDP	149
Table 3-34 Pharmacokinetic data for blood clearance and cumulative urine activity in receiving $^{186}\text{Re}$ -HEDP .....	150
Table 3-35 Data showing pharmacokinetics, biodistribution and bone localization of $^{153}\text{Sm}$ -EDTMP, $^{188}\text{Re}$ -HEDP and $^{186}\text{Re}$ -HEDP in experimental dogs.....	154
Table 3-36 Data showing pharmacokinetics and bone localization of $^{153}\text{Sm}$ -EDTMP in humans and animals.....	157
Table 3-37 Data showing pharmacokinetics and bone localization of $^{186}\text{Re}$ -HEDP and $^{188}\text{Re}$ -HEDP in humans and animals .....	158
Table 3-38 Pain scoring used to describe treated dogs.....	161
Table 3-39 Descriptive statistics for platelets for dogs (n=5) receiving $^{153}\text{Sm}$ -EDTMP.....	166
Table 3-40 Overall median survival time in dogs (n=16) receiving $^{153}\text{Sm}$ -EDTMP which were grouped for pain.....	168
Table 3-41: Necropsy and radiograph results at euthanasia showing the frequency of metastases and survival times found in twenty dogs receiving $^{153}\text{Sm}$ -EDTMP .....	169
Table 3-42 The median survival time and pain response for Group-2 dogs receiving $^{153}\text{Sm}$ -EDTMP plus carboplatin. ....	174
Table 3-43 Median survival time for Groups 1 and 2 dogs stratified for response to pain control.....	175
Table 3-44 Post-hoc analysis comparing differences in survival times stratified for pain response to therapy. ....	175
Table 3-45 Descriptive statistics and <i>P</i> values for platelets from treatment Group-2 dogs ..	176

Table 3-46 Descriptive statistics for white blood cell count (WBC) treatment Group-2 dogs .....	176
Table 3-47 Descriptive statistics and <i>P</i> values for platelets for combined Groups. ....	177
Table 3-48 Descriptive statistics and <i>P</i> values for white blood cell counts (WBC) for combined Groups.....	177
Table 3-49 The mean±SD uptake ratio (T/NTC) for Group-1 ( <sup>153</sup> Sm-EDTMP) and Group-2 ( <sup>153</sup> Sm-EDTMP plus carboplatin).....	180
Table 3-50 Descriptive statistics for platelets from treatment single-dose <sup>188</sup> Re-HEDP dogs .....	185
Table 3-51 Descriptive statistics for platelets from both treatment groups receiving <sup>188</sup> Re- HEDP.....	185
Table 3-52 Median survival time for treatment both groups receiving single or multiple doses of <sup>188</sup> Re-HEDP.....	189
Table 3-53: Organs found positive for metastases at euthanasia in dogs receiving <sup>188</sup> Re-HEDP .....	190
Table 3-54 Median survival time for dogs with osteosarcoma receiving <sup>153</sup> Sm-EDTMP (plus carboplatin) and <sup>188</sup> Re-HEDP.....	192
Table 3-55 Median survival time for pain response to treatment for the combined treatment groups (n=29).....	192
Table 3-56 Results from multivariate analysis of osteosarcoma dogs stratified by treatment group.....	193
Table 3-57 Results from multivariate analysis of osteosarcoma dogs with survival as the only dependent variable.....	193
Table 3-58 Median uptake ratios (T/NTC) comparing tumour counts (T) to non-tumour counts (NTC) for all treatment groups.....	194
Table 3-59 Statistical comparison between radiopharmaceuticals uptake ratios (T/NTC) ...	194
Table 3-60: Descriptive statistics for micro-autoradiography score results from high, moderate and low <sup>153</sup> Sm-EDTMP uptake areas of the osteosarcoma.....	209
Table 3-61 Results from ANOVA on ranks analysis comparing micro-autoradiography score results from high, moderate and low <sup>153</sup> Sm-EDTMP uptake areas.....	210
Table 4-1 Molecular structure and weight of PEI-MP.....	217
Table 4-2 Percentage yield of PEI-MP molecular weight fractions obtained by membrane ultrafiltration.....	218



Table 4-3 List of normal dogs used in experimental procedures using variously sized MW-fractions of <sup>99m</sup> Tc-PEI-MP molecules.....	219
Table 4-4 Pharmacokinetic data for various compartments for dogs receiving <sup>99m</sup> Tc-PEI-MP MW-fractions 50-100 kDa (+) and (-) .....	223
Table 4-5 Pharmacokinetic data for various compartments for dogs receiving <sup>99m</sup> Tc-PEI-MP 30-50 kDa (+) and (-) charged .....	224
Table 4-6 Pharmacokinetic data for various compartments for dogs receiving <sup>99m</sup> Tc-PEI-MP 20-30 kDa (n=4).....	226
Table 4-7 Pharmacokinetic data for various compartments for dogs receiving <sup>99m</sup> Tc-PEI-MP 10-30 kDa (n=4).....	228
Table 4-8 Pharmacokinetic data for various compartments for a dog receiving <sup>99m</sup> Tc-PEI-MP 3-10 kDa (n=1).....	229
Table 4-9 Pharmacokinetic data for various <sup>99m</sup> Tc-PEI-MP MW-fractions in urine.....	230
Table 4-10 Pharmacokinetic data for various <sup>99m</sup> Tc-PEI-MP MW-fractions in blood.....	230
Table 4-11 Statistical comparison of pharmacokinetic data from <sup>99m</sup> Tc-PEI-MP MW-fractions 10-30 (n=4) and 20-30 kDa (n=4) for the cardiac compartment .....	231
Table 4-12 Statistical comparison of pharmacokinetic data from <sup>99m</sup> Tc-PEI-MP MW-fractions 10-30 and 20-30 kDa for blood.....	231
Table 4-13 Statistical comparison of pharmacokinetic data from <sup>99m</sup> Tc-PEI-MP MW-fractions 10-30 and 20-30 kDa for the lung compartment.....	232
Table 4-14 Statistical comparison of pharmacokinetic data from <sup>99m</sup> Tc-PEI-MP MW-fractions 10-30 and 20-30 kDa for the liver compartment .....	232
Table 4-15 Statistical comparison of pharmacokinetic data from <sup>99m</sup> Tc-PEI-MP MW-fractions 10-30 and 20-30 kDa for the left kidney compartment.....	232
Table 4-16 Statistical comparison of pharmacokinetic data from <sup>99m</sup> Tc-PEI-MP MW-fractions 10-30 and 20-30 kDa for the right kidney compartment .....	232
Table 4-17 Statistical comparison of pharmacokinetic data from <sup>99m</sup> Tc-PEI-MP MW-fractions 10-30 and 20-30 kDa for urine.....	233
Table 4-18 Statistical comparison of pharmacokinetic data from <sup>99m</sup> Tc-PEI-MP MW-fractions 10-30 and 20-30 kDa for the cortical bone compartment .....	233
Table 4-19 Statistical comparison of pharmacokinetic data from <sup>99m</sup> Tc-PEI-MP MW-fractions 10-30 and 20-30 kDa for the trabecular bone compartment .....	233

Table 4-20 Statistical comparison of pharmacokinetic data from $^{99m}\text{Tc}$ -PEI-MP MW-fractions 10-30 and 20-30 kDa for the background (soft-tissue) compartment.....	234
Table 4-21 The population characteristics of the osteosarcoma dog Case-14.....	235
Table 4-22 Pharmacokinetic results for various compartments in the osteosarcoma dog receiving $^{99m}\text{Tc}$ -PEI-MP 10-30 kDa .....	237
Table 4-23 Pharmacokinetic data for blood for osteosarcoma dog $^{99m}\text{Tc}$ -PEI-MP 10-30 kDa .....	237
Table 4-24 Pharmacokinetic data for cumulative urine clearance in an osteosarcoma dog receiving $^{99m}\text{Tc}$ -PEI-MP 10-30 kDa .....	237
Table 4-25 List of normal dogs (n=4) used in experimental procedures for $^{153}\text{Sm}$ -PEI-MP 10-30 kDa.....	238
Table 4-26: Pharmacokinetic mean $\pm$ SD of the cardiac compartment in normal dogs given $^{153}\text{Sm}$ -PEI-MP (10-30 kDa) .....	239
Table 4-27: Pharmacokinetic mean $\pm$ SD of the lung compartment in normal dogs given $^{153}\text{Sm}$ -PEI-MP (10-30 kDa).....	240
Table 4-28: Pharmacokinetic mean $\pm$ SD of the liver compartment in normal dogs given $^{153}\text{Sm}$ -PEI-MP (10-30 kDa) .....	241
Table 4-29: Pharmacokinetic mean $\pm$ SD of the left kidney compartment in normal dogs given $^{153}\text{Sm}$ -PEI-MP (10-30 kDa).....	242
Table 4-30: Pharmacokinetic mean $\pm$ SD of the right kidney compartment in normal dogs given $^{153}\text{Sm}$ -PEI-MP (10-30 kDa) .....	243
Table 4-31: Pharmacokinetic mean $\pm$ SD of the trabecular bone compartment in normal dogs given $^{153}\text{Sm}$ -PEI-MP (10-30 kDa) .....	244
Table 4-32: Pharmacokinetic mean $\pm$ SD of the cortical compartment in normal dogs given $^{153}\text{Sm}$ -PEI-MP (10-30 kDa) .....	245
Table 4-33: Pharmacokinetic mean $\pm$ SD of the background compartment in normal dogs given $^{153}\text{Sm}$ -PEI-MP (10-30 kDa) .....	246
Table 4-34 Pharmacokinetic mean $\pm$ SD of the blood compartment in normal dogs given $^{153}\text{Sm}$ -PEI-MP (10-30 kDa) .....	247
Table 4-35 Cumulative urine activity for dogs receiving $^{153}\text{Sm}$ -PEI-MP (10-30 kDa).....	248
Table 4-36 Pharmacokinetic data and statistical results comparing $^{153}\text{Sm}$ and $^{99m}\text{Tc}$ labelled 10-30 kDa PEI-MP MW-fraction .....	249

Table 4-37 Pharmacokinetic data for blood comparing $^{153}\text{Sm}$ and $^{99\text{m}}\text{Tc}$ labelled 10-30 kDa PEI-MP MW-fractions.....	250
Table 4-38 Pharmacokinetic data for urine comparing $^{153}\text{Sm}$ and $^{99\text{m}}\text{Tc}$ labelled 10-30 kDa PEI-MP MW-fractions.....	251
Table 4-39 Data showing pharmacokinetics, biodistribution and bone localization for PEI-MP MW-fractions and labelled radionuclides in normal dogs and dogs with osteosarcoma.....	255
Table 5-1 Dosimetry results from various radiopharmaceuticals in normal dogs comparing radiation sensitive organs.....	257
Table 5-2 Dosimetry data for osteosarcoma dogs receiving various radiopharmaceuticals..	259
Table 8-1 Manually calculated decay correction factors (DF*) for radioisotopes used in the study.....	274
Table 8-2 An example of spread sheet calculations derived from a dynamic $^{153}\text{Sm}$ -EDTMP scintigraphy study in a normal dog.....	275
Table 8-3 An example of spreadsheet calculations derived from a 1-hour static scintigraphy study in a normal dog receiving $^{153}\text{Sm}$ -EDTMP.....	276
Table 8-4 An example of the percentage organ distribution calculations derived from a scintigraphy study in a normal dog receiving $^{153}\text{Sm}$ -EDTMP.....	277
Table 8-5 An example of calculations used to derive urine time-activity curves and body retention curves expressed as a percentage injected dose for a dog receiving $^{153}\text{Sm}$ -EDTMP. .....	278
Table 8-6 An example of calculations used to derive blood time-activity curves for a dog receiving $^{153}\text{Sm}$ -EDTMP.....	279
Table 8-7 An example of calculations used to derive organ activity (mCi) from %OD for a dog receiving $^{153}\text{Sm}$ -EDTMP.....	280
Table 8-8 An example of calculations used to derive the percentage injected dose (% ID) for a dog receiving $^{153}\text{Sm}$ -EDTMP.....	281
Table 8-9 An example of manual calculations used to derive AUC and residence time curves for a dog receiving $^{153}\text{Sm}$ -EDTMP.....	282
Table 8-10 Biodistribution and pharmacokinetic data for individual dogs undergoing dynamic scintigraphy receiving $^{153}\text{Sm}$ -EDTMP.....	283
Table 8-11 Biodistribution and pharmacokinetic data for individual dogs undergoing dynamic scintigraphy receiving $^{188}\text{Re}$ -HEDP.....	284

Table 8-12 Biodistribution and pharmacokinetic data for individual dogs undergoing dynamic scintigraphy receiving uncomplexed $^{186}\text{Re}$ and $^{186}\text{Re}$ -HEDP .....	285
Table 8-13 Whole body effective half-life ( $T_e$ ) for various radiopharmaceuticals .....	286
Table 8-14 Profile of osteosarcoma and multilobular osteosarcoma dogs receiving $^{153}\text{Sm}$ -EDTMP .....	287
Table 8-15 Radiographic description, tumour size, volume and mass in naturally occurring canine osteosarcomas following treatment with $^{153}\text{Sm}$ -EDTMP cases .....	291
Table 8-16 Descriptive statistics showing increasing tumour volume ratio from baseline over a 4 month period for dogs (n=9) receiving $^{153}\text{Sm}$ -EDTMP .....	302
Table 8-17 Raw data for haematology results for dogs receiving $^{153}\text{Sm}$ -EDTMP and $^{153}\text{Sm}$ -EDTMP plus carboplatin .....	303
Table 8-18 Descriptive statistics for haematology results for the $^{153}\text{Sm}$ -EDTMP and $^{153}\text{Sm}$ -EDTMP plus carboplatin group .....	304
Table 8-19 Raw data for histopathological scores from osteosarcoma sections .....	305
Table 8-20 Statistical Analysis of scores from osteosarcoma histological sections using ANOVA on Ranks .....	306
Table 8-21 Summary of cases with naturally occurring canine osteosarcomas following treatment with $^{188}\text{Re}$ -HEDP .....	307
Table 8-22 Radiographic description, tumour size, volume and mass in naturally occurring canine osteosarcomas following treatment with $^{188}\text{Re}$ -HEDP .....	308
Table 8-23 Raw data for haematology results for $^{188}\text{Re}$ -HEDP (single dose) and $^{188}\text{Re}$ -HEDP (multiple dose) .....	312
Table 8-24 Descriptive statistics for haematology results for the $^{188}\text{Re}$ -HEDP (single dose) and $^{188}\text{Re}$ -HEDP (multiple dose) .....	313
Table 8-25 Data corrected for baseline (1) showing increasing tumour volume over time for dogs receiving a single dose of $^{188}\text{Re}$ -HEDP .....	314
Table 8-26 Raw data from dogs receiving a tracer dose of $^{153}\text{Sm}$ -PEI-MP MW-fraction10-30 kDa .....	315
Table 8-27: The mean $\pm$ SD values for compartments derived from raw data in normal dogs (n=4) given $^{153}\text{Sm}$ -PEI-MP (MW 10-30 kDa) .....	316
Table 8-28 Raw pharmacokinetic data for various radiopharmaceuticals .....	317
Table 8-29 Descriptive statistics and ANOVA on Ranks of organ compartments from various radiopharmaceuticals used for comparative purposes in the discussion sections .....	319

Table 8-30 Descriptive statistics blood and urine for various radiopharmaceuticals .....	323
Table 8-31 Dosimetry results (mGy/MBq) for various organs derived from OLINDA software from normal dogs .....	324
Table 8-32 Dosimetry results derived using OLINDA software for dogs with osteosarcoma .....	326
Table 8-33 Self dose calculations for tumours .....	326

## LIST OF APPENDICES

Section 8.1.....	page 272
Section 8.2.....	page 273
Section 8.3 .....	page 274
Section 8.4.....	page 283
Section 8.5.....	page 287
Section 8.6 .....	page 315
Section 8.7.....	page 317
Section 8.8 .....	page 324

## SAMEVATTING

Primêre en metastatiese beenkankers is in beide volwasse en pediatriese pasiente vernietigende siektes weens die morbiditeit wat geassosieer word met been pyn. Die beheer van hierdie pyn met konvensionele behandelings, veral in die finale stadia en in gevalle waar daar veelvuldige uitsaaiings voorkom, kan problematies wees. Vir hierdie doel kan daar met 'n groter mate van sukses van been-soekende radiofarmaseutika gebruik gemaak word. Hierdie middels deponeer die radioaktiwiteit met 'n redelike mate van selektiwiteit in die teiken-gebied. Hierdie teiken-gerigte radioterapie is egter beperk tot pyn verligting aangesien beenmurgonderdrukking die dosisse tot sub-terapeutiese vlakke beperk. Pogings wat aangewend is om hierdie beperkings te oorbrug het prosedures ingesluit soos chemoterapie tesame met beenmurgoorplantings asook radiosensitisering en die ontwikkeling van nuwe radiofarmaseutika.

Vir die ontwikkeling van nuwe middels is eksperimentele werk op proefdier modelle noodsaaklik. Die gebruik van laboratorium knaagdier modelle word egter gekortwiek deur die dosimetriese beperkings a.g.v. die grootte van die diere asook die inherente beperkings van die xenoweefseloorplantings van mens tumourweefsels op proefdiere. Om hierdie probleem te oorkom, is daar in hierdie studie gebruik gemaak van honde met natuurlik voorkomende osteosarkome as 'n oorbruggings-model vir mens beenkanker.

Die kern hipotese van hierdie studie is dat natuurlik voorkomende hond osteosarkome kan dien as 'n navorsings-model vir 'n vergelykende studie oor die farmakokinetika (biodistribusie), dosimetrie, toksisiteit en terapeutiese effek van  $^{153}\text{Sm-EDTMP}$ ,  $^{188}\text{Re-HEDP}$ ,  $^{186}\text{Re-HEDP}$  en 'n nuwe toepaslik radionuklid gemerkte ligand, polietileeniminometielfosfoonsuur (PEI-MP). Die data wat vanaf bestaande radiofarmaseutika verkry is, is verder vergelyk met dié van PEI-MP wat gemerk is met  $^{99m}\text{Tc}$ ,  $^{153}\text{Sm}$  en  $^{186}\text{Re}$ .

Met hierdie nuwe en unieke ondersoek was dit moontlik om verskillende radiofarmaseutika in natuurlik voorkomende beenkanker dier modelle te evalueer. Die farmakokinetika en dosimetrie van die nuwe radionuklid gemerkte ligand (PEI-MP) kon ook gedokumenteer word. Die nut van hierdie studie is dat resultate wat vanaf prekliniese knaagdier proewe bekom is, vinniger via die natuurlike kanker model wat nader aan die mens is, oorgedra kan word om sodoende probleme t.o.v. kinetika en toksisiteit vroegtydig te identifiseer voordat daar met duur kliniese proewe begin word.

Oorspronklik was die formulering van die verwagte resultate van hierdie studie gebaser op die beperkte gepubliseerde gegewens op honde. Byvoorbeeld, daar bestaan geen beskrywing van die farmakokinetika of toksisiteit van  $^{188}\text{Re-HEDP}$  en  $^{186}\text{Re-HEDP}$  in honde nie.

Hierdie studie is in twee fases uitgevoer. Die eerste fase handel oor die evaluering van  $^{153}\text{Sm-EDTMP}$ ,  $^{188}\text{Re-HEDP}$  en  $^{186}\text{Re-HEDP}$  in die honde model. Die tweede fase handel oor die gedrag van die nuwe radionuklied gemerkte ligand, PEI-MP, wat die eienskappe van 'n ideale ligand vir hierdie doel vertoon, in die osteosarkoom honde model.

Die farmakokinetika resultate van  $^{153}\text{Sm-EDTMP}$  in normale honde ( $n=4$ ) was soortgelyk aan dié in gepubliseerde resultate vir honde en mense. Statistiese vergelykings met dié van mense het getoon dat die meerderheid resultate dieselfde was, wat geloofwaardigheid verleen aan die hipotese dat honde 'n geskikte model uitmaak vir navorsing op radiofarmaseutika vir eventuele menslike gebruik. Daar is egter verskille waargeneem deurdat die kinetika van uriene eliminerings-fase ( $t_{1/2-\beta}$ ) in normale honde en die osteosarkoom honde verskil het van dié van mense. Hierdie verskille kan moontlik verklaar word aan die hand daarvan dat die meerderheid van die mense wat gebruik is, bejaard was en waarskynlik nier probleme gehad het tesame met die bydraende tumourlas. Daar is egter 'n tendens waargeneem dat in honde met osteosarkome daar 'n verlengde urine uitskeidings-fase ( $t_{1/2-\beta}$ ) voorgekom het as by normale honde, wat die hipotese ondersteun dat die kinetika en biodistribusie resultate van honde soortgelyk is aan die gepubliseerde mens data. Die farmakokinetika en biodistribusie van  $^{188}\text{Re-HEDP}$  en  $^{153}\text{Sm-EDTMP}$  in normale honde is verder statisties vergelyk. Die langer uriene eliminerings-fase ( $t_{1/2-\beta}$ ) en verhoogde bloed retensie van  $^{188}\text{Re-HEDP}$  was waarskynlik die gevolg van 'n verlengde been-uitloging en sagteweefsel retensie, wat toegeskryf kan word aan die verskille in die antiresorptiewe vermoëns van die bisfosfonaat ligande, bv. EDTMP (lexidronan) het 'n 100-voudige groter antiresorptiewe vermoë as dié van HEDP (etidronate).

Aanvullende biodistribusie waarnemingstudies deur gebruik te maak van makro-en mikro-ouroradiografiese tegnieke is ook gedoen op weefsels van honde en Sprague-Dawley rotte. 'n Heterogene intratumour opname is in honde waargeneem terwyl in rotte die waargenome lokalisering van  $^{153}\text{Sm-EDTMP}$  in rooibeemurg areas 'n aanduiding kan wees van hoë stralingsdosise aan die bloed produserende elemente. Tesame hiermee is ook 'n hoë opname waargeneem by die metafisiale groei-plate wat die waarskynlikheid van groei-vertraging of groei-staking in groeiende kinders tot gevolg kan hê indien  $^{153}\text{Sm-EDTMP}$  aan hulle toegedien sou word.



Fase-1 kliniese proewe op honde met natuurlike osteosarkome het slegs milde toksisiteit vertoon met dosisse van 37MBq/kg (1nCi/kg) vir beide  $^{153}\text{Sm}$ -EDTMP en  $^{188}\text{Re}$ -HEDP. Tesame hiermee is 'n loods-studie uitgevoer met honde wat beide  $^{153}\text{Sm}$ -EDTMP en 'n karboplatien infusie tesame met die radiofarmaseutikum toediening gekry het, waarna daar drie siklusse karboplatien met drie weeklikse intervalle toegedien is. Geen verskille in toksisiteit kon waargeneem word tussen die groepe wat slegs  $^{153}\text{Sm}$ -EDTMP en dié wat addisioneel karboplatien ontvang het, nie. As 'n deel van die  $^{188}\text{Re}$ -HEDP kliniese toets, is drie honde met osteosarkomas 'n weeklikse dosis van 37MBq/kg  $^{188}\text{Re}$ -HEDP vir vier weke toegedien waar slegs milde toksisiteit waargeneem is. Daar was ongelukkig geen staking in die groei van die tumoure nie, en die tumoure in al die honde het progressie getoon. Die mediaan oorlewingstyd vir beide radiofarmaseutika behandelde honde was vier maande, wat aansienlik korter was as die tien maande mediaan oorlewingstyd van honde wat met chemoterapie en amputasie behandel is. Dit was verder opmerklik dat ses honde wat toedienings met beide  $^{99\text{m}}\text{Tc}$ -MDP ('n diagnostiese radiofarmaseutikum) en  $^{153}\text{Sm}$ -EDTMP gehad het, tumour sintigramme opgelewer het wat deurgaans laer  $^{99\text{m}}\text{Tc}$ -MDP opname-verhoudings (normale been tot kankeragtige been) getoon het as in die geval van  $^{153}\text{Sm}$ -EDTMP. In teenstelling hiermee, was dit nie die geval met die opname-verhoudings tussen die sintigramme van  $^{188}\text{Re}$ -HEDP en  $^{99\text{m}}\text{Tc}$ -MDP nie. Hierdie bevindinge beklemtoon weereens die antiresorptiewe eienskappe van die bisfosfonaat ligande. Sintigramme van nog drie honde wat met  $^{99\text{m}}\text{Tc}$ -MDP,  $^{153}\text{Sm}$ -EDTMP en  $^{99\text{m}}\text{Tc}$ -PEI-MP (10-30 kDa) gedoen is, het 'n variasie in die opname in dieselfde tumoure getoon. Van groter belang is die bevinding dat die opname verhoudings van die  $^{99\text{m}}\text{Tc}$ -MDP en  $^{153}\text{Sm}$ -EDTMP in die sintigramme 'n groot variasie met 'n koëffisiënt van variasie van 52% en 39% respektiewelik getoon het. Die opname-bereike van die  $^{99\text{m}}\text{Tc}$ -PEI-MP (10-30 kDa) sintigramme was egter kleiner met 'n variasie koëffisiënt van slegs 6%. Hierdie bevinding kan toegeskryf word aan 'n meer konsekwente opname verhoudings van die nuwe ligand PEI-MP wat moontlik verklaar kan word aandie hand van sy hipotetiese meganisme van opname: die verhoogde permeabiliteit en retensie (EPR) in die tumour vaskalatuur. Hierdie aspek benodig egter verdere ondersoek met groter getalle proefdiere.

In fase twee is die farmakokinetika en biodistribusie van die nuwe polimeer ligand PEI-MP ondersoek, waar dit aanvanklik met  $^{99\text{m}}\text{Tc}$  gemerk is. Verskeie fraksies met verskillende molekulêre massa reikwydtes is in honde ondersoek en vergelyk met gepubliseerde resultate wat in bobbejane verkry is. Die resultate wat met die honde studies verkry is, was soortgelyk

aan dié van die primaat studies. Soos in die geval van die primaat studies het die molekulêre massa en lading 'n beduidende rol in die farmakokinetika en biodistribusie gespeel. Die molekulêre massa fraksies van 10-30kDa en 20-30kDa het die belowendste vertoon t.o.v. die hipotetiese kriteria vir 'n ideale radiofarmaseitikum vir die doel van hierdie studie. Van hierdie twee fraksies was die 20-30kDa die meer aanvaarbare een weens sy vinniger opruiming uit die sisteem. Weens sy hoër opbrengs vanuit die fraksioneringsproses is die 10-30kDa fraksie gebruik vir verdere merkingsstudies met  $^{153}\text{Sm}$ . Die  $^{153}\text{Sm}$ -PEI-MP het egter 'n ander farmakokinetika en biodistribusie patroon as  $^{99\text{m}}\text{Tc}$ -PEI-MP (10-30kDa) vertoon. Die eliminasië fase ( $t_{1/2}\text{-}\beta$ ) van  $^{153}\text{Sm}$ -PEI-MP was langer met 'n gepaardgaande hoër lewer opname. Om hierdie verskynsel te verklaar, is van 'n rekenaar modellering vir bloedplasma (ECCLES) gebruik gemaak, wat voorspel het dat daar 'n dissosiasie van die  $^{153}\text{Sm}$  vanaf die PEI-MP in die bloed kan plaasvind, a.g.v. die vorming van  $^{153}\text{Sm}$ -sitraat. Die ECCLES bloedplasma model het ook voorspel dat die anioniese 10-30kDa PEI-MP 'n swak ligand sal wees vir kopleksering met  $^{166}\text{Ho}$ ,  $^{212}\text{Pb}$ ,  $^{213}\text{Pb}$  en  $^{89}\text{Sr}$ . Bruikbare komplekse behoort egter te vorm met  $^{186}\text{Re}$  en  $^{188}\text{Re}$  weens hulle posisie t.o.v.  $^{99\text{m}}\text{Tc}$  op die periodieke tabel. In 'n voorlopige studie is  $^{186}\text{Re}$ -PEI-MP 20-30kDa (n=2) en 30-50kDa (n=1) fraksies in honde ondersoek, wat soortgelyke resultate as dié met  $^{99\text{m}}\text{Tc}$ -PEI-MP opgelewer het.

Die biodistribusie en kinetiese data is verder ook gebruik vir 'n vergelykende dosimetriese studie tussen die verskillende radiofarmaseutika. Hierdie data het die hoë rooibeenmurg dosis vir  $^{153}\text{Sm}$ -EDTMP bevestig asook die verhoogde sagteweefsel dosis vir die HEDP gekomplekseerde radionukliede. Die stralingsdosis vir al die terapeutiese radiofarmaseutika was binne die gebied van 26Gy tot 44Gy, wat binne die stralingsdosis gebied val wat vir eksterne bundel radioterapie op honde osteosarkome gebruik word. Die gebrek aan tumour gevoeligheid in die geval van die terapeutiese radiofarmaseutika in vergelyking met dié van eksterne bundel radioterapie kan verklaar word aan die hand van die heterogene distribusie van die radiofarmaseutika in die tumoure asook die inhirente weerstand van osteosarkomasse teenoor onafgebroke lae-vlak straling-toedienings wat eie is aan radionuklied verval. Hierdie studie het aan die meeste verwagtings voldoen, behalwe in die geval van  $^{153}\text{Sm}$ -PEI-MP waar die interaksie met sitraat in die bloed die werking van die middel belemmer het. Alhoewel daar genoeg data beskikbaar was vir 'n vergelykende studie, het die vinnige verval van die  $^{188}\text{Re}$ -generator aanleiding gegee tot die voortydige inkorting van die  $^{188}\text{Re}$ -HEDP terapeutiese proewe.

## SUMMARY

Metastatic and primary bone cancers are devastating diseases of paediatric and adult humans because of the morbidity associated with bone pain. Controlling bone pain from multiple metastatic sites can be difficult in end-stage cancers using conventional therapies. Bone-seeking radiopharmaceuticals have been successful in this area as radiation can be delivered with moderate selectivity to the target. Unfortunately, targeted radiotherapy using radiopharmaceuticals have been relegated to palliative therapy as myelosuppression largely limits the radiation dose to sub-therapeutic levels. Efforts to overcome this therapeutic limitation include autologous bone marrow transplants in combination with chemotherapy-radiosensitization and the development of new radiopharmaceuticals. Development work using laboratory rodent models has been complicated by dosimetric limitations because of size and inherent problems with human xenografted tumour models in rodents. To address this need we studied naturally occurring canine osteosarcoma as a translational model for human bone cancer.

Central to our hypothesis was that naturally occurring canine osteosarcoma would serve as an investigational model for comparing the pharmacokinetics (biodistribution), dosimetry, toxicity, and therapeutic effect of  $^{153}\text{Sm}$ -EDTMP,  $^{188}\text{Re}$ -HEDP,  $^{186}\text{Re}$ -HEDP, and a novel ligand, polyethyleneiminomethyl phosphonic acid (PEI-MP). Data collected from existing radiopharmaceuticals was then compared to PEI-MP labelled with  $^{99\text{m}}\text{Tc}$ ,  $^{153}\text{Sm}$ , and  $^{186}\text{Re}$ .

This innovative and unique study allowed for the evaluation of various radiopharmaceuticals in a naturally occurring animal model of bone cancer, documenting the pharmacokinetics and dosimetry of a novel radiolabelled-ligand (PEI-MP). Benefits resulting from the successful completion of the study would allow more rapid transfer of rodent preclinical data into a naturally occurring cancer model more resembling to the human diseases and would thus more likely identify problems with pharmacokinetics and toxicity before proceeding to expensive clinical trials.

The expected outcomes of the study were originally formulated based on limited previous published data in dogs. For instance, no data exists describing the pharmacokinetics or toxicity of  $^{188}\text{Re}$ -HEDP and  $^{186}\text{Re}$ -HEDP in the dog. The study was conducted in two phases. The first phase deals with the evaluation of  $^{153}\text{Sm}$ -EDTMP,  $^{188}\text{Re}$ -HEDP, and  $^{186}\text{Re}$ -HEDP in the dog model. Phase-two was the development of a novel ligand (PEI-MP) in the dog model of osteosarcoma, which has the characteristics of an ideal ligand.

Pharmacokinetic results for  $^{153}\text{Sm}$ -EDTMP in normal dogs ( $n=4$ ) for blood were similar to published reports for dogs and human. When compared statistically to human data the majority of results were the same, lending credence to the hypothesis that dogs could serve as models for human radiopharmaceutical research. Normal dogs and the osteosarcoma dog did differ from human pharmacokinetics in the urine elimination phase ( $t_{1/2-\beta}$ ). This can most likely be explained by the tumour burden in the human research populations or due to the fact that most humans were aged and likely to have some renal disease. Certainly, the trend in dogs with osteosarcoma was to have a prolonged urine elimination phase ( $t_{1/2-\beta}$ ) compared to normal dogs which supported the hypothesis that the biodistribution and pharmacokinetics results from dogs were similar to human published data. Statistical comparisons were also made between normal dogs receiving  $^{188}\text{Re}$ -HEDP and  $^{153}\text{Sm}$ -EDTMP. The prolonged urine elimination phase ( $t_{1/2-\beta}$ ) and increased blood retention of  $^{188}\text{Re}$ -HEDP was most likely a reflection of prolonged bone washout and soft issue retention. This could be attributed to the differences between the antiresorptive capability of bisphosphonate ligands e.g., EDTMP (lexidronam) with a greater than 100-fold antiresorptive capability than HEDP (etidronate).

Additional observational biodistribution studies using macro- and micro-autoradiography techniques were also performed in canine tissue and Sprague-Dawley rats. Results from the studies showed heterogeneous uptake within tumours in dogs. In rats, localization of  $^{153}\text{Sm}$ -EDTMP in red marrow areas would lead to a high radiation dose to blood producing elements. In addition, high uptake was documented at the metaphyseal growth plate confirming the likelihood of a delay or cessation of growth if  $^{153}\text{Sm}$ -EDTMP were used in growing children.

Phase-one of the clinical trial in dogs with naturally occurring osteosarcoma identified only mild toxicity at the dosage rate of 37 MBq/kg (1 mCi/kg) for both  $^{153}\text{Sm}$ -EDTMP and  $^{188}\text{Re}$ -HEDP. In addition, a pilot trial was conducted in dogs receiving  $^{153}\text{Sm}$ -EDTMP which also received a carboplatin infusion at the time of the radiopharmaceutical administration followed by another 3 cycles of carboplatin at 3 weekly intervals. No differences in toxicity were noted between the carboplatin group and dogs receiving only  $^{153}\text{Sm}$ -EDTMP. As a part of the  $^{188}\text{Re}$ -HEDP clinical trial, 3 dogs with osteosarcomas received weekly dose of  $^{188}\text{Re}$ -HEDP at 37MBq/kg for 4 weeks in which only mild toxicity was noted. Unfortunately, there was no cessation in growth of the tumours, with all dogs showing progression. The median survival time for both radiopharmaceuticals was 4 months, significantly shorter than the 10-month median survival time for amputation and

chemotherapy. Interestingly six dogs that had  $^{99m}\text{Tc}$ -MDP and  $^{153}\text{Sm}$ -EDTMP showed scans of tumours that had consistently lower  $^{99m}\text{Tc}$ -MDP uptake ratios (normal bone compared to cancerous bone) compared to solely  $^{153}\text{Sm}$ -EDTMP. In contrast, this was not evident for uptake ratios between  $^{188}\text{Re}$ -HEDP and  $^{99m}\text{Tc}$ -MDP scans. Once again, this finding highlights the differences between the antiresorptive capabilities of the bisphosphonates ligands. Interestingly, another three dogs were scanned with  $^{99m}\text{Tc}$ -MDP,  $^{153}\text{Sm}$ -EDTMP, and  $^{99m}\text{Tc}$ -PEI-MP (10-30 kDa) showed a variation in uptake between scans of the same tumours. More importantly, the uptake ratios of  $^{99m}\text{Tc}$ -MDP and  $^{153}\text{Sm}$ -EDTMP scans showed wide variation with a coefficient of variance of 52% and 39% respectively. However, the range in uptake from the  $^{99m}\text{Tc}$ -PEI-MP (10-30 kDa) scan was narrow with a coefficient of variance of only 6%. This could be attributed to more consistent uptake ratio of the unique ligand PEI-MP and its hypothesized mechanism of action: enhanced permeability and retention (EPR) in tumour vasculature. This requires further investigation with larger groups.

In phase-two, the pharmacokinetic result for the novel ligand PEI-MP was initially studied labelled with  $^{99m}\text{Tc}$ . Various molecular weights were tested in normal dogs and compared to previously published results in baboons. Results from the dog studies were found to be similar to those from the primate study. As in the primate study, molecular weight and charge played a significant role in  $^{99m}\text{Tc}$ -PEI-MP pharmacokinetics. Increasing the size of the macromolecules and altering their charge resulted in marked changes in their pharmacokinetics and biodistribution. The PEI-MP molecular weight of 10-30 kDa and 20-30 kDa were the most promising and fulfilled the hypothesized criteria of an ideal radiopharmaceutical. In keeping with the aims of the study, the 20-30kDa polymer was considered more desirable because of its faster clearance. However, because of the limitations imposed by the percentage yield of the different molecular weights of the ligand during filtration, we decided to label the 10-30kDa molecular weight MW-fraction with  $^{153}\text{Sm}$ . Unexpectedly, the  $^{153}\text{Sm}$ -PEI-MP 10-30 kDa had a prolonged urine elimination phase ( $t_{1/2-\beta}$ ) associated with increased liver uptake when compared to  $^{99m}\text{Tc}$ -PEI-MP10-30 kDa. To explain this, computer modelling for blood plasma (ECCLES) was done which predicted that there would be some chemical dissociation of the  $^{153}\text{Sm}$  from the PEI-MP polymer in blood. This is due to interaction between the radiopharmaceutical and citrate, forming  $^{153}\text{Sm}$ -citrate. The ECCLES model for blood plasma also predicted that the anionic MW-fraction, PEI-MP 10-30kDa, would be a poor ligand complexed to  $^{166}\text{Ho}$ ,  $^{212}\text{Pb}$ ,  $^{213}\text{Pb}$ , and  $^{89}\text{Sr}$ , but was expected to be effective when complexed to  $^{186}\text{Re}$  or  $^{188}\text{Re}$ , based on their close proximity to

$^{99m}\text{Tc}$  on the periodic table. As a preliminary study  $^{186}\text{Re}$  was complexed to 20-30 kDa (n=2) and 30-50 kDa (n=1) MW-fractions and tested in dogs. The results were similar to  $^{99m}\text{Tc}$ -PEI-MP 10-30 kDa.

The biodistribution data and pharmacokinetic data were also used to do comparative dosimetry between radiopharmaceuticals. Not surprisingly, the dosimetry data confirmed the high red marrow dose for  $^{153}\text{Sm}$ -EDTMP and the increased soft-tissue dose of the radionuclides complexed to HEDP. The radiation dose to the tumour for all radiopharmaceuticals fell within the range of 26Gy to 44Gy. This is well within the range used to treat canine osteosarcoma using external beam radiotherapy. When compared to external beam radiotherapy, the probable lack of tumour response in our clinical trial relates to the heterogenous distribution of the radiopharmaceutical in the tumour and the inherent resistance of osteosarcoma cells to continuous low-dose radiation delivery (CLDR) inherent in radionuclide -particle decay.

The study met the majority of outcomes with the exception of labelling PEI-MP with  $^{153}\text{Sm}$ <sup>1</sup>. This was due to the interaction of the  $^{153}\text{Sm}$ -PEI-MP complex with citrate ions in blood. Rapid deterioration of the Rhenium-188 generator also led to earlier than expected curtailment of the  $^{188}\text{Re}$ -HEDP therapeutic trial although sufficient data was available to be used in a comparative study.

## Chapter 1. Introduction and Literature Study

### 1.1 Overview

Metastatic bone cancer and primary bone cancer (osteosarcoma) are devastating diseases of paediatric and adult humans. A predominant issue with these cancers is the severe pain that patients experience. Where people have multiple metastatic sites, controlling bone pain can be difficult and bone-seeking radiopharmaceuticals have been successful in this area. Lists of the radiopharmaceuticals used in the past are given below in Table 1-1<sup>2-6</sup>.

**Table 1-1 Bone-seeking radiopharmaceuticals**

Radiopharmaceutical	Trade name
Holmium-166	
Lutetium-177-EDTMP	
Phosphorous-32	
Rhenium-186-HEDP	
Rhenium-188-HEDP	
Samarium-153-EDTMP	Quadramet
Strontium chloride-89	Metastron
Tin(Sn)-117m-DTPA	
Radium-223	Alpharadin

In humans, metastatic disease is more common than primary bone cancer and is associated with end-stage disease, primarily from prostate or breast cancer. Recently reports of bone-seeking radiopharmaceuticals exerting an anticancer effect on osteosarcoma in humans and animals can be found in the literature<sup>7-13</sup>. Unfortunately, targeted radiotherapy using radiopharmaceuticals have for the most part been relegated to palliative therapy as myelosuppression largely limits the radiation dose. In an effort to overcome the myeloablative affects associated with higher therapeutic doses to the tumour, some researchers have used autologous bone marrow transplants<sup>10, 14</sup>. In a more recent report, the addition of chemotherapy radiosensitization has also been employed to improve tumour response to radiopharmaceuticals<sup>11, 12</sup>.

In developing new radiopharmaceuticals, preclinical research has for the most part been in rodent models with some exceptions<sup>15</sup>. Although helpful, rodent models have very different dosimetry results compared to humans and so extrapolation to clinical medicine is limited<sup>16</sup>. In the search for a better translational model, it is now more widely recognized that naturally occurring canine osteosarcoma is a good large animal model for primary bone cancer in humans and could serve as one for metastatic disease<sup>17</sup>. Indeed, in an abstract presented at an international meeting, the authors found canine and human osteosarcomas were remarkably similar genetically and greater differences were found between osteosarcoma types than between species<sup>18</sup>. This was confirmed by recent comparative genomic hybridization array (aCGH) and in-situ hybridization experiments in dogs with naturally occurring osteosarcoma<sup>19</sup>. Since a model's importance is also related to its availability, it is fortunate that canine osteosarcoma has a high incidence when compared to human osteosarcoma<sup>20</sup>.

The long-term goals of this study are to support the concept that naturally occurring canine osteosarcoma can be used as a radiopharmaceutical translation model to fill the gap between rodent models and human clinical medicine. The central hypothesis of the study was that naturally occurring canine osteosarcoma could serve as an investigational model for human osteosarcoma and for comparing the pharmacokinetics (biodistribution), dosimetry, and therapeutic effect of established therapeutic radiopharmaceuticals and a novel radiolabelled-ligand. More specifically the aims of this thesis were to propose the canine as a model for the use of established (<sup>153</sup>Sm-EDTMP, <sup>188</sup>Re-HEDP, and <sup>186</sup>Re-HEDP) radiopharmaceuticals by collecting pharmacokinetic (biodistribution), dosimetry, toxicity and survival data in dogs with and without osteosarcoma and comparing it with published human data (metastatic bone cancer). These data were then compared to a novel radiolabelled-ligand, polyethyleneiminomethyl phosphonic acid (PEI-MP) which has potential as tumour-seeking radiopharmaceutical with improved pharmacokinetic properties such as reduced radiation dose to bone marrow and other radiosensitive organs<sup>21</sup>.

This study is both innovative and unique because it allowed evaluation of various established radiopharmaceuticals in a naturally occurring model of bone cancer and it documents the pharmacokinetics, dosimetry of a novel radiolabelled-ligand (PEI-MP). Benefits accruing from the successful completion of the study would allow more rapid transfer of rodent preclinical data into a naturally occurring cancer model resembling more



the human form of these diseases and thus more likely to identify problems with pharmacokinetics and toxicity before proceeding to expensive clinical trials.

The expected outcomes of the study were originally formulated based on previously published data in dogs<sup>7, 15, 22</sup> and primates<sup>21</sup>. The study met the majority of outcomes with the exception of labelling of PEI-MP with  $^{153}\text{Sm}$ <sup>1</sup>. This was due to the interaction of the  $^{153}\text{Sm}$ -PEI-MP complex with citrate ions in blood. Rapid deterioration of the Rhenium-188 generator also led to earlier than expected curtailment of the  $^{188}\text{Re}$ -HEDP therapeutic trial although sufficient data was available to compare it to other radionuclides.

The study was conducted in two phases. The first phase (Chapter 3) deals with the evaluation of  $^{153}\text{Sm}$ -EDTMP  $^{188}\text{Re}$ -HEDP and  $^{186}\text{Re}$ -HEDP in the dog model. Phase-2 (Chapter 4) was the development of a novel ligand (PEI-MP) in the dog model of osteosarcoma, which would have the characteristics of an ideal ligand. Chapters 5 and 6 summarize the comparative aspects and conclusions of the two phases of the study

## 1.2 Bone Physiology

A brief review of normal bone physiology is necessary to understand the effects of primary and metastatic cancer on bone. Bone consists of three cell types, osteoblasts, osteocytes, and osteoclasts. Precursors of osteoblasts and osteoclasts originate in the bone marrow<sup>23, 24</sup>.

Osteoblast precursors are multipotent mesenchymal stem cells that give rise to bone marrow stromal cells, chondrocytes, muscles, and adipocytes<sup>23, 24</sup>. The primary growth factors responsible for initiating osteoblastogenesis are bone morphogenetic proteins (BMPs). Specifically BMP-2 and -4 initiate the process of differentiation from mesenchymal precursors to osteoblastic lineage. Further differentiation can be initiated by transforming growth factor  $\beta$  (TGF- $\beta$ ), platelet-derived growth factor (PDGF), insulin derived growth factors (IGFs), and fibroblast growth factors (FGF)<sup>23, 24</sup>. Osteoblasts are responsible for the production of osteoid (protein matrix) which becomes mineralized. Mineralization is under control of the osteoblast and is thought to regulate local conditions of calcium and phosphate to promote hydroxyapatite formation<sup>23, 24</sup>. The major product produced by osteoblasts is collagen type-1, which undergoes further extracellular processing to form collagen fibrils. Other proteins excreted are osteocalcin, osteonectin, glycosaminoglycans, bone sialoprotein, fibronectin, vitronectin, and thrombospondin, which are incorporated into the bone matrix<sup>23, 24</sup>. Osteoblasts end up either being incorporated into bone and become osteocytes or form

lining cells, which are on the surface of quiescent bone<sup>23</sup>. On the surface, osteoblasts express high amounts of alkaline phosphatase which is anchored to the external surface of the plasma membrane<sup>23</sup>. Osteocytes, osteoblasts, bone marrow stromal cells and endothelial cells communicate with each other and form a functional syncytium<sup>23,24</sup>. The osteocyte is postulated to function as a mechanosensory cell, which is then responsible for the initiation of modelling or remodelling activity of bone<sup>23</sup>.

Precursors of osteoclasts arise from hematopoietic cells of monocytic / macrophage lineage<sup>23</sup>. Osteoclasts cannot bind directly to collagen layers covering bone and require lining cells to release collagenase and remove the protein matrix<sup>23</sup>. It is postulated that the lining cells give the homing signal to osteoclasts that initiates bone resorption<sup>23,24</sup>. It is not surprising that a large number of cytokines and colony stimulating factors involved in haematopoiesis also affect osteoclast development<sup>23,24</sup>. Stimulating cytokines include interleukins -1, -3, -6, and -11, tumour necrosis factor (TNF), granulocyte macrophage-colony stimulating factor (GM-CSF), and M-CSF and c-kit ligand<sup>23,24</sup>. Inhibiting cytokines include Interleukins -4, -10, -18 and interferon- $\gamma$ <sup>23,24</sup>. Recent work has identified the role of TNF (Tumour Necrosis Family) superfamily receptors called receptor activator of nuclear factor- $\kappa$ B ligand (RANKL)<sup>24</sup>. RANKL from osteoblasts interacts with the RANK receptor on osteoclast precursors, resulting in activation, differentiation and fusion of osteoclast precursors into osteoclasts, thus promoting bone resorption<sup>24</sup>. The effects of RANKL are controlled by a decoy glycoprotein receptor, called osteoprotegerin (OPG), which regulates bone resorption<sup>24</sup>. It is now well recognized that primary bone cancers in humans and dogs can express RANKL, which would aid tumour growth, by resorbing bone<sup>25,26</sup>.

Morphologically osteoclasts are recognized as multinucleated cells with abundant mitochondria, lysosomes, and free ribosomes. The most remarkable feature is the ruffled border that is surrounded by a clear zone. The clear zone delineates the area of attachment to bone and seals off a distinct area of bone. The area below the osteoclast allows for a microenvironment suitable for bone resorption<sup>23,24</sup>. The osteoclasts secrete hydrogen ions via an ATPase proton pump and proteolytic enzymes to accomplish resorptive process. Proteolytic enzymes such as matrix metalloproteinase and cathepsin K, B and L are secreted by the osteoclast<sup>23,24</sup>. Osteoclasts also contain high levels of a phosphohydrolase enzyme, tartrate-resistant acid phosphatase (TRAPase). TRAPase is used to detect osteoclasts in bone specimens. Systemic hormones such as parathyroid hormone (PTH) and vitamin D<sub>3</sub> and calcitonin exert a significant effect on osteoblasts and osteoclasts. PTH and vitamin D<sub>3</sub> are

potent initiators of osteoclast formation. Nevertheless, it has been found that PTH and its analogue, teriparatide (recombinant human PTH) when given at low doses inhibits apoptosis in osteoblasts and can be used clinically for osteoporosis<sup>27</sup>. Calcitonin inhibits osteoclast development and promotes osteoclast apoptosis. Other hormones that have significant metabolic effects on bone are the sex hormones, glucocorticoids, and thyroid hormone.

The physiological processes of bone formation and resorption involved in remodelling are considered a unique temporary structure known as a basic multicellular unit (BMU)<sup>23, 24</sup>. The BMU consist of a team of osteoclasts at one end and osteoblasts at the other end, a central vascular capillary, a nerve supply and associated connective tissue<sup>23, 24</sup>. Each BMU travels from a point of origin to the target and in some cases continues beyond or until termination. In cortical bone, BMU's excavate a tunnel that is replaced by remodelled bone. In the case of trabecular bone, a trench is excavated and replaced. In humans about 1 million BMU are active at any one moment<sup>23, 24</sup>.

### 1.3 Human Bone cancer

Significant interest and effort in this cancer has led to the identification of numerous etiologic agents<sup>28-31</sup>. Several chemical agents such as beryllium, viruses such as the murine C-Type RNA (FBJ) that was subsequently found to contain the src-oncogene, and radiation were shown to be potent inducers of osteosarcoma<sup>32</sup>. Paget's disease, electrical burn, or trauma all are thought to be other factors that may contribute to the pathogenesis. Osteosarcoma arising from prosthetic surgical sites has been documented in the dog<sup>33</sup>. More recently, human patients with hereditary diseases such as Rothmund-Thomson syndrome, Bloom syndrome, and Li-Fraumeni syndrome were found to have an increased risk of having osteosarcoma<sup>29, 31</sup>. During the past few years, molecular analysis brought a wealth of new information about numerous genes that are associated with osteosarcoma and its clinical disease progression. From early studies, it was evident that high-grade osteosarcomas have significant propensity to aneuploidy<sup>32, 34</sup>. Cytogenetic analysis has identified chromosomal abnormalities that can be as high as 69%<sup>34</sup>. The addition of comparative genomic hybridization (CGH) techniques, has given new insights into chromosomal abnormalities<sup>29, 34</sup>. DNA sequence number increase and loss have been identified, and may be important factors in the development of osteosarcomas<sup>34</sup>. An interesting observation has been gene amplification such as ring chromosomes that have been associated with human parosteal osteosarcomas<sup>29, 31, 34</sup>. Oncogene and tumour suppressor gene-mutations have been identified

in canine and human osteosarcoma and are summarized in Table 2-2 on page 86.

Abnormalities in osteosarcoma cells can be categorized into self-sufficiency in growth signals, insensitivity to growth inhibitory signals, evasion of apoptosis, limitless replicative potential, sustained angiogenesis, and tissue evasion and metastasis<sup>35</sup>.

### 1.3.1 Self-sufficiency in growth signals

Tumour cells have the ability to proliferate without the external stimuli needed by normal cells. Amplified expression of certain oncogenes can mimic normal signalling. Tumour cells are also able to synthesize growth factors e.g., PDGF or TGF- $\alpha$ . Over expression of the growth factor receptors can also lead to cell hyper responsiveness. Furthermore, growth signal autonomy can also originate from downstream cytoplasmic components such as Ras-Raf-MAPK cascade leading to deregulation of growth signalling in human tumours. Expression of human epidermal growth factor receptor -2 (erbB-2) has been correlated to worse event-free survival in human osteosarcoma, aggressive tumour growth, promotion of metastatic potential<sup>28-31, 35</sup>. C-fos expression, an AP-1 transcription factor responsible for mediating growth signals, correlates with the development of osteosarcoma in transgenic mice and poor response to chemotherapy and metastatic disease in man<sup>29, 35</sup>. Correlations were also found for BMP, specifically BMP type-II receptors and metastases<sup>35</sup>.

### 1.3.2 Insensitivity to growth inhibitory signals

Multiple antiproliferative signals act to keep cells quiescent. Simplistically they block progression by forcing the cell into the G<sub>0</sub> phase of the cell cycle or block proliferation directly. Nearly all antiproliferative signals converge onto the retinoblastoma protein (pRb), which blocks proliferation by altering transcription factors that govern progression from G1 into the S-phase of the cell cycle. Once the pRb-pathway is disrupted (through mutation or signalling molecule), the cell becomes insensitive to antigrowth factors. TGF- $\beta$  is one of the best-known inactivating molecules of the p-Rb-pathway. Disruption of the pRb-pathway can be associated with the potential of a poor survival outcome<sup>29, 35, 36</sup>.

### 1.3.3 Evasion of apoptosis

Tumour cells acquire the ability to escape from apoptosis by changes in the normal apoptotic pathways. These pathways can be loosely divided into sensors and effectors. The

most common sensor pathway change is associated with mutation of p53 tumour suppressor gene. Effector pathways include cell surface receptors that bind survival factors IGF-1, IGF-2, and death factors TNF- $\alpha$  binding TNF-R1. The apoptosis pathway can occur via either mitochondrial or intracellular pathways, but the ultimate effectors are caspases that execute the programmed cell death pathway. It has been found that p53 alone may not be responsible for disease progression and that change together with co-expression of MDR1 gene protein (p-glycoprotein) or MDM2 may be more important<sup>32, 35, 37</sup>.

#### 1.3.4 Limitless replicative potential

All normal cells contain an intrinsic cell-autonomous program (telomeres) that limits cell replication resulting in senescence. Telomeres at the end of chromosomes undergo progressive shortening until a critical threshold is reached which leaves the ends of the DNA unprotected. This results in cell death. Cancer cells have the ability to achieve immortality by up-regulation of reverse transcriptase telomerase that adds hex nucleotide repeats to the end of telomeric DNA. This allows for unlimited multiplication of the cell<sup>35</sup>.

#### 1.3.5 Sustained angiogenesis

Tumours cell have the ability to induce and sustain angiogenesis from vascular quiescence. Tumours have the ability to change the balance between inducers and inhibitors of angiogenesis. An inducer of angiogenesis, VEGF has been correlated with pulmonary metastases<sup>35</sup>.

#### 1.3.6 Tissue evasion and metastasis

Canine osteosarcoma metastasizes to the lung early on in the disease. The reason for metastasis to the lung is unknown, but recent research has identified soluble factors called chemo kinases that have the ability to attract circulating breast cancer cells to the lung. In osteosarcomas, anomalous cadherin expression is associated with metastasis as are the oncogenes c-Met and c-Fos<sup>35</sup>. Although the understanding of these processes in osteosarcoma is still incomplete, they could be potential therapeutic targets in the future<sup>35</sup>.

## 1.4 Human Osteosarcoma

Bone sarcomas represent only 0.2% of all new cancers diagnosed; approximately 2,500 new cases are diagnosed in the United States annually<sup>32,38</sup>. The incidence is approximately three cases per million people<sup>38</sup>. Osteosarcoma is the most common primary bone tumour in humans and accounts for 20% of all bone malignancies<sup>18,38</sup>. A biphasic incidence pattern is observed in human osteosarcoma, with the early peak occurring in adolescence as a primary cancer and in the elderly as a secondary tumour associated with Paget's disease and irradiated bone<sup>32,38</sup>. The human osteosarcoma resembles canine osteosarcoma in histological appearance and biological behaviour<sup>17,39,40</sup>. In humans, osteosarcoma can arise in any bone but commonly occurs in the long bones of the lower extremity<sup>32,38</sup>. Metastases often do occur in the lungs, which is also the primary metastatic site in canines. Human cases show a metastatic rate 10-20% on presentation<sup>32,38</sup>. Radiographic techniques used in the staging and diagnosis of human osteosarcoma include radiographs, CT, scintigraphy and MRI<sup>41</sup>. Diagnostic ultrasound has been used in human osteosarcoma; however, it offers no additional information when compared to conventional imaging<sup>42</sup>. For metastatic disease, radiographs and CT are the most commonly used formats, but problems still exist with detection of metastasis to the lungs<sup>43</sup>. Table 1-2 below lists the classification of human osteosarcoma.

**Table 1-2 Classification of human osteosarcoma**

<b>Types of Human Osteosarcoma<sup>34</sup></b>
Conventional (intramedullary) osteosarcoma
Osteoblastic
Chondroblastic
Fibroblastic
Epithelioid
Giant-cell rich
Small cell
Telangiectatic
Cortex-associated osteosarcoma
Parosteal
Dedifferentiated parosteal
Periosteal
High-grade surface
Intracortical
Low-grade (central) osteosarcoma
Osteoblastoma-like osteosarcoma
Disease-associated osteosarcoma
Osteosarcoma in Paget's disease

<b>Types of Human Osteosarcoma</b> <sup>34</sup>
Osteosarcoma in fibrous dysplasia
Osteosarcoma in Mazabraud disease
Multicentric osteosarcoma
Post-irradiation osteosarcoma
Osteosarcoma in the gnathic bones

The staging system for human osteosarcoma is similar to the canine system, with histological type playing little role as a predictor of outcome<sup>17</sup>. Tumour grade, extent, and presence of metastasis have a significant effect on therapy<sup>38</sup>. Axial skeletal osteosarcoma carries a worse prognosis than appendicular osteosarcoma<sup>38</sup>. Response to neoadjuvant chemotherapy is probably the most important prognostic factor in human OSA. Other factors that also play a role are; presence of metastasis at presentation, duration of symptoms > 6 months, high grade, size or tumour volume and location (axial worse)<sup>38</sup>. Trans-articular skip is also considered to have a negative impact on survival and to increase the risk for metastasis<sup>38</sup>. Generally, surgery preceded by neoadjuvant chemotherapy is considered standard of care in humans with osteosarcoma<sup>32, 44</sup>. The response to chemotherapy as measured by bone necrosis at the time of surgery is the single most important predictor of outcome in human osteosarcoma<sup>32, 38</sup>. Local control and metastasis are significantly affected by chemotherapy. Surgery often includes limb-sparing techniques but may include amputation in more advanced cases<sup>32, 38</sup>. Conventional radiotherapy is typically not used in human osteosarcoma cases except peri-surgically for cytoreductive purposes<sup>38</sup>. However, radiopharmaceuticals are used where the standard of care therapy, either is contraindicated or has failed. Bruland *et al.*,<sup>45</sup> reported, <sup>153</sup>Sm-EDTMP was used in a primary osteosarcoma of the vertebra with good transient response to treatment. Franzius *et al.*,<sup>9</sup> reported a case of a 21-year old woman with unresectable pelvic osteosarcoma and multiple pulmonary metastases were treated with high-dose of <sup>153</sup>Sm- EDTMP (150 MBq/kg). The patient also received external radiotherapy of the primary tumour site and chemotherapy followed by autologous peripheral blood stem cell reinfusion. Within 48 hours after <sup>153</sup>Sm-EDTMP application, the patient had complete pain relief. Their conclusions were that these cases warranted further evaluation of feasibility and efficacy of this multimodal therapy combination of high-activity <sup>153</sup>Sm-EDTMP therapy, external radiation, polychemotherapy, and stem cell support for unresectable osteosarcomas. In a later study of more patients (n=6) Franzius *et al.*,<sup>8</sup> once again confirmed the feasibility of high-dose <sup>153</sup>Sm-EDTMP therapy. Between the two studies, it was concluded that <sup>153</sup>Sm-EDTMP in combination with external radiation and polychemotherapy seemed the most

promising. A third study by Anderson *et al.*,<sup>10</sup> reported thirty patients treated with high dose <sup>153</sup>Sm-EDTMP (1100 MBq/kg), however patients required peripheral-blood progenitor cells (PBPC) or marrow transfusions due to the myeloablative effects of <sup>153</sup>Sm-EDTMP. Transient symptoms of hypocalcaemia were noted at 30mCi/kg. Cytopenias also occurred in all patients and were dose-related. Recovery of haematopoiesis was problematic in only two patients that received the 1100 MBq/kg dose and PBPC grafts with less than  $2 \times 10^6$  CD34<sup>+</sup>/kg after day 14. The receptor CD34 is an early marker of hemopoietic stem cells and their number in harvested peripheral mononuclear cells are predictive of successful bone marrow engraftment. A linear relationship was found between injected dose and estimates of radioisotope bound to bone surfaces and bone marrow radiation dose. Pain reduction and elimination of opiates was seen in all patients. Even more recently, Anderson<sup>11</sup> employed adjunct chemotherapy in combination with <sup>153</sup>Sm-EDTMP. Loeb *et al.*,<sup>13</sup> also reported on a dose escalation study using <sup>153</sup>Sm-EDTMP in which the maximally tolerated dose was 44.8 MBq/kg (1.21 mCi/kg). Apart from <sup>153</sup>Sm-EDTMP, a single case report by Sawyer *et al.*,<sup>46</sup> sought to demonstrate the usefulness of targeted radiotherapy using <sup>186</sup>Re-HEDP as a method for dose escalation in the treatment of osteosarcoma.

## 1.5 Human Metastatic Bone Cancer

There are no consistent figures for the incidence of metastatic bone cancer, but of the one million people that die from cancer every year in the United States approximately 70% are either from breast, lung or prostate cancer<sup>2, 47</sup>, of this amount, it is estimated that as many as 350,000 will have metastatic bone cancer<sup>2, 47</sup>. Since the thesis is primarily focused on the metastatic component of breast and prostate cancer only these aspects will be discussed. A difference between the two types is that metastatic breast cancer predominately produces an osteolytic type of lesion, whereas prostate cancer produces an osteoblastic lesion in bone<sup>2, 47</sup>. On the other hand, a single metastatic tumour can have both osteolytic and osteoblastic areas and they should not be considered mutually exclusive<sup>2, 47</sup>. The following molecular pathways are proposed for bone metastasis in human disease. The tumour cell does not directly cause osteolysis but rather by activation of normal osteoclasts. The metabolic pathways, which lead to activation, are mediated by the production of parathyroid related-peptide (PTHrP)/parathyroid hormone (PTH) and Interleukin (IL)-1, -6, -11. These factors stimulate production via the osteoblast and stromal cells of RANKL. PTHrP also has a negative effect on the production of osteoprotegerin (OPG), OPG functions as a decoy receptor that prevents



binding of RANKL to RANK. Signalling through RANK in the osteoclast activates transcription factors AP1 and NF- $\kappa$ B, leading to osteoclast progenitors differentiating into mature osteoclasts<sup>2, 47</sup>. Differentiation of osteoclast leads to an increase in bone resorption and has been discussed earlier under bone physiology.

The osteoblastic lesion in human prostate cancer when undergoing metastasis produces a predominantly osteoblastic lesion. Production of factors such as fibroblast growth factors (FGFs), bone morphogenetic proteins (BMPs), platelet derived growth factor (PDGF), and transforming growth factor- $\beta$  (TGF- $\beta$ ) by cancer cells stimulate osteoblast activity and bone formation<sup>2, 47</sup>. Proteases, such as prostate specific antigen (PSA) induced by urokinase (uPA), can activate latent TGF- $\beta$ , release insulin growth factors (IGFs) from inhibitory binding proteins (IGF BPS), and inhibit PTHrP that promotes bone formation<sup>2, 47</sup>.

Diagnostic imaging for metastatic disease includes radiographs, CT, scintigraphy, and MRI. In most cases, this represents end stage disease and commonly the therapy is directed at palliation of bone pain. Analgesic therapy includes drug therapy, teletherapy, and radiopharmaceuticals. Commonly drugs used in the control of bone pain consist of non-steroidal anti-inflammatory drugs (NSAIDs), narcotic analgesics, and bisphosphonates. Teletherapy plays an important role in the treatment of metastatic bone cancer; however, it is generally confined to single lesions or lesions confined to regional areas. As part of palliative therapy, radiopharmaceuticals have played a large role in treating pain associated with metastatic disease and has been the subject of numerous reviews<sup>48-50</sup>. It is typically used when there are multiple metastatic lesions in the skeleton, which makes local treatment impractical and systemic treatment an attractive alternative<sup>49</sup>. The treatment is precise since the radiopharmaceutical targets the area of increased mineral turnover associated with the metastatic lesion<sup>49</sup>. The metastases could occur either as an expansile osteoblastic lesion (e.g. metastatic prostate cancer) or where the preponderance of bone mineralization is high or an expansile osteolytic lesion (e.g. metastasis breast cancer) where the bone turnover occurs at the periphery of the lesion due to an interaction of osteoclastic and osteoblastic activity. This allows for selective uptake and prolonged radiopharmaceutical retention in these areas<sup>49</sup>. Radiopharmaceuticals reported to be effective in bone pain palliation and cancer therapy are: Strontium-89-chloride (<sup>89</sup>Sr), Phosphorus-32-orthophosphate (<sup>32</sup>P), Rhenium-186-hydroxy ethylidene diphosphonate (<sup>186</sup>Re-HEDP), Rhenium-188-hydroxy ethylidene diphosphonate (<sup>188</sup>Re-HEDP), Samarium-153-ethylenediamine tetramethylene phosphonic acid (<sup>153</sup>Sm-EDTMP), Tin-117m-diethylene triamine pentaacetic acid (<sup>117m</sup>Sn-DTPA)<sup>51</sup>. More recently,

Lutetium-177-ethylenediamine tetramethylene phosphonic acid ( $^{177}\text{Lu}$ -EDTMP) and Radium-223-chloride have also been reported as alternatives to Sm-153-EDTMP<sup>4, 52-54</sup>.

## 1.6 Radiopharmaceuticals

Radioisotopes offer a unique method of radiation delivery when combined with ligands. Ligands function as targeting agents, which allow selective targeting of cancers for radiation dose delivery by the radioisotope. Collectively, these agents are known as radiopharmaceuticals. Radiopharmaceuticals administered to people and animals disappear from the organ or body by biological clearance and physical decay of the radionuclide. A detailed review follows.

### 1.6.1 Radionuclides

#### 1.6.1.1 Radiation Physics

Radionuclides can decay by spontaneous fission:  $\alpha$  decay;  $\beta^-$  decay;  $\beta^+$  decay; electron capture and isomeric transition<sup>55</sup>. For the purposes of this thesis only  $\beta^-$  decay will be considered as many therapeutic radionuclides decay by this process. Radionuclides that are neutron rich (i.e. their nucleus has a higher N/Z ratio compared to the stable nucleus), decay by  $\beta^-$ -particle emission along with an *antineutrino* ( $\bar{\nu}$ ). The *antineutrino* has little mass and no charge, and is needed to conserve energy in the decay process<sup>55</sup>. In  $\beta^-$  decay a neutron decays into a proton ( $p$ ) and a  $\beta^-$  particle. The process can be described by the Equation 1-1.



Beta ( $\beta^-$ ) particles are emitted with a variable energy from zero to the decay energy. The decay energy (transition energy) is described by the difference in energy between the parent and daughter nuclides<sup>56</sup>, and thus not all  $\beta^-$  particles emitted are of the same energy during radionuclide decay.  $\beta^-$ -particle decay is often followed by  $\gamma$ -ray emission, which is particularly helpful in imaging the distribution of the radiopharmaceutical in the body. The  $\beta^-$ -particles are the therapeutic contribution from the radionuclide and interact with the surrounding medium by *bremsstrahlung*, ionization, and excitation<sup>56</sup>. *Bremsstrahlung* occurs as electrons (i.e.  $\beta^-$  particles) pass through matter and are decelerated in the Coulomb field of the atomic nuclei, these results in continuous x-rays emissions. This process depends on increasing electron energy and increasing atomic number of the medium. For example if the medium were tungsten, a 10-MeV electron would lose 50% of energy, whereas a 100-MeV electron loses upwards of 90% of its energy<sup>56</sup>. See Table 1-3 on page 44 for beta-emitting

radionuclides commonly used in nuclear medicine. The distance travelled by the  $\beta^-$  particle is important in choosing a radionuclide and is expressed as *path length* and *range*<sup>57</sup>. By definition, *path length* refers to the total distance travelled by the  $\beta^-$ -particle in coming to rest, whereas *range* is the linear distance travelled from emission to end of trajectory. Since the path travelled by a  $\beta^-$ -particle is torturous, *range* as a rough guide can be assumed to be half the *path length*. A more recent approach is to report the *range* as “Continuous Slowing Down Approximation” (CSDA)<sup>58</sup>. See Table 1-4 on page 45 and Table 1-5 on page 46 which report the data for commonly used radionuclides and the *range* as CSDA. Berger *et al.*,<sup>58</sup> define the CSDA range as a very close approximation to the average *path length* travelled by a charged particle as it slows down to rest. In this approximation, the rate of energy loss at every point along the track is assumed to be equal to the total stopping power and energy-loss fluctuations are neglected. The CSDA range is obtained by integrating the reciprocal of the total stopping power with respect to energy. This value takes into account the density of the material ( $\text{g}/\text{m}^3$ ) and range (m) the radiation particle is passing through and is expressed in  $\text{g}/\text{cm}^2$ . These data are sourced from the Physical Data Reference of the National Institute of Standards and Technology, Physics Laboratory web site<sup>58</sup>. The torturous path travelled is due to relative masses of the  $\beta^-$ -particle when compared to orbital electrons, which is not significantly different. Thus significant collision energy loss (ionization, excitation *bremsstrahlung*), with recoil velocity change occurs when  $\beta^-$ -particles interact with orbital electrons<sup>57</sup>. This change, when compared to  $\alpha$ -particles of equal energy,  $\beta^-$ -particle have a much higher velocity and thus less time to interact with orbital electrons<sup>57</sup>. Therefore,  $\beta^-$ -particles have a lower specific ionization potential compared to  $\alpha$ -particles and have a good chance of passing through a cell without any interaction<sup>57</sup>. Table 1-3 on page 44 summarizes the physical properties of radionuclides that have been used in targeted radiotherapy for metastatic bone cancer and osteosarcoma.

**Table 1-3 Physical Characteristics of radionuclides used in radiotherapy**

Isotope	Physical Half-life (Tp) <sup>59</sup>	Max Pharmacokinetic Energy (MeV)	Gamma Emission Energy (keV)	% gamma emission
Tin(Sn)-117m	14.00±0.05 days	Auger conversion electrons (CE)* 0.13, 0.16	158	87
Samarium-153	46.29±0.0014 hours	0.80**	103	28
Rhenium-186	89.25±0.069 hours	1.07**	137	9
Strontium-89	50.5 days	1.46**	None	None
Phosphorous-32	14.26±0.003 days	1.70**	None	None
Holmium-166	26.79±0.023 hours	1.80**	81	7
Rhenium-188	17.00±0.022 hours	2.11**	155	10

Legend: The table summarizes the physical properties of radionuclides. \*- It should be noted that max energy emission of Tin(Sn)-117m is by Auger conversion electrons (CE), not Beta emission. Internal conversion is a radioactive decay process where an excited nucleus interacts electromagnetically with an electron in one of the lower atomic orbitals, causing a high-energy electron to be emitted from the radioactive atom, but not from a nucleon in the nucleus. \*\*- Beta Emission Energy

**Table 1-4 Stopping powers and range tables for radionuclides in cortical bone (International Commission on Radiological Protection [ICRP])**

Radionuclide <sup>58</sup>	Max Pharmacokinetic Energy MeV	Total Stopping Power MeV cm <sup>2</sup> /g	CSDA Range* g/cm <sup>2</sup>	Cortical Bone Density g/cm <sup>3</sup>	Range mm
Tin(Sn)-117m	0.13 (CE)	3.14	0.02	1.85	0.13
Samarium-153	0.80**	1.71	0.37	1.85	1.98
Rhenium-186	1.07**	1.67	0.49	1.85	2.63
Strontium-89	1.46**	1.66	0.79	1.85	4.25
Phosphorous-32	1.70**	1.67	0.94	1.85	4.00
Holmium-166	1.80**	1.67	0.94	1.85	5.06
Rhenium-188	2.11**	1.68	1.09	1.85	5.86

Legend: \*CSDA (Continuous Slowing Down Approximation) Range. CSDA range as a very close approximation to the average path length travelled by a charged particle as it slows down to rest. . The CSDA range is obtained by integrating the reciprocal of the total stopping power with respect to energy. This value takes into account the density of the material (g/m<sup>3</sup>) and range (m) the radiation particle is passing through and is expressed in g/cm<sup>2</sup>. From this table it is evident that Tin(Sn)-117m which decays by CE (conversion electrons) has a significant shorter range (0.13 mm) in cortical bone when compared to the beta emitters\*\*. The implication is then that in order for Tin (Sn)-117m to be effective therapeutically, it should be transported by the ligand into close proximity to the target e.g. the nucleus. Nevertheless, since the total stopping power of Tin (Sn)-117m is greater than that of the beta emitters, it could translate into an improved therapeutic effect if the ligand were successful.

**Table 1-5 Stopping powers and range tables for radionuclides in soft-tissue (ICRP)**

Radionuclide <sup>58</sup>	Pharmacokinetic Energy MeV	Total Stopping Power MeV cm <sup>2</sup> /g	CSDA Range* g/cm <sup>2</sup>	Soft-tissue Density g/cm <sup>3</sup>	Range mm
Tin(Sn)-117m	0.13 (CE)	3.59	0.02	1.00	0.21
Samarium-153	0.80**	1.89	0.33	1.00	3.31
Rhenium-186	1.07**	1.85	0.44	1.00	4.39
Strontium-89	1.46**	1.83	0.71	1.00	7.11
Phosphorous-32	1.70**	1.83	0.84	1.00	7.60
Holmium-166	1.80**	1.83	0.85	1.00	8.48
Rhenium-188	2.11**	1.84	0.98	1.00	9.84

Legend: \*CSDA (Continuous Slowing Down Approximation) Range. CE – Conversion Electrons. \*\*- Beta Emission Energy. The table summarizes the stopping powers and range tables for radionuclides in soft-tissue. The distance travelled by the particle in soft tissue is significantly longer (mm) when compared to bone. This is due in large part to the reduced density of soft-tissue since the stopping power is only marginally increased in soft tissue compared to cortical bone.

### 1.6.1.2 Radionuclide selection for targeted radiotherapy

Criteria governing the selection of the radionuclide for targeted radiotherapy to bone are particle range, physical half-life, gamma yield, chemistry, and the type of ligand. To be effective, the isotopes must fulfil certain requirements, these are <sup>7</sup>:

- minimum chemical toxicity
- a physical half-life of medium duration (approximately 2 to 8days) so as to provide optimum radio-biologic effect
- when combined to a ligand the radiopharmaceutical must have a high affinity for diseased bone in relation to normal bone
- minimal deposition outside the skeleton and within bone marrow
- the mode of radioactive decay should be principally beta-particle emission so that the deposition of energy is concentrated in the immediate vicinity of a lesion.

### 1.6.2 Radiopharmaceutical Ligands

By definition, a ligand is a molecule bound to a radionuclide by various bonds and collectively called a radiopharmaceutical. The chemical bonds involved are variable, but in the case of Lanthanides, it is by covalent bonding <sup>55</sup>. Ligands can be complex or simple molecules depending on the desired target in the body. The ligand determines how the radiopharmaceutical is going to behave in the body and is responsible for the pharmacokinetics and pharmacodynamics of the radiopharmaceutical. This in turn determines the biological half-life of the radiopharmaceutical. For the purpose of this study, only bone-seeking ligands from the largest group will be discussed as these belong primarily to the bisphosphonates group. In addition, the novel ligand polyethyleneiminomethyl phosphonic acid (PEI-MP) used in this research will be discussed.

#### 1.6.2.1 General Overview of Bisphosphonates and Cancer

Bisphosphonates form a class of drugs, which as a family are characterized pharmacologically by their ability to inhibit bone resorption and are pharmacokinetically similar in absorption,

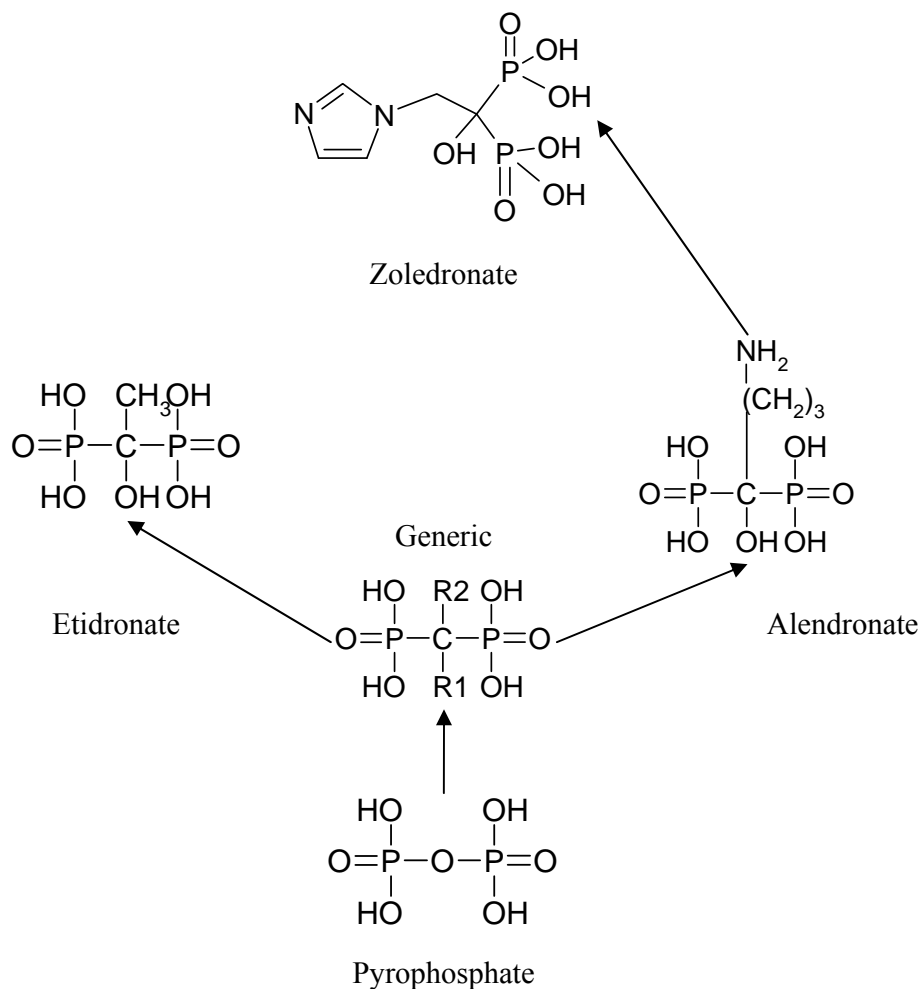
distribution, and elimination<sup>60-62</sup>. Bisphosphonates are used as therapeutic agents for osteoporosis and bone pain associated with metastatic disease, Paget's disease, hypercalcaemia of malignancy and in diagnostic nuclear medicine and targeted radiotherapy<sup>51, 51, 63, 64</sup>. Due to the increased use of bisphosphonates in cancer, guidelines for various solid tumours have been promulgated<sup>65, 66</sup>.

#### 1.6.2.1.1 Bisphosphonate Chemistry

Bisphosphonates have a structure similar to pyrophosphate (PPi), but with a carbon atom (geminal) substitution for the central oxygen atom<sup>67</sup>. Two additional covalent bonds (side chains) to the geminal carbon can be formed and are referred to as R<sub>1</sub> and R<sub>2</sub><sup>68</sup>. The ability of these side chains to bind carbon, oxygen, halogen, sulfur, or nitrogen atoms gives rise to numerous possibilities for the development of unique molecules<sup>68</sup>. As with PPi, bisphosphonates form a three-dimensional structure which is capable of binding divalent metal ions such as Ca<sup>2+</sup>, Mg<sup>2+</sup>, and Fe<sup>2+</sup> in a bi- / tri-dentate manner. Binding occurs by coordination of oxygen from the phosphonate group with the divalent cation. Affinity for Ca<sup>2+</sup> can be increased by manipulating the R<sub>1</sub> side chain such as the addition of a hydroxyl group, common to most bisphosphonates. The addition of a hydroxyl or primary amine group on the R<sub>2</sub> side chain allows for the formation of a tridentate conformation with more effective binding to hydroxyapatite<sup>68</sup>. See Figure 1-1 below. The aliphatic carbon chain (R<sub>2</sub>) length appears to be an important factor affecting the anti-resorptive capability of bisphosphonates<sup>63</sup>. For example, alendronate has 100-1000 times greater antiresorptive capacity than does etidronate<sup>69</sup>. Further manipulation of this primary R<sub>2</sub> chain amine to form a tertiary amine increases its potency<sup>70</sup>. The most potent bisphosphonates to date appear to be those that contain a tertiary amine in a ring structure e.g. zoledronate which has >10,000 times the potency of etidronate<sup>70</sup>. See Table 1-6 below for the chemical structure of bisphosphonates used in clinical medicine.



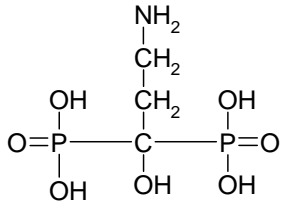
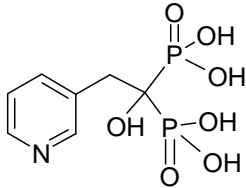
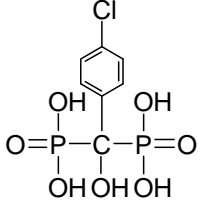
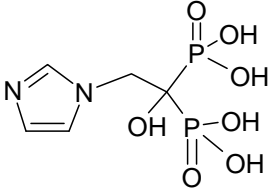
Figure 1-1 The development of bisphosphonates from pyrophosphate



Legend: The development of bisphosphonates from pyrophosphate by the substitution of the central oxygen by a carbon (geminal) atom is shown. The two main classes of bisphosphonates are represented by alendronate (amino-bisphosphonates) and etidronate (non amino-bisphosphonates). The presence of a primary amine group on the R<sub>2</sub> side chain offers significant improvement in therapeutic activity. Zoledronate is an example of a 3<sup>rd</sup> generation amino-bisphosphonate with a tertiary amine in a ring structure on the R<sub>2</sub> side chain. The addition of an OH group on the R<sub>1</sub> side chain enhances binding to hydroxyapatite<sup>61</sup>.

**Table 1-6 Bisphosphonates their uses, molecular weight (MW) and chemical structure**

Bisphosphonates	Uses	MW (kDa)	Chemical Structure
Alendronate	Medical therapy	0.221	$  \begin{array}{c}  \text{NH}_2 \\    \\  (\text{CH}_2)_3 \\    \\  \text{HO} \quad \text{OH} \\    \quad   \\  \text{O}=\text{P}-\text{C}-\text{P}=\text{O} \\    \quad   \quad   \\  \text{HO} \quad \text{OH} \quad \text{OH}  \end{array}  $
Clodronate	Medical therapy	0.240	$  \begin{array}{c}  \text{OH} \quad \text{Cl} \quad \text{OH} \\    \quad   \quad   \\  \text{O}=\text{P}-\text{C}-\text{P}=\text{O} \\    \quad   \quad   \\  \text{OH} \quad \text{Cl} \quad \text{OH}  \end{array}  $
Etidronate (HEDP)	Medical therapy Radiopharmaceuticals	0.202	$  \begin{array}{c}  \text{HO} \quad \text{CH}_3 \quad \text{OH} \\    \quad   \quad   \\  \text{O}=\text{P}-\text{C}-\text{P}=\text{O} \\    \quad   \quad   \\  \text{HO} \quad \text{OH} \quad \text{OH}  \end{array}  $
Ibandronate	Medical therapy	0.319	
Lexidronate (EDTMP)	Radiopharmaceuticals	0.428	
Medronate (MDP)	Diagnostic Nuclear Medicine	0.172	$  \begin{array}{c}  \text{OH} \quad \text{OH} \\    \quad   \\  \text{O}=\text{P}-\text{CH}_2-\text{P}=\text{O} \\    \quad   \\  \text{OH} \quad \text{OH}  \end{array}  $

Bisphosphonates	Uses	MW (kDa)	Chemical Structure
Pamidronate (APD)	Medical therapy Radiopharmaceuticals (rarely used)	0.231	
Risedronate	Medical therapy	0.283	
Tiludronate	Medical therapy	0.302	
Zoledronate	Medical therapy	0.272	

Legend: The bisphosphonates, HEDP, EDTMP and MDP are used as ligands in radiopharmaceuticals. EDTMP is the only amino bisphosphonate (N-nitrogen containing) in the group and is thus expected to have greater binding to hydroxyapatite when compared to HEDP or MDP.

### 1.6.2.2 Pharmacodynamics of Bisphosphonates

The principal target of bisphosphonates is bone and research has shown that the main effect of bisphosphonates is to inhibit bone resorption<sup>60, 61</sup>. It is thought that bisphosphonates are incorporated into the crystalline structure by way of exposed hydroxyapatite (lacunae). Reviews by Russell *et al* in 2008 and Ebetino *et al* in 2011 give detailed overview of the chemical interaction of bisphosphonates and bone hydroxyapatite<sup>62, 71</sup>. Briefly, the chemical reaction between bisphosphonates and hydroxyapatite is based on multiple effects, these include; the inhibition of de novo precipitation of calcium phosphate from solution, retard the transformation of amorphous to crystalline hydroxyapatite, and inhibit the aggregation and dissolution of hydroxyapatite crystals<sup>62, 71</sup>. This ability to bind strongly to bone mineral gives bisphosphonates (albeit, variable between drugs) their unique property of selective uptake by metabolic active bone due the exposure of hydroxyapatite crystals during bone resorption but also during bone mineralization<sup>62, 71</sup>.

Bisphosphonates are released during resorption by the osteoclast activity resulting in inhibition of osteoclastic activity<sup>60, 61</sup>. Experimentally, it has been shown that bisphosphonates disrupt intracellular metabolism that can lead to apoptosis<sup>60, 72</sup>. Since some bisphosphonates (etidronate, clodronate) resemble pyrophosphate (PPi), they can be incorporated into non-hydrolyzable analogues of ATP, therefore denying the osteoclast energy<sup>60, 72</sup>. It is likely that accumulations of these analogues would inhibit osteoclast function and cause apoptosis. The more potent nitrogen containing bisphosphonates (alendronate, pamidronate etc.) are not metabolized but act as transition state analogues of isoprenoid diphosphates, thereby inhibiting FPP synthase and perhaps additional enzymes of the mevalonate pathway<sup>60, 72</sup>. Inhibition of this pathway prevents the biosynthesis of isoprenoid compounds that are essential for the posttranslational farnesylation and geranylgeranylation of small GTPase<sup>72</sup>. GTPase are important signalling proteins that regulate cell processes such as, cell morphology, integrin signalling, membrane ruffling, endosome trafficking, and apoptosis<sup>60, 72</sup>. The process of apoptosis in osteoclast can be recognized by early detachment from bone with the loss of ruffled borders (area of intense proton-ATPase activity) and degradation of Golgi apparatus followed by nuclear pyknosis associated with condensation, margination of chromatin, and formation of

apoptotic bodies<sup>73</sup>. Enlargement and fusion of the nuclear envelope and appearance of ladder structures are characteristic of osteoclastic apoptosis. The majority are eliminated by macrophage phagocytosis. In some cases osteoclasts migrate into blood vessels with subsequent transport to other organs, most commonly the spleen<sup>73</sup>. It is also postulated that bisphosphonates may also have effect via osteoblasts<sup>60, 61</sup>.

Although bisphosphonates have similar physicochemical properties, their anti-resorptive capabilities differ significantly. Alendronate is approximately 700–fold more potent than etidronate in vitro, and this effect is retained in vivo. The aliphatic carbon chain length appears to be an important factor affecting anti-resorptive capability<sup>60, 61</sup>.

### 1.6.2.3 Pharmacokinetics of Bisphosphonates

Drug binding to plasma protein is a function of its lipophilicity, ionic binding, and electrostatic forces. Although bisphosphonates have a low lipophilicity they are at physiological pH (7.4) completely ionized and therefore expected to bind to plasma protein<sup>60, 61</sup>. They are indeed highly protein bound however; this binding is concentration, pH, and calcium-dependent. A concentration increase in the bisphosphonates in the blood leads to a corresponding increase in uncomplexed drug<sup>60, 61</sup>. There is also a species and drug variation in plasma protein binding with dogs and humans having a lower protein binding compared to rats, and clodronate is less bound than alendronate<sup>60, 61</sup>. Research has shown that hypocalcaemia states lead to lower bisphosphonate binding to albumin. Unexpectedly, the inverse situation (hypercalcaemia) has been shown experimentally not to lead to increase in binding. A change in pH from 6.6 to 8.6 shows a corresponding increase in binding from 50% to 98% respectively for alendronate<sup>60, 61</sup>. Researchers are unsure if bisphosphonates bind directly to albumin or alternatively to calcium, which in turn binds to albumin. It has also been shown in humans and dogs that alendronate is more bound than expected to albumin indicating other endogenous displacer or displacers<sup>60, 61</sup>.

To describe the pharmacokinetics of tissue distribution, a three-compartment model is the most appropriate. This model consists of the blood pool, bone or calcified tissue, and non-calcified tissue. With administration, there is a rapid distribution of bisphosphonates to noncalcified tissues. This distribution is transient and is cleared rapidly from this tissue and transferred to bone or excreted by the kidneys. Bone shows an increase in uptake over 1 hour indicating movement of bisphosphonates from noncalcified tissue to bone. Non-calcified tissue

can be made to retain bisphosphonates if high dosages are given by rapid injection. The reason is thought to be due to binding of the bisphosphonates at high concentrations with metals (calcium, iron, and magnesium) creating large complexes which are phagocytised by the liver and spleen<sup>60, 61</sup>. In mice, this has been shown to occur, as would be expected, with intravenous injection of clodronate not with intraperitoneal or subcutaneous injection. While this is experimentally important, it is unlikely that bisphosphonates will ever be given at high enough dosages clinically for this to occur.

Bone cannot be regarded as a single compartment but rather consisting of trabecular bone and cortical or compact bone. Since it is known that the trabecular bone is metabolically the most active and therefore receives more blood, correspondingly bisphosphonates show a higher accumulation in these areas. Trabecular bone would also have a proportionally larger amount of exposed hydroxyapatite crystals due to bone resorption mediated by osteoclastic activity, as would areas showing increased metabolic activity such as injuries or cancerous bone. There is also a saturable uptake in bone for bisphosphonates with increasing dose, which has been shown experimentally with alendronate, and other bisphosphonates<sup>63, 74</sup>. However if the dose is MW-fractionated and given over time, this effect seems to be attenuated<sup>60, 61</sup>. There is also a gender and age difference in uptake. Logically, younger animals have higher metabolic bone activity and therefore higher bisphosphonate uptake while gender differences of lower uptake were only observed in juvenile female rats compared to juvenile male rats<sup>60, 61</sup>, and no differences were found between adult rats. Where two bisphosphonates were administered together at high enough dosages, competitive binding to exposed hydroxyapatite crystals occurs<sup>60, 61</sup>.

Very little or no metabolism of bisphosphonates occurs within the body of all species and they are thus regarded as having low toxicity<sup>60, 61</sup>.

Elimination of bisphosphonates from bone occurs over a prolonged period as the drug is incorporated into bone and is only released when the bone undergoes resorption<sup>60, 61</sup>. The biological half-life is therefore dependent on the rate of bone turn over in the individual. Alendronate's half-life for has been estimated to be 300 days in dogs and 10 years in humans<sup>60, 61</sup>. In the rat, this elimination from bone follows a biphasic pattern, which is thought to be due to different turnover in different parts of the bone<sup>60, 61</sup>.

Elimination or excretion of bisphosphonates from the body is primarily through the kidneys. Research indicates the process is a concentration-dependent saturable active transport

mechanism<sup>60, 61</sup>. This process of excretion is not via the typical anion or cation renal transport systems since inhibitors of these systems, probenecid and cimetidine respectively, when given at high doses in rats, do not inhibit renal excretion of bisphosphonates<sup>60, 61</sup>. However, bisphosphonates do compete with each other this transport mechanism as research has shown that etidronate inhibits alendronate excretion<sup>60, 61</sup>.

To study the pharmacokinetics of bisphosphonates in the body they have been labelled to <sup>99m</sup>Tc or <sup>14</sup>C (Carbon-14). It is interesting to note that the radionuclide does affect organ distribution e.g., radiolabelled <sup>14</sup>C-pamidronate had a twofold greater uptake in bone than <sup>99m</sup>Tc labelled pamidronate<sup>60, 61</sup>.

#### 1.6.2.4 Side Effects of Bisphosphonates

Reports suggest that most bisphosphonates are relatively nontoxic because they are inert substances that do not undergo significant metabolism<sup>63, 75</sup>. However, adverse effects have been reported including, bone and renal toxicity, electrolyte abnormalities, and acute-phase reactions<sup>60, 65</sup>. As expected, bone, being the target organ of bisphosphonates, can be adversely affected by high doses of these drugs<sup>60, 65, 75</sup>. One potential adverse effect is referred to as “frozen bone” which occurs when bone remodelling and repair are inhibited to such an extent that the bone is weakened and fractures occur<sup>60, 65, 75, 76</sup>. The syndrome has been reported in the dog and occurs more frequently when using moderately high doses of non-amino-bisphosphonates such as etidronate<sup>60, 65, 77</sup>. Non amino-bisphosphonates are implicated due to their narrow therapeutic index, which is the difference in dose between inhibiting bone resorption and inhibition of normal bone repair and mineralization<sup>78</sup>. Newer amino-bisphosphonates are safer, as they inhibit osteoclastic activity at lower doses and have a wider anti-resorption to anti-mineralization ratio<sup>78</sup>.

Renal toxicity has also been reported to occur with bisphosphonate use<sup>75, 79-82</sup>. The apparent factors that affect renal toxicity include infusion rate and type of bisphosphonate. One report<sup>75</sup> indicated that a rapidly infused bisphosphonate could lead to acute renal failure and this could be prevented by slowing the infusion rate to less than 200 mg/hr. However, other clinical studies have not demonstrated renal toxicity in people receiving intravenous pamidronate infusions<sup>81, 83</sup> and no reports of renal toxicity have been found for dogs in the experimental or

clinical literature<sup>78</sup>. In experimental dogs poisoned with vitamin D3 and treated with pamidronate IV infusions for hypercalcaemia, no renal toxicity was observed<sup>84, 85</sup>. In a rat model, zoledronate was shown to be less nephrotoxic than pamidronate<sup>79</sup>. While not reported as occurring in experimental dogs, the following human side effects should be mentioned. These include inflammatory or acute-phase response<sup>75</sup>, various ophthalmic syndromes such as scleritis<sup>81</sup>, transient bone pain<sup>81</sup>, and hypocalcemia<sup>75</sup>.

Side effects associated with bisphosphonates generally occur for the following reasons: per os formulations such as alendronate are irritating to the oesophagus if dosed incorrectly; etidronate prevents bone resorption and mineralization, which can lead to pathological fractures and bone weakening<sup>77</sup>.

#### 1.6.2.5 Anti-Tumour Effects of Bisphosphonates

Most research into the antitumour effect of bisphosphonates has focused on metastatic bone disease due to prostate and breast cancer<sup>86</sup>. Nevertheless, some research has been done into the effects of bisphosphonates on osteosarcoma<sup>61, 87-95</sup>. Early results seem to show possible cytotoxic effects on osteosarcoma cell lines<sup>87, 96, 97</sup>.

It is well accepted that tumour cells in bone, especially breast cancer and myeloma cells, can stimulate osteoclast formation and activity leading to the release of growth factors or cytokines, which will further stimulate cancer cells' growth, and their secretion of osteolytic factors<sup>86, 96</sup>. Bisphosphonates are now currently the standard therapy for cancer hypercalcaemia in humans, for which an intravenous dose of 90 mg of pamidronate or 1500 mg of clodronate is recommended; the former compound is more potent and has a longer lasting effect<sup>72, 86</sup>. Repeated pamidronate infusions exert clinically relevant analgesic effects in more than half of patients with metastatic bone pain<sup>60, 65, 86</sup>. Regular pamidronate infusions can also achieve a partial objective response according to conventional Union for International Cancer Control (UICC) criteria and they can almost double the objective response rate to chemotherapy<sup>60, 65, 86</sup>. Lifelong administration of oral clodronate to patients with breast cancer metastatic to bone reduces the frequency of morbid skeletal events by more than one-fourth<sup>86</sup>. Two double-blind randomized placebo-controlled trials comparing monthly 90 mg pamidronate infusions to placebo infusions for 1-2 years in addition to hormone or chemotherapy in patients with at least one lytic bone metastasis have shown that the mean skeletal morbidity rate could be reduced by



30 to 40%<sup>86</sup>. The results obtained with intravenous bisphosphonates are generally viewed as better than those obtained with oral clodronate<sup>86</sup>. However, preference can be given to the oral route when bisphosphonates are started early in the process of metastatic bone disease in a patient receiving hormone therapy<sup>86</sup>. Because bisphosphonates are providing supportive care, reducing the rate of skeletal morbidity but evidently not abolishing it, the criteria for stopping their administration have to be different from those used for classic antineoplastic drugs, and they should not be stopped when metastatic bone disease is progressing<sup>86</sup>. Good results have been achieved in patients with multiple myeloma in people, and the consensus is that bisphosphonates should be started as soon as the diagnosis of lytic disease is made in myeloma patients. Clodronate and pamidronate have shown efficacy in reducing pain, hypercalcaemia episodes and slowing progression of osteolytic bone lesions<sup>96, 98</sup>.

Newer bisphosphonates have shown similar results to those achieved with pamidronate using monthly 6 mg infusions of ibandronate in patients with breast cancer metastatic to bone<sup>86</sup>. The tolerance of ibandronate could be better when compared to earlier bisphosphonates, and the drug has the potential to be administered as a 15 to 30 minute infusion. Zoledronate can also be administered safely as a 15 minute 4 mg infusion, and large-scale phase III trials have been completed<sup>86</sup>. These newer bisphosphonates will simplify the current therapeutic schemes and improve the cost-effectiveness ratio; they also have the potential to improve the therapeutic efficacy, at least in patients with an aggressive osteolytic disease or when given as adjuvant therapy<sup>60, 99</sup>. The results from a big, randomized phase 3 study comparing zoledronic acid and pamidronate in breast cancer or multiple myeloma patients with osteolytic lesions showed that the incidence of skeletal-related events (SREs), time to first SRE, and risk of developing a skeletal related events were similar between treatment groups<sup>99</sup>. In patients with solid tumours (excluding breast or prostate cancer) metastatic to the bone, only zoledronic acid demonstrated clinical efficacy<sup>99</sup>. In a randomised clinical trial by Saad *et al.*,<sup>100</sup> patients with hormone-refractory prostate cancer and bone metastases (n=643) received intravenously administered zoledronic acid (4 mg, 15 min infusion) or placebo (every 3 to 4 weeks). At 24 months, zoledronic acid significantly decreased the risk of developing skeletal complications by 36% compared with placebo. In contrast, Small *et al.*,<sup>101</sup> found in a previous prostate cancer study (n=236) that pamidronate was no more effective than placebo in reducing bone pain or skeletal related events after 6 months. However, the end point of the study was bone pain rather than

skeletal related events together with the advanced state of disease reduce the validity of cross-trial comparisons.

While bone turnover marker levels, such as N-telopeptide of type I collagen, have been shown to correlate with clinical response, additional studies are needed to confirm their ability to forecast response to bisphosphonate therapy<sup>99</sup>.

### 1.6.3 Clinically Relevant Bisphosphonate Ligands

#### 1.6.3.1 Clinical application of <sup>153</sup>Sm-EDTMP

The first report of <sup>153</sup>Sm-EDTMP used in canine bone tumours (n=40) was by Latimer *et al.*,<sup>7, 15</sup>. Dogs were randomized to receive either a single dose of 37 MBq/kg or two doses a week apart. No significant differences were found between the two groups, however early tumours and metastatic lesions appeared to show some response.

In a report by Moe *et al.*,<sup>102</sup>, <sup>153</sup>Sm-EDTMP was used to treat an osteosarcoma of the maxilla together with surgical debulking and the results were considered good. Straw *et al.*,<sup>103</sup> reported the use of <sup>153</sup>Sm-EDTMP in two dogs with mandibular osteosarcoma, one dog was lost to follow-up at 41 months and the other dog died of renal failure at 6.9 months with recurrence of the tumour at the primary local site. In 1998, Milner *et al.*,<sup>22</sup> reported on nine dogs with primary bone tumours that were treated with <sup>153</sup>Sm-EDTMP. All were tumours of the appendicular skeleton. The dogs were given a single injection of 37 MBq/kg (1 mCi/kg) of <sup>153</sup>Sm-EDTMP intravenously. Two dogs showed no response to treatment with an increase in bone pain, and were euthanized within 1 month. In one dog, a tumour of the scapula underwent complete involution and the dog was considered free of disease at 20 months post <sup>153</sup>Sm-EDTMP treatment. In the remaining dogs, all the primary tumours progressed over time and all the dogs had to be euthanized. Pain control in this cohort of dogs was not evident, except in the one dog that responded completely to treatment<sup>22</sup>. In a report by Aas *et al.*,<sup>104</sup> fifteen dogs were treated with <sup>153</sup>Sm-EDTMP. Dogs were given between one and four doses of <sup>153</sup>Sm-EDTMP at 36-57 MBq/kg. Their conclusions were that a favourable high tumour dose was achieved in the tumour compared to surrounding tissue, and in some cases, tumour growth was delayed. No serious side effects were observed. A report comparing <sup>153</sup>Sm-EDTMP to Sr-89 distribution in canine osteosarcoma bone found a more uniform distribution for Sr-89 in the cancer and a lower radiation dose to bone marrow<sup>105</sup>. Barnard *et al.*,<sup>106</sup> evaluated survival times and palliative

effects in 35 dogs given one to four doses of  $^{153}\text{Sm}$ -EDTMP at 37 MBq/kg. The overall median survival time was 100 days, which was not significantly different to dogs that had amputations without chemotherapy. They concluded that  $^{153}\text{Sm}$ -EDTMP might be useful in the palliation of pain in dogs with osteosarcoma.

In humans, Bruland *et al.*,<sup>45</sup> reported  $^{153}\text{Sm}$ -EDTMP was used in a primary osteosarcoma of the vertebra with good transient response to treatment. Franzius *et al.*,<sup>9</sup> reported a case of a 21-year old woman with unresectable pelvic osteosarcoma and multiple pulmonary metastases who was treated with high-dose of  $^{153}\text{Sm}$ -EDTMP (150 MBq/kg). The patient also received external radiotherapy of the primary tumour site and chemotherapy followed by autologous peripheral blood stem cell reinfusion. Within 48 hours after  $^{153}\text{Sm}$ -EDTMP application, the patient had complete pain relief. Their conclusions showed these cases warranted further evaluation of feasibility and efficacy of this multimodal therapy combination of high-activity  $^{153}\text{Sm}$ -EDTMP therapy, external radiation, polychemotherapy, and stem cell support for unresectable osteosarcomas. A later study of more patients (n=6) Franzius *et al.*,<sup>8</sup> once again confirmed the feasibility of high-dose  $^{153}\text{Sm}$ -EDTMP therapy. In this case, however, it was found that combination with external radiation and polychemotherapy seemed the most promising. In a 2002 study, Anderson *et al.*,<sup>10</sup> reported thirty patients were treated with high dose  $^{153}\text{Sm}$ -EDTMP (1100 MBq/kg). Patients required peripheral-blood progenitor cells (PBPC) or marrow transfusions due to the myeloablative effects of  $^{153}\text{Sm}$ -EDTMP. Transient symptoms of hypocalcaemia were noted at 30mCi/kg. A linear relationship was found between injected dose and estimates of radioisotope bound to bone surfaces and bone marrow radiation dose. Cytopenias also occurred in all patients and were dose-related. Recovery of haematopoiesis was problematic in only two patients that received the 1100 MBq/kg dose and PBPC grafts with less than  $2 \times 10^6$  CD34(+)/kg on day 14. Pain reduction and elimination of opiates were seen in all patients. More recently, Anderson *et al.*,<sup>11</sup> combined  $^{153}\text{Sm}$ -EDTMP with a radio sensitizer, gemcitabine. Fourteen patients were treated with 1110 MBq/kg  $^{153}\text{Sm}$ -EDTMP followed by gemcitabine one day after the  $^{153}\text{Sm}$ -EDTMP infusion. All patients received autologous stem cell reinfusion 2 weeks after  $^{153}\text{Sm}$ -EDTMP for expected grade 4 hematopoietic toxicity. Hemopoietic toxicity following a single infusion of gemcitabine (1,500 mg/m<sup>2</sup>) was minimal (pancytopenia), however, toxicity from a daily gemcitabine regimen (250 mg/m<sup>2</sup>/d x 4-5 days) was excessive (Grade 3 mucositis) in one of two patients. At the 6- to 8-week follow-up, there

were six partial remissions, two mixed responses, and six patients with progressive disease. In the 12 patients followed for greater than 1 year, there were no durable responses. They concluded that  $^{153}\text{Sm}$ -EDTMP combined with gemcitabine had a moderate palliative action in this poor-risk population, but additional measures of local and systemic control are required for durable control of relapsed osteosarcoma with osteoblastic lesions. Interestingly Lam *et al.*,<sup>107, 108</sup> investigated the combination of zoledronate and  $^{153}\text{Sm}$ -EDTMP in metastatic prostate cancer but they did not find that zoledronate influenced the uptake of  $^{153}\text{Sm}$ -EDTMP following repeated doses of each. In a single case report, the patient experienced long-term relief from bone pain and some decrease in size of the tumours<sup>107</sup>.

Loeb *et al.*,<sup>13</sup> reported on a dose finding study in patients with poor-prognosis osteosarcoma. The purpose of the study was to determine the maximally tolerated dose (MTD) of  $^{153}\text{Sm}$ -EDTMP that permits hematopoietic recovery within 6 weeks. They recruited patients with recurrent or refractory osteosarcoma with bone metastases. Patients were treated with increasing doses of  $^{153}\text{Sm}$ -EDTMP, beginning with 37 MBq/kg (1.0 mCi/kg) and followed initially with 40% increment dose level escalations, with a target dose-limiting toxicity (DLT) rate of 30%. The MTD of  $^{153}\text{Sm}$ -EDTMP was 44.8 MBq/kg (1.21 mCi/kg). DLTs were confined to hematologic toxicities, particularly delayed platelet recovery in two patients treated at a dose of 51.8 MBq/kg (1.4 mCi/kg). They concluded that patients with osteosarcoma who have been heavily pre-treated with chemotherapy could safely be given  $^{153}\text{Sm}$ -EDTMP with rapid hematologic recovery<sup>13</sup>.

### 1.6.3.2 Clinical Application of $^{188}\text{Re}$ -HEDP

In an early report, Knapp *et al.*,<sup>109</sup> evaluated two types of  $^{188}\text{Re}$ -labelled agents as potential treatments for cancer.  $^{188}\text{Re}$ -188-HEDP and  $^{188}\text{Re}$ -dimercaptosuccinic acid (DMSA) were applied for palliative treatment of pain associated with skeletal metastases, and the  $^{188}\text{Re}$ -RC-160 somatostatin analogue [cyclic NH<sub>2</sub>-(D)-Phe-Cys-Try-(D)-Trp-Lys-Val-Cys-Trp-NH<sub>2</sub>] for somatostatin-receptor-positive tumours in animals. The results of initial clinical studies with the two bone pain agents demonstrated good targeting to skeletal metastases, and use of  $^{188}\text{Re}$ -HEDP has resulted in pain palliation with minimal bone marrow suppression in the initial patient studies<sup>109</sup>.

In the first large study of several radiopharmaceuticals by Liep *et al.*,<sup>110</sup>, comparisons were made for efficiency of bone pain palliation. In addition, generator eluted <sup>188</sup>Re-HEDP was evaluated for suitability as a therapeutic agent. Forty-four patients (6 breast cancer and 38 prostate) were included and were treated with <sup>188</sup>Re-HEDP (n=16), <sup>186</sup>Re-HEDP (n=13) and <sup>89</sup>Sr (n=15) on pain symptoms and bone marrow function. They concluded that all radiopharmaceuticals were effective in pain palliation. The various radionuclides had no significant difference in the pain relief or the bone marrow impairment.

In a dose escalation study, Palmedo *et al.*,<sup>111</sup> determined the maximum tolerated dose of <sup>188</sup>Re-HEDP in prostate cancer patients with osseous metastases who were suffering from bone pain. Twenty-two patients received a single injection of escalating doses of <sup>188</sup>Re-HEDP [1.3 GBq (35 mCi), 2.6 GBq (70 mCi), 3.3 GBq (90 mCi) and 4.4 GBq (120 mCi)]. Blood counts and biochemical parameters and pain were measured for up to 6 months. Haematological toxicity (WHO grading) of Grade 3 or 4 was considered unacceptable. In the 1.3-GBq group, no haematological toxicity was observed. First haematotoxic results were noted in those patients receiving a dose of 2.6 GBq of <sup>188</sup>Re-HEDP. In the 3.3-GBq group, one patient showed a reversible thrombocytopenia of Grade 1, and another a reversible thrombocytopenia of Grade 2 and 3 and a reversible Grade 1 leukopenia. In the 4.4-GBq group, thrombocytopenia of grades 3 and 4 were observed in three patients (baseline thrombocyte count less than 200x10<sup>9</sup>/l), and leukopenia of Grade 3 was documented in one patient. The overall thrombocytopenia nadir\* occurred at week-4. The individual maximum percentage decrease in thrombocytes in the 1.3-, 2.6-, 3.3- and 4.4-GBq groups was 17%, 40%, 60% and 86%, respectively. In two patients, a transient increase in serum creatinine was observed (max. 1.6 mg/dl). Pain palliation was reported by 64% of patients, with a mean duration of 7.5 weeks. The response rate seemed to increase with higher doses, reaching 75% in the 4.4-GBq group. It is concluded that in prostate cancer patients, the maximum tolerated dose of <sup>188</sup>Re-HEDP is 3.3 GBq if the baseline thrombocyte count is below 200x10(9)/l. In patients with thrombocyte counts significantly above 200x10(9)/l, a dose of 4.4 GBq might be tolerable. Thrombocytopenia and leukopenia were the most important side effects. Pain palliation can be achieved in 60% to 75% of patients receiving

---

\* nadir is used to identify the lowest white cell count or platelet count reach during chemotherapy.

a dose of 2.6 GBq or more of  $^{188}\text{Re}$ -HEDP. The researchers concluded that larger studies were needed to evaluate the palliative effect of  $^{188}\text{Re}$ -HEDP.

In a later dose escalation study by the same group <sup>112</sup>, they investigated the effect of repeated doses of  $^{188}\text{Re}$ -HEDP in patients with progressive, hormone-resistant prostate carcinoma and bone pain. Their aim was to determine the pain palliation and the antitumour effect of  $^{188}\text{Re}$  HEDP treatments. Sixty-four patients were randomly assigned to one of two groups; Group A received a single injection, and Group B received two injections over an interval of 8 weeks. Patients were followed-up for pain palliation and clinical outcome until death. Low toxicity for both groups was reported, with no cases showing toxicity of greater than Grade 2 (WHO criteria).  $^{188}\text{Re}$ -HEDP was more effective in the repeated treatment Group (Group B), with a response rate of 92% and response time of 5.66 months ( $P=0.006$  and  $P=0.001$ ). In Group B, 11 of 28 patients (39%) had a prostate-specific antigen decrease of more than 50% for at least 8 weeks, compared with 2 of 30 (7%) patients in the single-injection Group (Group A). The median times to progression of Group A and Group B were 2.3 months (range, 0 to 12.2 months) and 7.0 months (range, 0 to 24.1 months), respectively ( $P=0.0013$ ), and the median overall survival times were 7.0 months (range, 1.3 to 36.7 months) and 12.7 months (range, 4.1 to 32.2 months), respectively ( $P=0.043$ ). It was concluded that when single-injection therapy was compared with repeated therapy, patients with advanced progressive hormone-refractory prostate carcinoma had enhanced pain palliation and improved progression-free and overall survival.

Li *et al.*, <sup>113</sup> examined the effects of  $^{188}\text{Re}$ -HEDP on different types of advanced cancer for the palliation of painful bone metastases. Sixty-one patients with painful bone metastases of lung, prostate, breast, renal, rhinopharyngeal, and bladder cancers were treated with 1.1 GBq (31 mCi) to 6.9 GBq (188 mCi)  $^{188}\text{Re}$ -HEDP. After treatment, the patients were followed at weekly intervals for the first 2 months and monthly thereafter for as long as 1 year. Hematologic function tests were also performed both before and after treatment for 6 weeks. Pain responses were scored according to a three-point pain-rating scale as complete, significant, and minimal. They reported prompt and significant relief of bone pain in 80% of patients overall. Of the specific tumour types, pain relief was achieved in 77% of patients with lung cancer, 80% with prostate cancer, 83% with breast cancer, 100% with bladder cancer, 50% with renal cancer, 50% with rhinopharyngeal cancer, and 87% of patients with other tumour types, with no severe side

effects or hematopoietic toxicity. They concluded that  $^{188}\text{Re}$ -HEDP was useful as a radiopharmaceutical agent for the treatment of painful bone metastases from various tumour types.

Another study of 27 patients with bone metastases from prostate cancer investigated the effect of  $^{188}\text{Re}$ -HEDP on pain relief, analgesic intake, and impairment of bone marrow function<sup>114</sup>. Patients were monitored 12 weeks before, and after therapy. Patients were treated with 2.7-3.5 GBq of  $^{188}\text{Re}$ -HEDP. Patients described an improvement on the Karnofsky performance scale from a mean of 74% to 85% 12 weeks after therapy ( $P = 0.001$ ). The pain score showed a maximum decrease from mean of 44% to 27% in the third to the eighth week after therapy ( $P = 0.009$ ). Seventy-six % of the patients described pain relief without increase of analgesic intake. Twenty % of the patients could discontinue their analgesics and were pain free. Mean platelet count decreased from  $(286 \text{ SD} \pm 75) \times 10^3 \mu\text{l}$  to  $(215 \text{ SD} \pm 92) \times 10^3 \mu\text{l}$ , and mean leucocyte count from  $(7.7 \text{ SD} \pm 1.5) \times 10^3 \mu\text{l}$  to  $(6.0 \text{ SD} \pm 1.9) \times 10^3 \mu\text{l}$  in the second to the fourth week after therapy. The maximal differences between the values of platelets and leucocytes before and after therapy were not statistically significant ( $P = 0.021$  and  $0.094$ ). They concluded that  $^{188}\text{Re}$ -HEDP was an effective radiopharmaceutical for palliative treatment of metastatic bone pain in prostate cancer and shows minimal bone marrow toxicity.

In a recent study, Liepe *et al.*,<sup>115</sup> (likely including previously reported cases<sup>110</sup>) compared the efficacy and toxicity in pain palliation of bone metastases of  $^{188}\text{Re}$ -HEDP,  $^{186}\text{Re}$ -HEDP, and  $^{153}\text{Sm}$ -EDTMP, and the volume seeker  $^{89}\text{Sr}$ . A total of 79 patients were treated for bone metastases from prostate and breast cancer. Pain symptoms, quality of life, and bone marrow function were studied. Over 73% of patients reported pain relief (77% after  $^{188}\text{Re}$ -HEDP, 67% after  $^{186}\text{Re}$ -HEDP, 73% after  $^{153}\text{Sm}$ -EDTMP, and 72% after  $^{89}\text{Sr}$ ). Fifteen % of patients could discontinue their analgesics and were pain-free. There were eight patients with a thrombocytopenia Grade 1, two patients with Grade 2 and one with Grade 3. The maximum nadirs of platelet and leukocyte counts were observed between the second to fifth weeks after treatment and were reversible within 12 weeks. There were no significant differences in pain palliation, Karnofsky performance status, and bone marrow toxicity between the different radionuclides. They concluded that all radiopharmaceuticals were effective in pain palliation without induction of severe side effects or significant differences in therapeutic efficacy or toxicity<sup>115</sup>.

The use of  $^{188}\text{Re}$ -HEDP has not been reported in naturally occurring canine osteosarcoma and was therefore considered an alternative to  $^{153}\text{Sm}$ -EDTMP for further research.

### 1.6.3.3 Clinical Application of $^{186}\text{Re}$ -HEDP

Maxon *et al* (1992) <sup>116</sup> reported in 43 metastatic bone cases that a single intravenous dose of  $^{186}\text{Re}$ -HEDP at approximately 34 mCi (1,258 MBq), resulted in a significant decrease in pain in 77% of patients following the initial injection, and in 50% of patients following a second treatment, with an average decrease in pain of about 60%. One in five treatments resulted in a complete resolution of pain. A mild, transient increase in pain was seen a few days post-injection in about 10% of the administered doses. Statistically significant but clinically unimportant decreases in total white blood cell counts and total platelet counts were observed within the first 8 weeks following the injection and no other toxicity was apparent <sup>116</sup>.

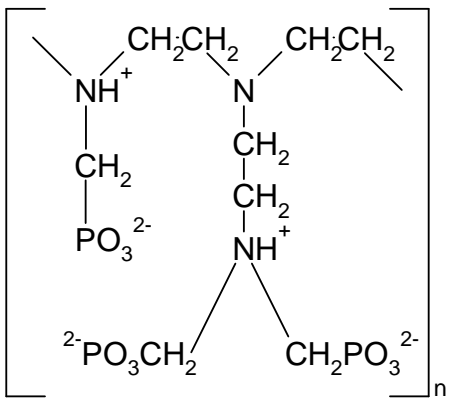
De Klerk *et al.*, <sup>117</sup> reported the results of a dose escalation studies with  $^{186}\text{Re}$ -HEDP as a bone-seeking radiopharmaceutical in patients with bone metastases originating from breast or prostate cancer describing toxicity, pharmacokinetics and bone marrow dosimetry, and the palliating effect on bone pain. The main side effect was thrombocytopenia, which proved to be the dose-limiting factor.  $^{186}\text{Re}$ -HEDP showed a significant usefulness in end-stage patients with metastatic bone pain <sup>117</sup>.

In addition, a summary of  $^{186}\text{Re}$ -HEDP clinical trials is given in a review by Lam *et al.*, <sup>2</sup>. Also, see section 1.6.3.2 for a review by Liepe *et al.*, <sup>115</sup> on  $^{188}\text{Re}$ -HEDP,  $^{186}\text{Re}$ -HEDP, and  $^{153}\text{Sm}$ -EDTMP, and  $^{89}\text{Sr}$ .



### 1.6.4 Novel Ligand Polyethyleneiminomethyl Phosphonic Acid (PEI-MP)

**Table 1-7: Chemical structure of PEI-MP**

Ligand	Potential use	MW (kDa)	Chemical structure
PEI-MP	Diagnostic Therapeutic	0.202 per unit	 <p>The diagram shows the chemical structure of the PEI-MP repeating unit enclosed in large square brackets with a subscript 'n'. The structure consists of two nitrogen atoms, each with a positive charge (NH<sup>+</sup> and N). The left nitrogen is bonded to a CH<sub>2</sub> group, which is further bonded to a PO<sub>3</sub><sup>2-</sup> group. The right nitrogen is bonded to a CH<sub>2</sub> group, which is further bonded to an NH<sup>+</sup> group, which is then bonded to a CH<sub>2</sub> group, which is finally bonded to a PO<sub>3</sub><sup>2-</sup> group. The two nitrogen atoms are also connected to each other via two ethylene chains (CH<sub>2</sub>CH<sub>2</sub>).</p>

An ideal radiopharmaceutical for the treatment of neoplastic and inflammatory (benign) bone disease would be a radiolabelled compound that predominantly accumulates in bone lesions with limited access to normal bone and other organs. A common target of radiopharmaceuticals is the capillary endothelial channel of cancerous tissue<sup>118</sup>. Neoplastic tissue's abnormal blood supply (increased permeability) and lack of lymphatics will selectively accumulate radiolabelled macromolecules<sup>119, 120</sup>. This enhanced “permeability and retention effect” (EPR) forms the basis for the development of the novel ligand PEI-MP<sup>120</sup>. In a previous non-human primate study, we investigated the application of variously sized macromolecules of <sup>99m</sup>Tc-PEI-MP<sup>21</sup>. The primary goal was to select a molecule that together with a β-emitting radioisotope would fulfil the criteria of an ideal radiopharmaceutical. An important aim of the study was to select a size of molecule to reduce radiation dose to vital structures or organs. PEI-MP was synthesized by condensation of polyethyleneimine, phosphonic acid, and formaldehyde followed by MW-fractionation into different molecular sizes by membrane ultrafiltration<sup>21</sup>. The pharmacokinetics and biodistribution of various <sup>99m</sup>Tc-PEI-MP MW-fractions (3 to 300 kDa MW) were investigated. From the results, macromolecules with sizes ranging from 30 to 300 kDa were characterized by excessive liver (21% to 57% retained activity at 4-hours) and kidney (40% retained activity at 4-hours) uptake and accompanying long residing times (T<sub>1/2</sub> up to 24 hr.). The percentage bone

uptake averaged at 8% for these particles excluding sizes 100 to 300 kDa where very little bone uptake was seen (less than 1%). In this case the blood clearance was also slow ( $T_{1/2}$  approximately 2 h). The MW-fraction size 10 to 30 kDa had comparatively low accumulation and short residence times in the liver (20%,  $T_{1/2} = 22 \pm 4$  min); and kidneys (18.4%,  $T_{1/2} = 20 \pm 3$  min) and although the bone uptake of 18% in this case was high, it is still low for a bone-seeking agent. These particles cleared the blood with  $T_{1/2} = 25 \pm 2$  minutes and seemed suitable for labelling with a therapeutic radio isotopic agent.

Results from the non-human primate study by Dormehl *et al.*,<sup>21</sup> lead to the formulation of research questions that were addressed in this investigation e.g. would PEI-MP accumulate in osteosarcomas in the canine model?

### 1.6.5 Toxicity Associated with Radiopharmaceuticals

Associated toxicities are a function of the biodistribution of the radiopharmaceutical, which in turn is related to the properties of the ligand and the radiation dose from the radionuclide. Most bone seeking radiopharmaceuticals have bisphosphonate ligands that are known to accumulate in areas of high bone turnover. These areas also correspond to some sites of active (red) marrow and therefore it is not surprising that the dose limiting toxicity of bone seeking radiopharmaceuticals is myelotoxicity. Complications of  $^{153}\text{Sm}$ -EDTMP treatment is primarily myelotoxicity but in some cases an increase in bone pain following treatment (flare response) is observed<sup>7, 7-10, 14, 104, 121, 122</sup>. In addition, the flare response could also be complicated by the reported acute-phase reaction associated with IV bisphosphonate use<sup>72</sup>. Myelotoxicity occurs 1 week after treatment and remains haematologically evident for 2 to 3 weeks<sup>7, 7, 122</sup>. Loeb *et al.*,<sup>13</sup> recently did a dose escalation study and found that 51.8 MBq/kg (1.4 mCi/kg) was associated with delayed platelet recovery and dose limiting neutropenia. The study was designed to have a dose limiting toxicity of 30% with the toxicity defined as a failure of haematological recovery at six weeks. The maximum tolerated dose was 44.8 MBq (1.21 mCi/kg) with a neutrophil and platelet nadir at four weeks.

Renal toxicity appears not to be significant even though  $^{153}\text{Sm}$ -EDTMP, in common with other bisphosphonates is cleared by the kidneys<sup>61</sup>. Even at myeloablative doses of  $^{153}\text{Sm}$ -EDTMP as reported by Franzius *et al.*,<sup>14</sup> and others, no renal toxicity was noted. Acute radiation nephritis is thought to occur only after exposure to radiation of more than 1000 cGy<sup>123</sup>. Lattimer

*et al.*,<sup>7</sup> did not report renal toxicity. Most bone seeking radiopharmaceuticals have similar toxicity profiles to <sup>153</sup>Sm-EDTMP and are reviewed in detail by Lam *et al.*,<sup>2</sup> in a 2007 publication. A detailed discussion on the mechanisms of radiation toxicity is dealt with under radiobiology.

## 1.7 Radiobiology.

Radiation exerts its effect by ionization of certain targets in the body. Traditionally, it was thought that ionization radiation (IR) exerted its effect by either directly damaging DNA via ionization or indirectly by generation of free radicals<sup>124</sup>. Damage is manifested by single or double strand breaks in the sugar phosphate backbone of DNA. Cross-linking between DNA strands and chromosomal proteins does occur. It is now known, apart from DNA damage, the cell membrane can also be an important target for radiation induced cell-death pathways. These include two independent signalling pathways that lead to a biphasic intracellular ceramide increase<sup>125</sup>. A transitory increase of ceramide that is DNA damage-independent is observed within minutes after radiation exposure because of sphingomyelinase acid activation. Sphingomyelinase catalyses the hydrolysis of sphingomyelin to ceramide, which in turn is an important stress messenger that promotes cell death. Several hours after irradiation, a second wave of ceramide accumulation is observed which is dependent on DNA damage leading to activation of ceramide synthase, which requires a signalling pathway involving ataxia telangiectasia-mutated gene (ATM). ATM activation by ionizing radiation stimulates DNA repair and blocks progression through the cell cycle. It is now suggested that that the late ceramide accumulation is also dependent on the early increase of ceramide and is rate limiting for the apoptotic process induced by radiation. This dependency makes ceramide an important factor in the radiation-induced apoptotic process at the cross-point of different signal transduction pathways<sup>125</sup>. The effects of IR on the mammalian cell is a complex process dependent on numerous genes which combined determines final outcome including repair with resumed proliferation, or unsuccessful repair leading to permanent arrest or mitotic catastrophe, or intrinsic apoptosis. All tissues have varying responses to IR termed radiation sensitivity. Understanding the cellular determinants of normal and cancerous tissue will allow us to tailor IR therapy to be more effective.

### 1.7.1 Cellular Determinants

There are several alternatives to cellular response to IR<sup>124</sup>. This indicates that there are control mechanisms that determine outcome according to cell type, cell state, level of damage, and environment. Three important decisive steps include: first, IR-induced damage that directs cells to apoptosis or DNA repair; second, after DNA repair the cellular mechanisms determine if the repair was successful and if the cell should resume proliferation; third, if the DNA repair was unsuccessful whether the cell must choose between irreversible growth arrest or mitotic catastrophe. The decision between apoptosis and cell cycle arrest with repair or growth arrest is largely determined by the tumour suppressor gene TP53<sup>124</sup>. Hemopoietic tissue and early embryonic cells only respond by apoptosis; however, fibroblasts are more strongly committed to growth arrest. It appears that an increased amount of p53 activation and its duration of activation, p53-responsive genes present in active chromatin, and p53 co-factors induce a cell to undergo apoptosis rather than growth arrest. If a cell does not undergo apoptosis then DNA repair would be its fate. The ability of a cell to repair its DNA depends on a number of factors: the cell type; phase of cell cycle; and the ability to take proper time to effectively repair the damage. Thus, unrepaired chromosomal breaks in dividing tissue would be lethal, but in differentiated tissue, it would be tolerable. Certain phases of the cell cycle are more sensitive to IR, such as mitosis, but less sensitive in S-phase. Mitosis is sensitive because chromatin is subjected to strong torsional stresses and DNA breaks have no chance of repair. S-phase is more resistant because DNA replication machinery is coupled to DNA repair. The time of maximum radio resistance is known as the clonogenic potential.

If cells escape apoptosis after irreparable DNA damage, they can undergo either mitotic catastrophe or irreversible growth arrest. Irreversible growth arrest is p53 dependent with the p53-dependent CDKN2A gene an important component. Mitotic catastrophe is recognized morphologically as cells undergoing aberrant mitosis, which leads to large multinucleated cells containing MW-fractions of broken chromosomes. These are usually non-viable. Since both cancerous and normal tissues are targets of IR when an animal or human undergoes therapy, it is important to consider them in more detail.

### 1.7.2 Normal tissues response to ionizing radiation

Normal tissues have variable radio sensitivity to IR based on a number of factors present in the tissue type. For example hemopoietic tissue is a population rapidly dividing cells replenished from stem cell populations, which make hemopoietic tissue exquisitely sensitive to IR<sup>124</sup>. The IR toxicity grading system used in our study can be seen in Table 1-8 on page 70. Logically more differentiated non-dividing cell populations, e.g., nervous tissue are more radiation resistant and are thus more tolerant of higher radiation doses. Signs of toxicity in differentiated tissue are only evident when the cells attempt to divide. Lethal radiation doses kill the animal or human via organ failures either from ablation of bone marrow or complications from intestinal syndrome<sup>124</sup>. However, there appear to be other factors other than proliferation that plays a role, e.g., some non-dividing tissues are sensitive to radiation. For example, recent research has identified p53 as an important determinant of tissue-specific radio sensitivity. Radiosensitive tissues have a high basal level of p53 and with genotoxic stress caused by IR, accumulate and activate apoptotic pathways. As previously mentioned, ceramide is an important mediator of the apoptotic pathway and apoptosis is dependent on the availability of the machinery for the process. Apoptosis prevails in tissue with a rapid turnover such as hemopoietic, hair follicles and certain layers of the GIT. Apart from apoptosis, other outcomes are possible for normal tissue that receives IR. Depending on the tissue type and IR dose received, reversible arrest with DNA repair followed by normal proliferation or permanent arrest in the case of fibroblasts or failed DNA repair with resultant mitotic catastrophe are possible<sup>124</sup>. The effect of IR on normal tissue is known as the bystander effect.

The effect of IR on normal organs can also be attributed to other factors such as apoptosis of vascular epithelia triggered by p53-independent ceramide mediated mechanism. In addition, death of the spinal cord neurons following radiation is because of p53 dependent death of oligodendrocytes. Fibrosis of organs such as the kidney, lung, mammary gland, and liver are due to cytokines such as TGF- $\beta$ <sup>124</sup>.

**Table 1-8 Canine Toxicity Grading Schemes**

Toxic Effect and Grade*	Signs
<b>Neutropenia</b>	
0	None
1	1,500-3,000 neutrophils/ $\mu$ l
2	1,000-1499 neutrophils/ $\mu$ l
3	500-999 neutrophils/ $\mu$ l
4	<500 neutrophils/ $\mu$ l
<b>Thrombocytopenia</b>	
0	None
1	100,000-199,000/ $\mu$ l
2	50,000-99,000/ $\mu$ l
3	< 20,000-50,000/ $\mu$ l
4	< 20,000/ $\mu$ l
<b>Anorexia</b>	
0	None
1	Inappetence
2	<3days duration
3	$\geq$ 3 days but <5days duration
4	$\geq$ 5 days duration
<b>Vomiting</b>	
0	None
1	Nausea
2	Sporadic, self-limiting
3	1-5 episodes/day, <2 days duration
4	6-10 episodes/day, 2 days, or requires hospitalization
<b>Diarrhoea</b>	
0	None
1	Soft stools
2	<2 days duration
3	$\geq$ 2 days duration
4	Bloody or requires hospitalization

Legend: \*Adapted from De Regis *et al.*, (2003) <sup>126</sup>. The average normal ranges (subject to some variability between laboratories) for canine blood cells are; neutrophils 3,000-11,400 neutrophils/ $\mu$ l, thrombocytes 200,000-450,000/ $\mu$ l. Chemotherapy is withheld from most dogs that are showing grade-3 toxicities. Grade-2 toxicities can be controlled with oral medication. Grade-3 toxicities require hospitalization and preantral drug and fluid administration.

### 1.7.3 Cancerous tissues response to ionizing radiation

The signalling pathway p53 is frequently inactivated in human and animal cancers; however, it can still be present in either the wild form or mutated form. Cancers that express wild-type p53 do undergo p53-dependent apoptosis. It is now generally accepted that in order for this to happen, the cancer should be derived from tissue that expresses high levels of wild-type p53, such as hemopoietic cells<sup>124</sup>. It has also been shown that wild-type p53 can also express resistance to apoptosis by up regulation of antiapoptotic genes, such as BCL2 family or loss of apoptosis machinery, such as transcriptional silencing of APAF1, or inhibition of caspase encoding genes. In addition, numerous tumours lose their sensitivity to extrinsic signalling including FAS, TNF, and TRAIL. This loss allows cells to escape the bodies' immune response. There is now more evidence to suggest that in the case of cancers with mutated p53 or low expression of wild p53, mitotic catastrophe plays a significant role in cell death. In order for mitotic catastrophe to occur, irreparable DNA damage must occur with loss of cell cycle checkpoint control. Mutations and activation of tumour suppressor genes and /or oncogenes leads to loss of checkpoint control. Those involved in the cell cycle include D1, RB, E2F and INK4a and in checkpoint control p53, ARF, 14-3-3- $\sigma$  and MDM2<sup>124</sup>. The majority of these genes have been documented in human and canine osteosarcoma shown in Table 2-2, see page 86. Some cell cycle checkpoints are more crucial, with G2/M being especially critical, and are most susceptible to IR. Experimentally it has been shown that mitotic catastrophe is a significant cause of cell death in 12 out of 14 solid tumour cell lines. It is worth noting that mitotic catastrophe and apoptosis are not mutually exclusive, and that mitotic catastrophe is often followed by apoptosis in apoptotic-competent cells.

Another consequence of IR in the absence of apoptosis and an alternative to mitotic catastrophe is irreversible growth arrest<sup>124</sup>. This process is typical for connective tissues response to IR but also found in lymphoid tumours where the apoptotic pathway is blocked by BCL2 overexpression. Irreversible growth arrest is reminiscent of replicative senescence (permanent growth arrest) a process that cells in culture undergo when their telomeres become critically short due to repeated cell division<sup>124</sup>. This process is p53 dependent and induces WAF1 transactivation. WAF1 and p53 are positive regulators of senescence.

The loss of wild type p53 in cancers has traditionally been viewed as a poor prognostic indicator. This concept is now being challenged since the loss of p53 may allow cells with damaged DNA to progress through G2M into catastrophic mitosis. In solid tumours, this maybe the more common cell death route post IR. Interestingly, inhibitors of p53 are being considered as a way to protect normal tissue from the effects of IR. Since living on earth carries an intrinsic risk of radiation exposure from environmental sources and the cosmos, cells have developed natural modulators apart from DNA repair mechanisms to protect the cell. These natural modulators include cytokines such as Il-1, stem cell factor (SCF), Il-12, and TNF that protect mice from myeloablative effects of IR. Daily oscillation of metabolic activity known as circadian rhythm also plays a role in cellular radio sensitivity. For example, mice are shown to be more radiosensitive at night than in the day. Another modulating effect, and arguably the most important, is the balance of redox chemicals near DNA. The concentration of oxygen (a radio sensitizer) and thiols (especially glutathione, a radio protectant) have a marked effect on the ability of IR to do damage. Hypoxic cells, commonly found in tumours, have a three times greater resistant to IR than oxygenated cells. Mechanism of this modulation appears to be linked to the generation or scavenging of free radicals<sup>124</sup>. In a similar manner, the intake of antioxidants, such as vitamin-E during IR therapy may reduce the efficacy of the treatment; however, this concept has since been challenged<sup>127</sup>.

#### 1.7.4 Principles of radiation therapy

Cell death due to radiation generally follows exponential pharmacokinetics. This means a given dose of radiation kills a fixed proportion of cells<sup>128</sup>. If one were to plot survival curves of cells logarithmically as a function of radiation dose, it would be a straight line<sup>128</sup>. Sublethal damage, which is repaired tissue damage, is responsible for the “shoulder region” on the dose response curve<sup>129</sup>. Once sublethal repair is saturated, cell killing increases exponentially as is seen on the dose response curve. If another dose of radiation is given after repair, sublethal damage accumulates and appears as a shoulder again on the dose response curve. Therefore, if sublethal damage repair is allowed to occur between radiation doses a greater total dose is required<sup>128</sup>.

In its response to radiation, tissue and cancers are governed by certain factors including<sup>128</sup>:



- Normal tissue reaction. The goal of radiation therapy is to administer a sufficiently high dose of radiation to reduce the surviving MW-fraction of clonogenic cancer cells to zero<sup>129</sup>. However, the surrounding normal tissue limits the maximum amount of radiation. This dose is known as the maximum tolerated dose (MTD). The MTD is determined by the type and volume of normal tissue that is in the irradiated volume, with the hope of controlling some MW-fraction of the tumour<sup>129</sup>. Normal tissue that expresses injury soon after or during radiation is known as acute responding tissue and is commonly rapidly proliferating tissue e.g., red marrow, skin, and GIT<sup>128</sup>. Late responding tissue e.g., bone, kidneys, muscle, neural tissue, and connective tissue may take months or years to express signs of radiation injury<sup>128</sup>. Late responding tissue reactions can be serious and some cases life threatening e.g., bone necrosis, and pulmonary fibrosis<sup>128</sup>.
- Tumour clonogen number (Tumour volume). Tumour clonogen number is related to the tumour volume and therefore larger tumours require a greater dose to control them. The greater the number of clonogens (heterogeneity) in a tumour, the more radiation is required to complete their eradication. It is logical that the earlier cancers are treated the better chance there is of controlling them.
- Tumour Hypoxia. Cancers have areas of hypoxia due to diffusion limitation and intermittent interruption in tumour blood flow<sup>128</sup>. Hypoxic cells are considered radioresistant by a factor of two or three<sup>129</sup>. An important factor in this resistance is the free radical damage (indirect effect) to DNA when oxygen reacts with the damaged DNA fixing the damage, thus making it non-reparable<sup>128</sup>. Reoxygenation describes a process whereby cells at some distance from blood vessels are in a chronically hypoxic state. By MW-fractionating radiation, the cells closest to the blood vessels would be more radiosensitive and die and thus shortening the distance between the blood vessels and hypoxic cancer cells, thus improving oxygen delivery to the hypoxic cells making them more radiosensitive<sup>130</sup>.
- Tumour proliferation rate. Because tumours are proliferating, they are considered acute responding tissue. The factors that play a significant role in tumour proliferation are; the MW-fraction of tumours cells proliferating, cell cycle time of the proliferating cells and cell loss factor<sup>128</sup>. Other factors that may play a role during MW-fractionated radiation are repair of radiation damage, re-population of stem cells, redistribution, or re-

assortment of cell in the cell cycle<sup>130</sup>. DNA *repair* occurs when the same total dose is delivered in several small MW-fractions instead of one large MW-fraction. Slow responding tissue has a greater capacity for repair; fortunately, most tumours are rapidly responding tissue. *Re-population* of cells is induced by MW-fractionated radiation and it is therefore not advantageous during treatment to prolong the intervals between doses. *Re-assortment* (proliferation) involves the reposition of cells in the cell cycle to a more sensitive phase such as mitosis. The most resistant phase is the late S-phase that allows cells to accumulate in this phase during irradiation. MW-fractionated radiation protocols allow cells to move out of this phase into the more radiation sensitive phases such as mitosis<sup>130</sup>.

- Biologically Effective Dose (BED). The BED is defined by the product of the total physical dose (TD) received by a tissue and a modifying factor (RE) for that tissue<sup>131</sup>. The factor RE is defined as the relative effectiveness per unit dose<sup>132</sup>. Each tissue type either cancerous or normal has its own BED even if the total physical dose and dose rate are the same<sup>131</sup>. Two important radiobiological parameters are required in the definition of RE: the tissue  $\alpha/\beta$  ratio and the sublethal damage recovery constant ( $\mu$ ) in normal tissue<sup>132</sup>. The  $\alpha/\beta$  ratios provides a quantitative indication of the sensitivity of a given tissue, normal or cancerous, to changes in MW-fractionation or dose rate and are derived from the Linear Quadratic (LQ) formulation<sup>132</sup>. The LQ formulation for a tissue are derived from a linear-scale logarithmic plot of cell survival MW-fraction against dose and assumes that lethal radiation is created in either of two ways: Type A or B. A Type A effect is a single lethal ionization event where the damage to DNA is such that it is non-repairable e.g., double strand break. Type B effect is where two, separate (single strand DNA breaks), sublethal ionizing events interact pairwise to create lethal damage<sup>132</sup>. The individual single-strand breaks (precursors to Type B damage) are assumed to be potentially repairable and thus sublethal<sup>132</sup>. The  $\alpha/\beta$  ratio is determined from the intersection point on the LQ plot where Type A and Type B damage are equal. The  $\alpha/\beta$  value (in units of Gy) is generally higher for tumours and early responding tissue (typical range, 5–25 Gy) than for late-responding normal tissues (typical range, 2–5 Gy) and some tumours (melanoma)<sup>132</sup>. As part of RE, the damage-recovery constant ( $\mu$ ) is inversely related to the sublethal damage repair half time; to the rate at which single-

strand DNA breaks repair<sup>132</sup>. The repair times are typically in the range of 0.5 to 3-hours and this is why, in external beam radiotherapy (where MW-fractions are approximately 24 hour apart), the sublethal damage remaining after each MW-fraction is usually fully repaired by the time of delivery of the next MW-fraction. It thus follows that if the damage from the first sublethal event repairs before the second event occurs, there will be no lethality. Sublethal, single-target damage is the key to understanding MW-fractionation and dose-rate effects because, unlike the case with Type-A damage, the amount of Type-B damage is reduced when there are opportunities for sublethal repair, which occurs when a treatment is protracted as with radionuclides or brachytherapy. Continuous low-dose-rate (CLDR) radiotherapy normally extends over periods of hours or days depending on the physical half-life of radionuclide. As with external beam radiation, the continuous delivery of radiation creates both lethal (fixed) and sublethal repairable damage (SLD). However, because CLDR therapy is protracted, the rate of dose delivery is relatively low; some of the SLD has an opportunity to repair itself while the radiation is being delivered. The SLD repair therefore takes place as treatment progresses. Thus, as with MW-fractionated external beam radiation, CLDR spares the normal tissues relatively more than the tumour, and the use of this modality confer, in principle, the same benefits as MW-fractionation. The radiobiological processes governing external beam radiation and CLDR are seen to be essentially identical<sup>133</sup>. Because of this, they may be incorporated within the LQ model to allow for quantitative comparison between the two modalities. Targeted radiotherapy (TRT) is a form of continuous radiation delivery during which the dose rate is not held constant but rises from zero to some maximum value and then drops back to zero. As with external beam radiation and CLDR, the delivery of radiation at varying dose-rates creates both lethal and sublethal damage. Because TRT radiation delivery normally takes hours or days, some of the SLD repairs while the radiation is being delivered, but the differential between creating new damage and the repair of existing sublethal damage will now also depend on the dose-rate being delivered at any particular time. When tumours and critical normal tissues are each subjected to the same dose-rate profile, the sparing argument is similar to that for CLDR and there will be a therapeutic benefit if the overall TRT dose rate is kept low. For TRT, however, the associated LQ formulation must take

account of the biological uptake and clearance pharmacokinetics in the targeted tumour or organ. This is because with TRT the critical dose-limiting tissues (e.g., the kidneys or bone marrow) may be anatomically distant from the tumour(s) to be treated and will likely be subjected to a quite different dose-time profile than the tumour. Although the radiobiological processes, which govern external beam radiation and TRT are essentially identical, the separation of the tumour and dose limiting target organs makes quantitative analysis of TRT rather more difficult.

## 1.8 Tumour Vasculature

Since most drugs must travel across biologic membranes to exert an effect, characteristics and interactions of the membrane and drug have important effects on the process of drug transport. The cell membrane is a bilayer of amphipathic-phospholipid molecules that endow the membrane with fluidity and flexibility. The bilayer is imperviousness to polar molecules and has a high electrical resistance<sup>134</sup>. Drug movement across this membrane is either by passive transfer or by active participation of the membrane. The passive transfer of drugs is dependent on the concentration gradient, molecular size, lipid solubility, and polarity. Traversing the membrane occurs by either diffusion or if the drug is sufficiently small, via filtration through aqueous channels or pores<sup>134</sup>. Some drugs and radiopharmaceuticals rely on the permeability of abnormal capillary endothelial channels to gain entry to and be retained in cancerous tissue; this phenomenon is known as the enhanced permeability and retention effect (EPR)<sup>119, 120, 135</sup>. The enhanced permeability is not always correlated to channels or to inter-endothelial pores in tumour blood vessels<sup>119</sup>. Blood borne molecules that reach cancer cells must pass through the chaotic blood supply, the microvascular wall, and the interstitial compartment, which involves diffusion and convection<sup>135</sup>. The fate, which awaits the molecules in the interstitium, are: to bind non-specifically to proteins (or other components), to bind specifically to the target, or be metabolized. Tumour vasculature comprises both co-opted blood vessels from the original network and vessels resulting from the angiogenic response of the host's vessels to cancer cells. The chaotic blood vessels in cancerous tissue leads to temporal and spatial heterogeneity in blood flow for the following reasons: elevated geometric and viscous resistance in blood vessels, coupling between high vascular permeability and elevated interstitial pressure, vascular modelling by intussusception, solid stress generated by proliferating cancer cells, and an

imbalance between pro- and anti-angiogenic molecules<sup>135, 136</sup>. Due to the variation in perfusion, the four regions that can be identified in tumours are: avascular necrotic region, semi necrotic region, stabilized microcirculation region, and an advancing front. The heterogeneity of the blood flow and vascular morphology is responsible for the heterogeneous distribution of molecules in cancers that increases proportionally with tumour weight. There are also changes in the metabolic microenvironment of solid cancers. The further one moves from the tumour vessels the more acidic and hypoxic the environment. This can be either an advantage or a disadvantage with therapy. Jain *et al.*,<sup>136</sup> have recently shown that solid cancers depend more on glucose than oxygen to maintain ATP levels. From experimental work, Jain<sup>137</sup> made the following conclusions about transport of molecule into cancers:

- Vascular permeability and hydraulic conductivity of tumours is generally higher than normal tissue and these vessels lack selective permeability.
- Positively charged molecules have a higher permeability.
- Not all tumour blood vessels are leaky.
- Leaky blood vessels have a finite pore size.
- Large pore sizes in tumours are due to large inter-endothelial junctions.
- Vascular permeability varies from tumour to tumour: from primary tumour to metastasis, within the same tumour over time, during growth phases of the tumour, tumour regression, and relapse of the tumour.
- The position of the tumour in the body will affect permeability even for the same tumour type.
- Hypothetically, host-tumour interactions control the secretion of cytokines associated with vascular permeability e.g., vascular permeability factor (VPF), vascular endothelium growth factor (VEGF) and its inhibitors.
- Experimentally, cancers exhibit higher interstitial fluid pressure compared to normal tissue, with a rapid fall off at the periphery. This results in less extravasation of the drug at the centre of a tumour than periphery.
- The average vascular surface area per unit tissue weight decreases with tumour growth and therefore, large tumours have a reduced trans-vascular exchange.

After a molecule reaches the tumour interstitium, movement within the tumour occurs by diffusion and convection. From research, Jain<sup>137</sup> drew the follow conclusion about tumour interstitium:

- For macromolecules, diffusion in tumour interstitium depends on the size of the tumour; within a 1 mm size tumour, diffusion by 1 mm would take days versus a 1 cm size tumour where 1 mm diffusion could take months.
- Collagen content of the interstitium significantly affects diffusion.
- There is significant non-specific binding of molecules in the interstitium.
- Functional lymphatics exist only on the periphery of tumours and even if lymphatics did form, they would collapse due to proliferating tumour cells.

Coomber *et al.*,<sup>138</sup> conducted a retrospective study to investigate the possibility that tumour vascularity may provide useful prognostic information; indicative of the role of vascularity in progression of cancer. Higher primary tumour vascularity was associated with detectable pulmonary metastases, and significantly lower vascularity in animals without metastatic disease at presentation.

## 1.9 Scintigraphic Technique and Equipment

### 1.9.1 Instrumentation

In nuclear medicine, radiation detecting devices are used to ascertain the intensity, presence, type and energy of the radiation<sup>55</sup>. Nuclear medicine clinical instrumentation can be divided into two groups: those required for the preparation and measurement of radiopharmaceuticals prior to administering it to the patient, and those that detect the distribution of radiation within the body. The former consist primarily of gas-filled detectors that function by way of gas molecule ionization due to radiation across which a current is applied<sup>55</sup>. The two instruments most commonly used are the Geiger-Müller counter and the dose calibrator. Scintillation cameras, or gamma cameras, are used to detect the distribution in the body of the radioisotope emitting gamma radiation in the patient. The camera consists of a collimator, sodium-iodide crystal detector, photomultiplier tubes, preamplifier, linear amplifier, pulse-height analyser, display and storage<sup>55</sup>. The camera is described in more detail in the following section.

### 1.9.1.1 Equipment and Imaging Quality Control

#### 1.9.1.1.1 Gamma Camera (Scintillation Camera)

A gamma camera consists of one or more flat crystal planes (or detectors) optically coupled to an array of photomultiplier tubes, the assembly of which is known as a "head", mounted on a gantry. The gantry is connected to a computer system that controls both the operation of the camera as well as acquisition and storage of acquired images. The system accumulates events, or counts, of gamma photons emitted from the patient that are absorbed by the crystal in the camera. Usually a large flat crystal of sodium iodide with thallium doping in a light-sealed housing is used. When a gamma photon leaves the patient (who has been injected with a radioactive pharmaceutical), it knocks an electron loose from an iodine atom in the crystal, and a faint flash of light is produced when the dislocated electron again finds a minimal energy state. The crystal scintillates in response to incident gamma radiation. This initial phenomenon of the excited electron is similar to the photoelectric effect and (particularly with gamma rays) the Compton effect. After the flash of light is produced, it is detected by the photomultiplier tubes (PMTs) behind the crystal and the number of fluorescent flashes (counts) is summed by the computer. The computer reconstructs and displays a two dimensional image of the relative spatial count density on a monitor. This reconstructed image reflects the distribution and relative concentration of radioactive tracer elements present in the organs and tissues imaged.

#### Signal processing

The gamma camera uses sets of vacuum tube photomultipliers (PMT). Generally each tube has an exposed face of about 75 mm in diameter and the tubes are arranged in hexagon configurations, behind the absorbing crystal. The electronic circuit connecting the photodetectors is wired so as to reflect the relative coincidence of light fluorescence as sensed by the members of the hexagon detector array. All the PMT's simultaneously detect the (presumed) same flash of light to varying degrees, depending on their position from the actual individual event. Thus the spatial location of each single flash of fluorescence is reflected as a pattern of voltages within the interconnecting circuit array. The location of the interaction between the gamma ray and the crystal can be determined by processing the voltage signals from the photomultiplier tubes; in simple terms, weighting the position of each photomultiplier tube by the strength of its signal and

then calculating a mean position from the weighted positions can determine the location. The total sum of the voltages from each photomultiplier is proportional to the energy of the gamma ray interaction, thus allowing discrimination between different isotopes or between scattered and direct photons.

### Spatial resolution.

In order to obtain spatial information about the gamma emissions from an imaging subject, a method of correlating the detected photons with their point of origin is required. The conventional method is to place a collimator over the detection crystal and PMT array. The collimator consists of a thick sheet of lead, typically 25 to 75 mm thick, with thousands of adjacent holes through it. The individual holes limit photons, which can then be detected by the crystal to a cone; the point of the cone is at the midline center of any given hole and extends from the collimator surface outward. Unfortunately, the collimator is also one of the sources of blurring within the image as lead does not totally reduce incident gamma photons so there can be some crosstalk between holes. Unlike a lens, as used in visible light cameras, the collimator reduces most (greater than 99%) of incident photons and thus greatly limits the sensitivity of the camera system. Large amounts of radiation must be present so as to provide enough exposure for the camera system to detect sufficient scintillation dots to form a picture. Other methods of image localization (pinhole, rotating slat collimator with Cadmium Zinc Telluride (CZT) detectors have been proposed and tested; however, none have entered widespread routine clinical use<sup>139, 140</sup>.

Most current camera system designs can differentiate two separate point sources of gamma photons located a minimum of 1.8 cm apart, at 5 cm away from the camera face. Spatial resolution decreases rapidly at increasing distances from the camera face that limits the spatial accuracy of the computer image. It becomes a fuzzy image made up of many dots of detected but not precisely located scintillation. A typical 64x64 resolution reconstructed image will have a pixel (smallest picture element) size ranging from 3 to 6 mm and represents 4,096 pixels.

### Imaging techniques using gamma cameras.

Scintigraphy ("scint") is the use of gamma cameras to capture emitted radiation from internal radioisotopes to create two-dimensional images. Single photon emission computed tomography (SPECT) imaging, as used in nuclear cardiac stress testing for example, is performed using gamma cameras, usually one, two or three detectors or heads, which are slowly



rotated around the patient's torso. Multi-headed gamma cameras can also be used for positron emission tomography (PET) scanning, provided that their hardware and software can be configured to detect 'coincidences' (near simultaneous events on 2 different heads). Gamma camera PET is markedly inferior to PET imaging with a purpose designed PET scanner. This is because scintillator crystals have a poor sensitivity for high-energy annihilation photons and the detector area is significantly smaller. However, given the low cost of a gamma camera and its additional flexibility compared to a dedicated PET scanner, this technique is still useful where the expense and resource implications of a PET scanner cannot be justified.

#### 1.9.1.1.2 Scintillation Camera Quality Control

##### Routine quality control

Quality control (QC) is required to ensure accurate image acquisition <sup>141</sup>. Weekly QC program for the camera should include the following: peaking the energy window at regular intervals depending on the radionuclide used, flood field acquisition for intrinsic uniformity, phantom bar imaging for spatial resolution and linearity, calculation of central field of view and useful field of view, and calculating the gamma camera crystal sensitivity and uniformity correction matrix for uniformity correction.

##### Imaging Quality Control

Artefacts associated with imaging should be corrected as they can influence image quality significantly. Common artefacts include septal penetration, poor resolution, field non-uniformity, and edge packing <sup>141</sup>.

Septal penetration occurs when low energy collimators are used with higher energy photons from the nuclide. The high-energy photons penetrate through the collimator septa resulting in significant loss of spatial resolution and degradation in image quality. Septal penetration can also occur where there is a focal area of intense uptake that results in a significant penetration of the collimator septa. To correct for this artefact, the correct collimator should be selected.

Poor resolution can occur in the following instances: camera to patient distance, incorrect pulse height analyser setting, movement, factors intrinsic to the camera, high-energy gamma emission, damaged collimator, low count density, digital matrix size, and mismatched collimator to gamma emission. Corrective measures are dependent on causes and are generally self-evident.

In low count densities using a smaller acquisition matrix increases count density without increasing acquisition times. However, the use of a general-purpose collimator is often considered an acceptable compromise.

Field non-uniformity is due to non-uniform detector response, which in turn is caused by defects, such as cracks, or hydrolyzation in the sodium iodide crystals. Other causes include defects in the light coupling or coupling grease resulting in ineffectual light transfer, poorly balanced or non-functional photomultiplier tube, and/or amplifiers leading to non-uniform field. Defects in the spatial circuitry, which determines the x, y location of the incident photon, will result in non-uniform fields. If the window of the pulse height analyser is above or below the photopeak, a honeycomb pattern is seen. Field non-uniformity may not be apparent in a correctly photopeak flood field image, only images obtained below or above the photopeak will show the honeycomb appearance. These artefacts require service personnel to correct the defect.

Edge packing occurs when an incident photon is recorded near the edge of a crystal and only part of the light spread is recorded, resulting in a high photon dense area. Correction of this artefact is done by repositioning of the region of interest (ROI) to the centre of the camera. This avoids over interpretation of possible pathology.

#### 1.9.1.2 Dose Calibrator Quality Control

Dose calibrators require the following quality control tests: precision, accuracy, linearity and geometry (regulatory requirements) <sup>141</sup>.

Daily QC involves zero calibration for background activity. Precision (constancy) testing uses a known source such as Cs-137 that allows for  $\leq \pm 10\%$  variation with repeated measure. Accuracy testing ensures that the measured activity is equivalent to true activity. Variation should not be  $> \pm 5\%$  for different radionuclides. Calibration for linearity occurs yearly and is an assessment of the calibrator's accuracy over a wide range of activity within a  $\pm 10\%$  error. Geometry testing is whether a source configuration, volume, or position has a significant effect on accuracy. An example of this is the depth of a radiation source in a medium, which reduces the measured activity.

### 1.9.1.3 Radiopharmaceutical Quality Control

Quality control of radiopharmaceuticals includes evaluating for radionuclide, radiochemical and chemical impurities<sup>141</sup>. Radionuclide purity measures the MW-fraction of total activity for the stated radionuclide and uses a dose calibrator that can detect activity for impurities<sup>142</sup>. Radiochemical purity (RCP) is the MW-fraction of stated radionuclide present in the stated chemical form and is measured using paper or thin-layer chromatography. The radiopharmaceutical to be tested for RCP is applied to the bottom chromoplate (origin), which is then placed into a solvent: acetone, saline, and methyl ethyl ketone. Time is allowed for the solvent to migrate via upward capillary attraction to separate out the chemical species of the radiopharmaceutical. When the solvent has reached the desired distance, the plate is dried and the distance travelled by the solvent, known as the solvent front ( $S_f$ ), is recorded. For the radioactive species the plate can be analysed using various methods, these include: autoradiography, chromatogram scanning, gamma camera imaging, and cutting and counting segments. Location of the radiopharmaceutical and the impurities along the column are recorded and are expressed as a MW-fraction of the distance travelled relative to the  $S_f$ . This MW-fraction is known as the relative front ( $R_f$ ) and is known for different radiopharmaceutical species. For example, in the labelling process of  $^{99m}\text{Tc}$ -MDP certain impurities can form free pertechnetate ion and hydrolysed/reduced technetium (H/R- $^{99m}\text{Tc}$ ). The RCP for  $^{99m}\text{Tc}$ -MDP can be determined by using two solvents with thin-layer chromatography. When using saline 0.9 % as the solvent, H/R- $^{99m}\text{Tc}$  remains at the origin ( $R_f = 0$ ) and both free pertechnetate and  $^{99m}\text{Tc}$ -MDP migrate with the  $S_f$  ( $R_f = 1$  for both). However, when the solvent methyl ethyl ketone (MEK) is used, only free pertechnetate ( $R_f = 1$ ) migrates with the solvent, and both H/R- $^{99m}\text{Tc}$  and  $^{99m}\text{Tc}$ -MDP remain at the origin ( $R_f = 0$ ).

Radiochemical purity can also be recognised during scintigraphic studies, for instance free pertechnetate is recognized by its accumulation in the salivary glands, thyroid glands, and stomach. Biological clearance is slow with persistence in the soft-tissue.

Therefore, for the purpose of the experimental work reported in this thesis, apart from the laboratory RCP procedures, we also injected uncomplexed/free  $^{153}\text{Sm}$  and  $^{99m}\text{Tc}$  into experimental dogs and the images were recorded and used for comparative imaging purposes.

#### 1.9.1.4 Variables Inherent within the Patient

Modified, unexpected, and often unusual imaging outcome can be due to a number of factors associated with the individual patient. These include: altered biodistribution, concomitant drug therapy, other medical procedures, inappropriate route or technique of administration, unanticipated or atypical pathophysiologic mechanism, radiopharmaceutical formulation problems<sup>141</sup>, adverse reactions and untoward side effects<sup>143, 144</sup> and drug interactions<sup>143, 144</sup>.

## Chapter 2. Experimental Design

### 2.1 Animal Model

The animal model used in the study to evaluate the effects of targeted radiotherapy was naturally occurring osteosarcoma of the dog. We propose that the research may provide information that could aid in the treatment of osteosarcoma as well as metastatic bone cancer in humans. To support the study of canine osteosarcoma as an animal model for primary bone cancer in man numerous articles have been published in the literature<sup>17, 39, 145-149</sup>. For comparative purposes Table 2-1 below highlights the clinical similarities between human and canine osteosarcoma<sup>145</sup>.

**Table 2-1: Comparative clinical aspects of canine and human osteosarcoma**

Variable	Dog	Human
Median Age (Range)*	8 (5-14) years	15 (10-25) years
Gender	1.5:1 Male: Female	1.5:1 Male: Female
BW	99% >20kg	Heavy
Site	77% long bones	90% long bones
Aetiology	Generally unknown	Generally unknown
Percentage confined to a single bone at presentation	80-90%	80-90%
Percentage histopathologically high grade tumours	95%	85-90%
Percentage aneuploidy**	75%	75%
Metastatic rate without chemotherapy	90% before 1 year	80% before 2 years
Metastatic Sites	Lung>bone>soft-tissue	Lung>bone>soft-tissue
Survival with chemotherapy	Significant	Significant
Radiosensitivity	Generally poor	Generally poor

Legend: \*The difference in the median age between dogs and humans has not been addressed in research. Nevertheless, genetically the tumours are similar in their chromosomal aberrations. \*\*Aneuploidy occurs during cell division when the chromosomes do not separate properly between the two cells resulting in an abnormal number of chromosomes. The most common aneuploidy in osteosarcoma is p53 mutations. Since different species have different numbers of normal chromosomes, the term "aneuploidy" refers to the chromosome number being different for that species.

Apart from the obvious clinical similarities as reported in Table 2-1, canine osteosarcoma has similar genetic and biochemical abnormalities to human osteosarcoma (see Table 2-2, below). Cytogenetic characterization of canine osteosarcoma, in comparison to the human disease, is now well advanced with the discovery of the canine genome<sup>19</sup>. A number of articles have recently identified remarkable cytogenetic similarities between the two species, Khanna *et al.*,<sup>18</sup> found canine and human osteosarcomas were surprisingly similar genetically, and greater differences were found between osteosarcoma types than between species. This was confirmed by recent comparative genomic hybridization array (aCGH) and in-situ hybridization experiments in dogs with naturally occurring osteosarcoma<sup>19</sup>. Indeed gene expression profiling has identified genes associated with long- and short-term survival in canine osteosarcoma<sup>150</sup>.

**Table 2-2: A summary of the mutated oncogene and tumour suppressor genes found in humans and dogs with osteosarcoma.**

Species	Oncogenes	Tumour suppressor genes
Canine	<i>c-myc</i> <sup>151</sup> , <i>MDM2</i> <sup>37</sup> .	<i>TP53</i> <sup>36, 37, 151-157</sup> , Retinoblastoma ( <i>Rb</i> ) <sup>36, 37</sup> .
Human	<i>c-myc</i> <sup>35</sup> , <i>MDM2</i> <sup>35</sup> , <i>SAS</i> <sup>34</sup> , <i>c-fos</i> <sup>34</sup> , <i>ERBB2</i> <sup>34</sup> .	<i>TP53</i> <sup>35</sup> , Retinoblastoma ( <i>Rb</i> ) <sup>35</sup> , <i>CDKN2A</i> (p16 <sup>INK4A</sup> , p14) <sup>34</sup> , <i>CDK4</i> <sup>34</sup> , cyclin D1 <sup>34</sup>

Legend: Mutated oncogenes and tumour suppressor genes reported to be common to both species are the *c-myc* and *MDM2*, and *TP53* and *Rb* respectively. *c-Myc* is a regulator gene that encodes for the transcription factor myc, which when mutated leads to persistent (constitutively) expression of multiple genes and uncontrolled growth. MDM2 protein is a negative regulator of the tumour suppressor p53 via a number of pathways. The p53 tumour suppressor protein along with pRb regulates the cell cycle conserving genomic stability by preventing mutations. Convention dictates that genes are abbreviated in italics e.g. *c-myc* and the encode gene product, if a protein, is preceded by the prefix p, e.g. p53. Nevertheless, this convention is often not followed.

### 2.1.1 Canine Osteosarcoma

In the dog, 85% of skeletal cancer is diagnosed as osteosarcoma (OSA). OSA usually affects middle-aged to old dogs with a median of 7 years. Young dogs may also be affected, especially the rib<sup>158</sup>. There is clearly a predilection for large and giant breeds of dogs as was found in a study by Ru *et al.*,<sup>159</sup> showing the risk of osteosarcoma increases with an increase in body weight, (breed) standard weight and (breed) standard height<sup>159</sup>. When compared to the

German Shepherd breed, the highest risk for osteosarcoma was found for giant large breeds<sup>159</sup>. A two-fold greater risk was observed for neutered dogs<sup>159</sup>. Smaller dogs do develop OSA and are reported to have a greater incidence of metastatic bone cancer when compared to large breeds<sup>160</sup>. There also appears to be a greater frequency of axial skeleton OSA with no predilection to the distal radius<sup>160</sup>. OSA has also been reported to undergo spontaneous remission<sup>161</sup>. The majority (75%) of OSA occurs in the appendicular skeleton. The metaphyseal region of long bones is the most common primary site, with the forelimbs being affected twice that of the hind limbs<sup>162</sup>. In the forelimb the distal radius and proximal humerus are the most common locations<sup>162</sup>. Unusual sites on the appendicular skeleton have also been reported these include: the patella<sup>163</sup>, femur head, proximal femur<sup>33</sup>, metatarsal and metacarpal bones<sup>164</sup>. On the axial skeleton, OSA has been reported to occur on the skull, mandible, zygomatic arch, nasal turbinates, and vertebrae<sup>103, 165-169</sup>. Extraskeletal OSA is rare, but OSA can occur in many and varied soft-tissues<sup>170-173</sup>. The accepted histopathological classification is based on a WHO series volume by Slayter *et al.*,<sup>174</sup> and is described in Table 2-3 seen below. Classification of OSA is based on the type and amount of matrix and characteristics of the cells: osteoblastic, chondroblastic, fibroblastic, poorly differentiated, and telangiectatic<sup>175</sup>. These subclasses of OSA have not demonstrated a difference in the biologic behaviour of dogs, however the histologic Grade 3 has been found to be an independent negative predictor of clinical outcome<sup>175</sup>.

**Table 2-3 Histopathological classification of canine osteosarcoma**

Malignant Bone Tumour	Position in bone	Description
Osteosarcoma	Marrow cavity	Poorly differentiated
		Osteoblastic
		Productive
		Chondroblastic
		Fibroblastic
		Telangiectatic
		Giant cell type
Osteosarcoma	Peripheral	Periosteal osteosarcoma
		Parosteal osteosarcoma
Multilobular tumour of Bone	Marrow cavity	Osteosarcoma like in appearance

Legend: The Table is a adapted from the WHO Series on tumours of domestic animals<sup>174</sup>. Canine osteosarcoma most commonly arises in the marrow cavity. The osteoblastic osteosarcoma is the more common clinical presentation found in dogs. The various forms of osteosarcoma arising from the marrow cavity are not associated with prognosis.

OSA is aggressive, with metastasis to the lungs arising early in the course of the disease. Less than 5 % of dogs have radiographically detectable pulmonary metastasis at presentation, approximately 90 % will die of metastasis within 1 year following amputation. Metastasis via the haematogenous route commonly occurs but, on rare occasions, extension to regional lymph nodes may occur<sup>175</sup>. The biologic behaviour of OSA of the mandible is an exception with dogs undergoing mandibulectomy having approximately a 70 % 1-year survival rate<sup>103</sup>.

Diagnostic work up of canine osteosarcoma (OSA) involves interpretation of good-quality radiographs of the local site taken in lateral and craniocaudal positions<sup>176</sup>. Radiographic abnormalities of bone affected by cancer vary from osteolysis to osteogenic changes. Bone tumours do not readily cross articular cartilage and primary lesions can remain monostotic. Tumours often extend into periarticular soft-tissues, and adjacent bones are at risk e.g., ulna with distal radius OSA due to extension through adjacent soft-tissue structures.

Radiological differential diagnoses of lytic proliferate or mixed pattern aggressive bone lesions, include primary bone tumour (osteosarcoma, chondrosarcoma, fibrosarcoma, hemangiosarcoma), multilobular osteochondrosarcoma, multiple cartilaginous exostoses, metastatic bone cancer, multiple myeloma or lymphoma of bone, systemic mycosis with bony localization, and bacterial osteomyelitis<sup>176</sup>. Signalment and history help to narrow the diagnostic possibilities. However, confirmation is based on histopathology. Radiographs primarily confirm radiologic detection of metastasis and four views are generally recommended to detect metastatic disease. Helical-CT has been reported in a comparison with conventional radiographs to improve detection of metastatic disease, however results were inconclusive and may over diagnose metastatic disease<sup>177</sup>. In an effort to identify the full extent of the primary OSA especially for limb salvage therapy, radiographs, CT, and MRI were compared<sup>178</sup>. Davis *et al.*,<sup>178</sup> reported that their measurements obtained by use of craniocaudal radiographic views were most accurate at predicting tumour length even though they underestimated tumour length substantially in one limb and slightly in another limb. Measurements made by CT were most accurate at predicting tumour length when intramedullary fibrosis was taken into account, but underestimated tumour length in one limb. Measurements made by MRI were least accurate but did not underestimate tumour length in any of the limbs. In contrast, a recent report<sup>179</sup> found MRI was accurate but overestimated actual tumour size by 3 SD±13%. Radiographs (craniocaudal), CT, and



scintigraphy overestimated tumour volume by 4 SD±26%, 27 SD±36%, 14 SD±28% respectively. Other findings included T1-weighted non-contrast images, which were superior in identifying intramedullary tumour margins in most instances. Contrast-enhanced images provided some important supplemental information.

Nuclear scintigraphy has also been used to determine the extent of OSA invasion in the adjoining bone<sup>180-184</sup>. Scintigraphy, in comparison to radiographs, overestimates the extent of the tumour due to inclusion of reactive bone, however Liebman *et al.*,<sup>180</sup> concluded that scintigraphy was beneficial in limb salvage workup. Nevertheless, caution was stressed because of the over estimation of tumour size resulting in dogs being excluded as candidates for surgery. Scintigraphy is also not specific for OSA, but rather identifies only areas of increased bone turnover<sup>184</sup>. Clinical staging of canine osteosarcoma uses the TNM classification system and is described in Table 2-4 below<sup>185</sup>.

**Table 2-4 Clinical staging of canine osteosarcoma**

Score	Definition
T0	No evidence of primary tumour
T1	Tumour confined to within bone medulla/cortex
T2	Tumour extending beyond periosteum
N0	Negative regional lymph node
N1	Positive regional lymph node (not commonly found)
M0	No evidence of metastases
M1	Distant metastases present

Legend: The TNM Classification of Malignant Tumours (TNM) is a cancer staging system that describes the extent of a cancer, where T describes the size of the primary tumor and whether it has invaded nearby tissue, N describes regional lymph nodes that are involved, M describes distant metastasis.

Diagnosis is primarily by bone biopsy and may be performed as an open incisional, closed needle, or trephine biopsy. Although closed biopsy with a Michelle trephine yields a diagnostic accuracy rate of 93.8 %, there is increased risk of creating pathologic fracture than with a smaller gauge needle. Jamshidi needle biopsy is less likely to be associated with complications and has an accuracy rate of 91.9 % for detecting tumour versus other disorders and an 82.3 % accuracy rate for diagnosis of the specific tumour subtype<sup>20</sup>.

Prognostic significance was found for serum alkaline phosphatase activity in dogs with appendicular osteosarcoma. High serum total alkaline phosphatase (TALP) and bone-specific alkaline phosphatase (BALP) activities before surgery were significantly associated with shorter survival and disease-free intervals in dogs undergoing surgery (amputation or limb-sparing procedure) and adjuvant chemotherapy<sup>186, 187</sup>.

Amputation of the effected limb has been reported to give a mean survival time of 19.8 weeks with 11.5 % alive at one year and 2 % at 2 years<sup>188-190</sup>. Currently the gold standard is still amputation together with cisplatin / carboplatin chemotherapy<sup>178, 191-193</sup>. Cisplatin, used either alone or in combination with doxorubicin (Adriamycin)<sup>194</sup> or liposome-encapsulated muramyl tripeptide-phosphatidylethanolamine (LMTP)<sup>195-197</sup>, has improved survival of dogs with osteosarcoma. It is recommended that adjuvant chemotherapy be administered as close to the time of surgery as possible, however it is still unknown if chemotherapy given early has any benefit on survival<sup>198</sup>. On average five doses of cisplatin at 70 mg/m<sup>2</sup> is administered every 3 weeks together with amputation or limb sparing. This protocol gives a median survival of 392 days, with a 1-year survival rate of 52 % and a 2-year survival of 31 %. Saline diuresis is vital in preventing nephrotoxicity, the dose-limiting toxicity in dogs, with cisplatin. Carboplatin, a less nephrotoxic drug than cisplatin, when used with appendicular OSA and amputation (four doses of carboplatin) gave a median survival of 321 days, and 35.4 % of dogs alive at 1 year<sup>199, 200</sup>. The advantage with carboplatin is that it can be given intravenously without the saline diuresis. Carboplatin together with amputation is dosed at 300mg/m<sup>2</sup> every 21 days. Toxicity is associated with myelosuppression, however the maximum tolerated cumulative dose has not been described. A number of reports using cisplatin / carboplatin combined with doxorubicin seem to have shown improved results<sup>194</sup>, nevertheless recent reports show no added advantage over single agent chemotherapy<sup>201</sup>. See Table 2-5 on page 91 for more detail on protocols and median survival times<sup>20</sup>.

**Table 2-5 A summary of the median survivals times of dogs with osteosarcoma receiving chemotherapy and surgery**

Drug	Regime	Survival
Cisplatin	70 mg/m <sup>2</sup> every 3 weeks for 4-5 cycles	Median 262-282 days 38-43% alive at 1 year 16-18% alive at 2 years
Carboplatin	300 mg/m <sup>2</sup> every 3 weeks for 4 cycles	Median 321 days 35.4% alive at 1 year
Doxorubicin	30 mg/m <sup>2</sup> every 2 weeks 5 cycles	Median 366 days 50.5% alive at 1 year
Doxorubicin and Cisplatin	Variable regime, dose reduction used	Median 300-470 days 37%-48% alive at 1 year
Doxorubicin and Carboplatin	Doxorubicin day 1 30mg/m <sup>2</sup> followed by carboplatin at day 21 300mg/m <sup>2</sup> . Cycle is repeated every 3 weeks for 4-6 cycles	Median 202 days

Legend: Adapted from Small Animal Clinical Oncology, 3<sup>rd</sup> Edition <sup>20</sup>. Single agent chemotherapy drug protocols are more commonly used for the treatment of osteosarcoma in dogs in comparison to human where multiple drug protocols are used. The majority of chemotherapy drugs are dosed using the meter squared (body surface area – [m<sup>2</sup>]) dosing tables as it is thought to be a better indicator of metabolic mass than body weight. Nevertheless, there are significant caveats when using this system e.g. variations in drug clearance between individuals.

Although most dogs function well with amputation, there is a large population of dogs that precludes the use of amputation as a treatment option for various reasons: size of the animal, breed, concurrent diseases, owners' resistance to amputation. In the search for an alternative treatment Heidner *et al.*, <sup>202</sup> reported the use of cobalt-60 radiation and intra-arterial cisplatin without amputation. Their reported overall survival times were a median of 34.3 weeks, when dogs with metastases were excluded the median survival was 46.9 weeks. Unfortunately, this treatment option is not always available. Another option is limb-sparing surgery, which encompasses tumour removal with bone reconstruction involving either cortical bone allografts or metal prostheses <sup>178, 192, 203-206</sup>. Limb-sparing surgery together with chemotherapy offers no significant advantage in survival times when compared with dogs treated with amputation and cisplatin. Logistics and complication include supply of allografts (bone bank), coordinated team effort, recurrent local disease, and allograft infection.

The use of radiopharmaceuticals in canine osteosarcoma has been reviewed in section 1.6.3 on page 58 and will not be discussed here.

Pain control in bone cancer is vital and particularly with aggressive bone tumours such as osteosarcomas<sup>207, 208</sup>. On initial diagnosis, all dogs with OSA should receive non-steroidal anti-inflammatory drugs (NSAIDS). Where the disease is diagnosed as advanced, the inclusion of narcotic analgesics should be considered. The use of bisphosphonates, such as pamidronate and alendronate should also be considered as an adjunct to normal pain therapy. Early reports indicate that bisphosphonates may be of benefit in pain control as well as exerting a direct effect on the cancer<sup>94 61</sup>

Multilobular osteochondroma sarcoma (MLO), a related cancer to OSA, is an uncommon bone tumour in dogs that recurs following incomplete surgical removal. In a 1998 report of 39 dogs by Dernell WS *et al.*,<sup>209</sup> surgery was performed on 37 dogs with 13 cases found to have incomplete margins. Incomplete resection, tumour grade, and tumour location were all found to have a significant effect on time to local recurrence.

### 2.1.2 Experimental Model Techniques for Quantitative Radiopharmaceutical Biodistribution: Data Acquisition and Analysis for Radiation Dose Estimates

The absorbed radiation dose to the body in targeted radiotherapy is vital when predicting probable tissue response to the therapy. Although direct measurement is preferable *in vivo*, this is not possible in the clinical setting<sup>210</sup>. The absorbed dose is derived from an estimate made from the following: localized uptake and retention (biodistribution), the known radiation decay data for the radionuclide, and simulations of radiation transport in anthropomorphic models<sup>210</sup>.

To understand the internal radiation dose received by the patient, a number of models have been proposed and are published as Medical Internal Radiation Dose (MIRD) pamphlets<sup>210</sup>. These pamphlets consist of mathematical representations of the human body (anthropomorphic models) that provide the absorbed radiation MW-fractions and organ masses. No model exists for dogs, thus we selected the 32 kg human model from MIRDOSE 3 software for the purposes of this study<sup>211</sup> as the average weight of the dogs in the study was comparable.

There are inherent errors with extrapolating external beam information to internally dosed emitters that have highly variable dose rates and are delivered over protracted periods of time<sup>210</sup>. In an effort to improve experimental design for this study, we followed recommendation

made in MIRD Pamphlet-16<sup>210</sup>. Recommendations made in the MIRD Pamphlet-16 are discussed in detail later under the following headings: MIRD Schema, data collection, temporal sampling, study category, data acquisition methods, analysis and processing of the data<sup>210</sup>. More accurate methods have been developed to calculate absorbed dose but were not implemented in this study including dose point kernels and Monte Carlo simulation<sup>212</sup>. Complimentary methods including blood and urine sampling and autoradiographic techniques were used in the study. Autoradiographic techniques employ either direct film measurements (employed in the study) or high-resolution detectors for imaging and direct digitization. At a cellular level microdosimetry employ electron microscopy autoradiography for distribution within cells<sup>212</sup>.

### 2.1.2.1 The MIRD Schema

The MIRD Schema consists of a number of Pamphlets that have been published over the years<sup>212</sup> and are reviewed in detail by Stabin in 1999<sup>212</sup>. The MIRD Schema's goal is an accurate determination of the time-dependent activity in the body tissues of a radiopharmaceutical (source e.g., trabecular bone) and its calculated absorbed dose to target regions (e.g., bone marrow) of the body. The term "region" designates sources of radiation in the body and designated targets for assessment of radiation-absorbed dose. The absorbed dose is defined as the energy absorbed per unit mass<sup>210</sup>. The mean dose in the MIRD Schema is given as:

#### Equation 2-1

$$\bar{D} = \tilde{A} \times S$$

Where  $\bar{D}$  is the mean absorbed dose in Gy or rad,  $\tilde{A}$  is the accumulated activity in Bq/sec or  $\mu\text{Ci/hr}$  and  $S$  is the mean absorbed dose per unit activity cumulated in Gy/Bq.sec or rad/ $\mu\text{Ci/hr}$ .  $S$  is given in the MIRDOSE 3 software for the specific anthropomorphic model (known as  $S$ -tables). The  $S$ -tables make the assumptions that the activity in the organs is homogenous and that the organ mass is standardized<sup>212</sup>. These assumptions can be erroneous since organs are often not homogenous and for obvious reasons, there are variations in organ size amongst individuals<sup>212</sup>. The absorbed dose to target can also be expressed as absorbed dose per unit administered activity,  $A_0$  (Bq or  $\mu\text{Ci}$ ) and the source region residence time  $\tau$ , defined as  $\tau = \tilde{A} / A_0$ . Therefore, the mean dose to the target per unit-administered activity is given as:

### Equation 2-2

$$\bar{D}/A_0 = \tau \times S$$

Time-dependent (biokinetic) factors: those incorporated within  $\tau$  or  $\tilde{A}$ , incorporate characteristics of both uptake and retention of activity in the region of interest (ROI), and include the physical half-life of the radionuclide and the biologic half-life of the radiopharmaceutical.

- Time-independent (physical) factors: those represented by  $S$ . These are types and energies of the radiation emitted, geometrical aspects, distance between them and composition of absorbing and intervening media of the source and target regions.

The three phases involved in the determination of the absorbed dose are:

- Data collection: identification of the source regions (which would be the ROI containing activity), the determination of temporal sampling and acquisition of counts or radioactivity within ROI.
- Data analysis: calculation of the activity in the ROI as a function of time. This would include calibration factors obtained from quantitative techniques
- Data processing: Integration of the time-activity curves to obtain the sum of all nuclear transitions, cumulated activity  $\tilde{A}$ , or residence time  $\tau$  for each source region (ROI).

The authors of newer computer software known as OLINDA/EXM<sup>213</sup> contend that the software expresses the dose equation in a more understandable concept:

### Equation 2-3

$$\bar{D} = N \times DF$$

Where  $N$  is the number of disintegrations that occurs in the source organ and is numerically equal to MIRD schema's source region residence time  $\tau$ , which is defined as  $\tau = \tilde{A}/A_0$ <sup>213</sup>. The contention is that the term disintegrations are more intuitive than residence times. The term  $DF$  is mathematically the same as  $S$  values derived from the MIRD Schema.

### 2.1.2.2 Data Collection

Identification of source regions for this study follows guidelines as recommended by Siegel *et al.*,<sup>210</sup>. To identify source regions accurately, four basic data groups that should be included are: imaging, whole-body or region counting, tissue sampling (blood) and excreta (urine). For the purposes of this study source regions were identified as areas in dog showing significant uptake. In most cases these were in the following order: cardiac region, liver, left kidney, right kidney, trabecular bone (metaphysis of the long bones), cortical bone (diaphysis of the long bones) and background (an area over a muscle group showing low uptake) and tumour areas. Blood sampling plus urine collection was designed into the study to meet the requirements of total body retention. The accuracy of using source regions lies with the possibility of overlap between organs. Software such as Sophy\* interfaced with the gamma camera† allowing for the drawing of region of interests (ROI) conforming to the shape of the source regions e.g. see Figure 3-2 on page 117.

Traditionally scintigraphy bone study consists of three phases. The first-phase is the flow phase, which demonstrates perfusion to the lesion for the first few seconds followed by the second-phase, which is the relative vascularity or blood-pool image, which is obtained in the first 5 minutes. The third or bone image phase is obtained 3 to 4-hours later and in some cases, a 24-hour scan is done. For the purposes of this study, in order to capture organ and bone biodistribution data, a dynamic-phase scan (1-minute acquisitions x 60 minutes) was done for the first hour, which encompasses a combination of phases-1 and -2 of the conventional bone study. This was followed by sequential 1-hour static scans for 3- to 4-hours which corresponds to phase-3 of a bone scan. Dynamic and static imaging allows for sequential acquisition of data over time for pharmacokinetic analysis of the radiopharmaceutical.

---

\* Sophy Forthmacs. Software Version 3.01, Copyright (c) 1995 SMV, Sophy Medical, B-1831 Diegem Kouterveldstraat 20, BELGIUM

† Camera: Siemens Orbiter Stand: 094-200024, Rev. A. 1989 Siemens Gammasonics, Inc. 2000 Nuclear Drive, DesPlaines, IL 60018. Camera Head: Siemens ZLC Digitrac Processor, 094-200013, Rev. F. 75 tubes. Collimator: 140 KEV Low Energy all-purpose Parallel Hole. Peak analyzer - Siemens Operators Terminal: 094-200011, Rev. E. 1989 Siemens Gammasonics, Inc. 2501 North Barrington Road, Hoffman Estates, IL 60195-7372, P.O. Box 957372.

### 2.1.2.3 Temporal Sampling

To meet the statistical requirements for dosimetry, a data acquisition protocol requires an adequate number of serial data collection points. The more data points collected the more accurate the data fit. To calculate the absorbed dose requires that the whole body uptake, washout, and long-term retention data be recorded. The pharmacokinetic models that can be recognized in the source regions are: instantaneous uptake (wash-in) with no biologic removal, instantaneous uptake with removal by both physical decay and biological elimination (washout), non-instantaneous uptake with no biological removal, non-instantaneous uptake with removal by both physical decay and biological elimination (washout)<sup>210</sup>. By definition, the uptake is described by the time to maximum concentration ( $T_{max}$ ). Washout is defined as the decrease from the  $T_{max}$  and is representative of the elimination from the ROI or central compartment, and is a function of the physical half-life of the radionuclide and the biological half-life of the radiopharmaceutical. This phase in blood commonly follows first order kinetics as represented in pharmacokinetic terms by a bi-exponential curve. The first part of the bi-exponential curve after  $T_{max}$  is denoted by the term  $t_{1/2-\alpha}$  and is representative of the distribution of the radiopharmaceutical to other compartments, followed by the second term  $t_{1/2-\beta}$ , which is representative of elimination from the body.

It is important to remember that biological washout may be longer than the physical half-life of the radionuclide and since the radionuclide is used as the tracer for biodistribution in the body, calculations to determine the biological half-life of a radiopharmaceutical must include radionuclide decay correction. See section 2.1.2.6 on page 100 for more details.

Serial sampling points were used in this study to determine the residence time for the particular radiopharmaceutical at the relevant source ROI. The residence time is defined by the area under the time-activity-curve (AUC) of accumulated activity  $\tilde{A}$  for a specific ROI, divided by the administered activity  $A_0$ . Siegel *et al.*, recommends 2 to 3 sampling points are required for each exponential phase of the retention curve<sup>210</sup>. For purposes of this canine study, the experimental design had serial sampling points every 1 second from the source ROI giving > 3 data points per phase of the exponential curve. Thus, multiple sampling points achieved accurate determination of residence times for the canine studies. Blood and urine were also serially collected for multiple time points. Multiple serial collections excludes errors with rapid uptake



where overestimation of the AUC due to too few collections points early on will overestimate the time to maximum concentration ( $T_{max}$ ). In the case of long retention times, too few collections point in the late phase of the washout will underestimate the AUC, especially in the case of radionuclide with a longer half-life e.g.,  $^{186}\text{Re}$   $T_{1/2} = 89$  hours<sup>210</sup>. To characterize long-term retention (tissue trapping or incorporation) sample points should be equal to multiples (2-5) of the effective half-life<sup>210</sup>. Unfortunately, this was not achievable in all cases due to the prolonged anaesthetic times of greater than 3-4 hours in some dogs. However, as discussed later in section 2.1.2.6 the dosimetry software, OLINDA calculates the long-term retention by fitting the data to infinity. By convention infinity would be equal to 10.5 times the half-life of the radionuclide<sup>122</sup>.

#### 2.1.2.4 Study Category

Siegel<sup>210</sup> recommends three general categories to describe the experimental status of a new radiopharmaceutical;

Category-1 where neither in-vivo animal studies nor human trials have been done;

Category-2 where data exist for at least two animal studies and initial human data exist:

Category-3 where extensive data exists and phase 1 and 2 clinical trials have been completed.

In Category-2 designed studies, the selection for sampling points can be based on the following information:

- Previously acquired data in other animals<sup>21</sup>.
- Computer modelling<sup>1</sup>.
- Assumption based on the physical half-life of the radionuclide or the effective biological half-life of the radiopharmaceutical in blood or ROI.
- The chemical and physical characteristics of the radiopharmaceutical based on the molecular weight (MW) and size and ionization potential<sup>210</sup>.

All the experimental work in this study was classified as Category-2.

#### 2.1.2.5 Data Acquisition

Measuring techniques used for data acquisition include the following: quantitative imaging using planar gamma camera (PGC) or tomographic SPECT or PET. For the purposes of this study, only aspects pertaining to PGC will be discussed. Factors that influence the accuracy

of quantitating radiation using PGC are <sup>210</sup>: energy resolution limitations, degradation of spatial resolution due to collimator septal penetration by high-energy photons and scattered radiation, statistical noise associated with low count densities and attenuation. Numerous review articles have been published and were used in the study preparation <sup>141</sup>.

Errors inherent in the single view PGC can be accommodated using conjugate view counting <sup>210</sup>. In cases where a single view PGC is used, a single-view effective point source method can be used <sup>210</sup>.

#### 2.1.2.5.1 Conjugate view counting

Conjugated view counting (CVC) employs an imaging method for quantification of radioactivity using a 180° opposed planar images (e.g., anterior-posterior view A/P) in combination with transmission data through the subject and a system calibration factor C <sup>210</sup>. This method provides correction for source thickness (ROI), inhomogeneity, and attenuation <sup>210</sup>. Information derived for attenuation, is done using a transmission scan, which involves counting an external source of radioactivity through the source ROI before the administration of the radiopharmaceutical. When using a single head system, a system calibration factor is required to convert the source ROI count rate into absolute activity. CVC uses mathematical formulas to explain following models:

##### Discrete Source Regions and Negligible Surrounding Background Activity:

This model makes the assumption for a single uniform source of uniform thickness embedded in a non-radioactive background. It is expressed in the formula where  $A_j$  represents a single discrete source region <sup>210</sup>;

##### **Equation 2-4**

$$A_j = \sqrt{\frac{I_A I_P f_j}{e^{-\mu_e t} C}}$$

The symbols  $I_A$  and  $I_P$  represent the conjugate-view counting pair (e.g., anterior posterior views) over time. The symbol  $f_j$  represents a correction for the source region attenuation coefficient and source thickness. The expression  $e^{-\mu_e t}$  represents the transmission factor across the patient taking into account thickness  $t$  through the ROI with the overall effective linear attenuation coefficient

$e_u$ . The attenuation coefficient is measured by the ratio of count rates for a particular radionuclide with and without the patient in position. The system calibration factor is  $C$  described as the count rate per unit activity and is obtained by counting a known source of activity for a fixed period of time in air relative to the gamma camera. The equation can also be solved for an overlapping source region.

#### Background Subtraction:

Background subtraction can be used for a single well-defined source region surrounded by regions of background activity. The ROI is often surrounded by radioactivity residing in surrounding soft-tissue. Equation 2-4 would overestimate the activity for that ROI because of contributions made from tissue overlying and below the ROI. Conventional background subtraction, where the background count rate is subtracted from the ROI count rate, does not consider the portion of the background equivalent to the source region volume. It may lead to underestimation of the ROI activity due to over subtraction of background. Selection of the ROI for background is therefore crucial and should avoid hot or cold areas e.g., blood vessels. A mathematical formula for background subtraction is given (uniform background activity) as a MW-fraction of the geometric mean counts;

#### **Equation 2-5**

$$F = \left\{ \left[ 1 - (I_{ADJ} / I_A)(1 - t_j / t) \right] \left[ 1 - (I_{ADJ} / I_P)(1 - t_j / t) \right] \right\}^{1/2}$$

Where  $I_A$  activity counted in the anterior view,  $I_P$  is the activity in the posterior view.  $I_{ADJ}$  is the activity recorded adjacent to the ROI,  $t$  denotes the body thickness at that point, and  $t_j$  is the ROI thickness. The  $F$  is applied as a factor to the geometric means  $F(I_A I_P)^{1/2}$ . Because the majority of the study was completed prior to publication of MIRD Pamphlet-16, only background subtraction was used in the canine study.

#### Correction for Scattered Photons:

The above equations are derived under the narrow-beam geometry in which the scatter effects are negligible. Using high-resolution collimators and narrow asymmetric energy windows can reduce scatter. However, in most cases, this is not achieved in nuclear medicine facilities and therefore scatter can be significant<sup>210</sup>. The sources of the error are due to scattered photons that

arise outside the ROI, which can introduce error into quantification of activity. A number of models are employed to correct for scatter, these are: pseudo extrapolation number, build-up factor method, multiple energy window techniques<sup>210</sup>. However, these were not used in the current study.

Whole body retention can also be determined using non-imaging techniques: external non-imaging radiation monitoring, tissue sample counting, and excreta counting. External monitoring can be estimated by placing a standard shielded sodium-iodine detector or other suitable survey meter, 3 to 7 m distant from the patient and recording the number of counts detected<sup>210</sup>. A source of known activity is used to calibrate the detector.

To determine accurately bone marrow dosimetry the haematocrit and red marrow fluid and extracellular fluid MW-fraction should be obtained. The temporal variation in activity is important in determining central compartment function and bone marrow dosimetry. Activity can be determined using gamma well counters\* or scintillation counters†. This study used multiple serial collections of 2 ml blood samples to determine central compartment activity over time. For calculation purposes, total blood volume for the dogs was estimated at  $75.00 \pm 6$  ml/kg<sup>214</sup>. Another approach is to use blood pool analysis generated from conjugate views of the heart (left ventricle or aorta)<sup>210</sup>. Although this technique has been validated, it does have inherent errors compared to blood collection. These occur because of overlapping ROI e.g., sternum, lungs or myocardium<sup>210</sup>. Whole body retention was calculated for the canine study by subtracting the total eliminated activity in urine (collected from multiple serial urine samples over 3-4 hours) from the total injected activity (all calculations were corrected for radionuclide decay).

#### 2.1.2.6 Data Processing

The activity [ $A_{ROI}(t)$ ] is derived from serial gamma camera measurements of the ROI and urine activity ( $A_{urine}$ ) plotted as a function of time ( $t$ ) which are used to give the area under the time-activity curve ( $\tilde{A}$ )<sup>210</sup>. The cumulated activity ( $\tilde{A}_h$ ) for a ROI is the sum of all the nuclear transitions for that area. The residence time ( $\tau_h$ ) is obtained by dividing the ROI cumulated activity ( $\tilde{A}_h$ ) by the administered dose ( $A_0$ )<sup>215</sup>.

---

\* Capintec counter (Model CRC-15R), Radioisotope Dose Calibrator

† Sodium-iodide well crystal counter linked to Oxford PCA 3 gamma spectrometer system

For all our experimental animals, the data was processed in the following manner to arrive at the mean absorbed dose (D) per ROI. The total body ( $A_{Body}$ ) retention of the radiopharmaceutical was calculated by subtracting the total accumulated urine activity ( $A_{urine}$ ) from the injected dose ( $A_0$ ). The calculation is represented by the equation below:

### Equation 2-6

$$\int_0^T A_{Body} \cdot dt = \int_0^T A_0 \cdot dt - \int_0^T A_{urine} \cdot dt$$

The integral ( $\int$ ) reflects the sampling over interval time ( $T$ ) of 0 to 4 hours. However,  $A_{Body}$  was composed of a number ROI that were identified during dynamic imaging and thus the equation can be written;

### Equation 2-7

$$A_{Body} = A_{Cardiac\ pool\ (Blood)} + A_{Lung} + A_{Liver} + A_{Kidney} + A_{Proximal\ humerus} \\ + A_{Humerus\ shaft} + (A_{Tumour})$$

Using published data<sup>216, 217</sup> and our phantom data<sup>16</sup>, the following assumptions were made for the bone regions of interest. We took the proximal humerus ROI to be primarily trabecular bone and the shaft ROI as cortical bone. We were able to show these assumptions were valid by subsequent research in the distribution of trabecular and cortical bone in the proximal and mid-shaft of the canine humerus, see Figure 2-1 below on page 103. The equation could therefore be expressed as follows:

### Equation 2-8

$$A_{Body} = A_{Cardiac\ pool\ (Blood)} + A_{Lung} + A_{Liver} + A_{Kidney} + A_{Trabecular\ Bone} + A_{Cortical\ bone} \\ + (A_{tumour})$$

From the time-activity curves, the percentage organ distribution (%OD) was calculated for each region of interest. The activity in the body was then used to determine the percentage-injected dose (% ID) for different ROI. The decay corrected % ID for each ROI and accumulated urine activity was entered into the OLINDA software package for exponential modelling (EXM module)<sup>213</sup>. This program allows the user to enter pharmacokinetic data (% ID) to fit to one or

more exponential terms<sup>218</sup>. The program extrapolates the data taking in to account the radiopharmaceuticals effective half-life ( $T_e$ ) which is a function of the physical half-life of the radionuclide ( $T_p$ ) and the biological half-life of the radiopharmaceutical ( $T_b$ ) in the body-organ<sup>219</sup>. The relationship between  $T_e$ ,  $T_p$  and  $T_b$  is given by the equation;

**Equation 2-9**

$$T_e = \frac{T_p \times T_b}{T_p + T_b}$$

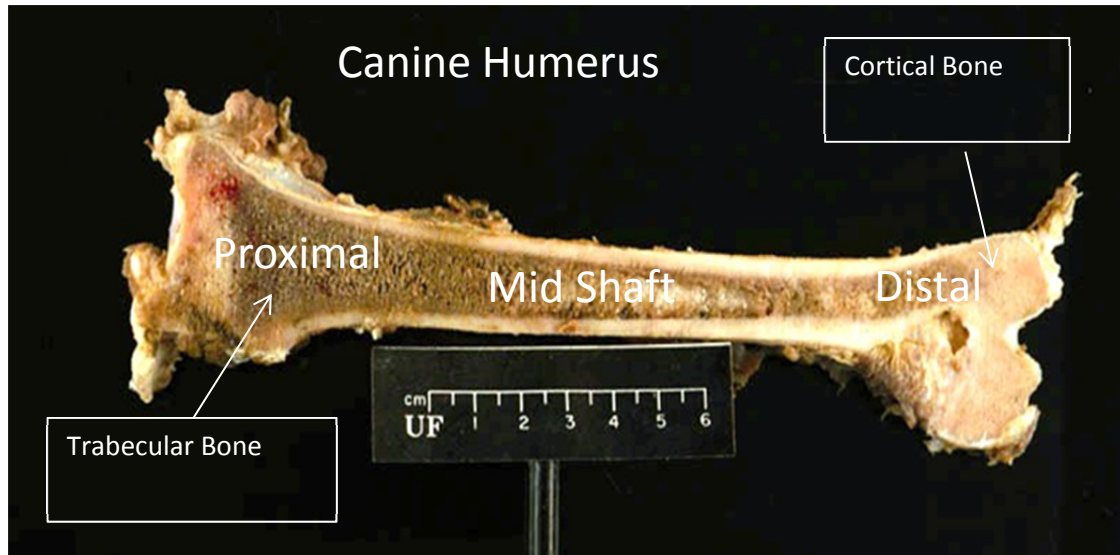
The program will then integrate the fitted time-activity curve to infinity and pass the integral ( $N$ ) back to the OLINDA pharmacokinetics input form for use in dose calculations<sup>218</sup>. The integral  $N$  is the number of disintegrations that occur in the source organs and are numerically equal to MIRD schema's source region residence time  $\tau$ , which is defined as  $\tau = \tilde{A}/A_0$ <sup>213</sup>. Using the previously described MIRDOSE Schema equation:

**Equation 2-10**

$$\bar{D}/A_0 = \tau \times S$$

The mean dose to the target per unit-administered activity (mGy/MBq) was derived using OLINDA  $S$ -value tables. In addition, we were able to compare the data from OLINDA with the University of Florida canine model<sup>16</sup>, which has dog specific  $S$ -value tables.

**Figure 2-1 A longitudinal section through the canine humerus showing the contribution of trabecular and cortical bone to the proximal and mid-shaft ROI.**



Legend: The longitudinal section through the humerus of a dog shows the relative contribution of red marrow (dark material) and fatty marrow (lighter material) in the bone. Pichardo *et al* (2011)<sup>220</sup> reported on the relative contribution of fatty tissue to regional sites in the canine humerus. Microscopically the midshaft and distal section is composed primarily of fat cells whereas the proximal humerus is predominately red marrow. The proximal humerus also consists of primarily trabecular bone.

#### 2.1.2.7 Compartmental Modelling

An alternative approach to direct calculating of  $\tilde{A}$  and  $\tau$  is to fit compartmental models to the measured data. This approach is used where it is impractical to measure all time-activity curves for all sources or when there is overlapping source ROI and the researcher wants to express it as a separate time-activity curve. The required known data here are the physiological interactions of these ROI with blood or the direct tissue measurements of the unknown source ROI. For compartmental modelling, a number of assumptions can be made these are: a compartment is a kinetically distinct, homogenous, and well-mixed unit; most models assume linear pharmacokinetics (first-order); and compartmental models are described by a set of differential equations, the parameters of which are the size of the compartment, and the rate coefficient for transfer between compartments<sup>210</sup>. A variety of computer software is available to solve for complex compartment models<sup>210</sup>. Compartment analysis was not done in this study.

## **Chapter 3. Characterization of Canine Osteosarcoma as a Translational Model for Human Bone Cancer Using the Radiopharmaceuticals: $^{153}\text{Sm}$ -EDTMP, $^{188}\text{Re}$ -HEDP and $^{186}\text{Re}$ -HEDP**

### **3.1 Overview**

While early reports exist describing biodistribution and some pharmacokinetic data for  $^{153}\text{Sm}$ -EDTMP (see Table 3-1, below on page 105) in dogs<sup>7, 15, 102, 104, 221, 222</sup>, none were found for  $^{188}\text{Re}$ -HEDP and only one for  $^{186}\text{Re}$ -HEDP<sup>223</sup>. Maxon *et al.*,<sup>224</sup> refers to using two dogs and finding the biodistribution data similar to humans, but does not report the data. None of these studies report time-activity curves that could be used for dosimetry calculations. In order to validate the dog model, primary data such as time-activity curves to describe the biodistribution for all three radiopharmaceuticals were needed. Additional data was also required e.g., bone marrow toxicity data. This section will test the hypothesis that normal dogs and dogs with naturally occurring osteosarcoma, when compared to published human pharmacokinetic, pharmacodynamic data, pain control, dosimetry and toxicity for  $^{153}\text{Sm}$ -EDTMP,  $^{188}\text{Re}$ -HEDP, and  $^{186}\text{Re}$ -HEDP will be similar in appearance making it a good radiopharmaceutical translational model. Positive results from this section will allow us to use the dog to test novel ligands conjugated to radionuclides in a preclinical animal model.



**Table 3-1 Data showing pharmacokinetics and bone localization of  $^{153}\text{Sm}$ -EDTMP in humans and animals**

Studies Parameter	Dogs (Appelbaum <i>et al.</i> , 1988) <sup>221</sup>	Rats (Goeckeler <i>et al.</i> , 1987) <sup>225</sup>	Rabbits (Goeckeler <i>et al.</i> , 1987) <sup>225</sup>	Baboons (Louw <i>et al.</i> , 1996) <sup>3</sup>	Human (Farhanghi <i>et al.</i> , 1992) <sup>226</sup>	Human (Bayouth <i>et al.</i> , 1994) <sup>122</sup>	Human (Brenner <i>et al.</i> , 2001) <sup>227</sup>
Subjects	6	5	5	6	22	19	18
Tumour Type	Normal animals	Normal animals	Normal animals	Normal animals	Skeletal metastases (multiple cancers types)	Skeletal metastases (type not reported)	Skeletal metastases (mainly prostate and breast carcinoma)
Whole Body (Skeleton)	50-66%	58.54±4.11%	66.3±4.98%	53%	Variable but positively correlated to the number of metastatic lesions	50.4±14 %	47.7%±11.2%
Soft-tissue	NR	NR	NR	NR	NR	No soft-tissue activity on images at 24 hrs.	12.7%±4.7%
Urine	33-50%	46.1±2.85%	34.3±4.4	46%	35.9±13.5%	49.6%	39.5%±13.8%
Blood ( $t_{1/2-\alpha}$ ) min	NR	NR	NR	NR	14 min	5.5±1.1 min	NR
Blood ( $t_{1/2-\beta}$ ) min	NR	NR	NR	NR	690 min	65.4±9.6 min	NR

Legend: Table 3-1 is a compilation of  $^{153}\text{Sm}$ -EDTMP pharmacokinetic data from the literature for humans and animals. The majority of authors make the statement that residual activity in the whole body 24 hours post injection equals skeletal  $^{153}\text{Sm}$ -EDTMP uptake. This was based on scintigraphic images showing mainly bone activity and little if any soft-tissue, blood or urine activity. Unfortunately no blood wash-in ( $t_{1/2-\alpha}$  = distribution phase) or wash-out ( $t_{1/2-\beta}$  = elimination phase) data from preclinical animal studies was reported. The lack of these data formed the basis of the research hypothesis for the canine  $^{153}\text{Sm}$ -EDTMP studies. (NR=data not reported)

**Table 3-2 Data showing pharmacokinetics and bone localization of <sup>186</sup>Re-HEDP and <sup>188</sup>Re-HEDP in humans and animals**

Studies Parameter	Human (Maxon <i>et al.</i> , 1988) <sup>228</sup>	Human (de Klerk <i>et al.</i> , 1992) <sup>229</sup>	Human (Brenner <i>et al.</i> , 2001) <sup>227</sup>	Rabbits (Brenner <i>et al.</i> , 2003) <sup>230</sup>	Human (Liepe <i>et al.</i> , 2003) <sup>231</sup>	Rat (Lin <i>et al.</i> , 1997) <sup>232</sup>
Radioisotope	<sup>186</sup> Re-HEDP	<sup>186</sup> Re-HEDP	<sup>186</sup> Re-HEDP	<sup>186</sup> Re-HEDP	<sup>188</sup> Re-HEDP	<sup>188</sup> Re-HEDP
Subjects	5	11	11	6	13	12
Tumour Type	Skeletal metastases	Skeletal metastases (prostate or breast carcinoma)	Skeletal metastases (mainly prostate and breast carcinoma)	Normal animals	Skeletal metastases (prostate carcinoma)	Normal animals
Tumour	NR	NR	NR	NR	1.45±0.68%	NR
Bone	NR	20%	21.8%±9.0%	31.2±1.5%	46.1±14.8%	NR
Whole Body	55%	20%	34.6%	47.4%	49.3±16.4%	48.27%
Soft-tissue	NR	NR	12.8%±5.4%	16.2±2.7%	NR	
Urine % ID	45-71%	71±6%	65.3%±12.8%	52.6±3.4%	41- 60%	51.73%
Blood t <sub>1/2</sub> min	NR	40.1±5%	NR	NR	NR	NR
Blood (t <sub>1/2</sub> -α) min	NR	NR	NR	NR	NR	NR
Blood (t <sub>1/2</sub> -β) min	NR	NR	NR	NR	NR	NR

Legend: Table 3-2 is a compilation of pharmacokinetic data for <sup>186</sup>Re-HEDP and <sup>188</sup>Re-HEDP radiopharmaceuticals studies. In contrast to <sup>153</sup>Sm-EDTMP, some researchers report soft-tissue uptake between 12% and 16%. Like <sup>153</sup>Sm-EDTMP, no blood wash-in (t<sub>1/2</sub>-α = distribution phase) or wash-out (t<sub>1/2</sub>-β = elimination phase) data from preclinical animal studies was reported. The lack of these data formed the basis of the research hypothesis for the canine <sup>188</sup>Re-HEDP studies. (NR=data not reported)

## 3.2 Research Hypothesis

3.2.1 Hypothesis: That normal dogs and dogs with naturally occurring osteosarcoma, when compared to published human pharmacokinetic, pharmacodynamic data, pain control, dosimetry, and toxicity for  $^{153}\text{Sm}$ -EDTMP,  $^{188}\text{Re}$ -HEDP, and  $^{186}\text{Re}$ -HEDP will be comparable, making it a good radiopharmaceutical translational model.

## 3.3 Specific Aims

In order to prove our hypothesis we propose the following research aims:

- 3.3.1 To determine biodistribution, pharmacokinetics, bone localization, dosimetry of  $^{153}\text{Sm}$ -EDTMP,  $^{188}\text{Re}$ -HEDP and  $^{186}\text{Re}$ -HEDP in the normal dog, using scintigraphy\*.
- 3.3.2 To determine the biodistribution, pharmacokinetics, bone localization, dosimetry of  $^{153}\text{Sm}$ -EDTMP and  $^{188}\text{Re}$ -HEDP in dogs with naturally occurring osteosarcoma using scintigraphy.
- 3.3.3 To compare the results from the canine biodistribution and pharmacokinetic studies of  $^{153}\text{Sm}$ -EDTMP with data available from the human literature.
- 3.3.4 To determine the effect of therapeutic dosages of  $^{153}\text{Sm}$ -EDTMP and  $^{188}\text{Re}$ -HEDP on survival, pain control in naturally occurring canine osteosarcoma.
- 3.3.5 To determine the macro and microscopy distribution of  $^{153}\text{Sm}$ -EDTMP in canine osteosarcoma and in normal rat bone using autoradiography techniques

## 3.4 Ethical approval

All research was done with approval of the Ethics Committee of the Pretoria Biomedical Research Centre, according to the guidelines of the National Code for Animal Use in Research, Education, Diagnosis, and Testing of Drugs and Related Substances in South Africa. Where client owned animals were used, informed, signed consent was first obtained. For an example of the information letter and consent form see Appendix, Section 8.1 & 8.2, pages 272 to 273.

---

\* By definition scintigraphy is the capture of emitted radiation by external detectors (gamma camera) to form two-dimensional images.

### 3.5 Materials and Methods for Scintigraphic Studies in Normal Dogs and a Dog with Osteosarcoma

#### 3.5.1 Samarium-153 Chemistry

$^{153}\text{Sm}$  ( $^{153}\text{Sm}$ ) is a radioisotope produced in a nuclear reactor. This is achieved by neutron irradiation of 99.06% enriched  $\text{Sm}_2\text{-}^{152}\text{-O}_3$  for a period of 50 to 60 hours which yields  $^{153}\text{Sm}^{233}$ . The yielded  $^{153}\text{Sm}$  has a specific activity of 1000 to 1300 Ci/g<sup>233</sup>. The physical characteristics of  $^{153}\text{Sm}$  are given in Table 3-3.

**Table 3-3 Physical Characteristics of  $^{153}\text{Sm}$**

$T_{1/2}$ (days)	Range in tissue (mm)	Beta Emission Energy ( $E_{max}$ , MeV)	Gamma Emission Energy (keV)	% Gamma yield
1.95 (46.7 hr)	0.32	0.8	103	28

$^{153}\text{Sm}$  is complexed to ethylenediamine tetramethylene phosphonic acid (EDTMP) to give a molecular complex of 1 ( $^{153}\text{Sm}$ ): 1 (EDTMP). EDTMP is synthesized by the Moedritzer and Irani method<sup>233</sup> from commercial precursors. EDTMP is also known as leixidronate and is considered a potent amino bisphosphonate with a multidentate binding capability<sup>225</sup>; see Table 1-6 (page 50) for the chemical structure of EDTMP. Ethylenediamine tetramethylene phosphonic acid is complexed with  $^{153}\text{Sm}$  in a single step by adding  $^{153}\text{Sm-Cl}_3$  to a freeze-dried pyrogen free preparation of EDTMP<sup>233</sup>.  $^{153}\text{Sm}$  has been complexed with other chelates but these were found to be unsatisfactory compared to EDTMP<sup>225</sup>. The complex  $^{153}\text{Sm-EDTMP}$  shows excellent stability with no measurable breakdown for at least 48 hours *in vitro* and *in vivo*<sup>225</sup>.

#### 3.5.2 Rhenium-188 Chemistry

Rhenium-188 ( $^{188}\text{Re}$ ) is a therapeutic radioisotope, which is produced from decay of the reactor-produced tungsten-<sup>188</sup>, parent ( $T_{1/2}$  69 days), and can be eluted on demand from the alumina-based tungsten-188 /rhenium-188 generator system<sup>109</sup>. The physical characteristics of  $^{188}\text{Re}$  are listed in Table 3-4.  $^{188}\text{Re}$  is commonly complexed with hydroxyethylidenediphosphonate (HEDP).

**Table 3-4: Physical characteristics of  $^{188}\text{Re}$** 

$T_{1/2}$ (days)	Range (mm)	Beta Emission Energy ( $E_{max}$ , MeV)	Gamma Emission Energy (keV)	% Gamma yield
0.704 (16.9 hrs.)	Max 11 Av. 3.8	2.116 (79%) 1.965 (20%)	155	15%

The generator is eluted with 0.9% saline to give  $^{188}\text{Re}$  as sodium perrhenate. Post-elutional concentration can be achieved using disposable tandem, ion-exchange columns where  $^{188}\text{Re}$  saline solutions are required with specific volumes  $> 500$  mCi/ml<sup>109</sup>. This may prove helpful in extending of the generators shelf life for up to a year, which would provide Rhenium at a reasonable cost for use as a therapeutic radioisotope.

Both  $^{188}\text{Re}$  and  $^{186}\text{Re}$  are chemically similar and are likely to react in a similar fashion to various ligands<sup>224</sup>. However  $^{186}\text{Re}$ , unlike  $^{99m}\text{Tc}$  (trace levels of Tc =  $10^{-4}$  M) or the carrier free tungsten-188 /rhenium-188 generator system, may contain large amounts of carrier ( $10^{-8}$  M)<sup>224, 234</sup>. In a study by Lin *et al.*,<sup>234</sup>  $^{188}\text{Re}$  was used as a Rhenium (Re) tracer. The influence of pH and concentrations of Re-carrier on the preparation of Re-HEDP were investigated. Rhenium-188-Tin-HEDP was prepared by reconstitution of a kit of lyophilized HEDP mixture, and tin chloride with a radioactive solution of perrhenate in saline. Various concentration of Re were used ranging from  $10^{-8}$  to  $10^{-3}$  M. High labelling efficiencies and similar chemical behaviours were obtained for all concentrations with or without carrier. However, biodistribution were found to differ between carrier free and carrier added  $^{188}\text{Re}$ -HEDP. This may significantly affect the preparation of  $^{188}\text{Re}$ -HEDP. Palmedo *et al.*,<sup>111</sup> report that microscopic amounts of stable Re (carrier) are required to form the correct chemical species, and if not added increased accumulation in soft-tissue and reduced bone accumulation is seen. This was also confirmed by Hsieh *et al.*,<sup>235</sup>. Typically a 20 ml saline elution  $^{188}\text{Re}$ -HEDP is concentrated to a volume of 1 ml saline. The 10  $\mu\text{l}$  of stable perrhenate (100  $\mu\text{mol}$   $\text{HReO}_4$  / ml saline 0.9%) is added per ml concentrated  $^{188}\text{Re}$  solution. One ml of this solution is sterilely filtered (0.22  $\mu\text{m}$ ) and added to a HEDP kit (containing 8.3 mg HEDP, 3.0 mg gentisic acid and 39 mg stannous chloride dihydrate). The vials are then heated between 90-100  $^{\circ}\text{C}$  for 15 minutes and then allowed to cool to room temperature. Neutralization is achieved by adding a sterile solution of sodium acetate trihydrate (39mg) and 10 $\mu\text{l}$  sodium hydroxide (32%) per ml yielding a final pH range of 5-6.

Interestingly, gentisic acid present in the  $^{188}\text{Re}$ -HEDP formulation has been found to reduce radiolytic degradation of certain ligands and may have a stabilizing effect on  $^{188}\text{Re}$ -labelled radiopharmaceuticals <sup>109</sup>.

Initial normal biodistribution and skeletal uptake in rats were assessed by Lin *et al.*, <sup>232</sup>. In addition, bony lesions in the tibia were created in three rabbits to explore uptake between normal and pathological bone (lesion/normal ratio L/N). The biodistribution data showed that the radioactivity in the bone tissue was as high as 1.877% ID/g at 1 hr. and that it climbed to 2.017% ID/g at 4 hr. The activity level in the kidney was highest at 1 hr. but declined rapidly throughout the study. The radioactivity in the lung, liver, muscle, spleen, testis, blood, and stool were all lower than 0.3 % ID/g at 1 hr. and declined rapidly. The biological half-life in bone was the longest (60.86 h). In contrast, the biological half-lives in muscle and blood were short (2.99 hr. and 6.21 hr. respectively). Most of the radiotracer was excreted by the urinary system. The lesion to normal bone (L/N) ratio was 4.23+/-0.21 in rabbits injected with  $^{188}\text{Re}$ -HEDP and 4.25+/-0.23 in those injected with  $^{99\text{m}}\text{Tc}$  methylene diphosphonate. Their conclusions suggested  $^{188}\text{Re}$ -HEDP is a very good potential candidate for the treatment of bone metastases because of the following characteristics: it is generator produced, it has a short half-life, it emits gamma rays suitable for imaging, there is highly selective uptake in the skeletal system and bone lesions, and it has a low non-target uptake with rapid clearance in non-osseous tissue <sup>232</sup>.

More recently Scheffler <sup>236</sup> reviewed the application of  $^{188}\text{Re}$ -HEDP as a reactor- or generator-produced nuclide for bone metastases therapy, and concluded it was potentially effective radiopharmaceutical for the treatment of metastatic bone cancer.

### 3.5.3 Rhenium-186 Chemistry

Rhenium-186 ( $^{186}\text{Re}$ ) appears directly below technetium on the periodic table and therefore a similar chemistry could be expected <sup>222</sup>. The  $^{186}\text{Re}$  isotope is produced by irradiating enriched  $^{185}\text{Re}$  <sup>50</sup>. The irradiated metal is dissolved in nitric acid, oxidizes to perrhenate. The dissolved metal is then complexed to HEDP. A low specific activity of obtained  $^{186}\text{Re}$  can complicate the process of labelling <sup>237</sup>. Physical characteristics are listed below in Table 3-5.

**Table 3-5: Physical characteristics of  $^{186}\text{Re}$** 

$T_{1/2}$ (days)	Range (mm)	Beta Emission Energy ( $E_{max}$ , MeV)	Gamma Emission Energy (keV)	% Gamma yield
3.8	0.64	1.07	137	9

Complexation can be difficult because of low specific activity and can result in differences in biodistribution with the early elution showing excellent skeletal uptake, while the latter showed more renal uptake<sup>222</sup>. Animal studies have shown high lesion-to normal bone ratios<sup>224</sup>. In humans, high tumours to marrow ratios (20:1) were found<sup>228</sup>.

#### 3.5.4 Model System and Sample size

To meet the aims and objectives as set out in paragraph 3.3.1 (on page 107), 11 normal dogs were sourced from the Police Dog School Roodeplaat Pretoria and transported to Pretoria Biomedical Research Centre. On arrival, the dog was housed in the designated kennels (approved for radioactivity use). Only a single dog was treated per day. The dogs were returned to the Dog School in the morning of the following day. The dogs were selected for uniformity of breed, gender, and age. Only dogs that were considered healthy by the veterinary staff of the Police Dog School were used. The average weight of the normal dogs was 30 kg (SD±3.28). Table 3-6 (below) displays the normal characteristics of the dogs. The exact ages of the dogs were not known, as these dogs were donations made to the Police Dog School by the public; however, all were judged to be young adults (18-36 months) based on their dentition and physical attributes. All the normal dogs were German Shepherds dogs (GSD).

To address objective 3.3.2 (on page 107), four dogs with histologically confirmed naturally occurring osteosarcomas underwent dynamic scintigraphy. The dog identified as Case-13 in Table 3-6 (see also Appendix, Table 8-14, page 287) received  $^{153}\text{Sm}$ -EDTMP. On admission, the dog was donated by owner due to the extensive nature of the osteosarcoma. Following the dynamic study, she was immediately euthanized and necropsied. Samples from the dog were also secured for autoradiography of the tumour. In addition, three clinical cases underwent dynamic scintigraphy with  $^{188}\text{Re}$ -HEDP followed by a therapeutic dose of the

radiopharmaceutical. The dogs are identified as Cases 1 to 3 in Table 3-6 (see also Appendix, Table 8-21, page 307). All owners signed the informed consent form prior to the study.

**Table 3-6 Population Characteristics of Normal and Osteosarcoma Dogs and Administered Radiopharmaceutical and Dose**

Dogs	Age (yrs.)	Breed	Body Weight (kg)	Sex	Radiopharmaceutical	Diagnostic Dose (MBq)
Normal Dog 1	Young adult	GSD*	27	M	<sup>153</sup> Sm-EDTMP	123.21
Normal Dog 2	Young adult	GSD	34	M	<sup>153</sup> Sm-EDTMP	107.30
Normal Dog 3	Young adult	GSD	27	M	<sup>153</sup> Sm-EDTMP	236.06
Normal Dog 4	Young adult	GSD	28	M	<sup>153</sup> Sm-EDTMP	236.80
Normal Dog 5	Young adult	GSD	29	F	<sup>153</sup> Sm <sup>+3</sup>	179.28
<sup>153</sup> Sm-EDTMP Case-13	13	Rottweiler	35	F	<sup>153</sup> Sm-EDTMP	255.67
Normal Dog 6	Young adult	GSD	34	M	<sup>188</sup> Re-HEDP	185.74
Normal Dog 7	Young adult	GSD	29	F	<sup>188</sup> Re-HEDP	168.35
Normal Dog 8	Young adult	GSD	35	M	<sup>188</sup> Re-HEDP	215.34
Normal Dog 9	Young adult	GSD	33	M	<sup>188</sup> Re-HEDP	193.14
<sup>188</sup> Re-HEDP Case-1	10	Pyr. Mt. dog**	60	F	<sup>188</sup> Re-HEDP	153.92
<sup>188</sup> Re-HEDP Case-2	7	Rottweiler	45	F	<sup>188</sup> Re-HEDP	230.51
<sup>188</sup> Re-HEDP Case-3	8	Rottweiler	56	M	<sup>188</sup> Re-HEDP	233.47
Normal Dog 10	Young adult	GSD	26	M	<sup>186</sup> Re	194.25
Normal Dog 11	Young adult	GSD	30	M	<sup>186</sup> Re-HEDP	200.25

\* GSD = German Shepherd Dog

\*\*Pyrenees Mountain dog

### 3.5.5 Experimental Design and Experimental Procedures

All dogs on the day of the procedure received sedation using medetomidine\* 0.1ml/10 kg intravenously through an intravenously 18-gauge cannula † placed in the cephalic vein on the forelimb. Induction of general anaesthesia, which followed, was by intravenous ketamine HCL at 3mg/kg intravenously and was maintained to effect by intravenous infusion of pentobarbitone (20mg/ml, 10 ml diluted in 200ml saline) at a constant rate of 20-30ml per

\* Domitor, Pfizer Animal Health, Pfizer Laboratories (Pty) Ltd, P O Box 783720, Sandton, 2196

† Jelco cannula, Critikon, Halfway House, Gauteng, South Africa



hour for the first 2 hours and then the infusion was discontinued for the last hour. The animals were all placed in a supine position as illustrated in Figure 3-1 see below.

**Figure 3-1 Positioning of dogs for dynamic scintigraphy.**



(i)



(ii)



(iii)



(iv)

Legend: Image (i) shows the position of the IV cannula placed in the femoral artery, to record blood pressure. Images (ii) & (iii) shows placement of jugular IV cannula for fluid and radioisotope administration, and blood sample collection. Image (iii) shows placement of the endotracheal tube and transducer for monitoring respiration. Image (iv) shows the dog positioned for scintigraphy and sampling. This supine position allowed imaging of vital organs and the upper skeleton.

A urinary catheter\* was then placed to sample urine produced during the three hours. The bladder was emptied immediately prior to administration of the radiopharmaceutical. Three lead electrocardiographic (ECG) monitoring was done for the duration of the scintigraphic dynamic study. Leads were placed using standard configuration for the dog, right front, left front and left hind leg. An intra-arterial catheter was placed in the left or right femoral artery and connected to a blood pressure (BP) transducer†. Oxygen saturation, ECG, BP, respiratory rate, and expired CO<sub>2</sub> were monitored for the duration of the study (3-hours).

The radiopharmaceuticals were prepared as per manufacturer's‡ instructions and checked for radiochemical purity at the laboratories of NECSA.

The normal dogs were given the radiopharmaceutical at an average total diagnostic dose of 184.66 MBq (SD±43.07). Scintigraphy was performed at the laboratory of the AEC Institute of Life Sciences using the Siemens Orbiter gamma camera§. The camera was fitted with a 140 keV low energy all-purpose parallel-hole collimator. The camera was calibrated for <sup>153</sup>Sm / <sup>188</sup>Re / <sup>186</sup>Re according to standard laboratory protocols for the radionuclide e.g., <sup>153</sup>Sm was calibrated to an energy level of 103 keV with a 15% window. The gamma camera was centred over the thorax and abdomen to include the heart, lungs, liver, kidneys and tumour. Both forelimbs were included to acquire data from the metaphysis of distal radius and cortical bone area. Data acquisition was performed as a dynamic study of 60 x 1 min frames for the first hour followed by single two-minute frames at two hours, three hours, and four hours on a countdown bolus injection of the radiopharmaceutical (matrix 64x64). Blood (heparin) and urine samples (labelled) were collected at fixed intervals for 3-hours, i.e. every 3 min for the first hour and then hourly for the blood samples, and for the urine every 5 min for the first hour, subsequently hourly. The activity and volume (total urine volume for each

---

\* Sabax feeding tube 17 french gauge

† Nihon Kohden Life Scope 12 Bedside Monitor: Model BSM-8500J/K. 31-4, Nishiochiai 1-chome, Shinjuku-ku, Tokyo 161 Japan

‡ South African Nuclear Energy Corporation (NECSA), P O Box 582, Pretoria, 0001, South Africa

§ Siemens Orbiter Stand: 094-200024, Rev. A.1989 Siemens Gammasonics, Inc. 2000 Nuclear Drive, DesPlaines, IL 60018. Camera Head – Siemens ZLC Digitrac Processor: 094-200013, Rev. F. 75 tubes.

time point) of each sample were measured\* and registered. These blood samples were centrifuged† and the plasma was archived and stored at -70 °C.

### 3.5.6 Data Analysis

From the dynamic studies, regions of interest (ROI) were drawn on the images over the following organs: cardiac, lungs, kidney, liver, trabecular, cortical bone, and tumour region(s). Trabecular bone ROI was centred over the proximal humerus and cortical bone ROI over the diaphyseal (midshaft) area of the humerus. Background ROI was centred over a well-muscled area of the front limb (triceps region). See Figure 3-2 below for the ROI selection. In the case of uncomplexed  $^{153}\text{Sm}^{+3}$  and  $^{186}\text{Re}$  the ROI were chosen based on the organs showing uptake e.g., liver in the case of  $^{153}\text{Sm}^{+3}$ .

Using Sopha Forthmacs software‡ the count rate, as an average count per pixel per ROI for each time point, was recorded and exported in comma-delimited file format into an Excel spreadsheet§. Because of the large volume of raw data collected for each dog, only examples of sequential calculations for a single dog (Normal Dog 1 listed in Table 3-6 on page 112) receiving  $^{153}\text{Sm}$ -EDTMP are in shown in Table 8-1 (page 274) to Table 8-9 (page 282) of the Appendix. The tables have detailed comments on how the calculations were performed on all dogs in the studies reported in this thesis.

Briefly, the data were tabulated in columns according to the ROI of the scintigraphic scan, typically these were: cardiac, lungs, liver, left kidney, right kidney, trabecular bone (proximal humerus), cortical bone (midshaft humerus), background, and tumour. All raw data was decayed corrected, and corrections were made for the errors in processing by the software in the decay corrected data by doing manual correction as described in Table 8-1 (page 274). Time-activity curves for each ROI were then plotted from these data. From the time-activity curves, the following pharmacokinetic data were calculated for each ROI; half-life ( $T_{1/2}$ ), time to maximum concentration ( $T_{\text{max}}$ ), percentage retention at 3-hours (% retention

---

\* Capintec counter (Model CRC-15R), Radioisotope Dose Calibrator

† Centrifuge

‡ Software: Sopha Forthmacs, Version 3.01 ©, 1995. Hardware: Sophy 256, 32 bit Nuclear Medicine Computer, XT 68020/25 CPU, Sopha Medical, B-1831 Diegem Kouterveldstraat 20, BELGIUM

§ Microsoft ® Excel 2002 (10.4524.4219) SP-2

at 3hr.), percentage organ distribution at 3-4 hours (% OD 3-4 hr.), see Table 8-4 (page 277). Blood clearance and cumulative urine curves were obtained from recorded data see Table 8-5 (page 278) and Table 8-6 (on page 279). For the percentage injected dose (% ID) calculations, data from the %OD, urine, and body activity were used; see Table 8-8 (page 281). These data were then described using descriptive statistics\*. The pharmacokinetic analysis of blood was done using pharmacokinetics software<sup>†</sup>. The software was used to calculate the  $t_{1/2\alpha}$  (distribution phase)  $t_{1/2\beta}$  (elimination phase) of the radiopharmaceutical in blood. This was necessary to be able to compare the pharmacokinetic human data with canine data.

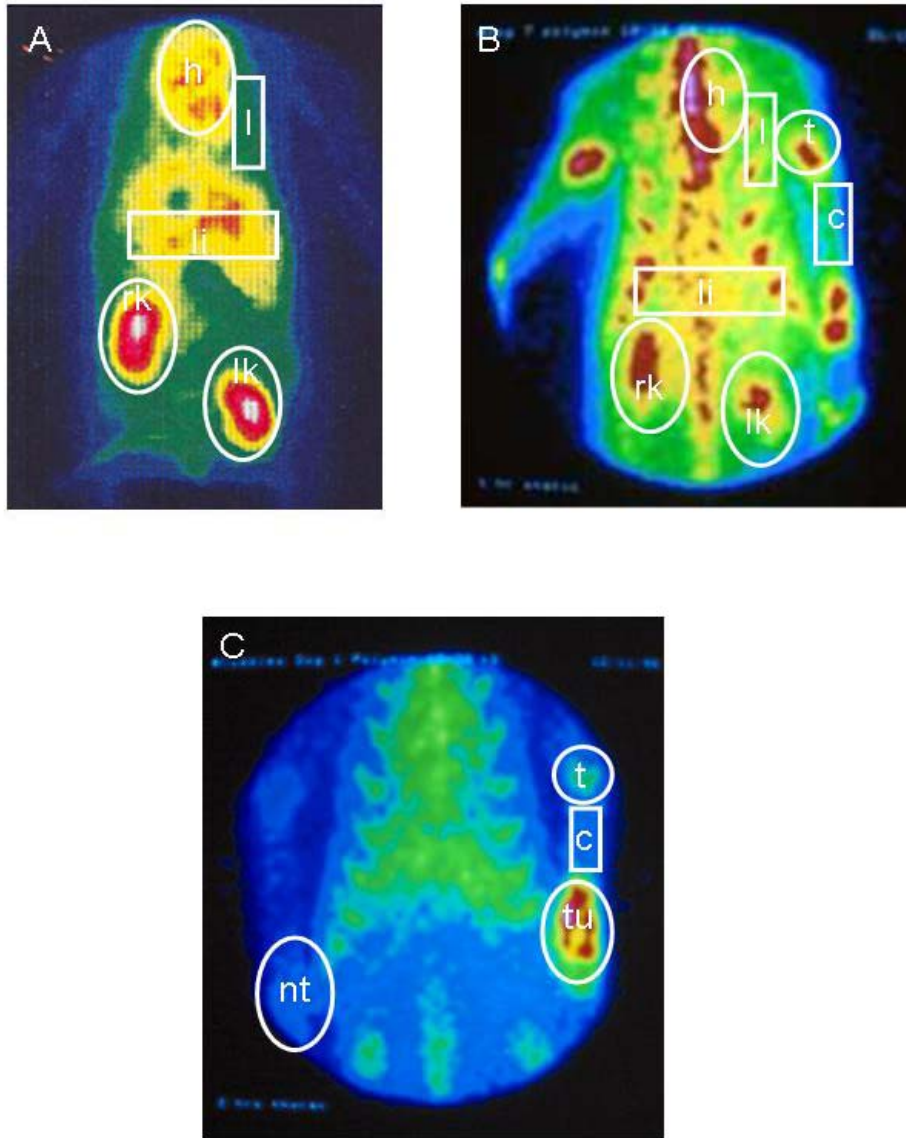
Dosimetric calculations are described in detail in section 2.1.2 (page 100) of the experimental design. Briefly, the decay corrected % ID for each ROI and accumulated urine activity was entered into the OLINDA software package for exponential modelling (EXM module)<sup>213</sup>. This program allows the user to enter pharmacokinetic data (% ID) to fit one or more exponential terms<sup>218</sup>. The program then integrated the fitted time-activity curve to infinity and passed the integral back to the OLINDA pharmacokinetics input form for use in dose calculations<sup>218</sup>. To verify the OLINDA's area under curve (AUC) calculations, manual calculations were done using the trapezoid method; see Table 8-9 (page 282). Initially, these data were used to calculate residence times for each ROI for inclusion in the Mirdose-3 software. However, OLINDA was the primary software used for dosimetry calculations, because decay corrected % ID could be entered directly into the EXM module unlike Mirdose-3 which requires an additional step to calculate of residence times<sup>213</sup>. In addition, with selection of the radionuclide in OLINDA, the software automatically adjusted the data for decay and the exponential curve was fitted to infinity based on the radionuclides physical half-life ( $T_p$ ).

---

\* SigmaStat<sup>®</sup> version 2.03. Jandel Corporation.

<sup>†</sup> (PK Solutions 2.0<sup>™</sup>) Summit Research Services, Pharmacokinetics and Metabolism Software. 68911 Open Field Dr. Montrose, CO 81401 USA

**Figure 3-2:  $^{153}\text{Sm}$ -EDTMP scintigraphic image showing areas selected as regions of interest (ROI) for normal and osteosarcoma dogs.**



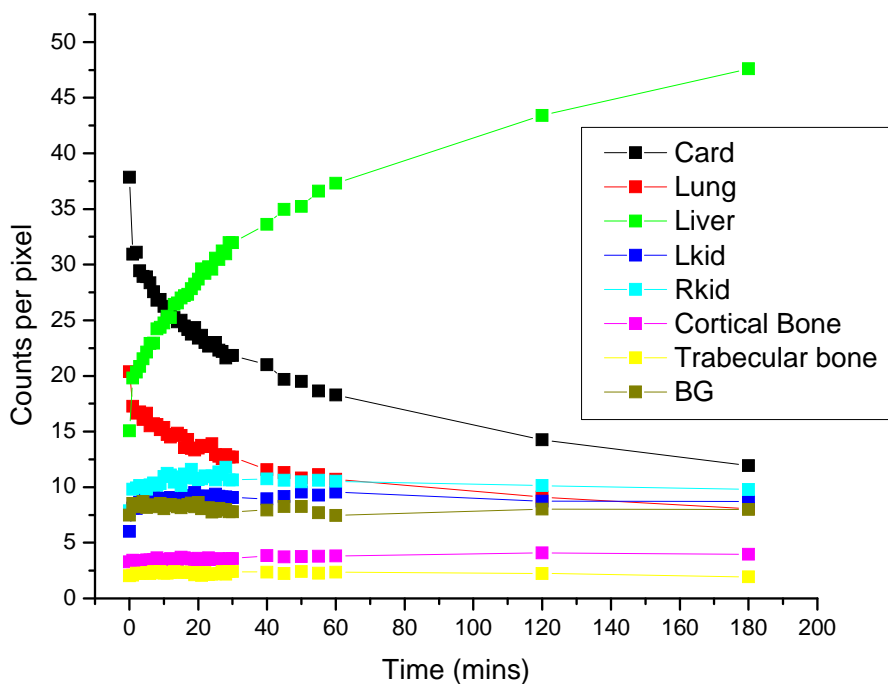
Legend: Image-A is an early frame taken at 2 seconds showing ROI for cardiac (h), lung (l), liver (liver), left (lk) and right kidney (rk). Image-B is a 60-second frame showing ROI for trabecular bone (t) and cortical bone (c). Image-C is a 24-hour scan showing ROI for trabecular bone (t), cortical bone (c), tumour bone (tu) and anatomically similar non-tumourous bone (nt).

### 3.6 Results for dogs receiving $^{153}\text{Sm-EDTMP}$ and uncomplexed $^{153}\text{Sm}^{+3}$

In compliance with Aim 3.3.1 on page 107, the results for dogs receiving  $^{153}\text{Sm-EDTMP}$  and uncomplexed  $^{153}\text{Sm}^{+3}$  are reported in this section. Specifically five normal dogs (Dogs 1-5, from Table 3-6 on page 112) and a single osteosarcoma dog ( $^{153}\text{Sm-EDTMP}$  Case-13, from Table 3-6) received a tracer dose of  $^{153}\text{Sm-EDTMP}$  for dynamic scintigraphy. Because of the large volume of dynamic raw data collected for each dog, only examples of sequential calculations for Dog 1 from Table 3-6 (on page 112) are in shown in Table 8-1 (on page 274) to Table 8-9 (on page 282) of Section 8.3 of the Appendix. The tables give detailed comments on how the biodistribution, pharmacokinetic and percentage injected dose calculations were made. The results for all biodistribution and pharmacokinetic studies for individual dogs can be found in the Appendix, Section 8.4 (on page 283), Table 8-10.

#### 3.6.1 Biodistribution data for a dog receiving uncomplexed $^{153}\text{Sm}^{+3}$ .

**Figure 3-3 Decay corrected time-activity curves for uncomplexed  $^{153}\text{Sm}^{+3}$**

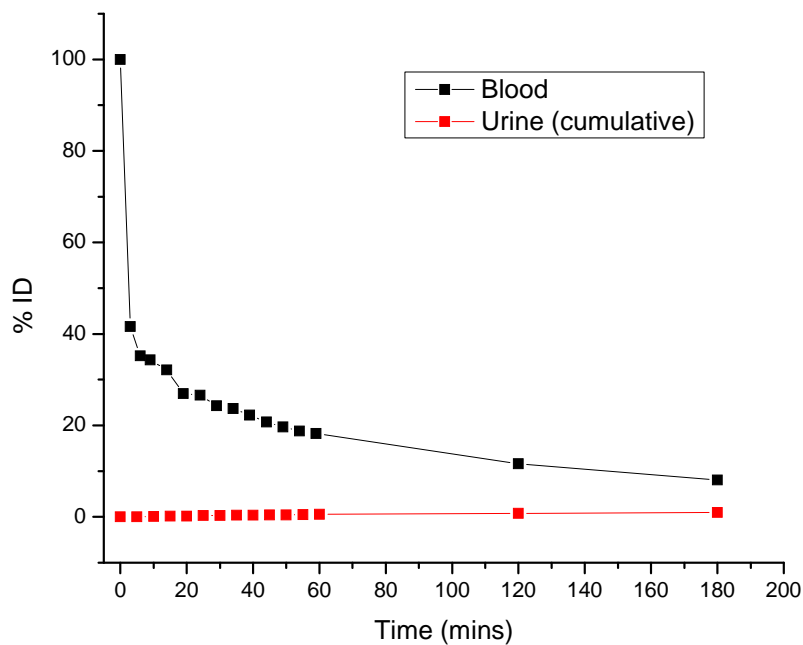


**Table 3-7 Pharmacokinetic data for all compartments in a normal dog receiving uncomplexed  $^{153}\text{Sm}^{+3}$**

Pharmacokinetic Parameter	Cardiac	Lung	Liver	Left kidney	Right kidney	Trabecular bone	Cortical Bone	Background
$T_{1/2}$ (min)	40.00	50.00	>180	>180	>180	>180	>180	>180
$T_{\text{max}}$ (min)	0.00	0.00	>180	19.00	12.00	7.00	>180	1.00
% retention 3 hr.'s*	28.00	35.00	Increasing	90.00	79.00	76.00	Increasing	89.00
% OD at 3-hours	11.94	8.06	47.62	8.7	9.77	3.97	1.94	7.99

\* The percent (%) retention at 3-hours was calculated by subtracting the %OD at 3-hours from the maxim recorded %OD for that ROI

**Figure 3-4 Time-activity curves showing  $^{153}\text{Sm}^{+3}$  clearance in blood and (cumulative) urine clearance**



**Table 3-8 Pharmacokinetic data for blood and cumulative urine clearance of uncomplexed  $^{153}\text{Sm}^{+3}$**

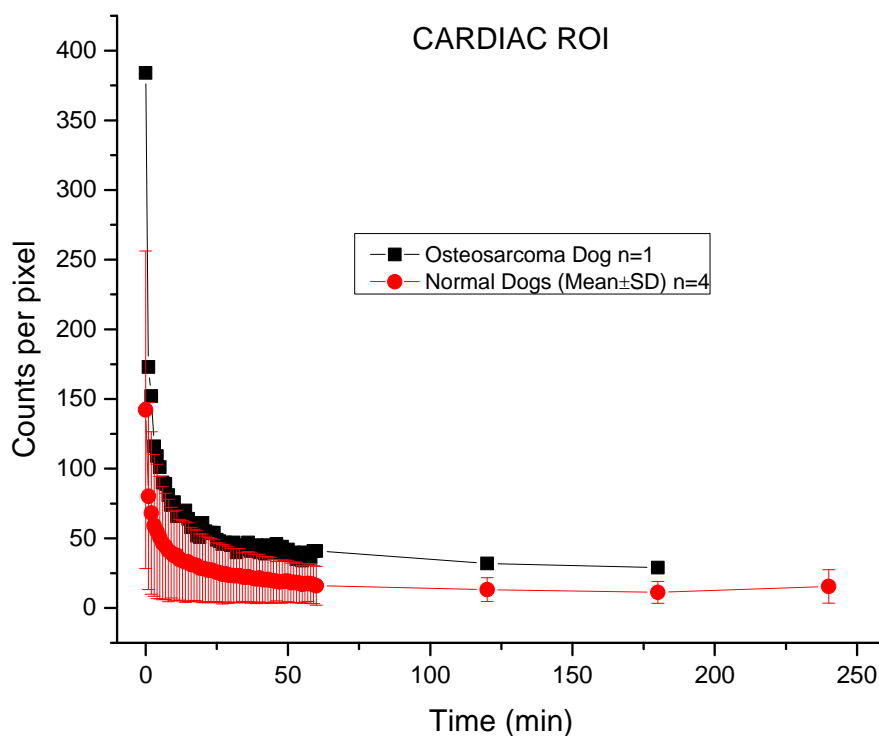
Isotope $^{153}\text{Sm}^{+3}$	Parameter	Normal dog (n=1)
<b>Blood</b>	$T_{1/2}$ (min)	44.00 min
	$t_{1/2-\alpha}$ (min)	7.87 min
	$t_{1/2-\beta}$ (min)	94.95 min
	% ID at 3-hours	8.07%
<b>Urine</b>	% ID eliminated at 3-hours	0.98%

The data above reports on the time-activity curves from a normal dog (Dog 5, see Table 3-6, page 112) receiving uncomplexed  $^{153}\text{Sm}^{+3}$ . The body showed significant soft-tissue retention, see Figure 3-3 above. It was clear from the data that uncomplexed  $^{153}\text{Sm}^{+3}$  showed considerable uptake and retention in the liver with minimal activity in urine within the first 3-hours post IV administration, see Table 3-8 above. The liver continued to accumulate uncomplexed  $^{153}\text{Sm}^{+3}$  for greater than 3-hours. The rationale for the single dog experiment was for radiopharmaceutical quality control purposes, because no biodistribution reports exist in the literature for uncomplexed  $^{153}\text{Sm}^{+3}$ . Scintigraphy would then potentially identify unexpected biodistribution that may have occurred due to impurities associated with radiopharmacy preparation or in-vivo instability<sup>142</sup>. This was indeed the case, as was seen later in experiments with  $^{153}\text{Sm-PEI-MP}$ ; see Section 4.6.5.1 (page 239).



3.6.2 Biodistribution data for the cardiac blood-pool in normal (n=4) and osteosarcoma (n=1) dogs receiving  $^{153}\text{Sm-EDTMP}$ .

**Figure 3-5 Time-activity curves for the cardiac ROI in normal and osteosarcoma dogs receiving  $^{153}\text{Sm-EDTMP}$**



**Table 3-9 Pharmacokinetic data for the cardiac compartment in dogs receiving  $^{153}\text{Sm-EDTMP}$**

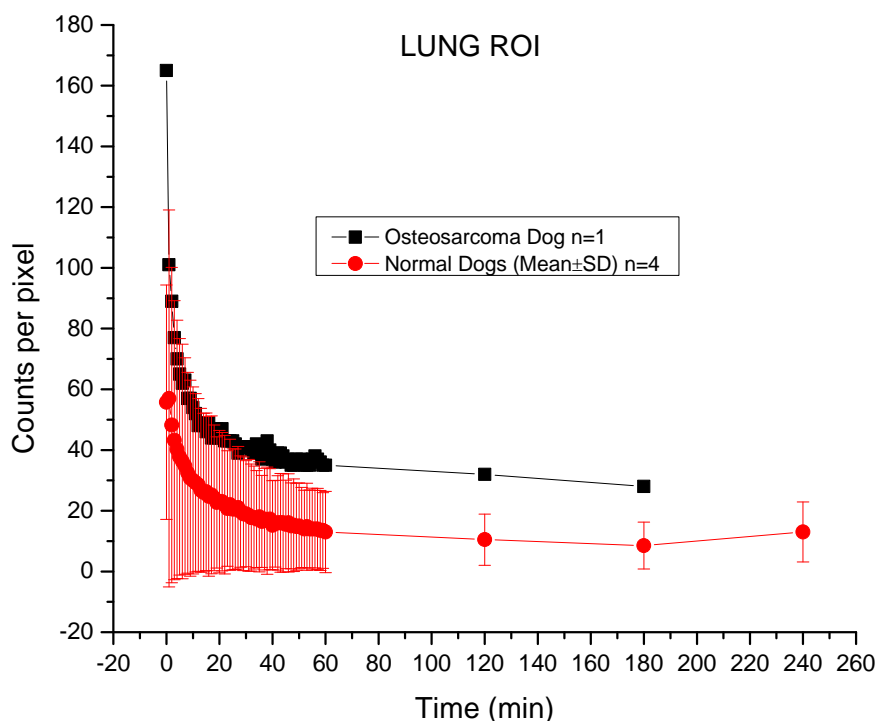
Cardiac	Normal dogs (n=4)		OSA dog (n=1)
	Parameter	Mean±SD	Value
	$T_{1/2}$ (min)	1.50±0.58	1.00
	$T_{max}$ (min)	0.00	0.00
	% OD at 3-hours	15.39±3.30	7.02

Legend: The time-activity curve for the cardiac ROI follows typical first-order pharmacokinetics as represented by the bi-exponential graph, see Figure 3-5 above. First-order pharmacokinetics (elimination) assumes that the amount of drug eliminated in a set

amount of time is directly proportional to the amount of drug in the body. If the natural log of the drug concentration versus time plot is linear, it generally can be assumed that the drug follows first-order elimination. This assumption was confirmed for the cardiac time-activity curve (Figure 3-5) by plotting the natural log of the y-axis versus time which resulted in a linear plot (data not shown). This is consistent with a one-compartment model with first-order elimination (washout). Since  $^{153}\text{Sm-EDTMP}$  was given intravenously, no uptake phase is evident thus  $T_{max} = \text{zero}$ . The cardiac ROI can be considered indicative of the blood pool (central compartment)<sup>210</sup>. The normal and osteosarcoma dogs showed similar  $T_{1/2}$  in the distribution phase (part of the washout phase) to other organ compartments (primarily kidney and bone) in the body as is evident in Figure 3-5 above. A higher percentage organ distribution (%OD) at 3-hours is evident in the normal dogs compared to the osteosarcoma dog. A possible explanation for the lower %OD in the osteosarcoma dog could be the increased radioisotope uptake by the tumour. Increased elimination via the kidneys of osteosarcoma dog was unlikely as 29.17% of the % ID was found in urine, compared to a mean of  $44.34 \pm 9.80\%$  in the normal dogs; see Table 3-19 (page 132).

3.6.3 Biodistribution for the lung ROI in Normal Dogs (n=4) and Osteosarcoma (n=1) receiving  $^{153}\text{Sm-EDTMP}$

**Figure 3-6 Time-activity curves for the lung ROI in dogs receiving  $^{153}\text{Sm-EDTMP}$**



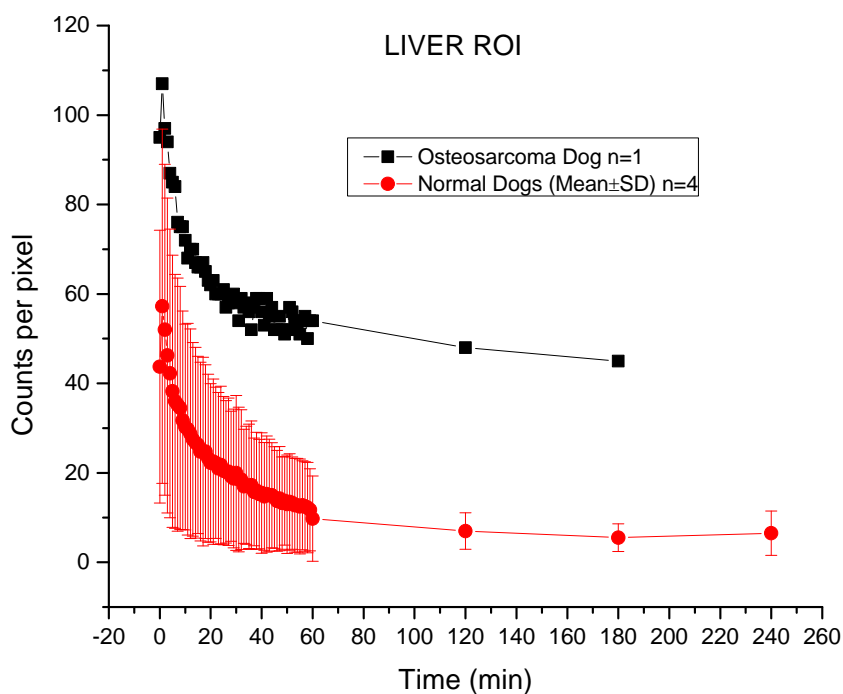
**Table 3-10 Pharmacokinetic data for the lung compartment in dogs receiving  $^{153}\text{Sm}$ -EDTMP**

Normal dogs (n=4)		OSA dog (n=1)
	Parameter	Mean $\pm$ SD
Lung	$T_{1/2}$ (min)	4.75 $\pm$ 4.11
	$T_{max}$ (min)	<1.00
	% OD at 3-hours	10.36 $\pm$ 3.15
		Value
		2.00
		0.00
		6.78

Legend: For the lung ROI little difference exists between the normal dogs and the osteosarcoma dog. No  $T_{max}$  was evident and therefore no accumulation of the radioisotope in the lungs. As seen in the cardiac ROI the osteosarcoma dog had lower retention and a shorter  $T_{1/2}$ . This ROI can be subject to error due to overlay of ribs, which can contribute to activity.

3.6.4 Biodistribution for the Liver ROI in Normal Dogs (n=4) and Osteosarcoma (n=1) receiving  $^{153}\text{Sm}$ -EDTMP

**Figure 3-7 Time-activity curves for the liver ROI in dogs receiving  $^{153}\text{Sm}$ -EDTMP**



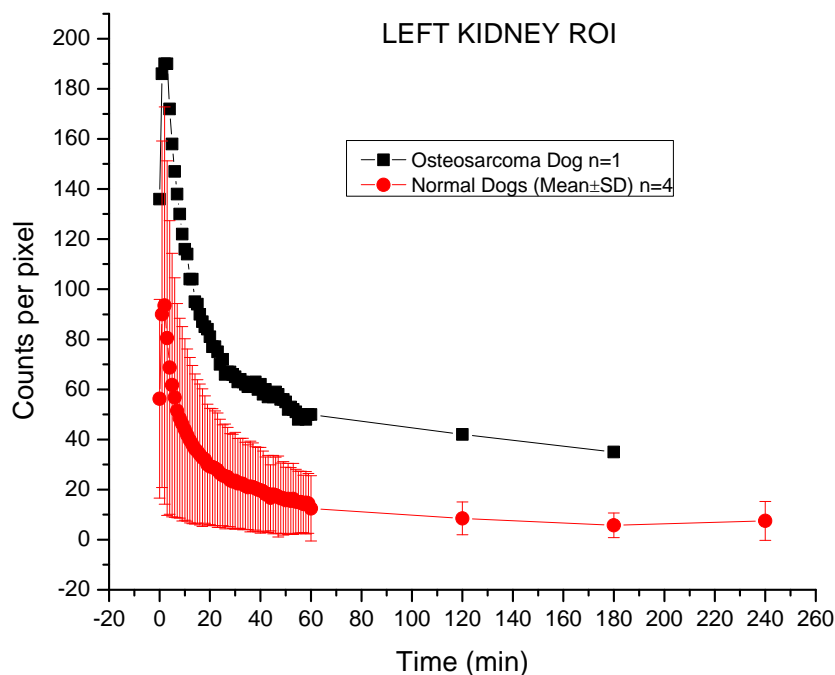
**Table 3-11 Pharmacokinetic data for the liver compartment in dogs receiving  $^{153}\text{Sm}$ -EDTMP**

Normal dogs (n=4)			OSA dog (n=1)
	Parameter	Mean±SD	Value
Liver	$T_{1/2}$ (min)	8.50±5.00	36.00
	$T_{max}$ (min)	0.75±0.50	1.00
	% OD at 3-hours	7.79±2.36	10.90

Legend: For the liver ROI the washout phase ( $T_{1/2}$ ) of radioisotope distribution, is delayed in the osteosarcoma dog. It appears to be due to retention of the radioisotope in the liver and not because of activity in blood. This assumption is made because blood clearances of the radioisotope between dogs are similar, see Figure 3-14 (page 130). Interestingly, reports in the literature do mention retention of bisphosphonates such as MDP in soft-tissue in normal human clinical cases<sup>227, 238-241</sup>. Post-mortem results of the dog did not identify significant changes in the liver.

3.6.5 Biodistribution for the Left and Right Kidney ROI in Normal Dogs (n=4) and Osteosarcoma (n=1) receiving  $^{153}\text{Sm}$ -EDTMP

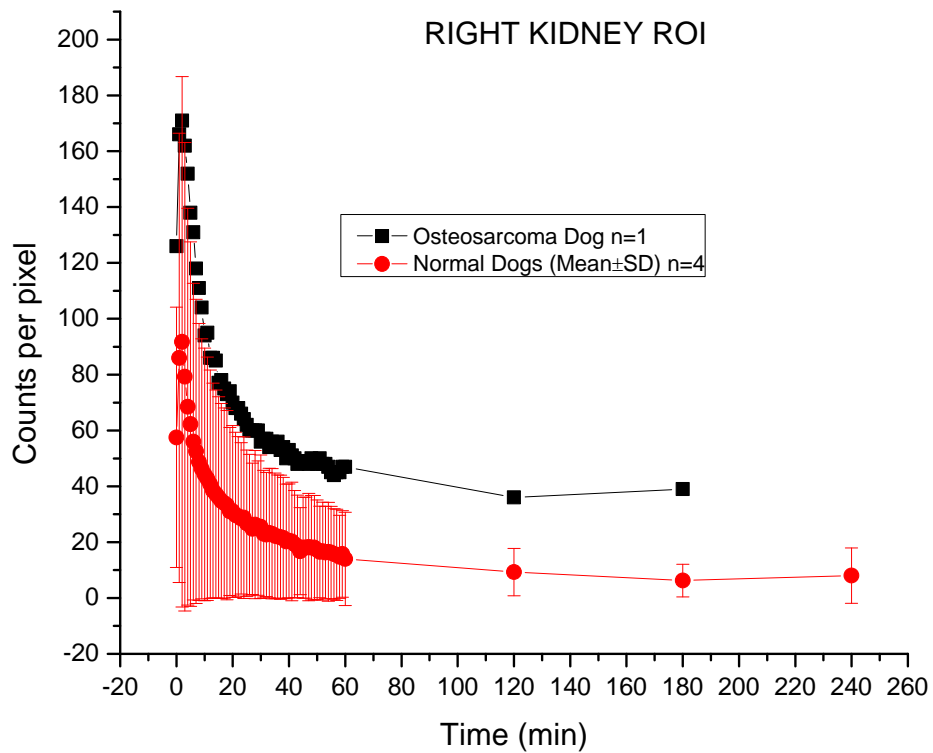
**Figure 3-8 Time-activity curves for the left kidney ROI in dogs receiving  $^{153}\text{Sm}$ -EDTMP**



**Table 3-12 Pharmacokinetic data for the left kidney compartment in dogs receiving  $^{153}\text{Sm}$ -EDTMP**

Normal dogs (n=4)		OSA dog (n=1)
	Parameter	Mean $\pm$ SD
Left Kidney	$T_{1/2}$ (min)	7.75 $\pm$ 0.50
	$T_{max}$ (min)	1.50 $\pm$ 0.58
	% OD at 3-hours	7.21 $\pm$ 1.40
		Value
		14.00
		2.00
		8.47

**Figure 3-9 Time-activity curves for the right kidney ROI in dogs receiving  $^{153}\text{Sm}$ -EDTMP**



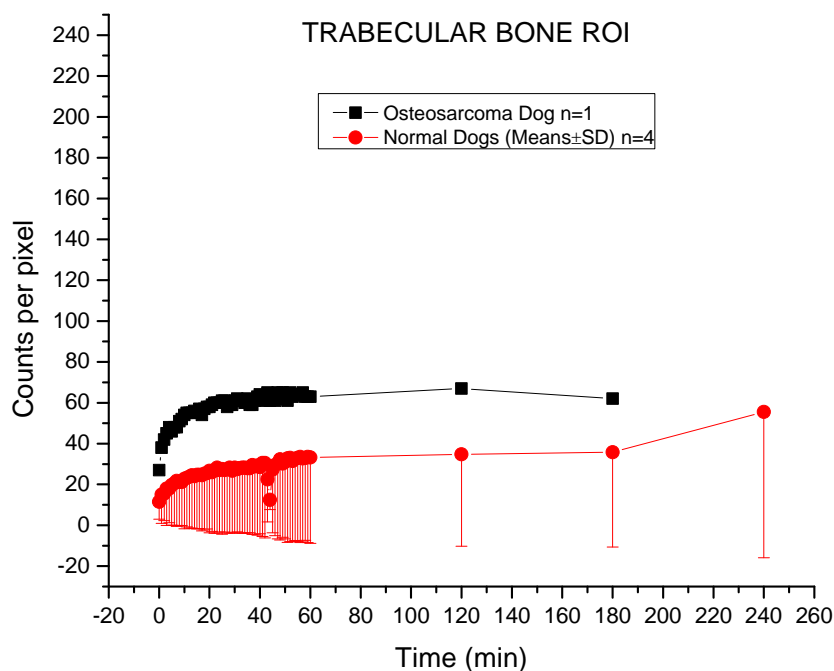
**Table 3-13 Pharmacokinetic data for the right kidney compartment in dogs receiving  $^{153}\text{Sm}$ -EDTMP**

	Normal dogs (n=4)		OSA dog (n=1)
	Parameter	Mean±SD	Value
Right Kidney	$T_{1/2}$ (min)	8.25±0.50	12.00
	$T_{max}$ (min)	1.50±0.58	2.00
	% OD at 3-hours	7.23±1.32	9.44

Legend: The time-activity curves for both kidneys showed only a mild increase in  $T_{1/2}$  for the osteosarcoma dog compared to normal dogs; see Figure 3-8 and Figure 3-9. This appears to be related to mildly prolonged elimination of  $^{153}\text{Sm}$ -EDTMP as the dog with osteosarcoma excreted less radioisotope in urine, see Table 3-19 (page 132). Renal  $T_{max}$  are similar for both normal dogs and osteosarcoma dog, see Table 3-12 and Table 3-13.

3.6.6 Biodistribution for the Trabecular Bone ROI in Normal Dogs (n=4) and Osteosarcoma (n=1) receiving  $^{153}\text{Sm}$ -EDTMP

**Figure 3-10 Time-activity curves for trabecular bone ROI in dogs receiving  $^{153}\text{Sm}$ -EDTMP**



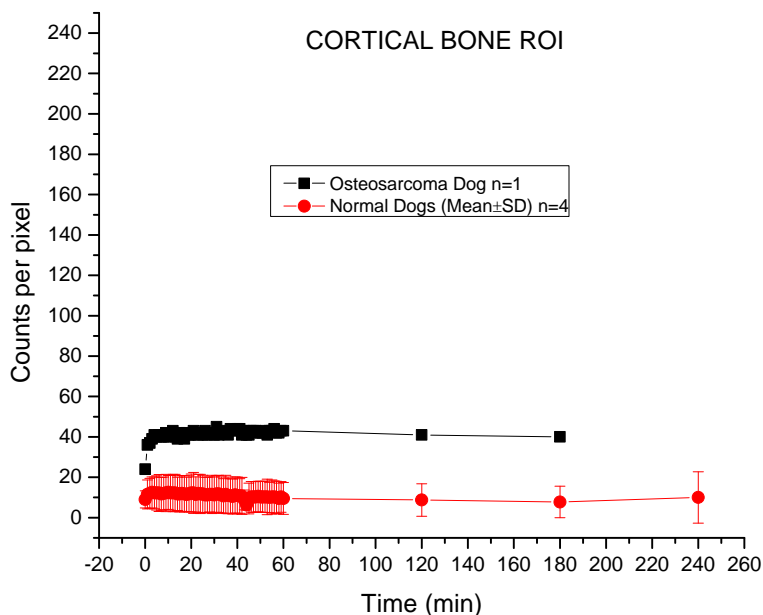
**Table 3-14 Pharmacokinetic data for trabecular bone compartment in dogs receiving  $^{153}\text{Sm-EDTMP}$**

Normal dogs (n=4)			OSA dog (n=1)
	Parameter	Mean±SD	Value
Trabecular Bone	$T_{1/2}$ (min)	>240	>180
	$T_{max}$ (min)	>240	120.00
	% OD at 3-hours	36.98±8.81	15.01

Legend: The time-activity curves for trabecular bone clearly confirm it as a target for bone seeking bisphosphonates such as  $^{153}\text{Sm-EDTMP}$ , see Figure 3-10 above. At the end of the dynamic scan,  $T_{max}$  had not been achieved in normal dogs indicating a long wash-in phase of distribution of greater than 240 minutes see Table 3-14. Redistribution from soft-tissue is the most likely reason for this accumulation after the initial wash-in phase, as the radioisotope is rapidly cleared from blood.  $T_{max}$  was achieved in the osteosarcoma dog at 120 minutes, which is in all likelihood due to redistribution to the tumour. Both normal dogs and the osteosarcoma dog had  $T_{1/2}$  of greater than 240 minutes, indicating a prolonged washout phase. This is in agreement with published canine data <sup>7, 15</sup>.

3.6.7 Biodistribution for Cortical Bone ROI in Normal Dogs (n=4) and Osteosarcoma (n=1) receiving  $^{153}\text{Sm-EDTMP}$

**Figure 3-11 Time-activity curves for cortical bone ROI in dogs receiving  $^{153}\text{Sm-EDTMP}$**



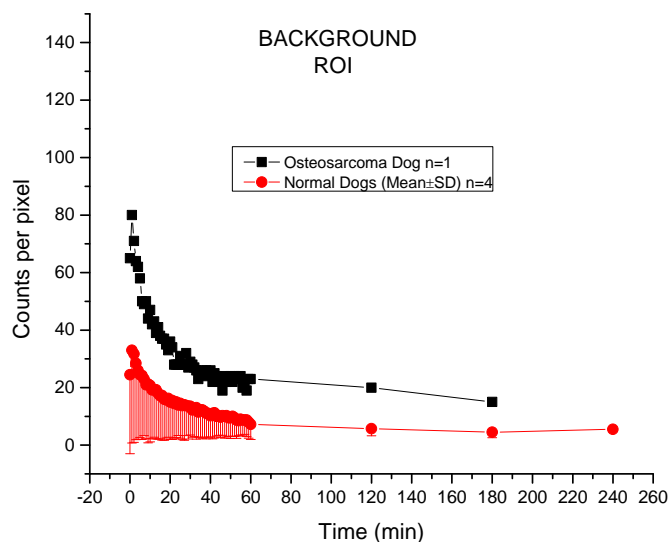
**Table 3-15 Pharmacokinetic data for cortical bone compartment in dogs receiving <sup>153</sup>Sm-EDTMP**

Normal dogs (n=4)		OSA dog (n=1)	
	Parameter	Mean±SD	Value
Cortical bone	T <sub>1/2</sub> (min)	>240	>180
	T <sub>max</sub> (min)	3.00	31.00
	% OD at 3-hours	10.97±1.76	9.69

Legend: The time-activity curves for cortical bone were different for cortical bone compared to trabecular bone see Figure 3-11 and Figure 3-10. The reason for these differences could be explained by the distribution of metabolically active red marrow (high vascularity) in trabecular bone ROI compared to predominately fatty marrow (low vascularity) in the cortical bone ROI, see Figure 2-1 (page 103). Thus, the cortical bone uptake was lower and the T<sub>max</sub> of 3 minutes was earlier than trabecular bone ROI. Nevertheless, the cortical bone retention at 3-hours and a T<sub>1/2</sub> of greater than 240 minutes were similar to trabecular bone; as would be expected for bone seeking radioisotopes <sup>61</sup>.

3.6.8 Biodistribution for the Background (soft-tissue) ROI in Normal Dogs (n=4) and Osteosarcoma (n=1) Dog Receiving <sup>153</sup>Sm-EDTMP

**Figure 3-12 Time-activity curves for background (soft-tissue) ROI in dogs receiving <sup>153</sup>Sm-EDTMP**





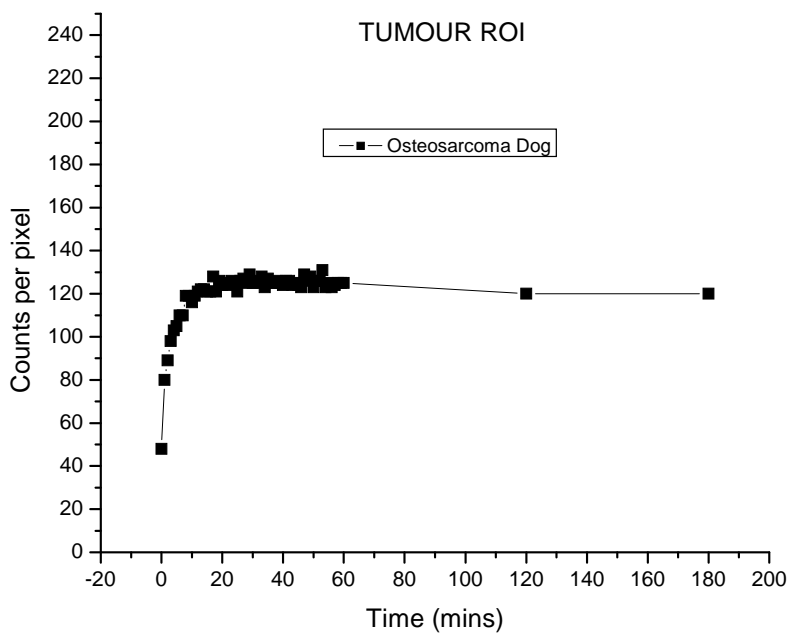
**Table 3-16 Pharmacokinetic data for background (soft-tissue) compartment in dogs receiving  $^{153}\text{Sm-EDTMP}$**

Normal dogs (n=4)		OSA dog (n=1)
	Parameter	Mean±SD
BG	$T_{1/2}$ (min)	15.50±3.70
	$T_{max}$ (min)	0.75±0.50
	% OD at 3-hours	4.66±2.52
		Value
		14.00
		1.00
		3.63

Legend: Background (Soft-tissue) showed a rapid wash-in phase of distribution ( $T_{max} \leq 1\text{min}$ ) for both the osteosarcoma and normal dogs. The washout phase ( $T_{1/2} = 14\text{-}15\text{ min}$ ) and elimination was similar to blood indicating little retention of radioisotope in the soft-tissue.

3.6.9 Biodistribution for the Tumour ROI in the Osteosarcoma (n=1) Dog Receiving  $^{153}\text{Sm-EDTMP}$

**Figure 3-13 Time-activity curves for the tumour ROI in a dog receiving  $^{153}\text{Sm-EDTMP}$**



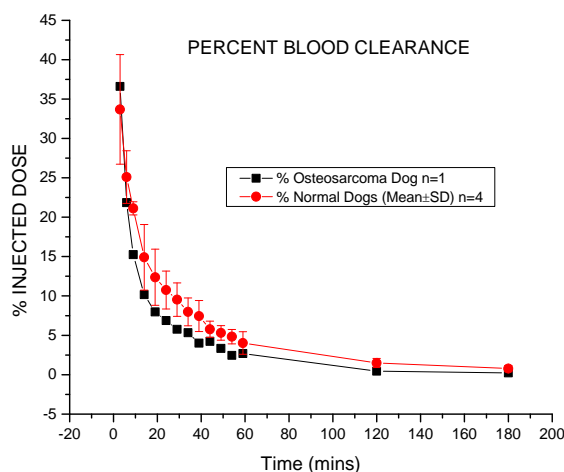
**Table 3-17 Pharmacokinetic data for the tumour compartment in a dog receiving <sup>153</sup>Sm-EDTMP**

Normal dogs (n=4)			OSA dog (n=1)
	Parameter	Mean±SD	Value
Tumour	T <sub>1/2</sub> (min)	NA	>180
	T <sub>max</sub> (min)	NA	53.00
	% OD at 3-hours	NA	29.06

Legend: The tumour ROI has a similar pattern of distribution to trabecular and cortical bone, and this is reflected in a T<sub>1/2</sub> of greater than 180 minutes see Figure 3-13 on page 129. However, T<sub>max</sub> was achieved earlier than for trabecular bone; a possible explanation could be the large soft-tissue component in osteosarcoma together with increased blood supply leading to a more rapid accumulation of <sup>153</sup>Sm-EDTMP. The tumour was large and had a significant soft-tissue component as seen in Figure 3-40 (page 197). The steepness of the slope for the wash-in phase of the tumour (Figure 3-13) compared to the more gradual slope for trabecular bone (Figure 3-10) is possibly an indication of increased blood supply aiding distribution. Challenging this assumption is a paper that has found that osteosarcoma have reduced blood supply to the bony parts of the tumour due to increased interstitial pressure when compared to neighbouring soft-tissue<sup>242</sup>. Interestingly a recent report in osteosarcoma in dogs showed that osteosarcomas with increased vascularity score had a greater chance of metastases and possible malignant transformation than tumours with lower numbers<sup>138</sup>.

3.6.10 Biodistribution in Blood for Normal Dogs (n=4) and Osteosarcoma (n=1) Dog Receiving <sup>153</sup>Sm-EDTMP

**Figure 3-14 Time-activity curves for blood in normal and osteosarcoma dogs receiving <sup>153</sup>Sm-EDTMP**



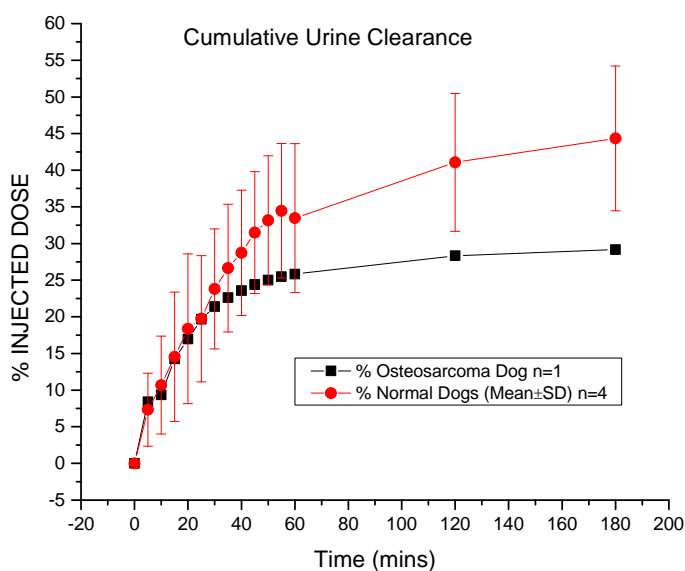
**Table 3-18 Pharmacokinetic data for blood clearance in dogs receiving  $^{153}\text{Sm-EDTMP}$** 

Normal dogs (n=4)		OSA dog (n=1)	
	Parameter	Mean $\pm$ SD	Value
Blood	$T_{1/2}$ (min)	15.61 $\pm$ 1.70	18.30
	$t_{1/2-\alpha}$ (min)	5.59 $\pm$ 0.66	6.29
	$t_{1/2-\beta}$ (min)	41.19 $\pm$ 31.86	31.86
	% ID at 3-hours	0.78 $\pm$ 0.39	0.23

An example (Dog 1) of the calculations used to develop the blood time-activity curve can be found in the Appendix, Table 8-6 on page 279. Individual data for normal dogs and the descriptive statistics can be found in the Appendix, see Table 8-10 (page 283). The time-activity curves for the normal dogs and the osteosarcoma dog were virtually identical for clearance of  $^{153}\text{Sm-EDTMP}$  from blood, and followed typical first order pharmacokinetics as represented by the bi-exponential graph, see Figure 3-14. Since  $^{153}\text{Sm-EDTMP}$  was given intravenously, no uptake phase is evident thus  $T_{max} = 0$ , see Table 3-18. Less than 1% of the ID was present in blood at 3-hours. The cardiac ROI is often represented as indicative of the blood-pool in nuclear medicine; however, our results show that actual measurement of activity in blood differs significantly from the cardiac ROI. The  $T_{1/2}$  for the cardiac ROI has a Mean $\pm$ SD of 1.5 $\pm$ 0.58 minutes compared to 15.61 $\pm$ 1.70 minutes for blood. Factors that may be responsible for this observation include: activity in adjacent or overlying structures e.g. ribs, activity in the myocardium. While the  $T_{1/2}$  for blood is helpful, a more accurate measure of blood pharmacokinetics are the pharmacokinetic parameters  $t_{1/2-\alpha}$  and  $t_{1/2-\beta}$ , where  $t_{1/2-\alpha}$  is the distribution half-life and  $t_{1/2-\beta}$  is the elimination half-life of  $^{153}\text{Sm-EDTMP}$ . These pharmacokinetic parameters may serve as a better description of the blood time-activity because they better describe the bi-exponential time-activity curves for radiopharmaceuticals in blood.

3.6.11 Biodistribution in Urine for Normal Dogs (n=4) and Osteosarcoma (n=1) Dog Receiving  $^{153}\text{Sm-EDTMP}$

**Figure 3-15 Time-activity curves showing (cumulative) urine clearance as a percentage of ID in dogs receiving  $^{153}\text{Sm-EDTMP}$**



**Table 3-19 Pharmacokinetic data for cumulative urine clearance in dogs receiving  $^{153}\text{Sm-EDTMP}$**

		Normal dogs (n=4)	OSA dog (n=1)
Urine	Parameter	Mean±SD	Value
	% ID cleared at 3-hours	44.34±9.80	29.17
	Time to 50% elimination of % ID	24.52±6.54	15.00

An example (Normal Dog 1) of the calculations used to develop the cumulative urine time-activity curve can be found in the Appendix, Table 8-5 (page 278). Individual data for normal dogs and descriptive statistics can be found in the Appendix, see Table 8-10 (page 283). At 3-hours, the % ID cleared in urine of  $^{153}\text{Sm-EDTMP}$  was 44.34±9.8 % for normal dogs compared to 29.17% for the osteosarcoma dog, see Figure 3-15. The tumour dog had reduced elimination of  $^{153}\text{Sm-EDTMP}$ , which could be attributed to a number of factors such as:

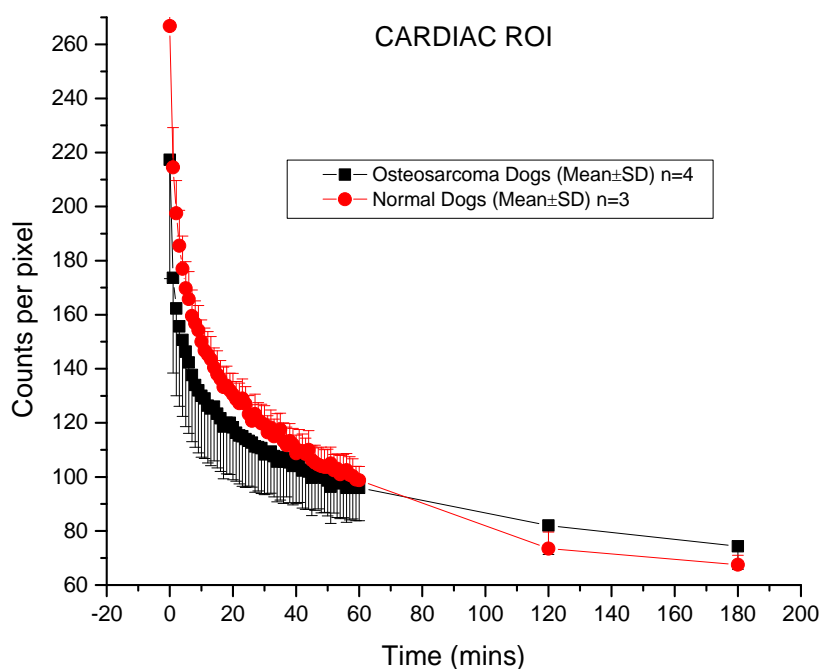
reduced renal perfusion because of non-steroidal anti-inflammatory use for pain, age related renal disease, greater isotope uptake by the tumour. Within 15 to 24 minutes, 50% of the injected dose of  $^{153}\text{Sm}$ -EDTMP was eliminated in the urine of the osteosarcoma and normal dogs with the balance requiring approximately 156 minutes to be eliminated see Figure 3-15.

### **3.7 Results for normal and osteosarcoma dogs receiving $^{188}\text{Re}$ -HEDP**

In compliance with Aim 3.3.1 (on page 107), the results for dogs receiving  $^{188}\text{Re}$ -HEDP are reported in this section. No studies for uncomplexed  $^{188}\text{Re}$  were done. In this section, we report on four normal dogs (Dogs 6-9, from Table 3-6 on page 112) and three dogs with osteosarcomas ( $^{188}\text{Re}$ -HEDP Cases 1 to 3, Table 3-6) which received a tracer dose of  $^{188}\text{Re}$ -HEDP for dynamic scintigraphy. As previously stated, because of the large volume of dynamic raw data collected for each dog, only examples of sequential calculations for Dog 1 from Table 3-6 are shown in Table 8-1 (on page 274) to Table 8-9 (on page 282) of Section 8.3 of the Appendix. The results for all biodistribution and pharmacokinetic studies for individual dogs receiving  $^{188}\text{Re}$ -HEDP can be found in the Appendix, Section 8.4, and Table 8-11 (on page 284).

3.7.1 Biodistribution for the Cardiac ROI in Normal Dogs (n=4) and Osteosarcoma (n=3) receiving  $^{188}\text{Re}$ -HEDP

**Figure 3-16: Time-activity curves for the cardiac ROI in normal and osteosarcoma dogs receiving  $^{188}\text{Re}$ -HEDP**



**Table 3-20 Pharmacokinetic data for the cardiac compartment in dogs receiving  $^{188}\text{Re}$ -HEDP**

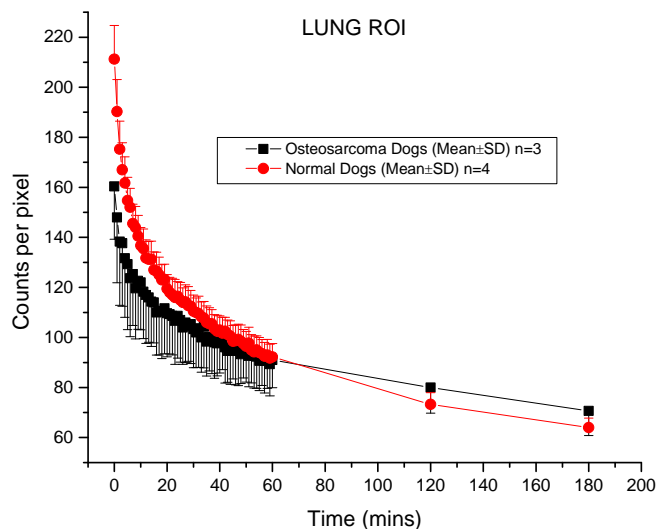
Organ		Normal dogs (n=4)	Osteosarcoma dogs (n=3)
Cardiac	Parameter	Mean±SD	Mean±SD
	$T_{1/2}$ (min)	15.61±6.91	16.38±10.13
	$T_{max}$ (min)	0.00	0.00
	% OD at 3-hours	15.00±0.82	14.67±1.53

Legend: The time-activity curve for the cardiac ROI follow typical first-order pharmacokinetics as represented by the bi-exponential graph, see Figure 3-16 above. Since  $^{188}\text{Re}$ -HEDP was given intravenously, no uptake phase is evident thus  $T_{max} = \text{zero}$ . The mean±SD washout phase ( $T_{1/2}$ ) for the osteosarcoma dogs was similar to normal dogs, see Table 3-20 above. Nevertheless, because the cardiac ROI may be a reflection of blood pool

pharmacokinetics, we examined the time-activity curves ( $T_{1/2}$ ) for blood, which identified differences in elimination between the groups, see Figure 3-25 (page 143). The mean $\pm$ SD % ID for blood at 3-hours was 7.77 $\pm$ 2.22 for osteosarcoma dogs compared to 4.83 $\pm$ 0.23 for normal dogs; see Table 3-29 on page 144. The mildly increased retention in the cancer dogs may be due to the older age of dogs, which are more likely to have age-related renal disease. However, no dogs with obvious renal disease were included in the study. Nevertheless, serum chemistry and urine specific gravity are not very sensitive indicators of renal disease. Therefore to examine the possibility of reduced renal clearance between the two populations, we compared the % ID eliminated in urine at 3-hours for both groups; see Table 3-30 on page 145. The mean $\pm$ SD for urine (% ID at 3-hours) was 30.59 $\pm$ 13.31 for osteosarcoma dogs compared to 52.31 $\pm$ 12.02 for normal dogs. While statistical analysis did not identify differences between groups for urine, the % ID at 3-hours did show a trend towards reduced clearance in the osteosarcoma group,  $P = 0.073^*$ . In conclusion, the cardiac pharmacokinetics were consistent with findings from the blood pool, which supports the role of the cardiac ROI as a reflection of blood pool pharmacokinetics.

### 3.7.2 Biodistribution for the Lung ROI in Normal Dogs (n=4) and Osteosarcoma (n=3) receiving $^{188}\text{Re}$ -HEDP

**Figure 3-17 Time-activity curves for the lung ROI in normal and osteosarcoma dogs receiving  $^{188}\text{Re}$ -HEDP**



\* Because the sample size was not large enough which resulted in a lower power (0.372), the desired power being 0.800, the negative statistical findings should be interpreted with caution.

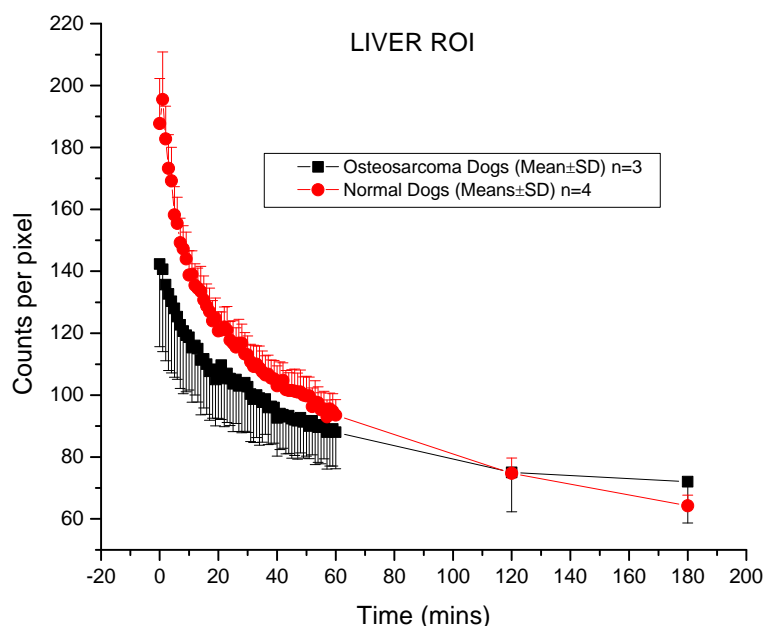
**Table 3-21 Pharmacokinetic data for the lung compartment in dogs receiving <sup>188</sup>Re-HEDP**

Organ		Normal Dogs (n=4)	Osteosarcoma Dogs (n=3)
Lung	Parameter	Mean±SD	Mean±SD
	T <sub>1/2</sub> (min)	21.73±8.04	36.27±2.69
	T <sub>max</sub> (min)	0.25±0.50	0.00
	% OD at 3-hours	14.00±0.82	13.67±0.58

Legend: The washout (T<sub>1/2</sub>) time-activity curve for the lung ROI followed typical first-order pharmacokinetics as represented by the bi-exponential graph, see Figure 3-17 above. The difference between groups for washout (T<sub>1/2</sub>) trended towards significance (P=0.07) (see Table 3-21 above). Nevertheless, because the lung ROI can be subject to error due to the overlay of ribs (which contributes to activity in the later stage of the scan) the results should be viewed with caution. Little difference existed between the normal dogs and the osteosarcoma dog for lung T<sub>max</sub>, and %OD at 3-hours.

3.7.3 Biodistribution for the Liver ROI in Normal Dogs (n=4) and Osteosarcoma Dogs (n=3) receiving <sup>188</sup>Re-HEDP

**Figure 3-18 Time-activity curves for the liver ROI in normal and osteosarcoma dogs receiving <sup>188</sup>Re-HEDP**





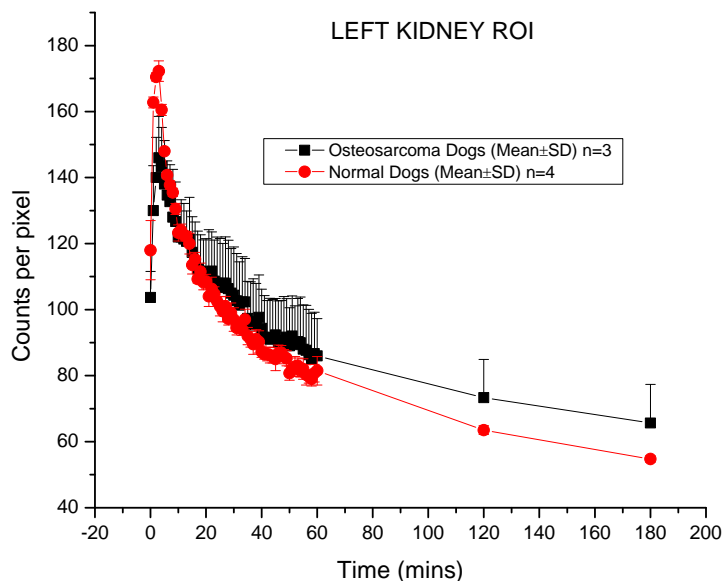
**Table 3-22 Pharmacokinetic data for the liver compartment in dogs receiving <sup>188</sup>Re-HEDP**

Organ		Normal Dogs (n=4)	Osteosarcoma Dogs (n=3)
Liver	Parameter	Mean±SD	Mean±SD
	T <sub>1/2</sub> (min)	24.86±6.95	48.41±43.43
	T <sub>max</sub> (min)	0.75±0.50	1.67±0.58
	% OD at 3-hours	14.25±0.50	13.67±1.53

Legend: The washout section of time-activity curve for the liver ROI followed typical first-order pharmacokinetics as represented by the bi-exponential graph see Figure 3-18 above. The difference between groups for washout (T<sub>1/2</sub>) was not statistically significant (see Table 3-22 above) because of the large standard deviation of the mean. There was no statistical difference between normal dogs and the osteosarcoma dogs for T<sub>max</sub>, and %OD at 3-hours.

3.7.4 Biodistribution for the Left and Right Kidneys ROI in Normal Dogs (n=4) and Osteosarcoma Dogs (n=3) receiving <sup>188</sup>Re-HEDP

**Figure 3-19 Time-activity curves for the left kidney ROI in normal and osteosarcoma dogs receiving <sup>188</sup>Re-HEDP**

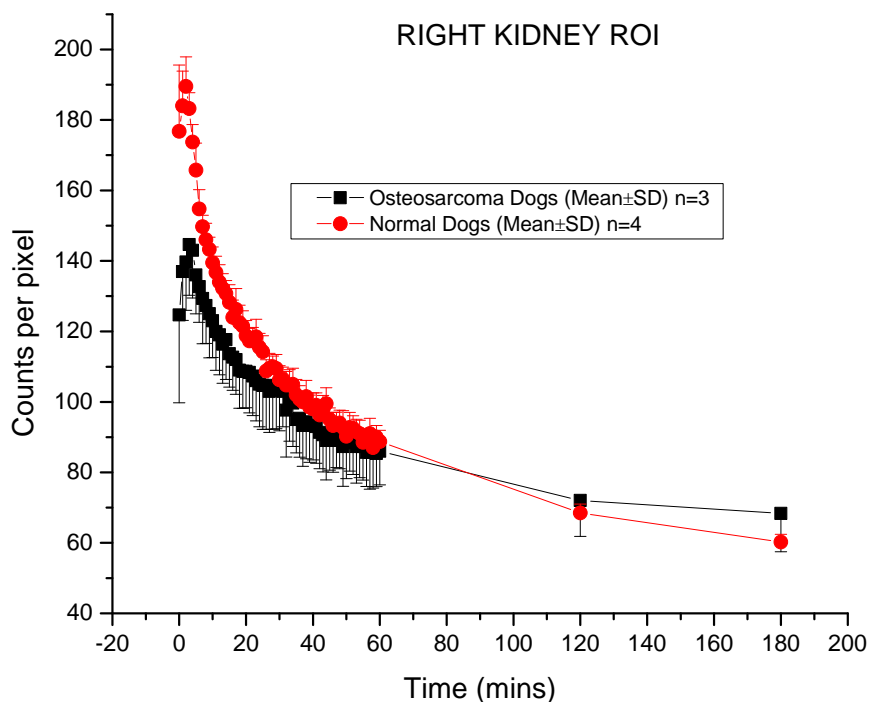


**Table 3-23 Pharmacokinetic data for the left kidney compartment in dogs receiving  $^{188}\text{Re}$ -HEDP**

Organ		Normal Dogs (n=4)	Osteosarcoma Dogs (n=3)
Left Kidney	Parameter	Mean±SD	Mean±SD
	$T_{1/2}$ (min)	27.97±5.12	32.37±17.04
	$T_{\text{max}}$ (min)	2.50±0.58	3.00±0.00
	% OD at 3-hours	12.25±0.50	13.00±1.73

Legend: The washout time-activity curve for the left kidney ROI follows typical first-order pharmacokinetics as represented by the bi-exponential graph, see Figure 3-19 above. No apparent differences between groups were found for  $T_{1/2}$ ,  $T_{\text{max}}$  and % OD at 3-hours for the left kidney.

**Figure 3-20 Time-activity curves for the right kidney ROI in normal and osteosarcoma dogs receiving  $^{188}\text{Re}$ -HEDP**



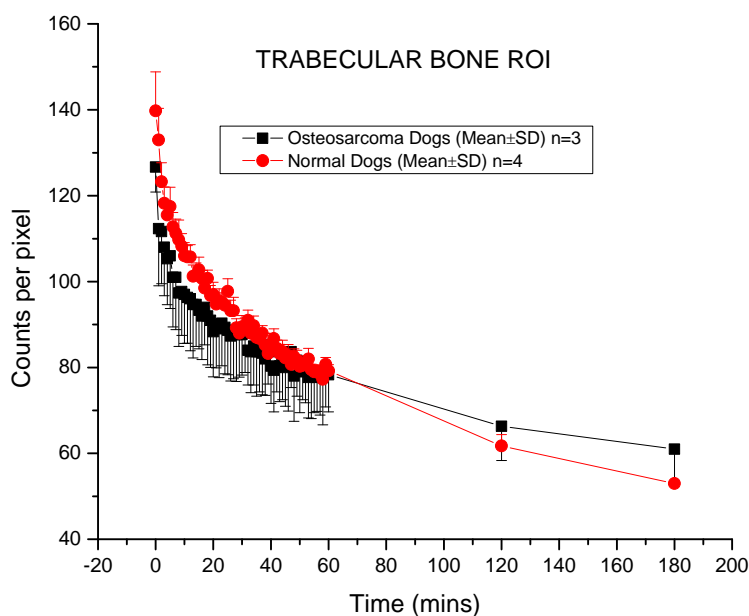
**Table 3-24 Pharmacokinetic data for the right kidney compartment in dogs receiving  $^{188}\text{Re}$ -HEDP**

Organ		Normal Dogs (n=4)	Osteosarcoma Dogs (n=3)
Right Kidney	Parameter	Mean±SD	Mean±SD
	$T_{1/2}$ (min)	25.70±7.73	40.93±24.13
	$T_{\text{max}}$ (min)	2.25±0.50	2.33±1.15
	% OD at 3-hours	13.25±0.96	13.67±1.53

Legend: The washout time-activity curve for the right kidney ROI follows typical first-order pharmacokinetics as represented by the bi-exponential graph, see Figure 3-20 above. No apparent differences between groups in retention in the kidney were evident as seen by the almost identical %OD at 3-hours, see Table 3-24 above. However, the wide SD of the mean for the right kidney  $T_{1/2}$  in the osteosarcoma dogs made statistical comparison difficult between groups; nevertheless, the mean did trend towards a longer renal  $T_{1/2}$  for the osteosarcoma dogs, which was in agreement with the  $T_{1/2}$  for cardiac, lung, liver and blood.

3.7.5 Biodistribution for the Trabecular Bone ROI in Normal Dogs (n=4) and Osteosarcoma Dogs (n=3) receiving  $^{188}\text{Re}$ -HEDP

**Figure 3-21 Time-activity curves for the trabecular bone ROI in normal and osteosarcoma dogs receiving  $^{188}\text{Re}$ -HEDP**



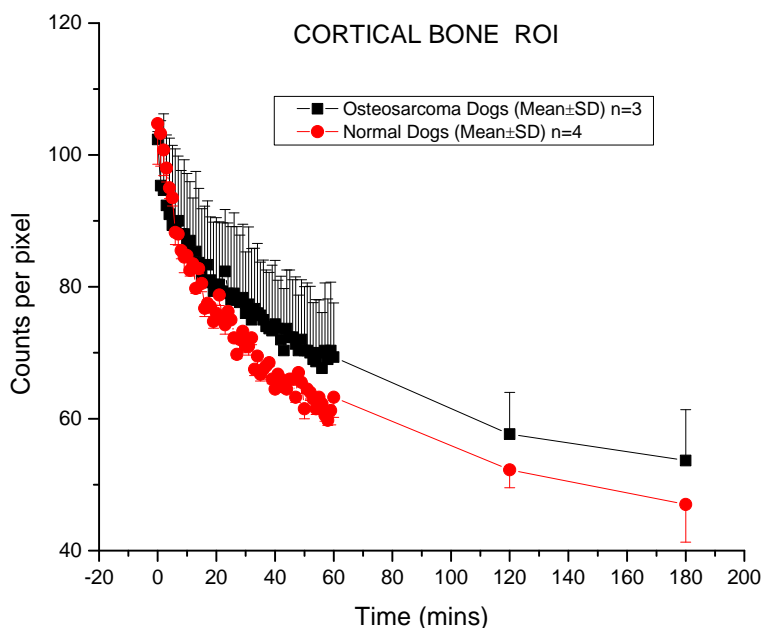
**Table 3-25 Pharmacokinetic data for trabecular bone compartment in dogs receiving  $^{188}\text{Re}$ -HEDP**

Organ		Normal Dogs (n=4)	Osteosarcoma Dogs (n=3)
Trabecular bone	Parameter	Mean±SD	Mean±SD
	$T_{1/2}$ (min)	69.71±7.11	63.02±4.27
	$T_{\text{max}}$ (min)	0.00	0.00
	% OD at 3-hours	11.75±0.96	12.00±0.00

Legend: The washout ( $T_{1/2}$ ) section of time-activity curve for the trabecular bone ROI followed typical first-order pharmacokinetics as represented by the bi-exponential graph see Figure 3-21 above. There was no statistical difference between normal dogs and the osteosarcoma dogs for  $T_{1/2}$ ,  $T_{\text{max}}$ , and %OD at 3-hours, see Table 3-25 above.

3.7.6 Biodistribution for the Cortical Bone ROI in Normal Dogs (n=4) and Osteosarcoma (n=3) dogs receiving  $^{188}\text{Re}$ -HEDP

**Figure 3-22 Time-activity curves for the cortical bone ROI in normal and osteosarcoma dogs receiving  $^{188}\text{Re}$ -HEDP**



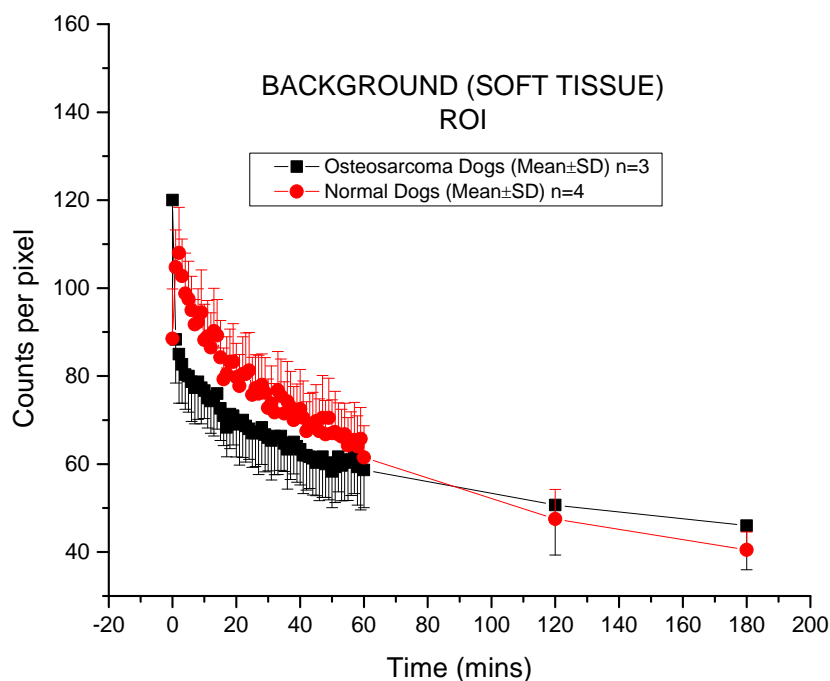
**Table 3-26 Pharmacokinetic data for cortical bone compartment in dogs receiving <sup>188</sup>Re-HEDP**

Organ		Normal Dogs (n=4)	Osteosarcoma Dogs (n=3)
Cortical bone	Parameter	Mean±SD	Mean±SD
	T <sub>1/2</sub> (min)	59.48±12.30	97.33±39.26
	T <sub>max</sub> (min)	1.00 ± 1.41	0.00
	% OD at 3-hours	10.50 ± 2.52	10.67 ± 1.15

Legend: The washout (T<sub>1/2</sub>) section of time-activity curve for the cortical bone ROI followed typical first-order pharmacokinetics as represented by the bi-exponential graph see Figure 3-22 above. There was no statistical difference between normal dogs and the osteosarcoma dogs for T<sub>1/2</sub>, T<sub>max</sub>, and %OD at 3-hours, see Table 3-26 above.

3.7.7 Biodistribution for the Background (Soft-tissue) ROI in Normal Dogs (n=4) and Osteosarcoma (n=3) dogs receiving <sup>188</sup>Re-HEDP

**Figure 3-23 Time-activity curves for the background (soft-tissue) ROI in normal and osteosarcoma dogs receiving <sup>188</sup>Re-HEDP**



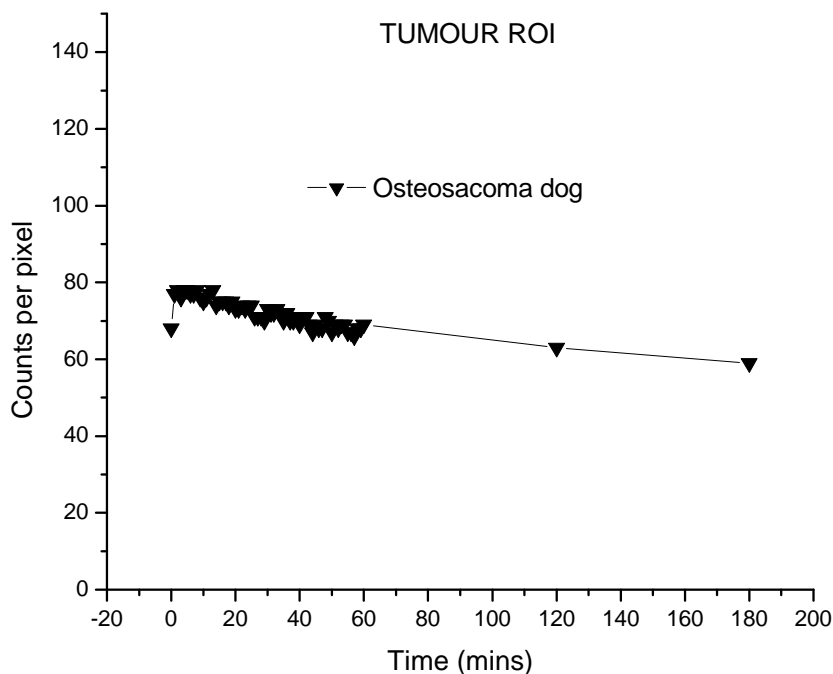
**Table 3-27 Pharmacokinetic data for background (soft-tissue) compartment in dogs receiving  $^{188}\text{Re}$ -HEDP**

Organ		Normal Dogs (n=4)	Osteosarcoma Dogs (n=2)
Background	Parameter	Mean±SD	Mean±SD
	$T_{1/2}$ (min)	57.51±6.44	52.50±3.54
	$T_{max}$ (min)	1.50±0.58	0.33±0.58
	% OD at 3-hours	9.25±2.22	8.67±1.15

Legend: The washout ( $T_{1/2}$ ) section of time-activity curve for the background ROI followed typical first-order pharmacokinetics as represented by the bi-exponential graph see Figure 3-23 above. There was no statistical difference between normal dogs and the osteosarcoma dogs for  $T_{1/2}$ ,  $T_{max}$ , and %OD at 3-hours, see Table 3-27 above.

3.7.8 Biodistribution for the Tumour in the Osteosarcoma Dog (n=1) receiving  $^{188}\text{Re}$ -HEDP

**Figure 3-24 Time-activity curves for the tumour in the osteosarcoma dog receiving  $^{188}\text{Re}$ -HEDP**



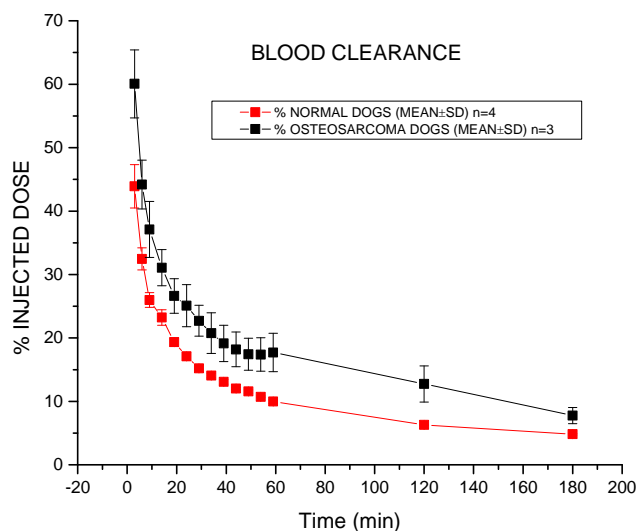
**Table 3-28 Pharmacokinetic data for the tumour compartment in a dog receiving <sup>188</sup>Re-HEDP**

Organ	Parameter	Value
Tumour	T <sub>1/2</sub> (min)	>180
	T <sub>max</sub> (min)	3
	% OD at 3-hours	13.29

Legend: In strong contrast to <sup>153</sup>Sm-EDTMP pharmacokinetics for trabecular bone (Figure 3-10, page 126), the <sup>188</sup>Re-HEDP dogs showed almost soft-tissue like pattern of washout for both trabecular and cortical bone, see Figure 3-21 and Figure 3-22. There was no prolonged wash in phase (T<sub>max</sub>) as was seen with <sup>153</sup>Sm-EDTMP. No differences were observed between normal and osteosarcoma dogs for T<sub>1/2</sub>, T<sub>max</sub>, and %OD at 3-hours. Time-activity curves for the tumour clearly confirm it as a target for bone seeking bisphosphonates such as <sup>188</sup>Re-HEDP see Figure 3-24. At the end of the dynamic scan (3-hours), T<sub>1/2</sub> had not been achieved; indicating a long washout phase of greater than 180 minutes, see Table 3-28 above. This is in sharp contrast to trabecular bone, which had a shorter washout phase. The mean±SD T<sub>1/2</sub> for trabecular bone in dogs with osteosarcomas was 63.02±4.27minutes, see Table 3-25 on page 140. Overall, this finding would most likely translate into a lower dose of radiation to normal bone marrow for dogs receiving <sup>188</sup>Re-HEDP compared to <sup>153</sup>Sm-EDTMP dogs.

3.7.9 Biodistribution in Blood for Normal (n=4) and Osteosarcoma Dogs (n=3) receiving <sup>188</sup>Re-HEDP

**Figure 3-25: Time-activity curves for blood in normal and osteosarcoma dogs receiving <sup>188</sup>Re-HEDP.**



**Table 3-29 Pharmacokinetic data for blood clearance in dogs receiving  $^{188}\text{Re}$ -HEDP**

Organ		Normal Dogs (n=4)	Osteosarcoma Dogs (n=3)
Blood	Parameter	Mean±SD	Mean±SD
	$T_{1/2}$ (min)	15.25±2.50	15.00
	$t_{1/2-\alpha}$ (min)	6.59±0.61	5.26±0.97
	$t_{1/2-\beta}$ (min)	92.19±9.87	104.92±29.16
	% ID at 3-hours	4.83±0.23	7.77±2.22

Legend: An example (Dog 1) of the calculations used to develop the blood time-activity curve can be found in the Appendix, Table 8-6 on page 279. Individual data and descriptive statistics for normal dogs and osteosarcoma dogs receiving  $^{188}\text{Re}$ -HEDP can be found in the Appendix; see Table 8-11 (page 284). The time-activity curves for  $^{188}\text{Re}$ -HEDP in the blood of normal dogs and osteosarcoma dogs were statistically identical, except for the % ID at 3-hours. The curves for blood followed typical first order pharmacokinetics as represented by the bi-exponential graph, see Figure 3-14. Since  $^{188}\text{Re}$ -HEDP was given intravenously, no uptake phase was evident, thus  $T_{max} = 0$ . The % ID at 3-hours was statistically different between groups  $P = 0.04$  (see Table 3-29 above) with the osteosarcoma dogs retaining almost twice as much activity at 3-hours compared to normal dogs. As discussed earlier, this is consistent with the earlier observation where the cardiac washout phase ( $T_{1/2}$ ) for the osteosarcoma dogs was twice as long as normal dogs see Table 3-20 on page 134. We hypothesized that the higher retention in the cancer dogs may be due to age-related renal disease. Indeed, while a statistical differences between the groups for urine activity could not be identified, the % ID at 3-hours did show a trend towards reduced renal clearance in the osteosarcoma group,  $P = 0.073^*$ . These results were also consistent with findings of a longer  $T_{1/2}$  for lung and liver ROI.

---

\* Because the sample size was not large enough which resulted in a lower power (0.372), the desired power being 0.800, the negative statistical findings should be interpreted with caution.



3.7.10 Biodistribution in Urine for Normal (n=4) and Osteosarcoma Dogs (n=3) receiving  $^{188}\text{Re-HEDP}$

Figure 3-26 Time-activity curves showing the cumulative dose in urine as a percentage of ID after renal clearance for dogs receiving  $^{188}\text{Re-HEDP}$

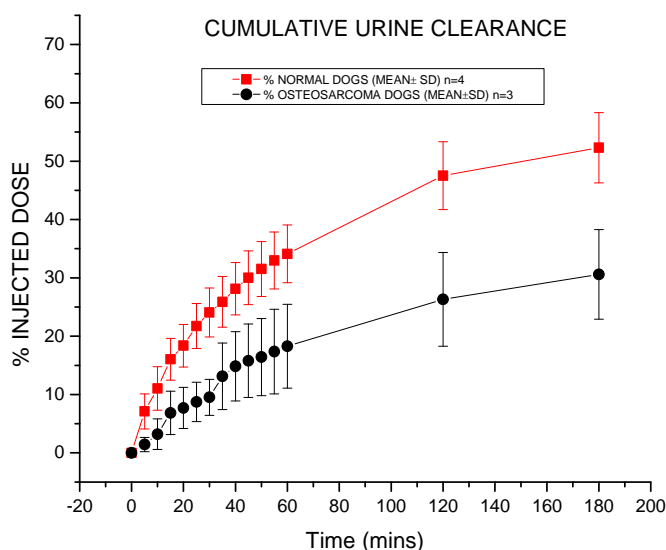


Table 3-30 Pharmacokinetic data for cumulative dose in urine after renal clearance for dogs receiving  $^{188}\text{Re-HEDP}$

Organ		Normal Dogs (n=4)	Osteosarcoma Dogs (n=3)
Urine	Parameter	Mean±SD	Mean±SD
	% ID eliminated at 3-hours	52.31 ± 12.02	30.59 ± 13.32
	Time to 50% elimination (min)	34.50 ± 8.43	45.00 ± 15.00

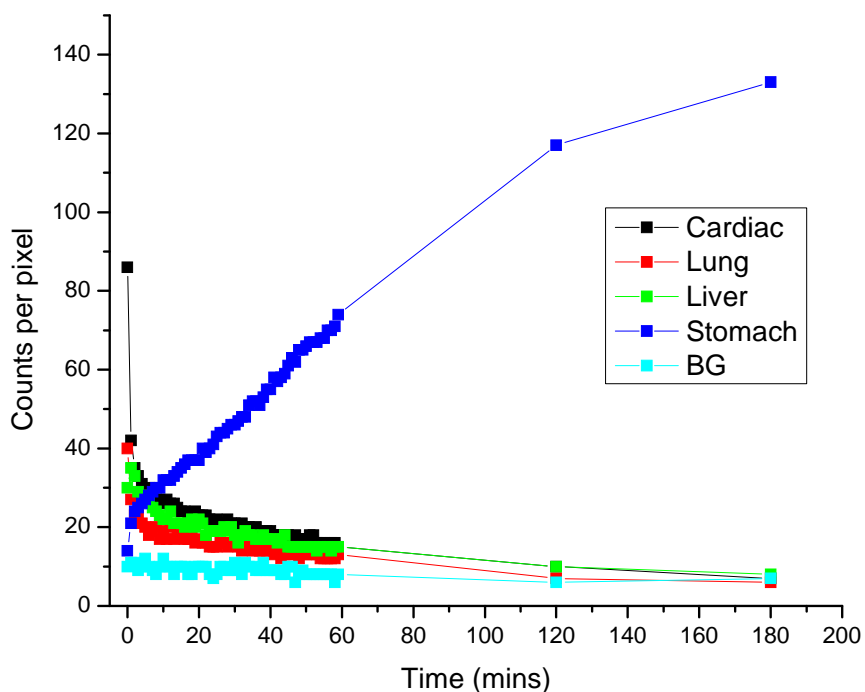
Legend: An example (Dog 1) of the calculations used to develop the cumulative urine time-activity curve can be found in the Appendix, Table 8-5 (page 278). Individual data for dogs receiving  $^{188}\text{Re-HEDP}$  can be found in the Appendix, see Table 8-11 (page 284). At 3-hours, the mean±SD was 52.31±12.02 % ID for normal dogs and 30.59 ±13.31 % ID for the osteosarcoma dog see Table 3-30 above. The osteosarcoma dogs showed a trend ( $P = 0.073$ ) towards reduced elimination of  $^{188}\text{Re-HEDP}$ , which could be attributed to a number of factors such as: reduced renal perfusion because of non-steroidal anti-inflammatory use for pain, age related renal disease, greater isotope uptake by the tumour. Within 34 to 45 minutes, 50% of the injected dose of  $^{188}\text{Re-HEDP}$  was eliminated in the urine of the normal and osteosarcoma dogs see Table 3-30 above.

### 3.8 Results for dogs receiving $^{186}\text{Re}$ -HEDP and uncomplexed $^{186}\text{Re}$

In compliance with Aim 3.3.1 on page 107 the results for dogs receiving  $^{186}\text{Re}$ -HEDP and uncomplexed  $^{186}\text{Re}$  are reported in this section. Specifically two normal dogs (Dogs 10 and 11, from Table 3-6 on page 112) received a tracer dose of  $^{186}\text{Re}$ -HEDP for dynamic scintigraphy. Because of the large volume of dynamic raw data collected for each dog, only examples of sequential calculations for Dog 1 from Table 3-6 are in shown in Table 8-1(on page 274) to Table 8-9(on page 282) of Section 8.3 of the Appendix. The tables give detailed comments on how the biodistribution, pharmacokinetic and percentage injected dose calculations were made. The results for all biodistribution and pharmacokinetic studies for individual dogs receiving  $^{186}\text{Re}$ -HEDP can be found in the Appendix, Section 8.4, and Table 8-12 (on page 285).

#### 3.8.1 Biodistribution results for a dog receiving uncomplexed $^{186}\text{Re}$

**Figure 3-27 Time-activity curves for a normal dog receiving uncomplexed  $^{186}\text{Re}$**

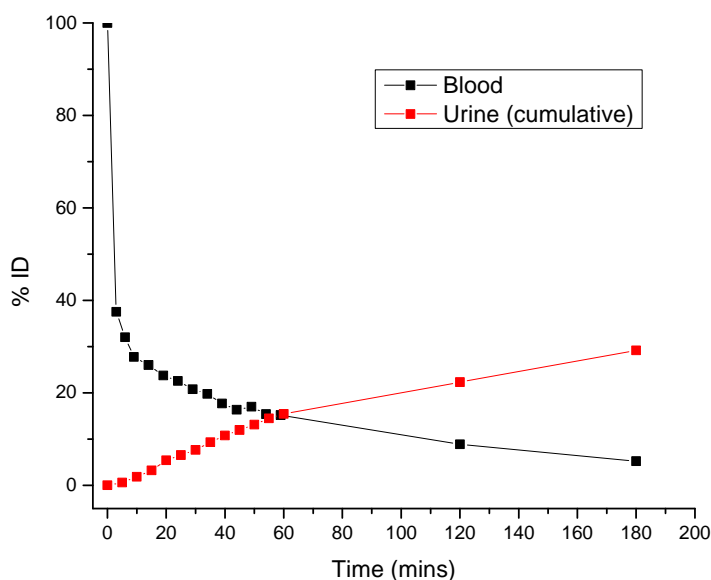


**Table 3-31 Pharmacokinetic data for all compartments in a normal dog given uncomplexed <sup>186</sup>Re**

Pharmacokinetic Parameter	Cardiac	Lung	Liver	Stomach	Background
T <sub>1/2</sub> (min)	1.00	5.00	36.00	Accumulating	26.00
T <sub>max</sub> (min)	0.00	0.00	1.00	Accumulating	1.00
% OD at 3-hours	4.35	3.73	4.97	82.61	4.35

Legend: The time-activity curves for a normal dog receiving uncomplexed <sup>186</sup>Re identified the stomach as the main organ of uptake with little evidence of washout over 3-hours. The TAC for both kidneys ROI could not be recorded due to the intense uptake in the gastric mucosa ROI which anatomically overlay both left and right kidneys thus masking their ROI. Nevertheless, renal clearance of uncomplexed <sup>186</sup>Re was confirmed by monitoring the radionuclide activity in urine, see Figure 3-28 below and Table 3-32 on page 148.

**Figure 3-28 Blood clearance and cumulative dose in urine after renal clearance as a percentage of ID for a dog receiving uncomplexed <sup>186</sup>Re**



**Table 3-32 Pharmacokinetic data for blood clearance and cumulative urine activity in receiving uncomplexed  $^{186}\text{Re}$**

Isotope $^{186}\text{Re}$	Parameter	Normal dog (n=1)
Blood	$T_{1/2}$ (min)	44.00 min
	$t_{1/2-\alpha}$ (min)	9.56 min
	$t_{1/2-\beta}$ (min)	80.22 min
	% ID at 3-hours	5.23%
Urine	% ID eliminated at 3-hours	29.20%

The rationale for the single dog experiment was for radiopharmaceutical quality control purposes, because no biodistribution reports exist in the literature for uncomplexed  $^{186}\text{Re}$ . Scintigraphy could potentially identify unexpected biodistribution that may occur due to impurities associated with radiopharmacy preparation or in-vivo instability<sup>142</sup>. The biodistribution study for uncomplexed  $^{186}\text{Re}$  showed a marked increase in uptake in the stomach over 3-hours with little evidence of washout from the organ (Figure 3-27 above). This finding has not previously been reported in the literature. The uptake in the stomach for uncomplexed  $^{186}\text{Re}$  was in sharp contrast to uncomplexed  $^{153}\text{Sm}$  which was characterised by increased liver and renal uptake; see Figure 3-3 (page 118). All other ROI showed time-activity curves typical for first order pharmacokinetics as represented by the bi-exponential curves in Figure 3-27. Remarkably, the pharmacokinetic parameters for blood  $T_{1/2}$ ,  $t_{1/2-\alpha}$  and  $t_{1/2-\beta}$  were similar to the pharmacokinetic findings for  $^{186}\text{Re}$ -HEDP, see Table 3-32 above and Table 3-34 on page 150. Nevertheless, only 29.20% of the ID at 3-hours was eliminated in urine in the uncomplexed  $^{186}\text{Re}$  study compared to 67.02% in the  $^{186}\text{Re}$ -HEDP study, confirming moderate renal clearance of uncomplexed  $^{186}\text{Re}$ . In contrast, only 0.98% of the ID was cleared in urine at 3-hours in the uncomplexed  $^{153}\text{Sm}$  study compared to 44.34% for  $^{153}\text{Sm}$ -EDTMP; confirming very little renal clearance of the uncomplexed  $^{153}\text{Sm}$  radionuclide (Table 3-8 on page 120).

3.8.2 Biodistribution results for a dog receiving  $^{186}\text{Re}$ -HEDP

Figure 3-29 Time-activity curves for a normal dog receiving  $^{186}\text{Re}$ -HEDP

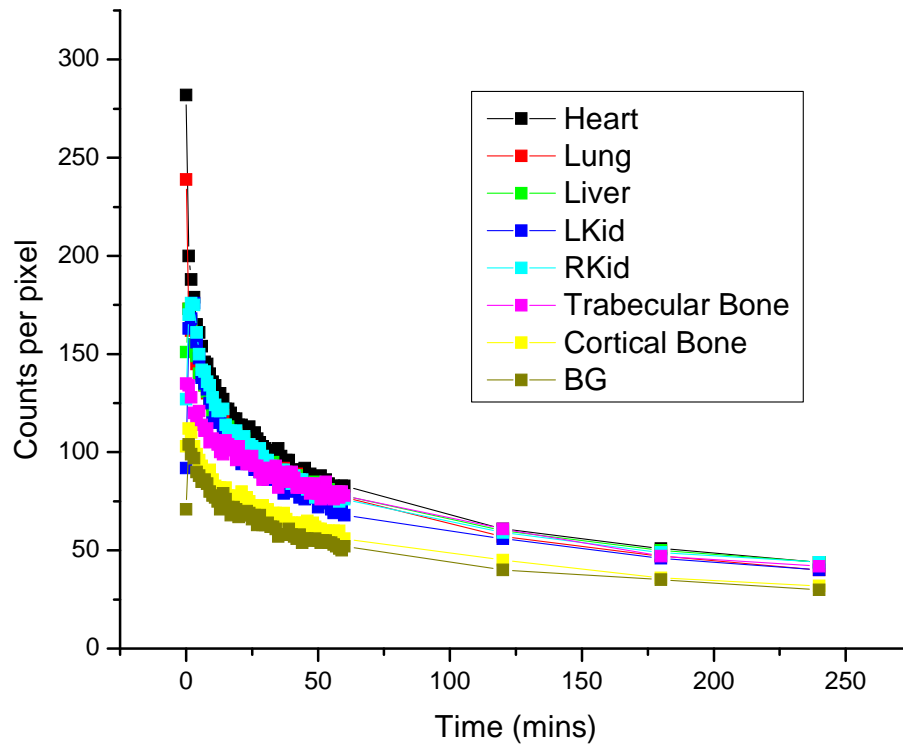
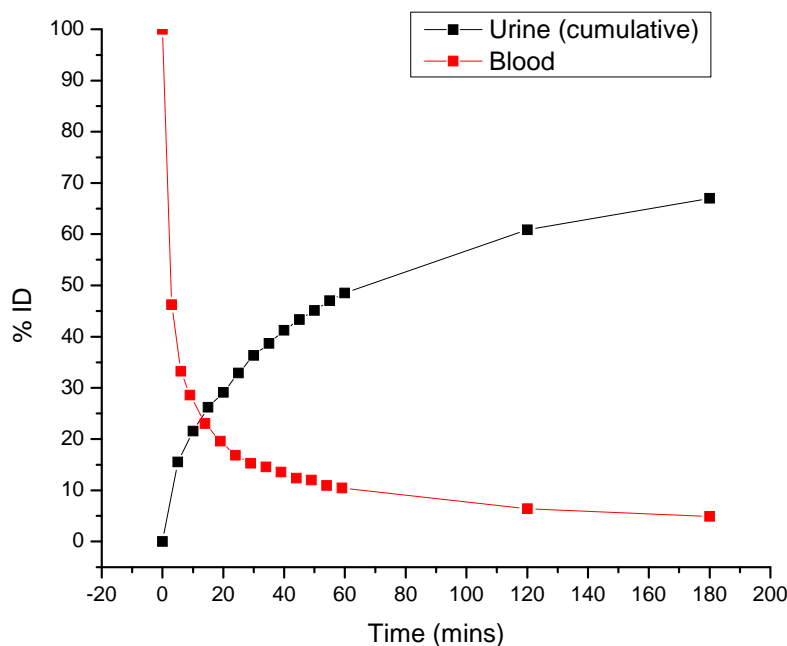


Table 3-33 Pharmacokinetic data for all compartments in a normal dog given  $^{186}\text{Re}$ -HEDP

Pharmacokinetic Parameter	Cardiac	Lung	Liver	Left kidney	Right kidney	Trabecular bone	Cortical Bone	Background
$T_{1/2}$ (min)	8.28	13.54	26.14	24.00	24.81	68.00	44.00	41
$T_{max}$ (min)	0.00	0.00	1.00	3.00	3.00	0.00	1.00	1.00
% OD at 3-hours	14.08	12.96	13.80	12.82	13.66	13.10	10.00	9.58

**Figure 3-30 Blood clearance and urine clearance (cumulative) as a percentage of ID in a normal dog receiving  $^{186}\text{Re}$ -HEDP**



**Table 3-34 Pharmacokinetic data for blood clearance and cumulative urine activity in receiving  $^{186}\text{Re}$ -HEDP**

Isotope $^{186}\text{Re}$ -HEDP	Parameter	Normal dog (n=1)
Blood	$T_{1/2}$ (min)	14.00 min
	$t_{1/2-\alpha}$ (min)	5.83 min
	$t_{1/2-\beta}$ (min)	88.12 min
	% ID at 3-hours	4.88%
Urine	% ID eliminated at 3-hours	67.02%

Legend: The time-activity curves for  $^{186}\text{Re}$ -HEDP are similar to  $^{188}\text{Re}$ -HEDP data, with prolonged blood  $t_{1/2-\beta}$  when compared to  $^{153}\text{Sm}$ -EDTMP, which showed more rapid clearance of the radiopharmaceutical. The %OD at 3 hours of  $^{186}\text{Re}$ -HEDP in trabecular bone (13.10%) was significantly lower than for  $^{153}\text{Sm}$ -EDTMP (36.98%) but similar to  $^{188}\text{Re}$ -HEDP (11.75%). This was not unexpected since both rhenium nuclides were labelled with the HEDP and as previously reported; HEDP has a lower affinity for bone compared to EDTMP, see section 1.6.2.1 on page 47. The normal  $^{186}\text{Re}$ -HEDP dog cleared 67.02% of the ID in urine at 3-hours compared to  $44.34 \pm 9.8\%$  for  $^{153}\text{Sm}$ -EDTMP and  $52.31 \pm 12.02$  for  $^{188}\text{Re}$ -HEDP.

### 3.9 Results comparing canine pharmacokinetics and biodistribution for $^{153}\text{Sm}$ -EDTMP, $^{188}\text{Re}$ -HEDP, and $^{186}\text{Re}$ -HEDP

In order to compare various radiopharmaceuticals with each other in the dog model, primary data such as time-activity curves to describe the biodistribution for  $^{153}\text{Sm}$ -EDTMP,  $^{188}\text{Re}$ -HEDP, and  $^{186}\text{Re}$ -HEDP were collected and recorded in the Appendix, Section 8.4, Table 8-10 (on page 283) to Table 8-12 (on page 285). In addition, pharmacokinetic data were also acquired, including; blood  $T_{1/2}$ ,  $t_{1/2-\alpha}$ ,  $t_{1/2-\beta}$  and urinary clearance of the three radiopharmaceuticals. These radiopharmaceutical data, where appropriate e.g.,  $n \geq 3$ , were then compared with each other using an ANOVA on Ranks, significance was set at  $P < 0.05$ . Table 8-29 on page 319 of the Appendix gives detailed results from the statistical analyses. A summary of the results can be seen in Table 3-35 on page 154.

The pharmacokinetic and biodistribution results for  $^{153}\text{Sm}$ -EDTMP in normal dogs ( $n=4$ ) for blood were  $t_{1/2-\alpha}$   $5.59 \pm 0.66$  and  $t_{1/2-\beta}$   $41.19 \pm 2.16$  minutes with  $0.78 \pm 0.39$  percentage of injected dose (% ID) retained at three hours, see Table 3-35 below.  $^{153}\text{Sm}$ -EDTMP was rapidly cleared from the body with  $44.34 \pm 9.8$  % of the ID in urine at 3-hours. Since little other activity was noted in tissues or blood ( $0.78 \pm 0.39$  % ID) other than bone at 3-hours, the assumption can be made that the whole body retention\* of  $^{153}\text{Sm}$ -EDTMP ( $50.52 \pm 6.86$  % ID) equals bone retention i.e. the effective half-life ( $Te$ )<sup>†</sup>. The pharmacokinetic and biodistribution results for  $^{188}\text{Re}$ -HEDP in normal dogs ( $n=4$ ) for blood were  $t_{1/2-\alpha}$   $6.59 \pm 0.61$  and  $t_{1/2-\beta}$   $92.19 \pm 9.86$  minutes and  $52.31 \pm 12.02$  % ID was cleared in urine at 3-hours. However, significantly more activity was found in blood at 3-hours ( $4.82 \pm 0.23$  % ID) compared to  $^{153}\text{Sm}$ -EDTMP. Even so, the gamma image showed little activity in specific organs, other than background, when compared to bone at 3-hours. Whole body retention at 3-hours was  $43.27 \pm 12.09$  % ID, and was likely to decrease further due to washout from bone. Results were only available for a single normal dog receiving  $^{186}\text{Re}$ -HEDP. The pharmacokinetic and biodistribution data for blood were  $t_{1/2-\alpha}$   $5.83$  and  $t_{1/2-\beta}$   $88.12$  minutes and  $67.02$  % ID was cleared in urine at 3-hours. At 3-hours,  $4.88$  % ID was found in blood, see Table 3-35 below.

---

\* Whole body retention is calculated by subtracting the cumulative dose % ID cleared by the kidneys in urine from the total injected dose. Note: The % ID at 3 hours is corrected for radionuclide decay.

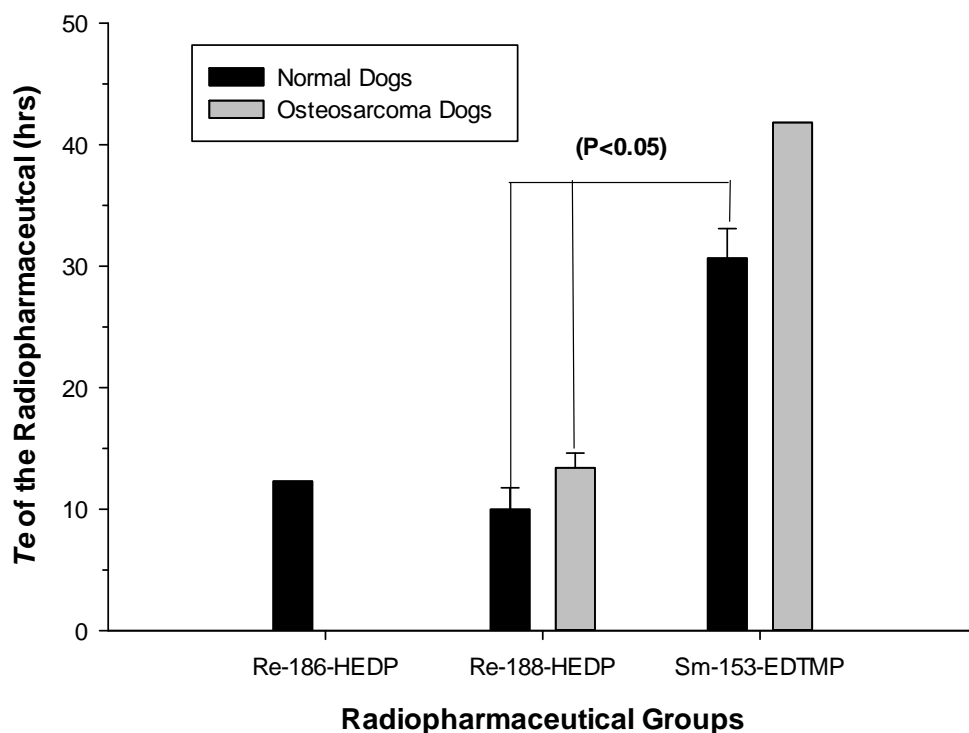
† The  $Te$  is derived from the Equation 2-9 on page 101 and is a function of the physical half-life of the radionuclide ( $Tp$ ) and the biological half-life of the radiopharmaceutical ( $Tb$ ) in the body-organ<sup>219</sup>.

Statistical comparisons were made only between normal dogs receiving  $^{188}\text{Re}$ -HEDP and  $^{153}\text{Sm}$ -EDTMP, and three tumour bearing dogs who received  $^{188}\text{Re}$ -HEDP, see Table 3-35 below. Statistical differences ( $P < 0.05$ ) were found for  $t_{1/2-\beta}$  (elimination phase) and retention in blood at 3-hours between normal dogs receiving  $^{153}\text{Sm}$ -EDTMP and dogs receiving  $^{188}\text{Re}$ -HEDP. The longer  $t_{1/2-\beta}$  and increased blood retention (% ID) of  $^{188}\text{Re}$ -HEDP are a reflection of prolonged bone washout of the radiopharmaceutical i.e. reduced stickiness of  $^{188}\text{Re}$ -HEDP to bone. This can be explained by the >100-fold weaker antiresorptive ability of HEDP (etidronate), a non-amino-bisphosphonate, compared to the amino-bisphosphonate ligand EDTMP (lexidronam). The only statistically significant finding between dogs with osteosarcoma and normal dogs given  $^{188}\text{Re}$ -HEDP was the increased retention (% ID) of the radiopharmaceutical in blood, which was higher for the osteosarcoma cases. The trend in the dogs with osteosarcoma receiving either  $^{153}\text{Sm}$ -EDTMP ( $n=1$ ) or  $^{188}\text{Re}$ -HEDP ( $n=3$ ) was for greater retention of the radiopharmaceuticals in the whole body and less in the urine at 3-hours compared to normal dogs see Table 3-35 below.

For comparative purposes, we calculated the effective half-life ( $T_e$ ) for whole body retention for the three radiopharmaceuticals in normal dogs and dogs with osteosarcoma. The whole body retention of the % ID is calculated by subtracting total % ID (decay corrected) found in urine at 3-hours from a 100% (i.e. % total injected dose). The ( $T_e$ ) data can be found in Section 8.4 of the Appendix, Table 8-13 on page 286. The individual radiopharmaceuticals in normal dogs and dogs with osteosarcoma were compared with each other and where applicable an ANOVA was performed on the data. Only three sets of data could be analysed statistically, these were; normal dogs receiving  $^{153}\text{Sm}$ -EDTMP (Mean $\pm$ SD, 30.66 $\pm$ 2.45 hrs.) and normal (9.98 $\pm$ 1.77) and osteosarcoma dogs (13.40 $\pm$ 1.20) receiving  $^{188}\text{Re}$ -HEDP. Results from the comparison between groups and other  $T_e$  for single dogs can be found in Figure 3-31 below. A significant difference ( $P < 0.05$ ) was found between  $^{153}\text{Sm}$ -EDTMP and both  $^{188}\text{Re}$ -HEDP dog groups. Thus, the  $T_e$  from  $^{188}\text{Re}$ -HEDP is less than the  $T_e$  than for  $^{153}\text{Sm}$ -EDTMP because of the shorter physical ( $T_p$ ) and biological ( $T_b$ ) half-life of  $^{188}\text{Re}$ -HEDP. This finding supports the hypothesis that the dog is more likely to show myelosuppression with repeated or higher doses of  $^{153}\text{Sm}$ -EDTMP than with  $^{188}\text{Re}$ -HEDP. Indeed this was a later study finding in dogs receiving repeated doses of  $^{188}\text{Re}$ -HEDP. While only single data points were available for a diseased dog receiving  $^{153}\text{Sm}$ -EDTMP and a normal dog receiving  $^{186}\text{Re}$ -HEDP in Figure 3-31, they do support the findings for the other groups.



**Figure 3-31 A comparison of whole body effective half-life ( $T_e$ ) for various radiopharmaceuticals in dogs**



Legend: The  $T_e$  half-life for  $^{188}\text{Re}$ -HEDP (normal and osteosarcoma dogs) when compared to  $^{153}\text{Sm}$ -EDTMP were statistically different ( $P < 0.05$ ). This finding supports the hypothesis that the dog is more likely to show myelosuppression with repeated or higher doses of  $^{153}\text{Sm}$ -EDTMP than with  $^{188}\text{Re}$ -HEDP.

**Table 3-35 Data showing pharmacokinetics, biodistribution and bone localization of <sup>153</sup>Sm-EDTMP, <sup>188</sup>Re-HEDP and <sup>186</sup>Re-HEDP in experimental dogs**

Studies Parameter	<sup>153</sup> Sm-EDTMP Normal dogs (n=4)	<sup>153</sup> Sm-EDTMP Osteosarcoma dogs (n=1)	<sup>188</sup> Re-HEDP Normal dogs (n=4)	<sup>188</sup> Re-HEDP Osteosarcoma dogs (n=3)	<sup>186</sup> Re-HEDP Normal dog (n=1)	ANOVA P-value
<b>Tumour %OD</b>	NA	20.59	NA	15	NA	NA
<b>Bone % ID at 3-hours</b>	45.81±10.20	50.24	43.27±12.09	46.64(61.64±11.34)	28.1	NS
<b>Urine % ID eliminated at 3-hours</b>	44.34±9.8	29.17	52.31±12.02	30.59±13.31	67.02	NS
<b>Blood % ID at 3-hours</b>	0.78±0.39*	0.23	4.82±0.23*	7.76±2.22*	4.88	<i>P</i> <0.005
<b>Blood (t<sub>1/2-α</sub>) min</b>	5.59±0.66	6.29	6.59±0.61	5.26±0.97	5.83	NS
<b>Blood (t<sub>1/2-β</sub>) min</b>	41.19±2.16**	31.86	92.19±9.86**	104.92±29.16**	88.12	<i>P</i> <0.005

\* Identifies the groups that were compared to each other for % ID in blood at 3-hours using ANOVA. Dogs receiving <sup>153</sup>Sm-EDTMP were statistically different from both groups of dogs receiving <sup>188</sup>Re-HEDP.

\*\*Identifies the groups that were compared to each other for t<sub>1/2-β</sub> in blood at 3-hours using ANOVA. Dogs receiving <sup>153</sup>Sm-EDTMP were statistically different from both groups of dogs receiving <sup>188</sup>Re-HEDP.

NS = not statistically significant

### 3.10 Results from a comparison between canine and human data for $^{153}\text{Sm}$ -EDTMP, $^{188}\text{Re}$ -HEDP, and $^{186}\text{Re}$ -HEDP

As outlined in section 3.3.3 the biodistribution and pharmacokinetic results from the canine studies were compared with data from the human literature. Three human studies with skeletal metastases, Bayouth *et al.*,<sup>122</sup> Farhanghi *et al.*,<sup>226</sup> and Brenner *et al.*,<sup>227</sup> had sufficient data to compare with the canine  $^{153}\text{Sm}$ -EDTMP pharmacokinetic data, see Table 3-36 on page 157. Only a single  $^{188}\text{Re}$ -HEDP human study skeletal metastases study by Liepe *et al.*,<sup>231</sup> was found to have sufficient data to compare with normal and osteosarcoma dogs receiving  $^{188}\text{Re}$ -HEDP, see Table 3-37 on page 158. For comparative purposes, data from two human skeletal metastases  $^{186}\text{Re}$ -HEDP studies and a single normal dog from our study are also reported in Table 3-37 on page 158.

The publications were analysed and the number of patients in the study, biodistribution and pharmacokinetic data were recorded. Specifically the following human data were recorded; the % ID at 3-4 and 24 hours for the whole body-skeleton, % ID at 3-4 hours for urine, % ID at 30 minutes in blood, and pharmacokinetic data for blood  $t_{1/2-\alpha}$ ,  $t_{1/2-\beta}$ . The biodistribution and pharmacokinetic data were entered into the statistical program as the mean, standard deviation and the number of individuals in each study. The canine and human data were checked for normal distribution and then compared using a one-way-ANOVA. Due to the limitations of the study, no 24-hour canine whole-body and urine % ID data were available to compare to human 24-hour data. However, when the 3-hour canine data were compared to the human data, no statistical differences were found ( $P = 0.99$ ), see Table 3-36 (page 157). This finding could be explained by the observed rapid binding of  $^{153}\text{Sm}$ -EDTMP to bone and rapid renal clearance within the first 3-hours in both species, leaving only a negligible amount of % ID to be cleared after 3-hours.

The only statistical parameter for  $^{153}\text{Sm}$ -EDTMP found to be different between canines and humans was  $t_{1/2-\beta}$  for blood ( $P < 0.001$ ). Blood  $t_{1/2-\beta}$  denotes the elimination phase of  $^{153}\text{Sm}$ -EDTMP from the body. While the result was statistically different, it is probably not clinically important and may be a reflection of decreased renal clearance of  $^{153}\text{Sm}$ -EDTMP in older people with advanced metastatic skeletal disease. The statistical parameters for  $^{188}\text{Re}$ -HEDP which were found to be different between canines and humans was the % ID in bone at 3-hours ( $P < 0.05$ ) and

the % ID cleared in the urine by 3-hours ( $P < 0.05$ ). However, the difference was between dogs with osteosarcoma and normal dogs and humans. This could be explained by the difference in tumour uptake since the canine osteosarcoma competes with normal bone for radiopharmaceutical uptake and more  $^{188}\text{Re}$ -HEDP was cleared in the urine at 3-hours compared to the human study. Competition for uptake could also be the reason for the difference between normal and tumour bearing dogs, although more  $^{188}\text{Re}$ -HEDP was cleared in the urine at 3-hours in the normal dogs. The normal dogs were also a more homogenous group i.e., German shepherd dogs, whereas the tumour bearing dogs were small mixed population. Interestingly whole body retention for all three populations receiving  $^{188}\text{Re}$ -HEDP were not statistically different ( $P = 0.132$ ). Urine clearance of the % ID at 3-hours did differ between canines and humans, although this maybe artificial since the urine clearance of the % ID at 48-hours in humans<sup>231</sup> when compared to normal dogs was not different. The likelihood of population differences cannot be excluded.

Overall, the comparison supports the applicability of the canine  $^{153}\text{Sm}$ -EDTMP and  $^{188}\text{Re}$ -HEDP pharmacokinetic data as a preclinical model for human research.

**Table 3-36 Data showing pharmacokinetics and bone localization of  $^{153}\text{Sm}$ -EDTMP in humans and animals**

Studies Parameter	Study Population Normal dogs	Study Population Osteosarcoma dog	Human (Farhanghi <i>et al.</i> , 1992)	Human (Bayouth <i>et al.</i> , 1994)	Human (Brenner <i>et al.</i> , 2001)	ANOVA P-value
Subjects	4	1	22	19	18	NA
Tumour Type	None	Osteosarcoma	Metastatic carcinomas	Metastatic carcinomas	Metastatic carcinomas	NA
Tumour % ID	NA	20.59%	NR	NR	NR	NA
Whole Body % ID at 3-hours	50.52±6.86% (3-hours)*	50.24%(3-hours)*	NR	50.4±14% (24 hours)*	47.7±11.2%*	0.99
Urine % ID eliminated at 3-hours	44.34±9.8%*	29.17%*	35.9±13.5% (24 hrs.)* 30% (4 hrs.)	49.6%	39.5±13.8%*	0.25
Blood % ID at 30 min	9.53%±2.13%*	6.87%*	9.6±2.8%*	20%	NR	0.96
Blood % ID at 3-4hours	0.78±0.39%*	0.23%	1.3±0.7%*	NR	NR	0.17
Blood ( $t_{1/2-\alpha}$ ) min	5.59±0.66 min*	6.29 min	14 min	5.5±1.1 min*	NR	0.88
Blood ( $t_{1/2-\beta}$ ) min	41.19±2.16 min*	31.86 min	690 min**	65.4±9.6 min*	NR	<0.001*

Legend: Where available, only human data reporting a mean, standard deviation, and numbers were compared using a one-way ANOVA. For example, for whole body % ID, the canine group could be compared with the human groups reported by Bayouth *et al.*,<sup>122</sup> and Brenner *et al.*,<sup>227</sup>. For urine % ID, the canine group could be compared with the human groups reported by Farhanghi *et al.*,<sup>226</sup> and Brenner *et al.*,<sup>227</sup>. At no time could all three studies compared together except for whole body % ID, due to missing data from human studies.

\*Denotes the population groups that were compared with each other. Only  $t_{1/2-\beta}$  for blood was found to be statically different between the canine group and the human group as reported by Bayouth *et al.*,<sup>122</sup>.

\*\* The human  $t_{1/2-\beta}$  reported by Farhanghi *et al.*,<sup>226</sup> is significantly longer than that reported for the canine study and the Bayouth study. The significance of this finding is not discussed by Farhanghi *et al.*,<sup>226</sup> but is likely due to differences in pharmacokinetic modelling of blood activity.

**Table 3-37 Data showing pharmacokinetics and bone localization of  $^{186}\text{Re-HEDP}$  and  $^{188}\text{Re-HEDP}$  in humans and animals**

Studies Parameter	Study Population Normal Dogs	Study Population Osteosarcoma Dogs	Human (Liepe <i>et al.</i> , 2003)	Study Population Normal Dog	Human (de Klerk <i>et al.</i> , 1992)	Human (Brenner <i>et al.</i> , 2001)	ANOVA P-value
Radioisotope	$^{188}\text{Re-HEDP}$	$^{188}\text{Re-HEDP}$	$^{188}\text{Re-HEDP}$	$^{186}\text{Re-HEDP}$	$^{186}\text{Re-HEDP}$	$^{186}\text{Re-HEDP}$	
Subjects	4	3	13	1	11	11	NA
Tumour Type	Normal	Osteosarcoma	Skeletal metastases (prostate CA)	Normal	Skeletal metastases. (prostate and breast CA)	Skeletal metastases (prostate and breast CA).	
Tumour % ID	NA	4.17±0.23	1.45±0.68%	NA	NR	NR	NA
Bone % ID at 3 hours	43.27±12.09%*	16.41±5.04*	46.1±14.8%*	28.1%	20%	21.8%±9.0%	<0.001*
Whole Body % ID at 3 hours	47.69±12.02%*	69.41±13.32%*	49.3±16.4%*	32.98%	20%	34.6%	0.132
Soft-tissue % ID at 3 hours	15.25±2.5%	6.80±3.00	NR	0.40%	NR	12.8%±5.4%	NA
Urine % ID eliminated at 3 hours	52.31±12.02%*	30.59±13.31%*	20±10%* (60±12%at48hrs)	67.02%	71±6%	65.3%±12.8%	<0.001*
Blood % ID at 3- 4hours	4.82±0.23	7.76±2.22	NR	4.88%	40.1±5%	NR	NA
Blood ( $t_{1/2-\alpha}$ ) min	6.59±0.61 min	5.26±0.97 min	NR	5.83 min	NR	NR	NA
Blood ( $t_{1/2-\beta}$ ) min	92.19±9.86 min	104.92±29.16 min	NR	88.12 min	NR	NR	NA

\* Denotes the population groups that were compared with each other. Two of the three pharmacokinetic parameters examined were found to be different between population groups. However, for the % ID in bone the difference was between normal dogs and tumour bearing dogs and humans and tumour bearing dogs. The difference between dogs and humans for the % ID cleared in urine at 3-hours could be artificial since it was extrapolated from Figure 3 in Liepe *et al.*, 2003<sup>114</sup>. At 48-hours, the difference was not apparent.

### **3.11 Materials and methods for the therapy group of dogs with osteosarcoma and multilobular osteochondrosarcoma receiving <sup>153</sup>Sm-EDTMP**

#### **3.11.1 Model System and Sample size**

As previously described, canine osteosarcoma is a recognized animal model for human osteosarcoma and should also serve as a useful model for metastatic bone cancer<sup>39, 145, 146, 149, 243, 244</sup>. To meet the aims and objectives as set out in Aim 3.3.4, twenty dogs (Cases 1 to 20, see Table 8-14, page 287) with radiologically and/or histologically diagnosed osteosarcoma (n=17) and multilobular osteochondrosarcoma (n=3) were enrolled into the study. Ethical approval and client consent was obtained prior to enrolment into the study, see Appendix section 8.1 (page 272). Dogs were excluded if evidence of lung metastases were found or if the dogs had evidence of compromised organ function e.g., azotaemia.

#### **3.11.2 Experimental Design and Experimental Procedures**

All dogs underwent full clinical examinations and radiographs of the primary tumour site as well as the following radiographs of the thorax, left and right lateral views, and dorsal-ventral and ventral-dorsal views. Only cases found to be free of radiological evidence of lung metastases and with signed consent were included in the study. The sizes of primary tumours and tumour stage were recorded from radiographs and are reported in the Appendix Table 8-15 (on page 291). The size of the tumour was determined by measuring the length of the tumour along the long axis of the bone followed by the maximum measurement in a cranial-caudal orientation followed by a lateral to medial (maximum) measurement (always at 90 degrees to each other)<sup>22</sup>. The margins were defined as those areas showing abnormal bone changes associated with bone tumours such as periosteal reaction, loss of cortical bone. The tumour volume was calculated from the equation for the volume of an ellipsoid (Volume =  $\pi/6(\text{length}) \times (\text{width}) \times (\text{height})$ ), the ellipsoid is considered a more applicable representation of the tumour volume than a rectangle<sup>245</sup>. This volume was then divided by itself to give a baseline value of 1, all subsequent measurements (monthly) were recorded and divided by the initial value to give a ratio of increase in size by the tumour, see Appendix, Table 8-16 (page 302). The cases were staged using the TNM method for bone tumours<sup>246</sup> were T0 = no evidence of a primary tumour, T1 = tumour confined to within bone medulla/cortex, T2 =

tumour extending beyond periosteum, M0 = no evidence of metastases and M1 = distant metastases present. For individual staging, see Appendix, Table 8-14 (page 287).

Most of the dogs with appendicular tumours were found to be lame in the affected limb and in some cases non-weight bearing. Thirteen out of seventeen dogs were confirmed by biopsy or post-mortem to have osteosarcomas. The other 4 dogs were considered to be radiographically (site, radiographic appearance, progression with metastases obvious at euthanasia) typical for appendicular osteosarcoma. Case-9 was an exception, which was classified as an aggressive primary bone tumour involving the whole wing of the scapula (Table 8-15, page 291). Nine dogs underwent an initial bone scan using  $^{99m}\text{Tc}$ -MDP as a possible indicator of tumour uptake by  $^{153}\text{Sm}$ -EDTMP and thus the likelihood of successful treatment <sup>7</sup>. The IV diagnostic dose of  $^{99m}\text{Tc}$ -MDP varied between 185 and 592 MBq depending on body weight. Three hours post injection light sedation was achieved using medetomidine HCl (Domitor 1mg/ml, Ciba) at 0.1 ml/10kg and ketamine HCL (3mg/kg). Scanning was then immediately done using a Siemens Orbital gamma camera (low energy collimator) (energy peak 140 keV, window 15%). Images of two-minute duration were acquired in 64 x 64-word mode. Reference regions of interest (ROI) were identified at the tumour site and at the same location on the contra lateral limb. Counts per pixel were recorded for the tumour (T) and contra-lateral ROI (NTC=non-tumour counts) and calculated as a ratio (T/NTC) which are reported in Appendix Table 8-14 (page 287). Regrettably,  $^{99m}\text{Tc}$ -MDP results for Case-3 scan were not recorded, as these were lost.

$^{153}\text{Sm}$ -EDTMP (Atomic Energy Corporation of South Africa [Pty.] Ltd) was given to the first nine cases 7 days after  $^{99m}\text{Tc}$ -MDP scan. The therapeutic dose of 37 MBq/kg was given as an IV bolus over a 30-second period via an indwelling catheter. The catheter was flushed following administration of  $^{153}\text{Sm}$ -EDTMP using 5 ml sterile saline solution to ensure complete administration of the calculated dose. In the case of last nine dogs a therapeutic dose of 37 MBq/kg  $^{153}\text{Sm}$ -EDTMP was given immediately followed by a scan 24 hours later (all calculated T/NTC are based on  $^{153}\text{Sm}$ -EDTMP 24 hour scans). All cases returned monthly or bi-monthly for follow-up radiographs of the thorax and primary tumour site. The size of the primary tumour and evidence of metastases were recorded as reported above. Blood samples were collected from the cephalic vein (EDTA tubes, Becton Dickinson, Vacutainer Systems, Europe) for haematology in some dogs (n=5) at two and 4 weeks post-



treatment. Blood samples were not taken in other cases (n=13) for the following reasons e.g., owner non-compliance, distance from the faculty, cost of tests.

For ethical reasons all dogs were given a non-steroidal anti-inflammatory, piroxicam\* at 0.3mg/kg once every second day for pain control and misoprostol† at 2-5µg/kg twice daily to prevent gastric ulceration. This was done at least 14 days prior to radioisotope treatment as pain control could have been attributed to piroxicam rather than <sup>153</sup>Sm-EDTMP. The owners were requested to monitor improvement in limb function over time, and for other signs associated pain such as loss of appetite. Pain was scored based on the following grouping; poor pain control, moderate and good pain control, see Table 3-38 below.

**Table 3-38 Pain scoring used to describe treated dogs.**

Scoring	Description
Poor pain control	Dog carries leg at all times, evidence of constant pain, vocalization.
Moderate pain control	Mild lameness evident at all times, some sensitivity on deep palpation.
Good pain control	No lameness or no pain on palpation. Limb has good function.

Legend: The subjective pain scoring system was devised for the study and the investigator did the scoring. Other scoring systems have been devised use lameness monitoring using force-plate Systems. These were not available to the researcher

### 3.11.3 Data Analysis

Descriptive statistics were used to describe the patient demographics such as age, body weight, and gender‡. The Kolmogorov-Smirnov test was used to determine whether data were normally distributed and variances were equal. Using linear regression, tumour size was plotted over time and examined for trends§. Comparisons were also made between groups for haematology using ANOVA of repeated measures\*. The Kaplan-Meier product-limit method was used to analyse data for duration of survival time. The log-rank test was used to examine the effect of several variables on survival, these were: sex, tumour size at diagnosis, histopathological description, presence of metastasis at death, position of the osteosarcoma

\* Feldene, Pfizer Laboratories [Pty] Ltd, Sandton

† Cytotec, G D Searle [SA] [Pty] Ltd, Johannesburg

‡ SPSS, Inc. (1997). SigmaStat version 2.03. www.spss.com

§ SPSS, Inc. (2002). SigmaPlot for Windows, version 8.02. www.spss.com

on the skeleton (axial vs. appendicular), site of the tumour on the skeleton (skull vs. distal radius etc.), pain control, uptake ratios, and treatment\*. Survival time was calculated from treatment to the time of death.

### 3.11.4 Results

#### 3.11.4.1 Population data

The patient details were recorded and are reported in Appendix, Table 8-14 (see page 287). Of the 20 dogs enrolled in the study, 15 were female and 5 male. The most common breed entered into the study were Rottweiler's (n=6) followed by German Shepherd dogs (n=2), other single large breed dogs (n=11), and a small mixed breed (n=1). The mean±SD age of the dogs with osteosarcoma was 7.55±2.85 years with a mean±SD body weight (BW) of 38.52 ± 11.95 kg. Fifteen dogs presented with osteosarcoma of the appendicular skeleton and five with axial skeletal osteosarcomas. Dogs with appendicular osteosarcomas all presented with obvious signs of lameness, see Appendix, Table 8-14 (see page 287). In most cases, lameness was the primary reason for presentation to the veterinarian. In cases where the axial skeleton was involved (pelvis, zygomatic arch and skull), the presenting signs were pain on manipulation and or a firm hard mass. Most dogs presented to the study were receiving nonsteroidal anti-inflammatories (NSAIDs) as prescribed by the primary veterinarian. These included phenylbutazone, meloxicam, piroxicam, ibuprofen, and aspirin. On enrolment into the study, all dogs received piroxicam at 0.3mg/kg once a day until euthanasia or until side effects were seen. If gastrointestinal signs were observed, the dose of piroxicam was reduced to every second day. A single dog (Case-12) required discontinuation of all NSAIDs due to significant gastrointestinal bleeding, resulting in a clinical anaemia. This dog received ibuprofen prior to entry into the study. Description of individual tumours and scanned in radiographs were recorded and can be found in Appendix 1, Table 8-15 (see page 291). Radiographs of dogs with appendicular (n=15) osteosarcoma identified six distal radius, four proximal humerus, two distal femurs, two scapulae, and one distal tibial bone tumour. The axial skeleton had four skull primary bone tumours (zygomatic, nasal, orbit, and

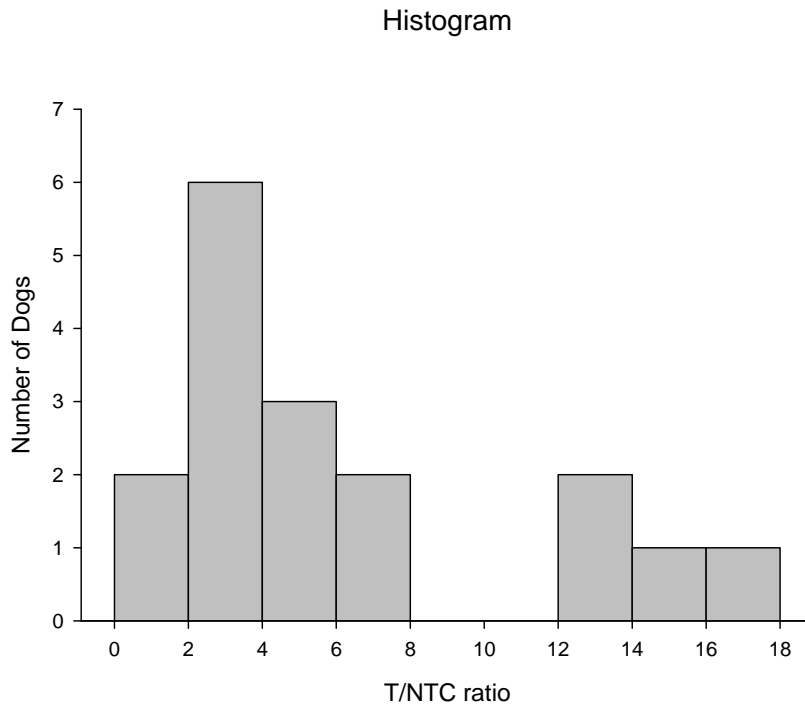
---

\* StatSoft, Inc. (2003). STATISTICA (data analysis software system), version 6.  
www.statsoft.com.

posterior skull) and pelvic osteosarcoma. All dogs were staged radiographically and the majority (n=18) were staged T2 (tumour extending beyond periosteum) with only two dogs staged as T1 (tumour confined to the bone marrow). No evidence of regional node involvement or distant metastases were found on enrolment in to the study.

Of the 20 dogs enrolled, 19 dogs received  $^{153}\text{Sm}$ -EDTMP at 37 MBq/kg (1mCi/kg). One dog (Case-11) was lost to follow-up and another (Case-13) did not receive a therapeutic dose of  $^{153}\text{Sm}$ -EDTMP, but rather a tracer dose of  $^{153}\text{Sm}$ -EDTMP and underwent a 3-hour dynamic scan. Because of the advanced nature of the osteosarcoma, the dog was immediately euthanized following the dynamic scan and was necropsied. This dog was used in an autoradiography study; see Section 3.16 on page 194. All dogs excluding Case-13 underwent static 24-hour bone scans following  $^{153}\text{Sm}$ -EDTMP administration and the uptake in the tumour (T) and opposite normal limb (NTC) were recorded. Cases 1-4 and 6-9 also had MDP bone scans 1 week prior to the  $^{153}\text{Sm}$ -EDTMP study. The mean  $^{153}\text{Sm}$ -EDTMP uptake ratio (T/NTC) for all the dogs (n=17), excluding cases 3, 11, and 12, was  $6.32 \pm 5.03$ . However, a histogram evaluation of the uptake ratios did show a bimodal distribution; see Figure 3-32 below. Unfortunately, due to the small number of cases the reason for the bimodal distribution could not be adequately explained. When the case-matched (Cases 1, 4, 6 and 9. See Table 8-14 on page 287) mean uptake ratios (n=4) of the preliminary  $^{99\text{m}}\text{Tc}$ -MDP ( $4.23 \pm 2.39$ ) bone scan were compared to the uptake ratios of the  $^{153}\text{Sm}$ -EDTMP ( $8.22 \pm 4.86$ ) scan, no statistical difference were found ( $P = 0.21$ ). This is in agreement with previous reports by Lattimer *et al.*, who found no difference between  $^{99\text{m}}\text{Tc}$ -MDP and  $^{153}\text{Sm}$ -EDTMP uptake ratios<sup>15</sup>. Interestingly the coefficient of variance (standard deviation / mean) for  $^{99\text{m}}\text{Tc}$ -MDP and  $^{153}\text{Sm}$ -EDTMP and were 0.54 and 0.59 respectively, indicating a wide standard deviation of the mean the uptake ratios between tumours, but not between radiopharmaceuticals.

**Figure 3-32: A histogram of osteosarcoma dogs (n=17) receiving  $^{153}\text{Sm-EDTMP}$  showing the distribution of T/NTC uptake ratios.**



Legend: The histogram above illustrates the distribution of the tumour to contralateral limb (T/NTC) uptake ratios for dog with osteosarcoma receiving  $^{153}\text{Sm-EDTMP}$ . The mean uptake was  $6.32 \pm 5.03$  for all dogs (n=17). The presence of bimodal peaks indicated the variability of uptake between tumours. Four dogs had uptake ratios of greater than 10:1. As will be shown later the increased uptake was not associated with improved survival or pain control.

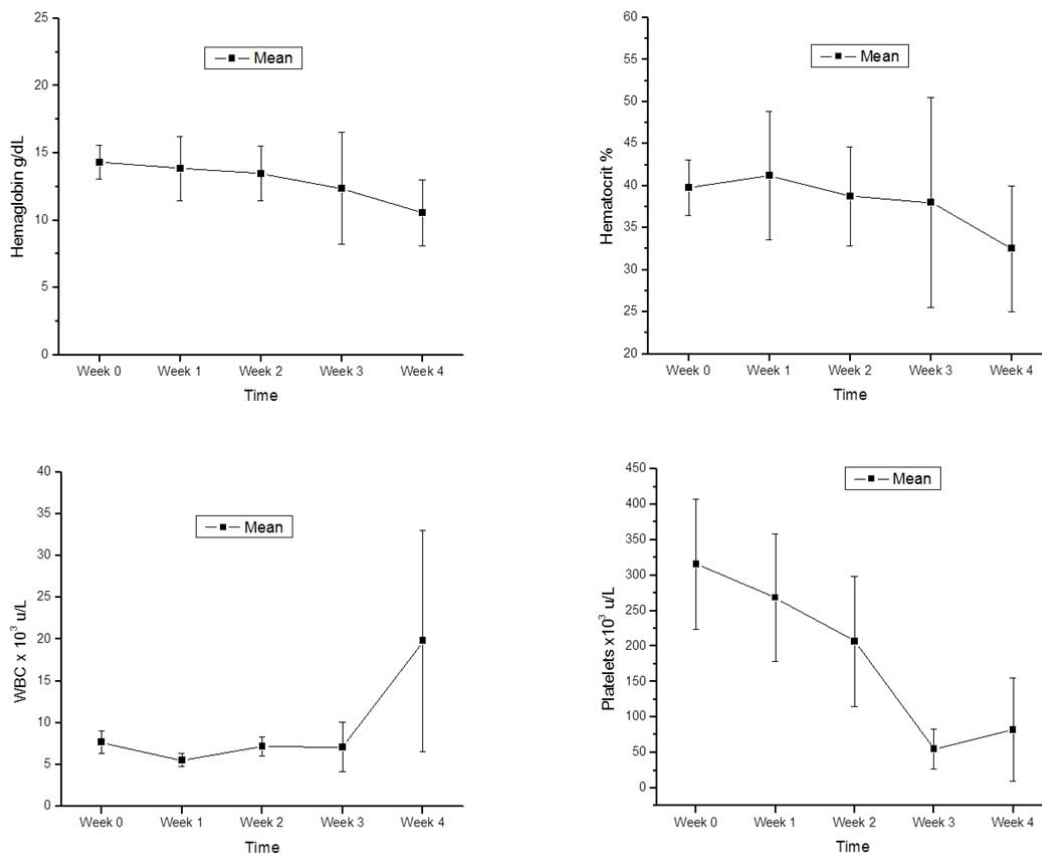
#### 3.11.4.2 Response to treatment

##### *Haematology*

Haematology results were examined and were found complete for five dogs. Raw data and descriptive statistics for haemoglobin, haematocrit, white blood cell (WBC) and platelet count, are displayed graphically in Figure 3-33 on page 165 and tabulated in the Appendix, Table 8-17 (see page 303) and Table 8-18 (see page 304). Comparisons between the means (One Way Repeated Measures ANOVA) for weekly haemoglobin ( $P = 0.936$ ), haematocrit ( $P = 0.979$ ) and WBC ( $P = 0.124$ ) values were not statistically significant. Nevertheless, a statistical difference was found between the mean weekly platelet values ( $P = 0.043$ ). A post-hoc analysis found platelets at week-3 to be statistically ( $P < 0.05$ ) different (lower) from

week-0 (baseline). The platelet descriptive statistics are reported in Table 3-39 on page 166. Using the WHO grading for toxicity the platelet counts at week-3 were considered Grade 2 toxicity<sup>126</sup>. While week-3 was the only time that there was a statistical significant difference compared to week-0 (baseline), the platelet count at week-4 was lower than clinically acceptable and was considered Grade 1 toxicity. The time to recovery could not be determined as no samples were collected after 4 weeks.

**Figure 3-33** Graphs representing haemoglobin, haematocrit, white blood cell and platelets values for dogs (n=5) receiving <sup>153</sup>Sm-EDTMP



Legend: The graphs display the four measured haematology parameters for the study. While only changes in platelet counts at week-3 were statistically significant, clinically relevant trends were seen at week-4. For instance, the platelet count at week-4 was still clinically relevant although not statistically different from baseline, since it fell below the lower normal range of  $200 \times 10^3 \mu\text{L}$ . While some changes were noted for the haematocrit and haemoglobin they were not outside the normal range. The WBC count at week-4 could be considered elevated, nevertheless only two dogs contributed to the values and may not be significant. It

is possible that the WBC count elevation could be due to a rebound effect of the bone marrow, although the WBC count at no time appeared decreases below normal range. Week-1 did show a mild change downwards from the baseline (week-0).

**Table 3-39 Descriptive statistics for platelets for dogs (n=5) receiving  $^{153}\text{Sm}$ -EDTMP**

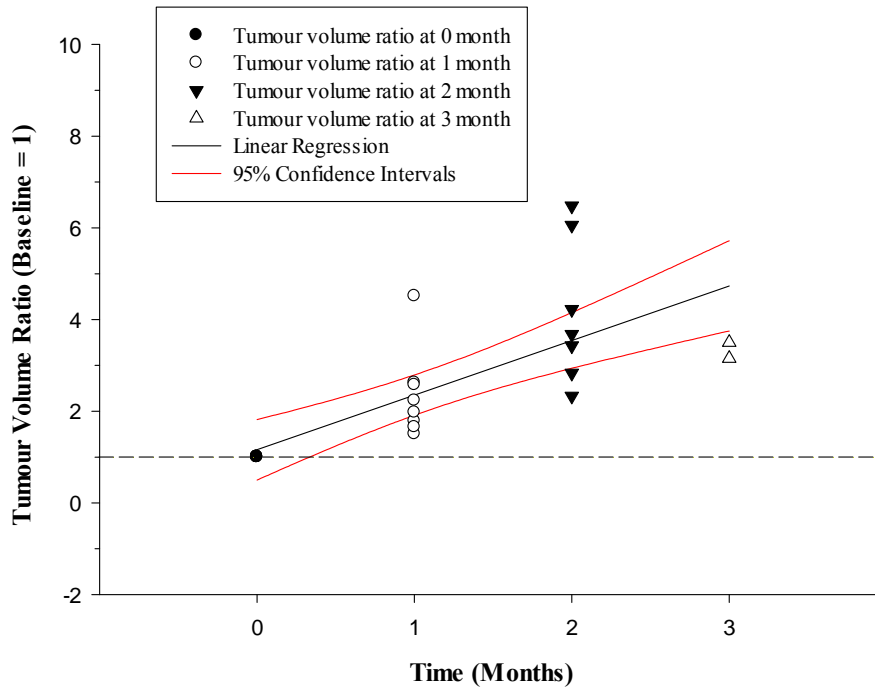
Sample weeks	Number of cases	Platelet counts Mean $\pm$ SD $\mu$ /l	<i>P</i> value
Week-0	5	315.60 $\pm$ 205 x 10 <sup>3</sup> $\mu$ /l	Baseline
Week-1	5	268.40 $\pm$ 201 x 10 <sup>3</sup> $\mu$ /l	NS
Week-2	5	207.00 $\pm$ 205x 10 <sup>3</sup> $\mu$ /l	NS
Week-3	3	54.61 $\pm$ 48 x 10 <sup>3</sup> $\mu$ /l	<i>P</i> < 0.05
Week-4	2	82.1 $\pm$ 103 x 10 <sup>3</sup> $\mu$ /l	NS

Legend: The normal range of platelets in blood for the dog is between 200-500 x 10<sup>3</sup>  $\mu$ /l. Some variation exists depending on the reference laboratory. Week-0 was considered the control and all weeks were compared to week-0 using a One-Way-Repeated-Measures ANOVA. Only week-3 was found to be statistically different from week-0. NS=not significant compared to week-0

#### *Tumour Volume*

Radiographs were used to monitor tumour progression over time. These were calculated from 3-dimensional measurements and recorded over time as described in the experimental design; and reported in Appendix; see Table 8-15 on page 291. The calculated median tumour volume (n=18) was 33.26 ml (25<sup>th</sup> percentile = 21.76 ml, 75<sup>th</sup> percentile = 67.82 ml). The measurements were corrected for the change from baseline (baseline = 1). The results are reported in the Appendix; see Table 8-16 on page 302. Using linear regression for statistical analysis, nine dog were analysed and all tumours showed an increase in size over 4 months with a correlation coefficient of  $R = 0.739$  ( $R^2 = 0.546$ ). The linear regression results are reported below, see Figure 3-34.

**Figure 3-34 Plotted tumour volumes from baseline regressed over time for dogs (n=9) receiving  $^{153}\text{Sm-EDTMP}$**



Legend: The baseline is represented by a broken-line at 1 along the y-axis. The baseline calculation was made to be able to compare tumours volume changes over time. A linear regression model was used to plot the change over time. From this graph it is apparent that  $^{153}\text{Sm-EDTMP}$  had little apparent effect on the tumours as they continued to grow.

### *Pain Control and Survival*

Only 16 out of 18 dogs were evaluable for response to pain control; raw data are reported in the Appendix, see Table 8-14 on page 287. Only two cases had a good response to treatment, seven cases had a moderate response and seven had a poor response to treatment based on criteria defined in Table 3-38 on page 161. Acute exacerbation (flare response) of clinical signs of pain and lameness was seen in three dogs. These dogs had degenerative joint disease at the time of enrolment e.g., hip dysplasia, which may have contributed to the flare response. The dogs also fell into the group of poor responders to pain control. Nevertheless, a flare response has been well documented in humans receiving  $^{153}\text{Sm-EDTMP}$  <sup>7, 7-10, 14, 104, 121,</sup>

The overall median survival of the dogs (n=16) receiving a therapeutic dose of  $^{153}\text{Sm}$ -EDTMP was 4 months (25<sup>th</sup> percentile = 5 months; 75<sup>th</sup> percentile = 3 months). The survival data were examined for variables (age, body weight, sex, tumour location, stage, tumour uptake, and response to pain control) which may have influenced survival. Only poor pain control was found to be negatively correlated to survival ( $P = 0.05$ ). The median survival times and percentiles for the different pain groups are reported in Table 3-40. Since one of the primary goals of the  $^{153}\text{Sm}$ -EDTMP treatment was pain control, it is not surprising that the lack of pain control would have a negative impact on survival for this population. The median survival time of 4 months for this population compares poorly with the 6-month median survival time for dogs undergoing amputation alone for osteosarcoma.

**Table 3-40 Overall median survival time in dogs (n=16) receiving  $^{153}\text{Sm}$ -EDTMP which were grouped for pain.**

Pain response to treatment	n	Median survival time (months)	25 <sup>th</sup> percentile	75 <sup>th</sup> percentile
Poor	7	2.0	1.0	3.0
Moderate	7	4.0	4.0	6.0
Good	2	6.0	6.0	24.0

### 3.11.4.3 Histopathology and Necropsy results

#### 3.11.4.3.1 Biopsy and Histopathology

Twelve tumours were classified histopathologically as osteosarcomas and three as multilobular osteochondrosarcoma (MLO); see Appendix Table 8-14 on page 287. Five dogs did not have histopathology, but were classified radiographically as primary aggressive bone tumours consistent with osteosarcoma; see Appendix, Table 8-15 on page 291.

Histopathologically the osteosarcomas were classified as osteoblastic (n=5), fibroblastic (n=3), mixed (n=3) and telangiectic (n=1). The histopathological sub-classifications were not correlated with survival, although a negative finding should be viewed cautiously as the groups were small. Nevertheless, the finding of no histopathological sub-classification correlation with survival is consistent with reports found in the literature.

#### 3.11.4.3.2 Necropsy and metastases results reported at the time of euthanasia.



Of the twenty cases in the study, eighteen cases were examined for evidence of metastases at the time of euthanasia by either necropsy and/or radiographs; see Appendix, Table 8-14 on page 287. Two cases (Cases 11, 17) were lost to follow-up. Radiographs in twelve cases confirmed metastases and full necropsies were done in nine cases. Soft-tissue metastases were confirmed in five out of nine necropsies and the frequencies of organ involvement are reported in Table 3-41 below. The most common sites were the lungs (5/9) followed by the spleen (3/9). A single dog (Case-7) had metastatic disease in multiple soft issue structures. This dog underwent an amputation at 4 months for progression of the primary tumour, which in all probability allowed for greater spread of the osteosarcoma. The necropsy findings of the lung (5/9) as the primary metastatic site are consistent with published reports.

**Table 3-41: Necropsy and radiograph results at euthanasia showing the frequency of metastases and survival times found in twenty dogs receiving  $^{153}\text{Sm}$ -EDTMP**

Case Number	Lungs	Spleen	Heart	Liver	Kidneys	GIT	Muscle	Survival (months)
1	+							1
2	+							1
3	+							3
4*	+	+	-	-	-	-	-	4
6*	-	-	-	-	-	-	-	3
7*	+	+	+	+	+	+	+	6
8*	+	+	-	-	-	-	-	7
9*	-	-	-	-	-	-	-	48
10	+							4
11	Lost to follow-up							
12*	-	-	-	-	-	-	-	2
13**	-	-	-	-	-	-	-	0
14*	+	-	-	-	-	-	-	4
15*	+							2
16	+							6
17	Lost to follow-up							
18	-							5
19*	+	-	-	-	-	-	-	4
20	+							3

Legend: The table above lists the soft-tissue metastatic in the dogs receiving a therapeutic dose of  $^{153}\text{Sm}$ -EDTMP. Dogs identified with an asterisks (\*) underwent full necropsy (9/18) and had thoracic radiographs taken for metastases. Lung metastases were identified in 66% (12/18) cases at the time of euthanasia. Two dogs were lost to follow-up. \*\* Case-13 was euthanized immediately after the scintigraphy studies were performed. The dog was used for autoradiography studies.

### **3.12 A Pilot study: Radiosensitization using $^{153}\text{Sm}$ -EDTMP and carboplatin**

#### **3.12.1 Justification**

It was apparent from the results of the previous therapeutic trial as described in Section 3.11 (on page 159), that  $^{153}\text{Sm}$ -EDTMP as a single therapeutic agent was showing only marginal efficacy in controlling pain and improving survival in dogs with osteosarcoma. Therefore, as a deviation from the original specific aim as outlined in Section 3.3.4 (page 107), consideration was given to ways to improve the therapeutic effect of  $^{153}\text{Sm}$ -EDTMP on survival and pain control in dogs with osteosarcoma. Radiosensitization (RS) using chemotherapy was considered a possible option because of previously reported studies using adjunct carboplatin and RS<sup>247-255</sup>. Douple *et al.*,<sup>252</sup> developed a rationale for coordinating the administration of carboplatin with radiation to enhance cancer therapy. Their approach was based on review of the reported beneficial effects attributed to the interaction between cisplatin or other platinum analogues and radiation. The two major beneficial effects were: RS of hypoxic cells with platinum during irradiation, and potentiation of cell kill with platinum complexes administered after irradiation. Both effects are expected to result in an improved therapeutic ratio. They also presented evidence for carboplatin RS, with an enhancement ratio (ER) of 1.8 occurring in Chinese hamster lung cells (V79) that were irradiated in culture under hypoxic conditions. Potentiation of radiation therapy in mice bearing a transplanted mouse mammary tumour (MTG-B) was reported as a supra-additive tumour growth delay when 60 mg/kg carboplatin was administered either 30 minutes before or immediately after 20 Gy of X-irradiation. They concluded that the increased efficacy of radiation therapy used in conjunction with carboplatin supported the premise that carboplatin could be used to potentiate radiation therapy<sup>252</sup>. More evidence supporting RS with carboplatin was reported in a research study where carboplatin in combination with the radioisotope,  $^{89}\text{Sr}$ , resulted in improvement in pain control<sup>251</sup>. Based on the above reports we hypothesized that  $^{153}\text{Sm}$ -EDTMP combined with carboplatin would result in improved pain control and tumouricidal effect in dogs with osteosarcoma compared to  $^{153}\text{Sm}$ -EDTMP as a single therapeutic agent.

#### **3.12.2 Research Hypothesis**

3.12.2.1 Hypothesis: That dogs with naturally occurring osteosarcoma when treated with

$^{153}\text{Sm}$ -EDTMP and adjunct carboplatin would have improved pain control and survival compared to dogs that received only  $^{153}\text{Sm}$ -EDTMP.

In order to prove the hypothesis the following research aim was proposed.

### 3.12.3 Specific Aim

3.12.3.1 To determine the effect of therapeutic dosages of  $^{153}\text{Sm}$ -EDTMP and carboplatin radiosensitization on survival, pain control, and myelosuppression in dogs with naturally occurring osteosarcoma.

### 3.12.4 Ethical approval

Deviation from the original  $^{153}\text{Sm}$ -EDTMP therapeutic protocol was approved by the Ethics Committee of the Pretoria Biochemical Research Centre, according to the guidelines of the National Code for Animal Use in Research, Education, Diagnosis, and Testing of Drugs and Related Substances in South Africa. All clients gave informed and signed consent before enrolment into the study.

### 3.12.5 Materials and Methods for Dogs receiving $^{153}\text{Sm}$ -EDTMP and carboplatin with osteosarcoma

#### 3.12.5.1 Model System and Sample size

To meet the objectives as set out in paragraph 3.12.2 above, six dogs with naturally occurring osteosarcoma were enrolled into the study; see Appendix, Table 8-14 (Cases 21-26) on page 287. Dogs were excluded if evidence of lung metastasis was found or if the dogs had evidence of compromised organ function e.g., azotaemia.

### 3.12.6 Experimental Design and Experimental Procedures

All dogs underwent full clinical examinations and radiographs of the primary tumour site as well as the following radiographs of the thorax, left and right lateral views, and dorsal-ventral and ventral-dorsal views. Only cases found to be free of radiological evidence of lung metastases and with signed consent were included in the study. The sizes of primary tumours were recorded from radiographs as described previously in 3.11.2 (on page 159) and results were recorded in the Appendix; see Table 8-14 (Cases 21-26) on page 287.

All the dogs had appendicular tumours and were found to be lame in the effected limb and in some cases, non-weight bearing. All six dogs were confirmed by biopsy to have osteosarcomas. Anaesthesia induction and maintenance and catheter placement followed previously described methods. Positioning for the scan also followed previously described methods. The dogs were induced, and 150 mg/m<sup>2</sup> carboplatin mixed in 500 ml normal saline was started as a one-hour infusion. Thirty minutes into the infusion, 37 MBq/kg <sup>153</sup>Sm-EDTMP (Atomic Energy Corporation of South Africa [Pty.] Ltd) was given as an intravenous bolus through a different catheter. The catheter was flushed following administration of <sup>153</sup>Sm-EDTMP using 5 ml sterile saline solution to ensure complete administration of the calculated dose. A scan was done 24 hours later and uptake was recorded for the tumour and contralateral limb. Because of known bone marrow toxicity of both agents, weekly blood samples for haematology were collected from the cephalic vein (EDTA tubes, Becton Dickinson, Vacutainer Systems, Europe).

The results from the bone scan were recorded in Table 8-14 on page 287. For ethical reasons all dogs were given a non-steroidal anti-inflammatory, piroxicam\* at 0.3mg/kg once every second day for pain control and misoprostol† at 2-5µg/kg twice daily to prevent gastric ulceration. This was done at least 14 days prior to radioisotope treatment as pain control could have been attributed to piroxicam rather than <sup>153</sup>Sm-EDTMP. The owners were requested to monitor for improvement in limb function over time, and for other signs, which could be associated with pain such as loss of appetite. Pain was scored in a similar manner as previously described in Table 3-38 (on page 161) and recorded as poor, moderate or good pain control in the Appendix; see Table 8-14 on page 287.

### 3.12.7 Data Analysis

Descriptive statistics were used to describe the patient demographics such as age, body weight, and gender‡. Dogs treated with <sup>153</sup>Sm-EDTMP alone were identified as Group-1 and dogs treated with <sup>153</sup>Sm-EDTMP plus carboplatin as Group-2. A comparison was made

---

\* Feldene, Pfizer Laboratories [Pty] Ltd, Sandton

† Cytotec, G D Searle [SA] [Pty] Ltd, Johannesburg

‡ SPSS, Inc. (1997). SigmaStat version 2.03. www.spss.com

between uptake ratios from Group-1 and Group-2 using the student's t test\*. In addition, tumour size was plotted over time using a linear regression model and examined for trends†. Comparisons were also made between groups for haematology using ANOVA of repeated measures\*. Using univariate analyses, the following parameters were also examined for their effect on survival; sex, tumour size at diagnosis, histopathological description, presence of metastasis at death, position of the osteosarcoma on the skeleton (axial vs. appendicular), site of the tumour on the skeleton (skull vs. distal radius etc.), pain control, uptake ratios, and treatment‡.

### 3.12.8 Results

#### 3.12.8.1 Patient Data

Patient details were recorded and reported in the Appendix; see Table 8-14 on page 287. Six dogs were entered into the study, of which one was female and five male. Breeds entered in the study were Rottweiler (n=2), Doberman (n=2), and large crossbred dogs (n=2). The mean±SD age of the dogs with osteosarcoma was 9.67±1.86 years and the mean±SD body weight (BW) was 48.67±8.69 kg.

#### 3.12.8.2 Concurrent medication and pain control

All the dogs had osteosarcomas of the appendicular skeleton and on presentation had obvious signs of lameness. In most cases, lameness was the primary reason for presentation to the veterinarian. Most dogs presented to the study were receiving non-steroidal anti-inflammatories (NSAIDS) as prescribed by the primary veterinarian. These included phenylbutazone, meloxicam, piroxicam, ibuprofen, and aspirin. On entry into the study, all dogs then received piroxicam at 0.3mg/kg once days until euthanasia or until side effects were seen. If gastrointestinal signs were observed, the dose of piroxicam was reduced to every second day.

---

\* SPSS, Inc. (1997). SigmaStat version 2.03. [www.spss.com](http://www.spss.com)

† SPSS, Inc. (2002). SigmaPlot for Windows, version 8.02. [www.spss.com](http://www.spss.com)

‡ StatSoft, Inc. (2003). STATISTICA (data analysis software system), version 6. [www.statsoft.com](http://www.statsoft.com).

Five dogs had a good response to treatment and one had a moderate response to treatment. The median survival times for Group-2 dogs based on response are listed below in Table 3-42. Acute exacerbation (flare response) of clinical signs of pain and lameness was seen in one dog. This dog had degenerative joint disease in all joints that may have contributed to the flare response. This is consistent with previous the findings in the Group-1, where three dogs with degenerative joint disease showed a flare response (see the results section 3.11.4.2 on page 164 - *Pain Control and Survival*). A direct comparison was made between Groups 1 & 2 for pain control. The dogs receiving carboplatin responded well to treatment and only one dog had a moderate response while five had a good response (Table 3-42 below) compared to only two dogs having good response in Group-1, see Table 3-40 on page 168.

**Table 3-42 The median survival time and pain response for Group-2 dogs receiving <sup>153</sup>Sm-EDTMP plus carboplatin.**

Pain response to treatment	n	Median survival time (months)	25 <sup>th</sup> percentile	75 <sup>th</sup> percentile
Poor pain control	None	-	-	-
Moderate pain control	1	3	NA	NA
Good pain control	5	6.5	3.04	9.73

When the Group-1 and 2 were compared for differences in survival times, stratified for pain response or group, no statistical differences were found. When the dogs were grouped together as a whole, the overall median survival was 4 months (6 months-25<sup>th</sup> percentile and 3 months for the 75<sup>th</sup> percentile). A statistical difference for survival between poor and moderate pain control was previously reported in Group-1 (see Table 3-40 on page 168), this difference was still present when the groups were combined ( $P < 0.011$ ); see Table 3-44 on page 175. Given that Group-2 contributed five dogs with a good pain response and only one to moderately pain response, poor versus good pain response was also statistically significant ( $P < 0.01$ ), see Table 3-43 and Table 3-44 below. Notwithstanding there was no statistical difference in survival between moderate and good pain response to therapy, there was a trend towards significance ( $P = 0.084$ ), see Table 3-44 below.

**Table 3-43 Median survival time for Groups 1 and 2 dogs stratified for response to pain control**

Pain response to Treatment	n	Median survival time (months)	25 <sup>th</sup> percentile	75 <sup>th</sup> percentile
Poor pain control	7	2.00	1.00	3.00
Moderate pain control	8	4.00	5.00	3.25
Good pain control	7	6.50	16.40	3.00

**Table 3-44 Post-hoc analysis comparing differences in survival times stratified for pain response to therapy.**

Pain Response Comparisons	<i>P</i> Value	Significant
Poor vs. Moderate Response	0.011	Yes
Poor vs. Good Response	0.010	Yes
Moderate vs. Good Response	0.084	No

### 3.12.8.3 Haematology

#### 3.12.8.3.1 Comparison of haematology results within Group-2 (<sup>153</sup>Sm-EDTMP + carboplatin)

A comparisons between the weekly means for haemoglobin ( $P = 0.087$ ) and haematocrit ( $P = 0.203$ ) values were not statistically significant for dogs receiving <sup>153</sup>Sm-EDTMP plus carboplatin. Statistical differences were found between weekly means for platelet counts and white blood cell counts (WBC). A post-hoc multiple comparison procedure was used to identifying which weeks were different. Descriptive statistics are reported in Table 3-45 and Table 3-46 below. Platelets counts for week-2 were found to be statistically lower than baseline (Week-0). White blood cell count at week-2 was found to be statistically lower than baseline (Week-0) and week-4 was found to be statistically higher than baseline (Week-0). Using the WHO grading for toxicity, the platelet toxicity was a Grade 2 at week-2. Even though the WBC at 2 weeks was lower than baseline it was not at a clinical significant level.

**Table 3-45 Descriptive statistics and *P* values for platelets from treatment Group-2 dogs**

Group-2 Sample weeks	n	Mean±SD Platelet count x 10 <sup>3</sup> µl	<i>P</i> value
Week-0	5	304.60±222.10	Baseline
Week-1	5	274.60±201.86	NS
Week-2	5	91.60±94.08	<i>P</i> <0.05
Week-3	4	195.25±201.23	NS
Week-4	3	173.00±138.27	NS

Legend: Only week-2 was found to be statistically different from the baseline week-0. Recovery from the nadir at week-2 was rapid, although the mean value was still below the clinically recognised lower range of the normal dog platelet count of 200 x 10<sup>3</sup>µl. NS=not significant compared to week-0

**Table 3-46 Descriptive statistics for white blood cell count (WBC) treatment Group-2 dogs**

Group-2 Sample weeks	n	Mean±SD WBC x 10 <sup>3</sup> µl	<i>P</i> value
Week-0	5	9.48±3.53	Baseline
Week-1	5	8.59±3.25	NS
Week-2	5	5.35±1.29	<i>P</i> <0.05
Week-3	4	7.26±2.51	NS
Week-4	3	13.61±5.14	<i>P</i> <0.05

Legend: While WBC at week-2 was found to be statistically lower than baseline (Week-0) and week-4 was found to be statistically higher than baseline (Week-0) these results were not considered clinically significant as the WBC range for normal dogs is 5-15 x 10<sup>3</sup>µl. NS=not significant compared to week-0.

### 3.12.8.3.2 A comparison for haematology results between treatment Groups-1 and -2

In order to determine if there was a difference between Group-1 and -2 for haematological response to therapy; comparisons were made between treatment groups for weekly haemoglobin, haematocrit, WBC, and platelets counts. Interestingly no significant differences were found for any parameter between treatment groups; allowing for the effects of differences in weeks. This indicates that the use of carboplatin infusion did not contribute significantly to toxicity. As expected, differences were found between weeks when the Groups were combined. Statistical significant differences were found between week-4 and baseline (week-0) for WBC (*P* = 0.001) and week-2 and -3 and the baseline (week-0) for



platelets ( $P = 0.001$ ). Descriptive statistics are reported below in Table 3-47 for platelet counts and Table 3-48 for white blood cells. The results are also graphically represented in Figure 3-35 and Figure 3-36 on page 179.

**Table 3-47 Descriptive statistics and  $P$  values for platelets for combined Groups.**

Combined Groups Sample weeks	Mean $\pm$ SEM* Platelet count x $10^3\mu\text{l}$	$P$ value
Week-0	310.10 $\pm$ 30.53	Baseline
Week-1	271.50 $\pm$ 30.53	NS
Week-2	149.30 $\pm$ 30.53	$P < 0.05$
Week-3	112.18 $\pm$ 38.75	$P < 0.05$
Week-4	217.75 $\pm$ 47.22	NS

Legend: Week-2 and week-3 were statistically different from the baseline week-0. The lower normal range for platelets in the dog is  $200 \times 10^3\mu\text{l}$ . Using the WHO grading for toxicity, week-2 and -3 are consistent with Grade-1 toxicity. NS=not significant compared to week-0

**Table 3-48 Descriptive statistics and  $P$  values for white blood cell counts (WBC) for combined Groups**

Combined Groups Sample weeks	Mean $\pm$ SEM WBC count x $10^3\mu\text{l}$	$P$ value
Week-0	8.57 $\pm$ 1.23	Baseline
Week-1	7.06 $\pm$ 1.23	NS
Week-2	6.27 $\pm$ 1.23	NS
Week-3	6.48 $\pm$ 1.56	NS
Week-4	16.60 $\pm$ 1.90	$P < 0.05$

Legend: While week-4 is statistically different from week-0, the mean falls close to the upper normal range of  $15 \times 10^3\mu\text{l}$  for WBC in dogs. NS=not significant compared to week-0

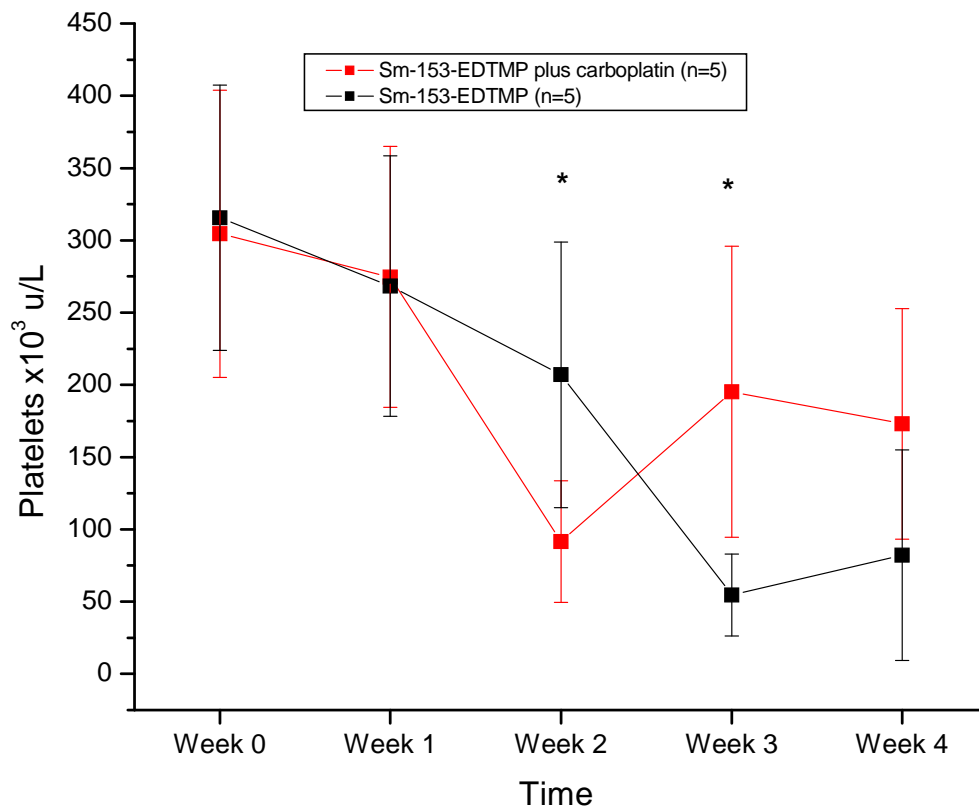
The individual data for platelet counts and WBC counts in Group-1 and Group-2 were combined and are graphically represented in Figure 3-35 and Figure 3-36 below. From Figure 3-35 it is apparent that the platelet count nadir of Group-2 ( $^{153}\text{Sm-EDTMP} + \text{carboplatin}$ )

---

\* The standard error of the mean (SEM) refers to an estimate of that standard deviation and is computed from the sample of data being analyzed and helps to determine the differences between more than one sample of information e.g. the means of Group-1 and Group-2.

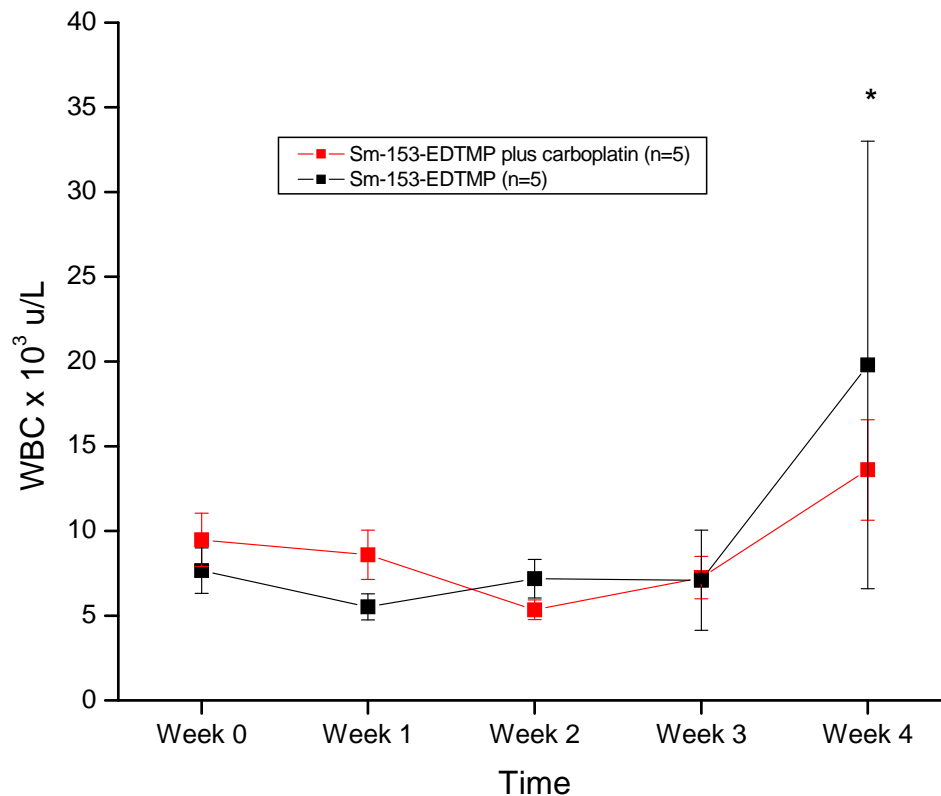
occurred a week earlier than Group-1. This could be due to the effect of carboplatin because of its associated toxicities e.g. thrombocytopenia.

**Figure 3-35 Platelet counts for dogs receiving  $^{153}\text{Sm}$ -EDTMP (Group-1) and  $^{153}\text{Sm}$ -EDTMP + carboplatin (Group-2)**



Legend: The statistically significant weeks are identified with an \*. The lower normal range for platelets in the dog is  $200 \times 10^3 \mu\text{l}$ . Using the WHO grading for toxicity, week-2 and -3 are consistent with Grade-1 toxicity.

**Figure 3-36 White blood cell count for dogs receiving  $^{153}\text{Sm-EDTMP}$  (Group-1) and  $^{153}\text{Sm-EDTMP}$  + carboplatin (Group-2)**



Legend: The statistically significant weeks are marked with an \*. While week-4 is statistically different from week-0, the mean falls close to the upper normal range of  $15 \times 10^3 \mu\text{L}$  for WBC in dogs.

#### 3.12.8.4 Radiographic evaluation of Group-2

Description of individual tumours and scanned in radiographs are recorded in the Appendix; see Table 8-15 on page 291. The appendicular skeleton radiographs identified five distal radius and one distal femur osteosarcomas. Radiological staging of all dogs found primary tumours breaking through the medulla and cortex with no evidence of metastases and were thus staged as T2N0M0. The radiological appearance of all tumours in Group-2 was osteoblastic in description in contrast to more variation in Group-1.

### *Tumour Volume*

Radiographs were used to monitor tumour progression over time. Changes in tumour volume were calculated as previously described in Section 3.11.2 on page 159 and are recorded in the Appendix; see Table 8-15 on page 291. The calculated median tumour volume (n=5/6) for Group-2 was 27.49 ml (25<sup>th</sup> percentile = 22.91 ml, 75<sup>th</sup> percentile = 58.91 ml). When compared to Group-1, where the median tumour volume (n=18/20) was 33.26 ml (25<sup>th</sup> percentile = 21.76 ml, 75<sup>th</sup> percentile = 67.82 ml) there was no statistical difference ( $P = 0.65$ ). As for Group-1, all tumours in Group-2 progressed over time. The tumour volume data is not shown graphically.

### 3.12.8.5 Scintigraphy

All dogs underwent 24-hour static bone scans following <sup>153</sup>Sm-EDTMP administration and carboplatin. Comparing uptake ratio's between Groups found that the dogs receiving carboplatin had a statistically higher uptake ratio ( $P= 0.019$ ). However, this difference did not translate into increased survival and the data may be biased, as Group-2 comprised only distal radial osteosarcomas, which were radiologically osteoblastic in appearance. Osteoblastic osteosarcomas are reported to have higher uptake ratios in the literature but were not significantly different in our groups.

**Table 3-49 The mean±SD uptake ratio (T/NTC) for Group-1 (<sup>153</sup>Sm-EDTMP) and Group-2 (<sup>153</sup>Sm-EDTMP plus carboplatin)**

Treatment Group	n	Uptake Ratio Mean±SD
Group-1 ( <sup>153</sup> Sm-EDTMP)	15	5.76±4.83
Group-2 ( <sup>153</sup> Sm-EDTMP plus carboplatin)	6	11.23±2.88

Legend: There was a statistically significant difference between groups ( $P= 0.019$ ).

#### 3.12.8.6 Histopathology and Necropsy results

All six osteosarcomas in Group-2 were classified histopathologically as osteosarcomas and were sub-classified as osteoblastic. The Group-2 data was insufficient to make comparison with Group-1 dogs based on the sub-classification of osteosarcomas and its effect on survival. The six cases from Group-2 were examined for evidence of metastases at the time of euthanasia; the radiological results are reported in the Appendix; see Table 8-14 on page 287 and Table 8-15 on page 291. Metastases were confirmed by radiographs (n=6). As for Group-1, the lungs were the primary metastatic site in all Group-2 cases at the time of euthanasia. One dog (Case-26) developed a bony lesion 3-months post treatment at the same site in the opposite radius. It was not seen at the time of the time of the original diagnosis of osteosarcoma but could a synchronous primary osteosarcoma.

### **3.13 Materials and methods for the therapy group of dogs with osteosarcoma receiving $^{188}\text{Re}$ -HEDP**

#### 3.13.1 Sample size

In order to satisfy the aims and objectives as set out in paragraphs in 3.3.4., seven dogs with naturally occurring osteosarcoma were enrolled in the  $^{188}\text{Re}$ -HEDP study; see Table 3-6 on page 112 and Table 8-21 on page 307 of the Appendix. Dogs were excluded if evidence of lung metastasis was found or if the dogs had evidence of compromised organ function e.g., azotaemia.

#### 3.13.2 Experimental Design and Experimental Procedures

The  $^{188}\text{Re}$ -HEDP dogs followed identical experimental design and procedures protocols as described for  $^{153}\text{Sm}$ -EDTMP dogs. The only difference was the setting and calibration of the gamma camera. The camera was fitted with a 140 keV low energy all-purpose parallel hole collimator (a high energy collimator was not available for this camera) and was calibrated for  $^{188}\text{Re}$  using a standard laboratory protocol to an energy level of 115 keV and 15% window. The gamma camera was centred over the thorax and abdomen to include the heart, lungs, liver and both kidneys (and in some cases tumour); see Figure 3-2 on page 117. Both

forelimbs were included to acquire data from the metaphysis of distal radius and cortical bone area. Static scans were obtained at 24 hours in all seven dogs with osteosarcoma.

In all cases, a therapeutic dose of 37 MBq/kg  $^{188}\text{Re}$ -HEDP was given followed by static scan 24-hours later (all calculated T/NTC are based on  $^{153}\text{Sm}$ -EDTMP 24-hour scans). All cases returned monthly or bi-monthly for follow-up radiographs of the thorax and primary tumour site. The size of the primary tumour and evidence of metastases were recorded as previously reported in Section 3.11.2 on page 159. Blood samples were collected from the cephalic vein (EDTA tubes, Becton Dickinson, Vacutainer Systems, Europe) for haematology in dogs (n=7) before treatment and weekly for 4 weeks post-treatment.

Two dogs received additional weekly doses of 37 MBq/kg  $^{188}\text{Re}$  HEDP for 4 weeks and blood was monitored weekly for 4 weeks. For ethical reasons all dogs were given a non-steroidal anti-inflammatory, piroxicam\* at 0.3mg/kg once every second day for pain control and misoprostol† at 2-5µg/kg twice daily to prevent gastric ulceration. This was done at least 14 days prior to radioisotope treatment as pain control could have been attributed to piroxicam rather than  $^{188}\text{Re}$  HEDP. The owners were requested to monitor improvement in limb function over time, and for other signs associated pain, such as loss of appetite. Pain response to therapy was scored (poor, moderate, or good response) as previously reported in Table 3-38 on page 161 and results were recorded in the Appendix; see Table 8-21 on page 307.

### 3.13.3 Data Analysis

Descriptive statistics were used to describe the patient demographics such as age, body weight, and gender‡. The dogs were divided into two groups based on treatment. Group-1 (n=5) was a single-dose of  $^{188}\text{Re}$ -HEDP and Group-2 (n=2) was multiple-doses of  $^{188}\text{Re}$ -HEDP. Data were tested for normality and equal variance using Kolmogorov-Smirnov test.

---

\* Feldene, Pfizer Laboratories [Pty] Ltd, Sandton

† Cytotec, G D Searle [SA] [Pty] Ltd, Johannesburg

‡ SigmaStat for Windows Version 3.00 © 1992-2003 and SigmaPlot for Windows Version 8.02 © 1986-2001 SPSS Inc

Parametric data is reported as Mean±SD (range) and nonparametric data as median and IQR (inter-quartile range 25<sup>th</sup> percentile to 75<sup>th</sup> percentile). A comparison was made between uptake ratios from Group-1 and Group-2 using the one-way ANOVA\*. Differences between these groups were identified using (post-hoc) pair wise multiple comparison procedures (Holm-Sidak method or Dunn's Method). Using linear regression, tumour size was plotted over time and examined for trends\*. Comparisons were also made between groups for haematology using ANOVA of repeated measures\*. The following parameters were also examined (Kaplan-Meier survival curves, Log Rank method) for their effect on survival and included sex, tumour size at diagnosis, histopathological description, presence of metastasis at death, position of the osteosarcoma on the skeleton (axial vs. appendicular), site of the tumour on the skeleton (skull vs. distal radius etc.), pain control, uptake ratios, and treatment\*. Differences between groups were identified using (post-hoc) pair wise multiple comparison procedures (Bonferroni Method). For all analyses, values of  $P < 0.05$  were considered significant.

### **3.14 Results from the therapy group of dogs with osteosarcoma receiving <sup>188</sup>Re-HEDP**

#### **3.14.1 Patient Demographics**

Patient details were recorded and reported in the Appendix; see Table 8-22 on page 308. Seven dogs were entered in the study, of which four were female and three male. The most common breed entered in the study were Rottweiler (n=3) followed by single Pyrenean Mountain dog, Irish Wolf hound, Whippet and Labrador retriever. The mean±SD age of the dogs with osteosarcoma was 9.35± 2.69 years with a mean±SD body weight (BW) of 42.49± 19.69 kg. Unfortunately, due to the small number of patients, age and BW could not be used to for survival analysis.

#### **3.14.2 Concurrent medication and pain control**

Most dogs presented to the study were receiving concurrent non-steroidal anti-inflammatories (NSAIDS) as prescribed by the primary veterinarian. These included phenylbutazone, meloxicam, piroxicam, ibuprofen, and aspirin. On entry into the study, all dogs were changed to receive piroxicam 0.3mg/kg once daily until euthanasia or until side effects were seen. If gastrointestinal signs were observed, the dose of piroxicam was reduced to every second day.

A single dog (Case-3) required discontinuation of all NSAIDs due to significant gastrointestinal bleeding, resulting in a clinical anaemia. This dog received ibuprofen prior to the study, which is known to cause gastrointestinal ulcers in dogs. Cases were reported as having an overall poor, moderate or good response to therapy as described in Table 3-38 on page 161. The results were recorded in Table 8-21 on page 307 of the Appendix. Three dogs achieved good pain control (cases 1, 2, and 4), two had moderate control (cases 3 and 7), and two had poor control (Cases 5 and 6).

### 3.14.3 Haematology

Haematology results were examined and found complete for five dogs in the single-dose group and two in the multiple-dose groups. Raw data and descriptive statistics are displayed graphically in Figure 3-37 on page 186 and tabulated in the Appendix: see Table 8-24 on page 313.

#### 3.14.3.1 Statistical analysis of haematology results for the Group-1(single-dose) and Group-2 (multiple-dose) <sup>188</sup>Re-HEDP treatment groups.

Haematology results for Group-1 and Group-2 are graphically represented in Figure 3-37 on page 186.

##### *Single Dose <sup>188</sup>Re-HEDP*

Comparisons between means (One Way Repeated Measures ANOVA) for weekly haemoglobin ( $P = 0.149$ ) and WBC ( $P = 0.396$ ) values were not statistically significant. Statistical significance was observed between the mean weekly haematocrit ( $P = 0.048$ ) and platelet count values ( $P = 0.043$ ). While haematocrit did achieve significance with the ANOVA, more stringent post-hoc tests did not identify a significant difference between weeks. Although, week-4 appeared to be trending towards significance ( $P = 0.09$ ). Platelets at week-3 and -4 were found to be statistically ( $P < 0.05$ ) different from the baseline week-0. The lower platelet counts for the single-dose group at week-3 and -4 were considered Grade-1 toxicity. The nature of the toxicity was only mild and would not have precluded dose escalation or repeated therapy with <sup>188</sup>Re-HEDP. Descriptive statistics and  $P$ -values for the single-dose Group-1 and the combined Groups are reported in Table 3-50 below.



**Table 3-50 Descriptive statistics for platelets from treatment single-dose  $^{188}\text{Re}$ -HEDP dogs**

Group-1 Single-dose $^{188}\text{Re}$ -HEDP	N	Platelet count $\times 10^3 \mu\text{l}$ Mean $\pm$ SD	P value
Week-0	5	380.00 $\pm$ 69.38	Baseline
Week-1	5	338.40 $\pm$ 145.69	NS
Week-2	5	310.20 $\pm$ 64.53	NS
Week-3	5	185.60 $\pm$ 113.31	$P < 0.05$
Week-4	5	194.60 $\pm$ 128.10	$P < 0.05$

Legend: The lower range for platelet count in normal dogs is  $200 \times 10^3 \mu\text{l}$ . NS=not significant compared to week-0

*Multiple Dose  $^{188}\text{Re}$ -HEDP*

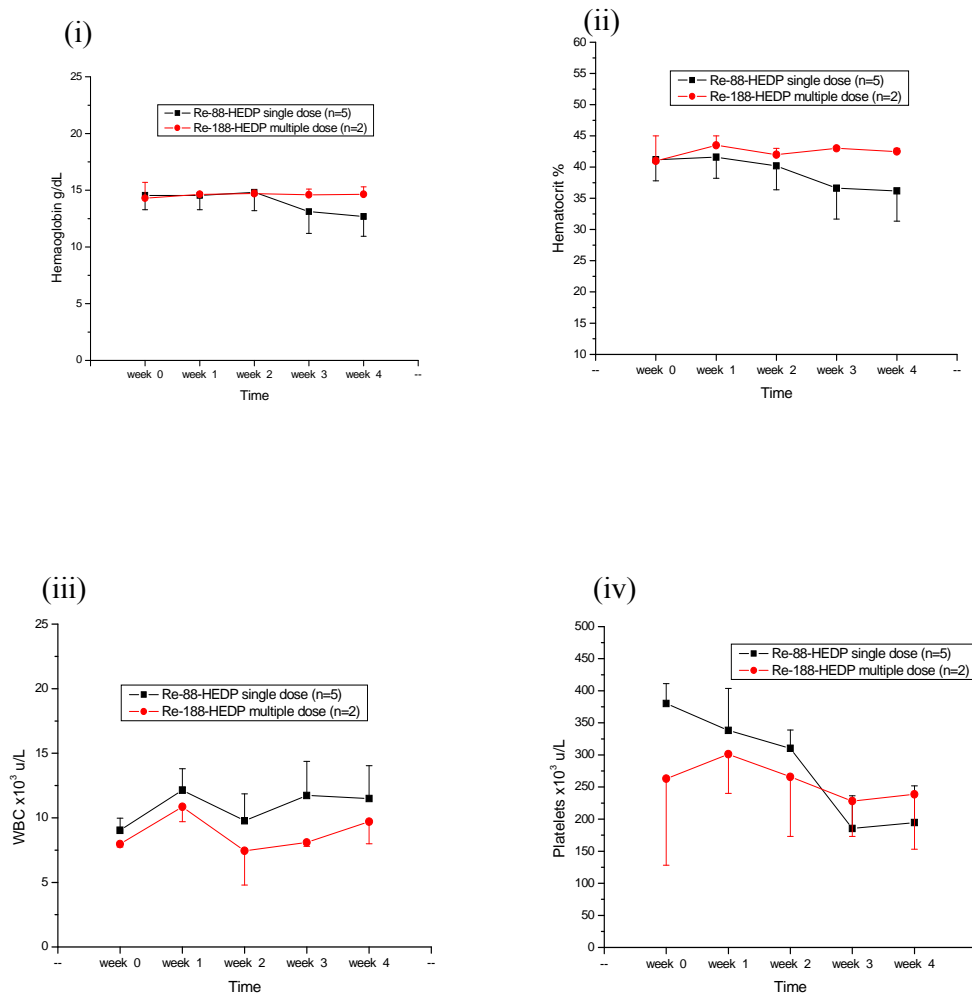
Only two cases were completed in this group, which did not allow for further statistical analysis between groups. Nevertheless when the data were combined ( $n=7$ ), haematocrit was no longer statistically significant, but the platelet count remained significant at week-4 and -5 ( $P = 0.05$ ). Once again, in the more stringent post-hoc analyses, platelets for week-3 and -4 were found to statistically different from week-0. The lower platelet counts for the combined group at week-3 and -4 were considered Grade-1 toxicity. The toxicity grade of the two dogs receiving multiple doses weekly doses of  $^{188}\text{Re}$ -HEDP was also on Grade-1; see Figure 3-37 on page 186. Thus, the nature of the toxicity was only mild and would not have precluded dose escalation or continued repeated therapy with  $^{188}\text{Re}$ -HEDP. Descriptive statistics for the combined group and are reported in Table 3-51 below.

**Table 3-51 Descriptive statistics for platelets from both treatment groups receiving  $^{188}\text{Re}$ -HEDP**

Combined groups	n	Platelet count $\times 10^3 \mu\text{l}$ Mean $\pm$ SD	P value
Week-0	7	346.57 $\pm$ 112.00	Baseline
Week-1	7	327.71 $\pm$ 125.40	NS
Week-2	7	297.57 $\pm$ 78.26	NS
Week-3	7	197.71 $\pm$ 99.98	$P < 0.05$
Week-4	7	207.14 $\pm$ 117.62	$P < 0.05$

Legend: The lower range for platelet count in normal dogs is  $200 \times 10^3 \mu\text{l}$ . NS=not significant compared to week-0.

**Figure 3-37 Haematology results for Group-1 (single-dose) and Group-2 (multiple-dose) <sup>188</sup>Re-HEDP dogs**



Legend: The graphs show the results for (i) haemoglobin, (ii) haematocrit, (iii) white blood cell (WBC) and (iv) platelet counts over 4 weeks. Only haematocrit (ii) and platelet count (iv) were found to be statistically significant from baseline (week-0) values, although the haematocrit was not significant in post-hoc analyses. The gradual trend downwards for platelet counts for both groups was obvious from the graph (iv) and became clinically and statistically significant at week-3 and -4. The lower range for platelet count in normal dogs is  $200 \times 10^3 \mu\text{l}$ . The WBC (iii) count did not change significantly with time in contrast to the observed increase in WBC count seen with dogs receiving <sup>153</sup>Sm-EDTMP and carboplatin; see Figure 3-33 on page 165 and Figure 3-36 on page 179.

#### 3.14.4 Radiographic evaluation

Description of individual tumours and scanned in radiographs were recorded in the Appendix; see Table 8-22 on page 308.

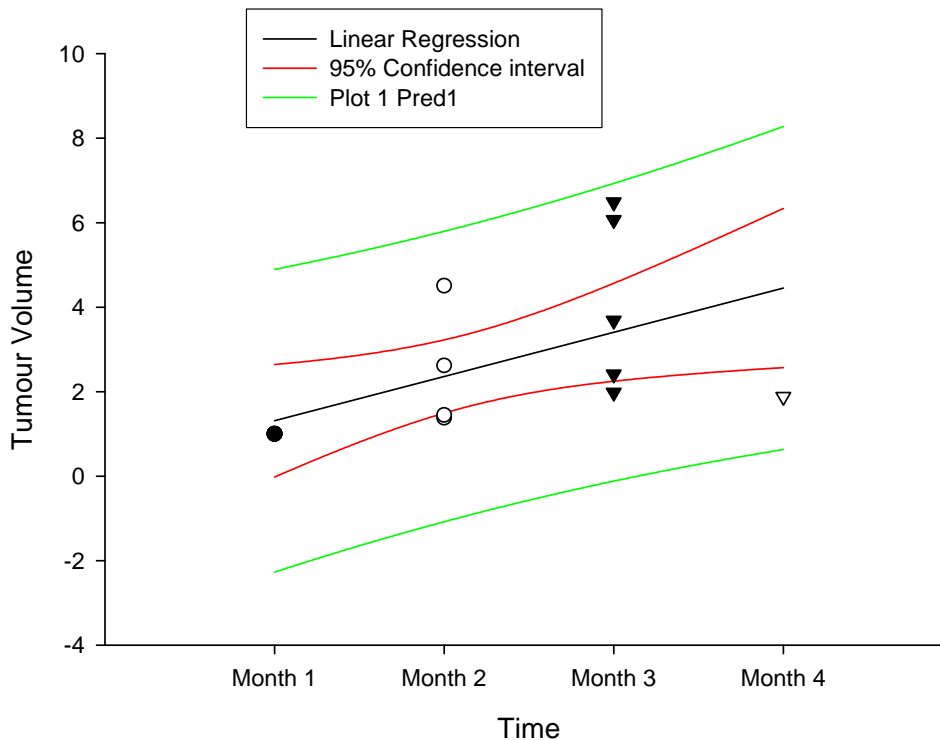
##### *Anatomic Location*

Radiographs identified two distal radiuses, three proximal humeri, one rib, and one nasal tumour. On admission, all dogs were staged as T2N0M0 e.g., tumours that had broken through the cortex and were no longer confined to the medulla. Cases were also grouped according position on the skeleton e.g., axial (n=2) or appendicular (n=5).

##### *Tumour Volume*

Radiographs were used to monitor tumour progression. Figure 3-38 on page 188 is a linear regression shown progression of tumours over time. This was calculated from three-dimensional measurements and recorded overt time as previously described and recorded in the Appendix; see Table 8-22 on page 308. The measurements were corrected for baseline (baseline=1), see Appendix, Table 8-25 on page 314. Using linear regression for statistical analysis all tumours showed progression over 4 months ( $R=0.557$ ,  $R^2=0.31$ ), see Figure 3-38 on page 188. The effect on tumour size on survival was not evaluated.

**Figure 3-38 Plotted tumour volumes from baseline regressed over time for dogs (n=5) receiving a single-dose of  $^{188}\text{Re}$ -HEDP**



Legend: The baseline is represented by 1 along the y-axis. The baseline calculation was made to be able to compare tumours volume (n=5) change over time. A linear regression model was used to plot the change over time. From this graph it is apparent that  $^{188}\text{Re}$ -HEDP had little apparent effect on the tumour volumes as they continued to grow over time.

### 3.14.5 Scintigraphy

Six out of seven dogs underwent static 24-hour bone scans following  $^{188}\text{Re}$ -HEDP administration. The mean $\pm$ SD uptake ratio (T/NTC) for all six dogs was 1.69 $\pm$ 0.59. Uptake ratios were not recorded after the primary scan in the two dogs that received multiple-doses of  $^{188}\text{Re}$ -HEDP. Two dogs, Case-1 and -4 (see Appendix, Table 8-21 on page 307) had a  $^{99\text{m}}\text{Tc}$ -MDP scan of their tumours a week prior to the  $^{188}\text{Re}$ -HEDP treatment. The median T/NTC uptake ratio at 3-hours for  $^{99\text{m}}\text{Tc}$ -MDP scan was 11.36 compared to 2.62 for the  $^{188}\text{Re}$ -HEDP. Unfortunately insufficient numbers of scans of  $^{99\text{m}}\text{Tc}$ -MDP and  $^{188}\text{Re}$ -HEDP in the same dogs precluded statistical evaluation of these results. Nevertheless, this was the

cases when the  $^{188}\text{Re}$ -HEDP uptake ratio (T/NTC) was observed to be statistically lower than  $^{153}\text{Sm}$ -EDTMP uptake ratios, see Table 3-59 on page 194 for details.

### 3.14.6 Treatment

The dogs were divided into two groups based on treatment received, five dogs in Group-1 received a single dose of 37 MBq/kg  $^{188}\text{Re}$ -HEDP, and two dogs in Group-2 received four weekly doses of 37 MBq/kg  $^{188}\text{Re}$ -HEDP.

#### *Treatment and Survival*

The two treatment groups were examined for their effect on survival using Kaplan-Meier survival analysis (Log Rank). The two groups were not statistically different from each other for survival time ( $P = 0.51$ ). The median survival times per treatment group are listed Table 3-52 below.

**Table 3-52 Median survival time for treatment both groups receiving single or multiple doses of  $^{188}\text{Re}$ -HEDP**

Median survival time (months)	Group-1 (Single-dose)	Group-2 (Multiple-dose)
25 <sup>th</sup> percentile	2 months	2.7
Median	4	3.25
75 <sup>th</sup> percentile	4	7

Overall, median survival time for all (n=7) dogs receiving  $^{188}\text{Re}$ -HEDP in the study was 3-months with an interquartile range (IQR) of 2- to 6-months.

### 3.14.7 Histopathology and Necropsy results

#### 3.14.7.1 Biopsy and Histopathology

All seven dogs were classified histopathologically as osteosarcomas. Histopathological tumour sub-classification identified three osteoblastic, two telangiectic and one chondroblastic and one unknown. Because of the small number of cases in the study, no survival time comparisons could be made between histopathological sub-classification of tumours.

### 3.14.7.2 Necropsy and metastases results reported at the time of euthanasia

Seven cases were examined for evidence of metastases at the time of euthanasia see Appendix, Table 8-21 on page 307 . Only two cases underwent full necropsy, the remaining five were staged using physical examination, radiographs of the abdomen and chest and ultrasound. Soft issue metastases were confirmed in five out of seven cases (71%). The soft-tissue structure involved and frequency are reported in Table 3-53 below. The common sites were the lungs, spleen and other soft-tissue (GI). Case-2 and -5 received multiple doses of  $^{188}\text{Re}$ -HEDP and had complete necropsies performed. Of prime interest were the kidneys and bladder wall because of the repeated radioisotope doses. No changes were expected in bone marrow, as these were not reflected in the haematology results. Necropsy report found changes in bladder wall of both dogs. Changes were described as alternatively mild diffuse subepithelial subacute inflammation with fibrosis and outspoken cytoplasmic vacuolization of bladder epithelium. Both cases had mild plasmacytic lymphocytic interstitial nephritis of the kidneys. After receiving multiple doses of  $^{188}\text{Re}$ -HEDP, Case-2 also underwent a  $^{99\text{m}}\text{Tc}$ -DTPA study to evaluate glomerular filtration. Results from this study were within normal limits for the dog.

**Table 3-53: Organs found positive for metastases at euthanasia in dogs receiving  $^{188}\text{Re}$ -HEDP**

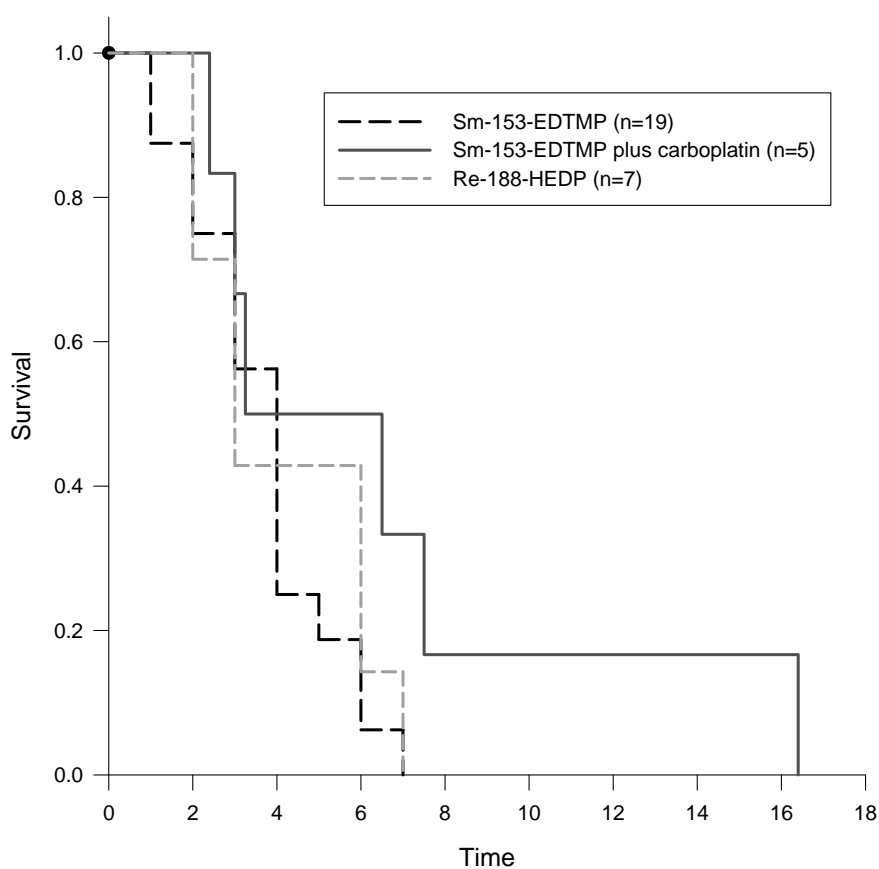
Case Number	Lungs	Spleen	Heart	Liver	Kidneys	Other Soft-tissue	Median Survival (months)
1	+	+	-	-	-	+	7
2*	-	-	-	-	-	-	6
3	+	-	-	-	-	-	3
4	+	+	-	-	-	-	6
5*	-	-	-	-	-	-	2
6	-	-	-	-	-	-	2
7	-	-	-	-	-	+	3

Legend: Cases identified by an asterisks (\*) had full necropsies done at the time of euthanasia. All other cases were staged using radiographs and ultrasound examinations. Other soft-tissue structures included the gastrointestinal tract and the regional draining lymph nodes.

### 3.15 Survival comparison between dogs receiving $^{153}\text{Sm}$ -EDTMP and $^{188}\text{Re}$ -HEDP

#### 3.15.1.1 Univariate analysis between treatment groups

**Figure 3-39 Kaplan-Meier survival curve for dogs with osteosarcoma receiving  $^{153}\text{Sm}$ -EDTMP (plus carboplatin) and  $^{188}\text{Re}$ -HEDP**



Legend: The y-axis scale is proportional to the number dogs surviving e.g. 1.0 = 100%. The x-axis is time in months. Each step downwards of the survival curves are dogs that have died due to the effects of the osteosarcoma.

**Table 3-54 Median survival time for dogs with osteosarcoma receiving  $^{153}\text{Sm}$ -EDTMP (plus carboplatin) and  $^{188}\text{Re}$ -HEDP**

Treatment Groups	n	Median survival time (months)	75 <sup>th</sup> percentile	25 <sup>th</sup> percentile
$^{153}\text{Sm}$ -EDTMP	19	4.00	2.00	4.00
$^{153}\text{Sm}$ -EDTMP+Carboplatin	5	3.25	3.00	7.50
$^{188}\text{Re}$ -HEDP (single + multiple dose groups)	7	3.00	2.00	6.00
All Groups	31	4.00	3.00	6.00

The Log-Rank Survival Test was used to compare treatment groups, no statistically significant difference was found between treatment groups ( $P = 0.21$ ). The overall median survival time for all the treatment groups combined was 4-months (IQR 3.00, 6.00 months). This is significantly different from the reported median survival time (11-12 months) in the literature for dogs with osteosarcoma where the standard of care is amputation followed by chemotherapy; see Table 2-5 on page 91.

**Table 3-55 Median survival time for pain response to treatment for the combined treatment groups (n=29)**

Pain Response	n	Median Time	75 <sup>th</sup> percentile	25 <sup>th</sup> percentile
Good	8	6	3.25	6.50
Moderate	9	4	4	5
Poor	12	2	2	3

As a combined treatment group, poor pain control was a predictor of a short survival ( $P = 0.015$ ) see Table 3-55 above. As stated before this is hardly surprising since predictably dogs that were not controlled for pain would very likely be euthanized. Only 28% (8/29) were considered to have good pain control in this study.

### 3.15.1.2 Multivariate Analysis

After multivariate analysis (Cox's Proportional Hazard Model) of the whole population stratified for treatment, only one statistically significant prognostic variable was identified for survival, this was uptake ratio ( $P = 0.004$ ), see Table 3-56. Dogs with a higher uptake ratio >10 had a shorter survival. This is in contrast to  $^{153}\text{Sm}$ -EDTMP as group where the negative



prognostic variable were poor pain control ( $P = 0.046$ ), although, the uptake group ratio approached significance at  $P = 0.075$ ; see Table 3-43 on page 175.

**Table 3-56 Results from multivariate analysis of osteosarcoma dogs stratified by treatment group**

Variable	<i>P</i> -value
Breed	0.223
Age Group	0.483
Gender	0.374
Affected bone	0.149
Skeletal location	0.884
Stage	0.736
Histopathology	0.511
Uptake ratio (T/NTC)	<b>0.004</b>
Metastases	0.795
Pain Response	0.817
Tumour volume	0.597

After multivariate analysis (Cox's Proportional Hazard Model) of the whole population with survival as the only dependent variable, increased uptake ratio was once again a statistically significant negative prognostic variable for survival ( $P = 0.025$ ), see Table 3-57 below. Once again, unlike  $^{153}\text{Sm}$ -EDTMP group alone, poor pain response to treatment for combined groups was not a negative prognostic predictor of survival.

**Table 3-57 Results from multivariate analysis of osteosarcoma dogs with survival as the only dependent variable**

Variable	<i>P</i> -value
Breed	0.122
Age Group	0.168
Gender	0.554
Affected bone	0.164
Skeletal location	0.762
Stage	0.732
Histopathology	0.670
Uptake ratio (T/NTC)	<b>0.025</b>
Metastases	0.764
Pain Control	0.699
Treatment groups	0.261
Tumour volume	0.733

### 3.15.2 Uptake ratios (T/NTC) comparison between radiopharmaceuticals

Because of the significance of uptake ratios as a prognostic indicator of survival, the differences in uptake were compared between treatment groups. Twenty-eight dogs had complete uptake data and descriptive statistics are reported below in Table 3-58 below. Statistical analysis of the data found that the T/NTC ratio for dogs receiving  $^{153}\text{Sm}$ -EDTMP with or without carboplatin infusion were significantly higher than the T/NTC ratio for  $^{188}\text{Re}$ -HEDP.

**Table 3-58 Median uptake ratios (T/NTC) comparing tumour counts (T) to non-tumour counts (NTC) for all treatment groups.**

Treatment Group	n	Median	25%	75%
$^{153}\text{Sm}$ -EDTMP	16	3.71	2.59	7.30
$^{153}\text{Sm}$ -EDTMP Carboplatin	6	12.11	10.73	12.65
$^{188}\text{Re}$ -HEDP	6	1.38	1.35	2.00

**Table 3-59 Statistical comparison between radiopharmaceuticals uptake ratios (T/NTC)**

Comparison	<i>P</i> <0.05
$^{153}\text{Sm}$ -EDTMP vs. $^{188}\text{Re}$ -HEDP	Yes
$^{153}\text{Sm}$ -EDTMP vs. $^{153}\text{Sm}$ -EDTMP+Carboplatin	No
$^{153}\text{Sm}$ -EDTMP+Carboplatin vs. $^{188}\text{Re}$ -HEDP	Yes

## 3.16 Materials and Methods for $^{153}\text{Sm}$ -EDTMP autoradiography in the dog with osteosarcoma and the rat

### 3.16.1 Model System and Sample size

To meet the objectives as set out in paragraph 3.3.5 on page 107 a single rat and dog were included in the study. The 12-week old (juvenile) rat was a female Sprague-Dawley sourced from the Pretoria Biomedical Research Institute. A second matched control rat was included as a negative control in the autoradiography section. The dog was Case-13 and its details were recorded in the Appendix, see Table 8-14 on page 287.

### 3.16.2 Experimental Design and Experimental Procedures

Both animals underwent dynamic three-hour scintigraphy studies as described in the experimental design and procedures section; see section 3.5.5 on page 112.

#### 3.16.2.1 Rat autoradiography

The rat was anesthetized via intraperitoneal injection of 0.1 ml pentobarbitone (60 mg/kg) solution. The lateral tail vein was cannulated using a 25-gauge Jelco catheter. The rat was positioned directly on the inverted gamma camera head. The collimator was protected from possible radioisotope contamination by a thin plastic sheet. The rat was given 37 MBq/kg <sup>153</sup>Sm-EDTMP intravenously and immediately scanned as described in 3.5.5. Following the three-hour scan, the rat was euthanized using 1 ml of pentobarbitone 6% solution. A single matched control rat was also euthanized in a similar fashion. The rats were immediately dissected and tissue samples were harvested, these included liver, spleen, kidney, and femur. Duplicate samples were also collected for routine haematoxylin and eosin (H&E) staining and were placed in buffered formalin and marked as sample or control. These were processed using standard laboratory protocols. The tissue samples for autoradiography were immediately taken to the Institute of Pathology (College of Medicine, University of Pretoria), where the samples were processed using standard protocols for fresh frozen sections. Single sections, 2 µm thick, were cut from the sample and negative control rat tissue and were placed side by side on glass microscope slides. The sections were identified and etched (diamond point pen) on the slide as + or -. Multiple slides were made for proximal femur, liver, and kidney. The autoradiography slides were then ready for darkroom processing.

#### Darkroom Procedures

The slides are immersed in preheated (42 °C) autoradiography emulsion\* to cover both sections. The slide was then removed from the emulsion to allow the adherent emulsion coating on the slide to dry. Positive and negative controls for the developing processes were used with every batch of slides developed. Controls were made by taking emulsion-coated slides without sections and exposing one to light (positive control), and leaving the other unexposed (negative control). Following immersion, the slides were placed on a drying rack

---

\* NTB 2 autoradiography emulsion. Eastman Kodak Co. Rochester New York.

in a horizontal position. The slides required 1 hour to dry completely. The slides were then placed in a closed plastic slide box container with a desiccant sachet (silica gel). The slide container was then placed in a refrigerator (at 4 °C) in the dark room to allow for adequate exposure of the emulsion by the radioisotope. The exposure time was on average 8 to 12 hours. Following the elapsed time, the slides were then removed from the fridge and allowed to warm to room temperature. The slides were then placed in a glass slide holder used for staining multiple slides and placed in a developing solution\* for 3 min and then the developing process was stopped by placing the slides into distilled water for 10 sec. The slides were then fixed for a further 8 min in fixer† and then washed using distilled water initially and then tap water for 5 min.

The slides were then allowed to dry on a drying rack for 2 hours and could now be exposed to light and further processing. Slides were then stained with Diff-Quik‡ stain without the fixator (methanol) stage. The photographic emulsion coating the slide stained blue, but was partially removed with a methanol wash (3-min). The slides are then cover slipped to preserve the sections and allowed to dry for 1 hour. The slides are then evaluated microscopically for distribution of the radiopharmaceutical.

#### 3.16.2.2 Dog autoradiography

The dog, Case-13, was euthanized immediately following the dynamic scan using 1ml/kg pentobarbitone (200mg/ml). The solution was given via the intravenously catheter described in 3.5.5. Figure 3-40 on page 197 shows the lateral radiograph and 24-hour static scintigraphic image from Case-13 with areas from the osteosarcoma selected for autoradiography. Sections were selected using radiographs from the middle of the osteosarcoma and areas of reactive bone e.g., Codman's Triangle.

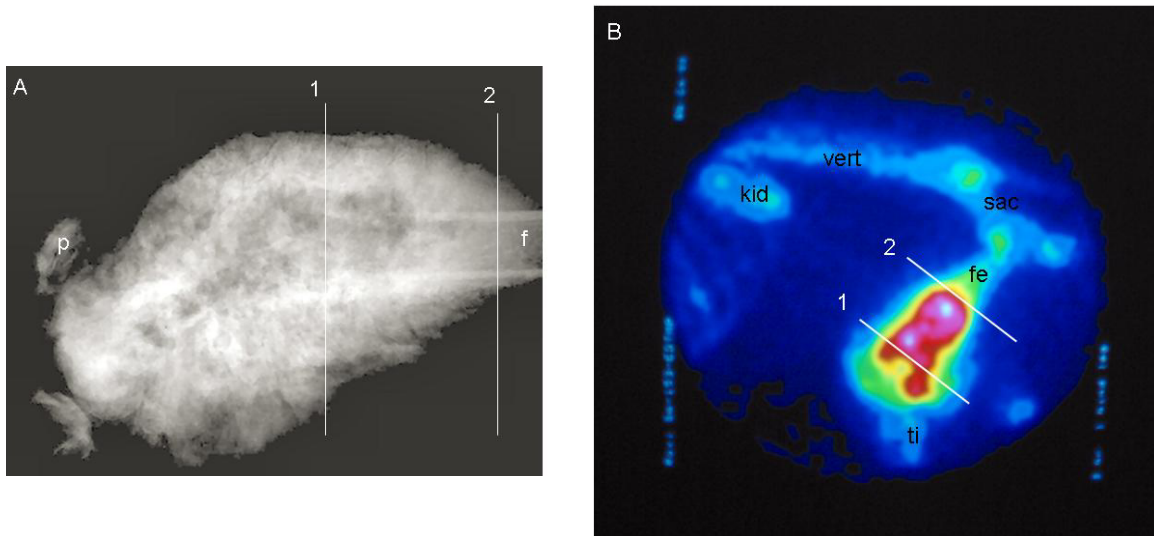
---

\* Kodak Dektol Developer. Eastman Kodak Co. Rochester New York

† Kodak Sodium Fixer. Eastman Kodak Co. Rochester New York

‡ Diff-Quik staining kit. Dade Behring South Africa (Pty) Ltd, P O Box 50726, Randjesfontein 1683

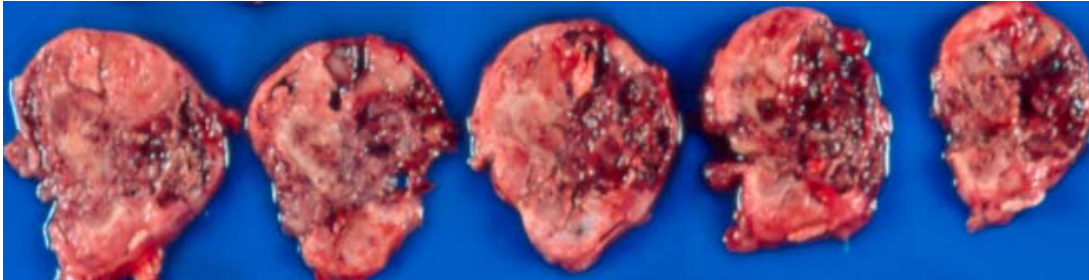
**Figure 3-40 A lateral radiograph (A) and 24-hour scintigraphic ( $^{153}\text{Sm-EDTMP}$ ) image (B) of the distal femur from Case-13.**



Legend: White lines numbered 1 and 2 on A and B show the areas (sections) selected for autoradiography. For orientation in A, the patella is labelled p and the diaphysis of the femur is labelled f. In B abbreviations are used to designate organs and skeletal components, kid (kidney), vert (lumbar vertebrae), sac (sacrum), fe (femur) and ti (tibia).

A post mortem was done shortly after euthanasia in the necropsy room at the Pretoria Biomedical Research Institute. The femur was dissected out and 1 cm thick sections were cut transversely using a band saw as shown in Figure 3-41 below.

**Figure 3-41: Transverse osteosarcoma sections taken from the distal femur from Case-13**



The sections (see 1&2) were dried using paper towel to remove excess blood and placed in plastic packets and vacuum-sealed using a commercial vacuum sealer\*. Radiographs were taken of the sections. In a dark room, the sealed sections were then placed directly on to standard x-ray film in the same orientation as for the radiographs and kept in a dark room for 12-hours. The film was then developed using an automated film developer. An area of low and high radioisotope deposition was identified on the radiographs and 2mm square, biopsies were taken from these sites for micro-autoradiography. These sections were processed using the same protocols as described for the rat tissue e.g., H&E staining and quick frozen sections. Negative controls were also used.

### 3.16.3 Results

#### 3.16.3.1 Normal Rat Macro- and Micro-autoradiography

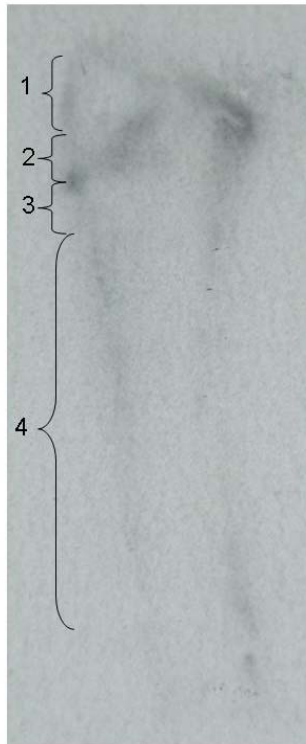
##### 3.16.3.1.1 Macro-autoradiography.

A section from the femur showed uptake in the region of the metaphyseal growth plate, periosteum, endosteum and epiphysis, see Figure 3-42.

**Figure 3-42: Macro-autoradiography image of the proximal femur.**

---

\* Freshlock™ Vacuumsealer Model No. FP155



Legend: The outline of the bone (in black) is from fixing of the silver salt by radioactive decay from the  $^{153}\text{Sm}$  isotope. The physis (2) and metaphysis (3) show the most radioisotope uptake when compared to the diaphysis (4) and epiphysis (1)

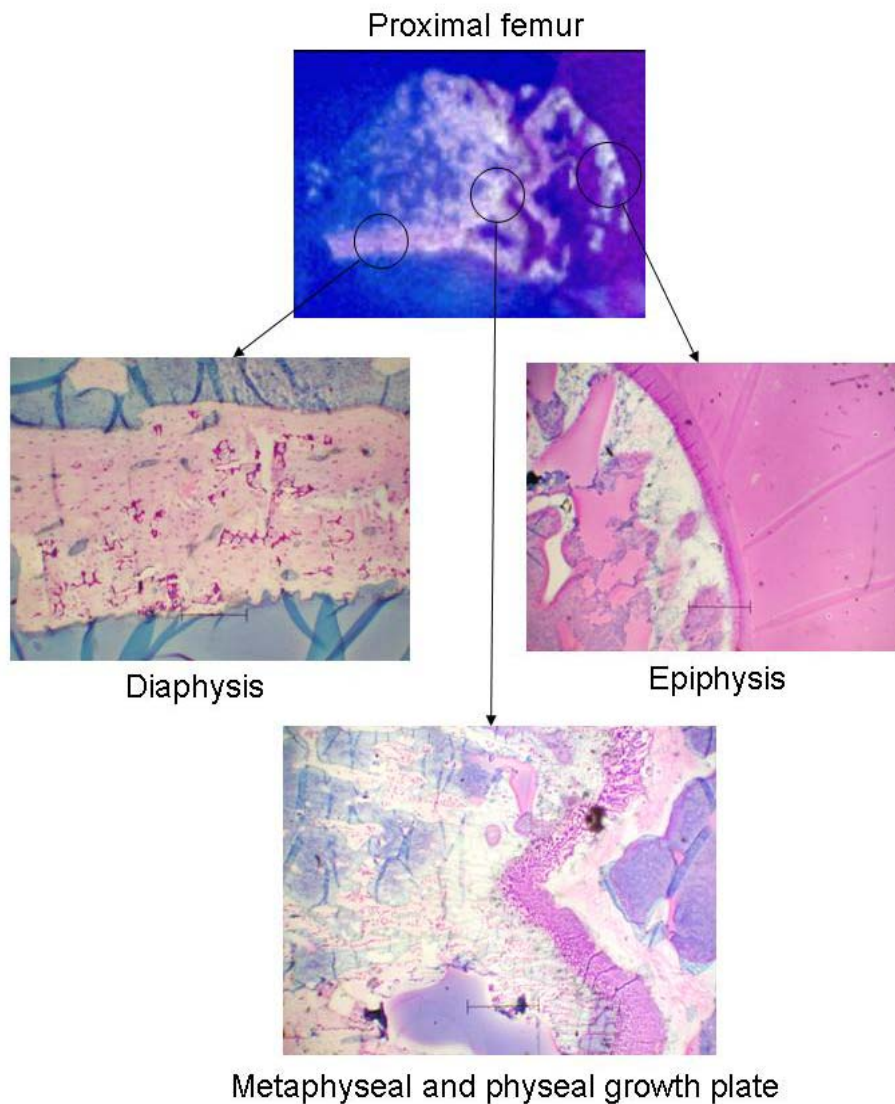
#### 3.16.3.1.2 Micro-autoradiography

Areas from the rat's proximal femur were selected for study using light microscopy see Figure 3-43 on page 200. These areas were then photomicrographed\*.

---

\* Nikon Labophot Microscope, Multiple objects x10 – x100. Images were digitally recorded using Nikon COOLPIX 4500 via lens attachment (Leitz, Periplan x10) fitted with custom made reticle (I-bar = 2mm).

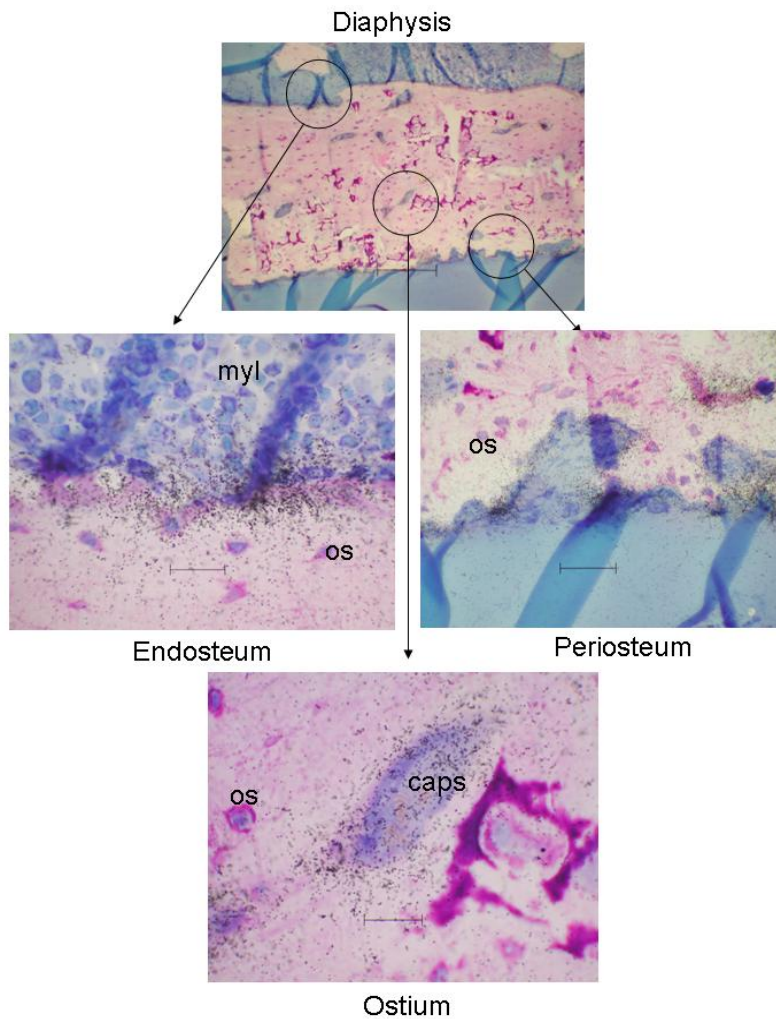
**Figure 3-43: Photomicrograph sections from the proximal rat femur showing areas of interest. These areas correspond to increased radioisotope uptake. Diff-Quik (X 40, I-bar = 50  $\mu$ m)**



Legend: The areas chosen in the proximal femur of the rat were based on the macro-autoradiography image of the proximal femur in Figure 3-42 on page 198. These areas corresponded to high uptake of  $^{153}\text{Sm-EDTMP}$  in the rat's femur. Importantly the metaphyseal growth plate section is critical for bone growth in juvenile animals and humans. High doses of radiation to the metaphyseal growth plate could lead to cessation of growth on length of the bone.

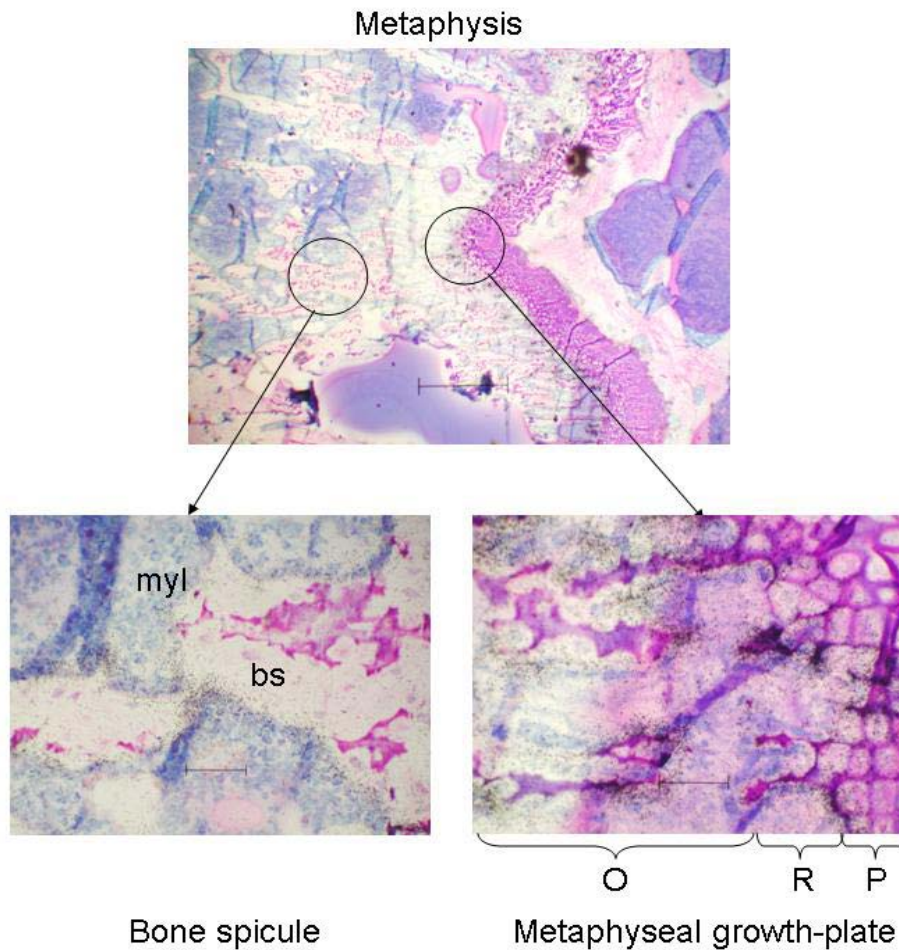


**Figure 3-44: Photomicrograph sections selected from the diaphyseal region of bone.**



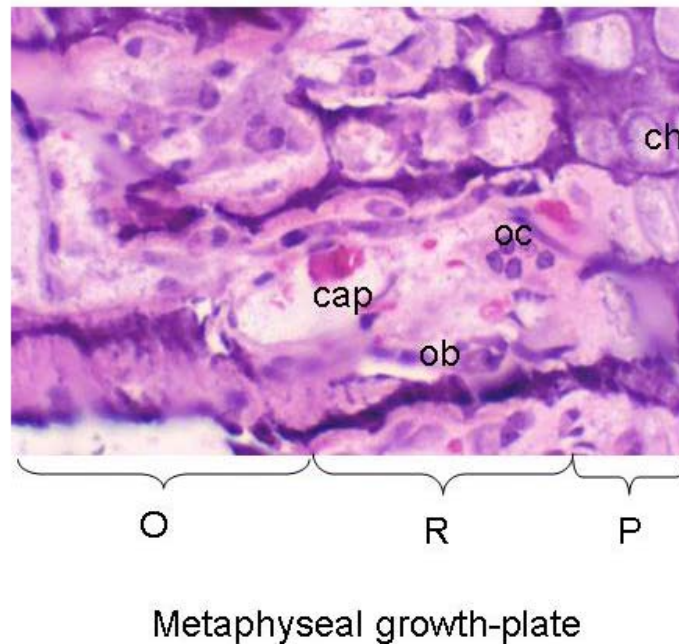
Legend: The endosteum shows high uptake (black granules are conversion of the silver salt by radioactive decay from the  $^{153}\text{Sm}$  isotope) of  $^{153}\text{Sm}$ -EDTMP on the surface adjacent to myeloid tissue (myl). This layer consists of lining cells derived from osteoblasts and collagen and is an area of resorption and osteoclastic activity in growing bone. Osteocytes (os) can be seen incorporated into the bone matrix. The periosteal layer also shows uptake indicative of metabolically active bone. The periosteal layer consists of lining cells and collagen and in growing bone is an area of bone deposition. Central canalicular capillaries (cap) in the ostium also showed increase uptake indicating diffusion from the capillary. Diff-Quik. Photomicrographs show the endosteum (X 1000), periosteum (X 400) and ostium (X 1000) (I-bar= 5  $\mu\text{m}$  at X 400, 2  $\mu\text{m}$  at X 1000)

**Figure 3-45: Photomicrographs sections selected from the metaphyseal region of the bone.**



Legend: The bone spicule (bs) shows uptake on the surface as seen with the endosteum and periosteum layers. This would explain the myelosuppressive effect of  $^{153}\text{Sm-EDTMP}$ , as the myeloid tissue (myl) lies in close proximity to the bone spicule. The metaphyseal growth plate showed the highest uptake as seen in this section and in Figure 3-42. The zone labelled *P* is the area of proliferation and hypertrophy of chondrocytes. R and O zones represents the area of resorption and calcification due to capillary invasion and osteoblastic and osteoclastic activity. This is the area of intense uptake and appears centred around osteoblastic and osteoclastic activity. Diff-Quik. Photomicrographs show the bone spicule (X400) and metaphyseal growth-plate (X400) (I-bar= 5  $\mu\text{m}$ )

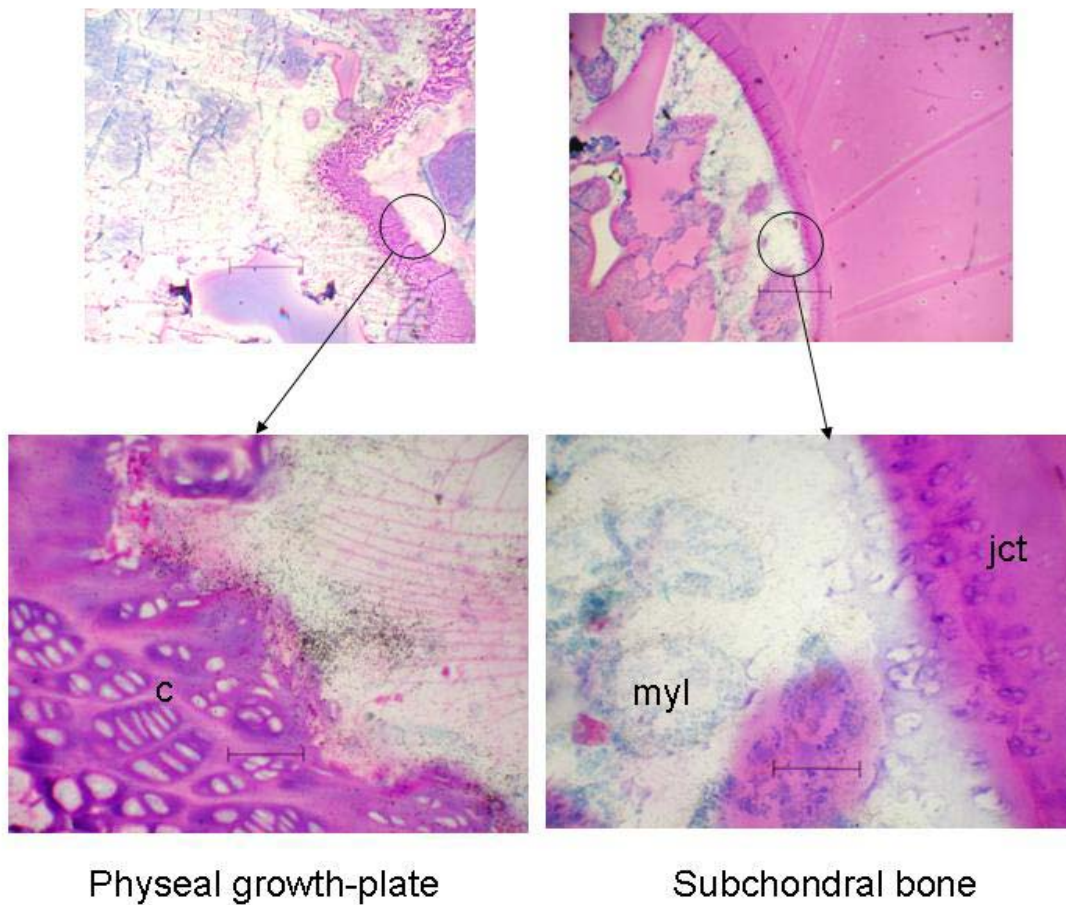
**Figure 3-46: A photomicrograph of an H&E from the metaphyseal region of the proximal femur.**



Legend: The area shows the normal histology of H&E section from the metaphyseal growth plate in the rat. The purpose of the slide was to illustrate in detail the microstructures present in the metaphyseal growth plate. While the previous autoradiography sections have good detail, some cellular detail is lost due to processing for autoradiography. The section is taken from the same area as the sections in Figure 3-45 on page 202, showing intense uptake of  $^{153}\text{Sm}$ -EDTMP. Osteoclastic (multinucleate cells) (oc) and osteoblastic (ob) and capillary (cap) invasion can be seen in the R zone adjacent to hypertrophied chondrocytes (ch) in the P zone. Zone O represents the area of ossification (calcification) by osteoblast entering with invading capillaries. The resulting trabeculae of bone are called primary spongy bone. Haematoxylin and eosin (X1000)

**Figure 3-47: Photomicrographs sections selected from the epiphyseal and joint region of the bone.**

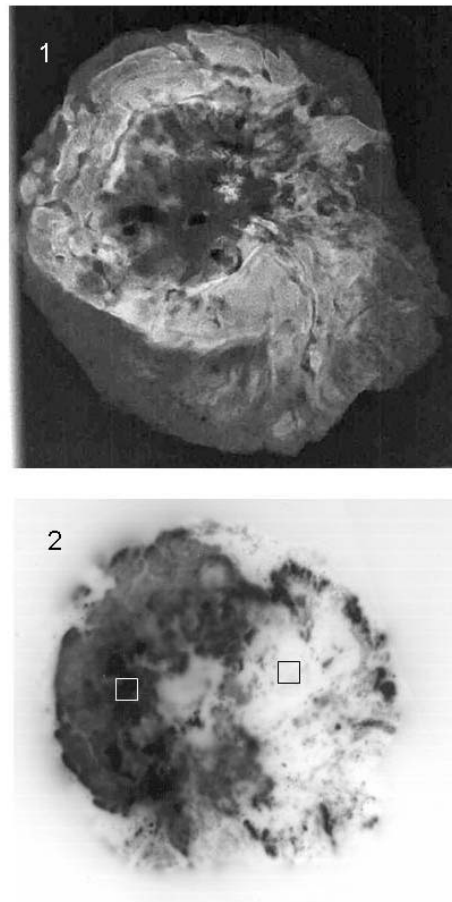
### Epiphysis and Joint cartilage



Legend: The physal growth plate also shows increased uptake on the epiphyseal side of the growth plate, similar to the metaphyseal side, but less intense. The area adjacent to the joint capsule, which is composed of spongiform bone shows uptake on the surface of the bone spicules. No uptake was noted in cartilage. Diff-Quik (X400) (I-bar= 5  $\mu$ m)

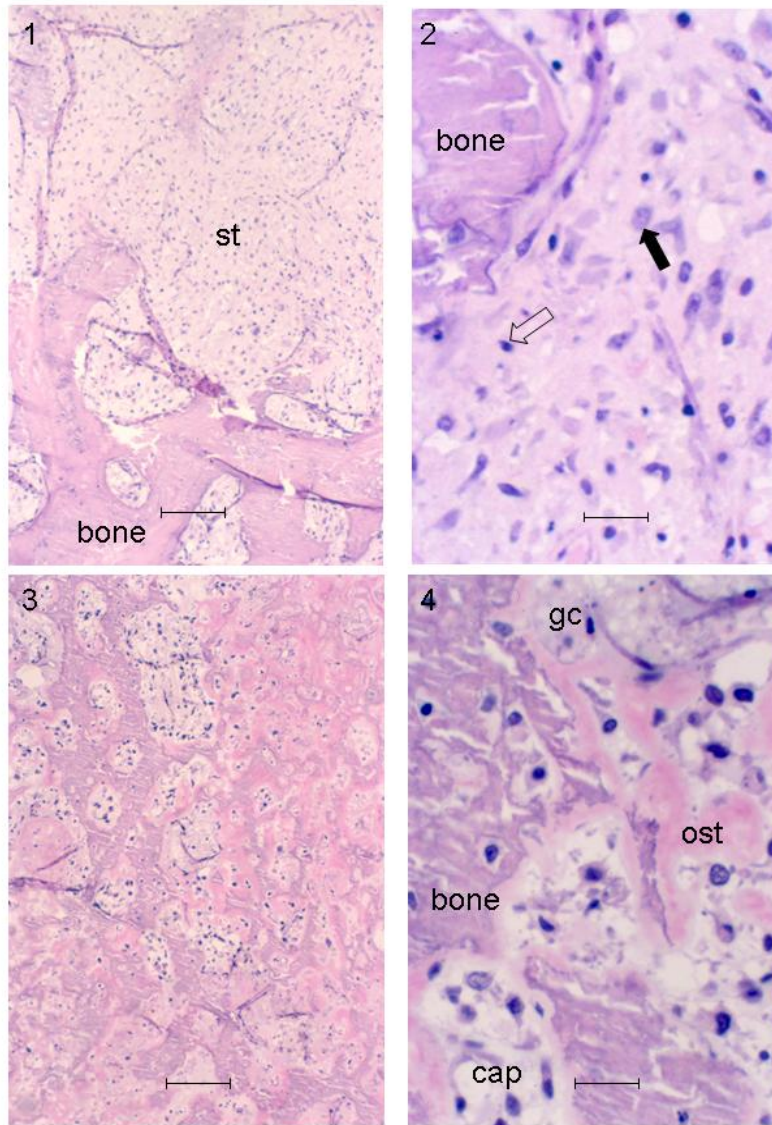
### 3.16.3.2 Dog macro- and micro-autoradiography

**Figure 3-48: Matching radiograph and macro autoradiograph images taken from the same area of the distal femur of the osteosarcoma dog (Case-13).**



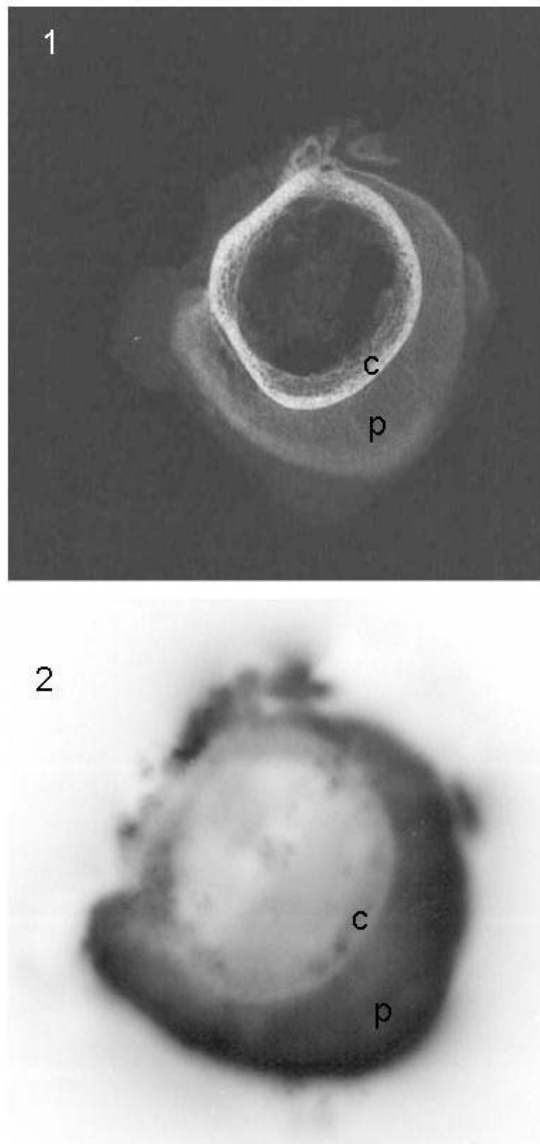
Legend: The radiograph in Image-1 (tumour section 1 from Figure 3-40 on page 197) shows complete effacement of normal bone architecture by the osteosarcoma. Image-2 is a macro autoradiograph of the same section, showing heterogeneous deposition of the radioisotope ( $^{153}\text{Sm}$ -EDTMP) within the tumour. As described in the material and methods, the radioactive decay of the  $^{153}\text{Sm}$  isotope in the sample fixes the silver salt in the X-ray plate emulsion. Samples (3mmx3mm) were taken from areas of poor (white box) and high uptake (dark box) to evaluate cell type, see Figure 3-49 on page 206

**Figure 3-49: Photomicrographs taken from areas (see Figure 3-48) of low (Images -1 and -2) and high (Image -3 and -4) radioisotope uptake.**



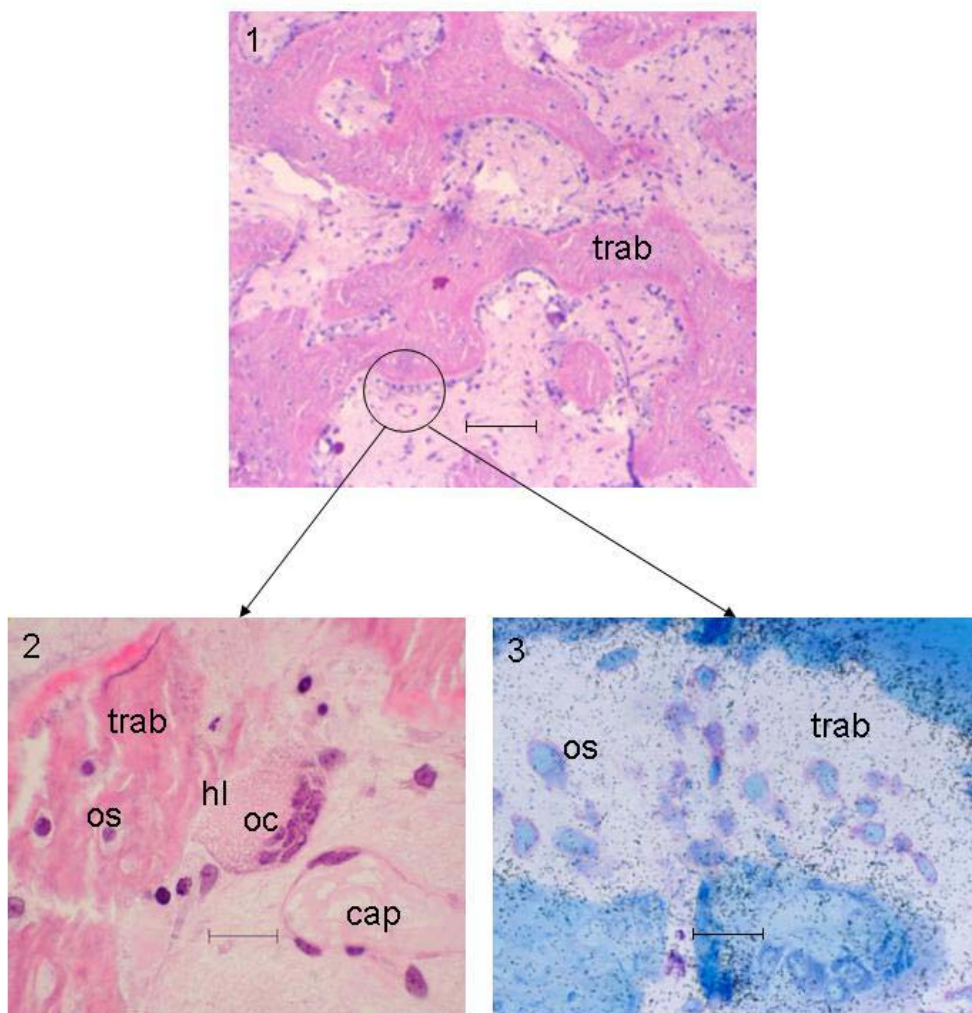
Legend: Image 1 shows an area soft-tissue (st) and bone not well supplied with capillaries. Image-2 shows a magnified section from image-1 showing some pyknotic nuclei (open arrow) and some viable spindle shaped cells (closed arrow). This is in an area of low uptake. Images-3 and -4 (high uptake) show an area of increased metabolic activity as evidenced by the capillaries (cap) and light pink-staining osteoid (ost) formation. In addition, bizarre giant cells can also be seen. Haematoxylin and eosin (Images -1 and -3 X100, I-bar 20  $\mu$ m; Images -2 and -4 X500, I-bar 4  $\mu$ m)

**Figure 3-50: Image-1 is a radiograph of the section (section-2 see Figure 3-40) taken from the diaphyseal area of the femur of Case-13.**



Comments: The radiograph shows a periosteal reaction (p), covering the cortex (c). No evidence of bony destruction can be seen. Image-2 is a macro autoradiograph of the same section showing intense uptake (dark) of the  $^{153}\text{Sm}$ -EDTMP in the periosteal layer. As described in the material and methods, the radioactive decay of the  $^{153}\text{Sm}$  isotope in the sample fixes the silver salt in the X-ray plate emulsion. Sections from the periosteum were taken and evaluated histopathologically see Figure 3-51 on page 208.

**Figure 3-51: Photomicrograph images from stained sections taken from the diaphyseal area of the femur of Case-13.**



Legend: Images 1, 2 and 3 are photomicrographs of the periosteal reaction (p) reported in Figure 3-50 on page 207. Images -1 and -2 are stained with haematoxylin and eosin (Image-1 X100, I-bar 20  $\mu\text{m}$ ; Image-2 X1000, I-bar 2  $\mu\text{m}$ ). Image-3 is stained with Diff-Quik (X1000, I-bar 2  $\mu\text{m}$ ). Image-1 shows the trabecular nature of the bony reaction. Image-2 shows details of the numerous osteoclasts (oc) found in the section. The multinucleate osteoclast can be seen adhered to the bone known as Howship's lacunae (hl). This is the area of bone resorption by the osteoclast. Adjacent to the lacunae, are osteocytes (os) imbedded in the bone matrix. Numerous capillaries (cap) are evident in the sections. Image-3 shows the deposition of radioisotope as fine black granules on the trabeculae (trab) surface.



### 3.16.3.2.1 Statistical analysis of areas of high and low $^{153}\text{Sm}$ -EDTMP uptake in the osteosarcoma

In order to explain the uptake of  $^{153}\text{Sm}$ -EDTMP in the osteosarcoma and its possible effect on tumour cells the number of live cells and the amount of blood supply to the three areas were quantified in H&E sections. Three histopathological sections were taken from the osteosarcoma shown in Figure 3-49, on page 206. The sections were from areas of high, moderate and low  $^{153}\text{Sm}$ -EDTMP uptake. Five areas at 400-power magnification were counted from each section and recorded in the Appendix; see Table 8-19 on page 305. The areas were scored for capillary, osteoblast, osteoclast and pyknotic nuclei density based on an in-house scoring system e.g. where a score of 0 meant no cells, to a score of 4 meaning cells were seen in five out of five fields; see Appendix, Table 8-19 on page 305. The data were then tested using ANOVA on ranks and results were reported in the Appendix; see Table 8-20 on page 306. A summary of the descriptive statistics and comparison between sections is reported below in Table 3-60 and Table 3-61 on page 210

**Table 3-60: Descriptive statistics for micro-autoradiography score results from high, moderate and low  $^{153}\text{Sm}$ -EDTMP uptake areas of the osteosarcoma.**

$^{153}\text{Sm}$ -EDTMP uptake in Histopathology Sections	Median Capillary Score
Moderate	1.0
None	0.0
High	4.0
	Osteoblast Score
Moderate	4.0
None	1.0
High	3.0
	Osteoclast Score
Moderate	0.0
None	0.0
High	4.0
	Pyknotic Nuclei Score
Moderate	2.0
None	3.0
High	1.0

Legend: Scoring system for the three histopathology sections was based on a score of 0 to 4 for capillary, osteoblast, osteoclast and pyknotic nuclei density. Where 0 = no evidence of capillaries or cells, 1 = structure or cell found in only 1/5 areas, 2 = structure or cell found in only 2/5 areas, 3 = structure or cell found in only 3/5 areas and 4 = structure or cell found in only 5/5

---

 areas

**Table 3-61 Results from ANOVA on ranks analysis comparing micro-autoradiography score results from high, moderate and low  $^{153}\text{Sm}$ -EDTMP uptake areas**

Histopathology Parameter	$^{153}\text{Sm}$ -EDTMP uptake Histopathology Sections	$P < 0.05$
Capillary Score	High vs. None	Significant
	High vs. Moderate	No
	Moderate vs. None	No
Osteoblast Score	Moderate vs. None	Significant
	Moderate vs. High	No
	High vs. None	No
Osteoclast Score	High vs. None	Significant
	High vs. Moderate	No
	Moderate vs. None	No
Pyknotic Nuclei Score	High vs. None	Significant
	None vs. Moderate	No
	Moderate vs. High	No

Legend: The high uptake sections were statistically different ( $P < 0.05$ ) from the no-uptake sections for capillaries, osteoclasts and pyknotic cells, but not from moderate uptake. Moderate uptake was only statistically different from no-uptake for osteoblast ( $p < 0.05$ ).

It was clear from the results in Table 3-60 and Table 3-61 (above) that areas of low  $^{153}\text{Sm}$ -EDTMP uptake had correspondingly low capillary density, but a higher density of pyknotic nuclei. Conversely, areas of high capillary density correspondingly had high uptake of  $^{153}\text{Sm}$ -EDTMP and higher scores for osteoclasts and osteoblasts. Therefore, since the bloodstream carries radiopharmaceuticals and there is significant variation in capillary density in the osteosarcoma, it is not surprising that the uptake of  $^{153}\text{Sm}$ -EDTMP in the tumour is heterogeneous. Nevertheless areas of low uptake did have what appeared to be viable neoplastic cells and because of the poor dose delivery of the radiopharmaceutical, these cells may contribute to regrowth of the osteosarcoma.

### 3.17 Section Discussion

In previous reported Sections 3.9 (on page 151) and 3.10 (on page 155) the results of the dog model were presented and discussed using primary data such as time-activity curves to describe the biodistribution of the  $^{153}\text{Sm}$ -EDTMP,  $^{188}\text{Re}$ -HEDP, and  $^{186}\text{Re}$ -HEDP. In addition, pharmacokinetic data were also acquired and reported, including blood  $t_{1/2-\alpha}$  and  $t_{1/2-\beta}$  and urinary clearance of the three radiopharmaceuticals. The results from these studies supported the hypothesis that normal dogs and dogs with naturally occurring osteosarcoma, when compared to published human biodistribution, pharmacokinetics, bone localization, dosimetry, pain control, dosimetry and toxicity for  $^{153}\text{Sm}$ -EDTMP,  $^{188}\text{Re}$ -HEDP, and  $^{186}\text{Re}$ -HEDP will have similar experimental data making it a good radiopharmaceutical translational model.

In addition observational biodistribution studies were done using macro- and micro- autoradiography techniques. The purpose was to observe the distribution of  $^{153}\text{Sm}$ -EDTMP within a tumour and in surrounding bone marrow elements. Results from the studies showed heterogeneous uptake of the radiopharmaceutical within tumours. Not surprisingly, poor distribution was found in areas of poor blood supply, with apparently viable (seen histologically) tumour cells. The heterogeneity of the uptake of the radiopharmaceutical in cancer has implication for dosimetry to tumours, as it is obvious that parts of the tumour would receive a lower dose or no dose of radiation resulting in sub-therapeutic dose delivery. The studies in normal rats confirmed the propensity of  $^{153}\text{Sm}$ -EDTMP to localize especially in red marrow areas, thus leading to high radiation dose to blood producing elements. In addition, high uptake was documented at the metaphyseal growth plate, confirming the likelihood of a delay or cessation of growth if  $^{153}\text{Sm}$ -EDTMP were used in growing children.

To monitor myelosuppressive effects and therapeutic response of  $^{153}\text{Sm}$ -EDTMP (n=26) and  $^{188}\text{Re}$ -HEDP (n=7) a clinical trial was conducted in dogs with naturally occurring osteosarcoma. Dogs receiving  $^{153}\text{Sm}$ -EDTMP at 37 MBq/kg (1 mCi/kg) showed only mild bone marrow toxicity (Grade 2). In the case of  $^{188}\text{Re}$ -HEDP, only mild (Grade 1) bone marrow toxicity was noted for all seven dogs. Two dogs received repeated doses of (x4)  $^{188}\text{Re}$ -HEDP, with no statistical difference in haematological parameters between single doses or multiple doses. This could be explained by the lower  $T_e$  of  $^{188}\text{Re}$ -HEDP compared to  $^{153}\text{Sm}$ -EDTMP, see Figure 3-31 on page 153. It can then be speculated that higher and

repeated doses of  $^{188}\text{Re}$ -HEDP may be possible. The literature reports the maximum tolerated dose of  $^{153}\text{Sm}$ -EDTMP as 93MBq/kg (2.5mCi/kg)<sup>256, 257</sup>. Typically,  $^{188}\text{Re}$ -HEDP is dosed at a similar rate of 37 MBq/kg.<sup>114</sup> Even though  $^{188}\text{Re}$ -HEDP has a more energetic  $\beta$ -emission compared to  $^{153}\text{Sm}$ -EDTMP, and the expected myelotoxicity would be worse, it was not observed in the dog study.

There was no cessation in growth of the tumours and all dogs were euthanized because of progression of the tumours. The median survival was 4-months, which is significantly shorter than the 10 to 12-month median survival for amputation and chemotherapy reported in the literature. In an effort to improve response to  $^{153}\text{Sm}$ -EDTMP, we studied the concurrent administration of a carboplatin infusion with the radiopharmaceutical. This decision was based on reports in the literature, which found that carboplatin acted as a radio sensitizer that improved survival when used together with teletherapy<sup>247, 249, 251, 258</sup>. No differences in toxicity were noted between the carboplatin group and dogs receiving only  $^{153}\text{Sm}$ -EDTMP. As a group, the dogs receiving only  $^{153}\text{Sm}$ -EDTMP had a mean $\pm$ SD uptake ratio of 5.76 $\pm$ 4.83. When the uptake ratio of the carboplatin group was compared to dogs receiving only  $^{153}\text{Sm}$ -EDTMP, there was a significant difference ( $P<0.05$ ). The carboplatin group had a higher uptake ratio of 11.23 $\pm$ 2.88. This however did not translate into improved survival and the data may have been skewed because of patient selection.

Interestingly six dogs that had both  $^{99\text{m}}\text{Tc}$ -MDP and  $^{153}\text{Sm}$ -EDTMP scans of their tumours, had consistently lower (45.42 $\pm$ 11.94 %) uptake ratio for  $^{99\text{m}}\text{Tc}$ -MDP scan compared to  $^{153}\text{Sm}$ -EDTMP. This could be explained by the differences in the binding (antiresorptive capacity) of bisphosphonate ligand to bone. This was again seen when six dogs that received  $^{188}\text{Re}$ -HEDP also had  $^{99\text{m}}\text{Tc}$ -MDP scans, however in this case the uptake ratios were not different, confirming the similar behaviour of the ligands MDP and HEDP; both are non-amino bisphosphonates.

## Chapter 4. Radiolabelled Polyethyleneiminomethyl Phosphonic Acid (PEI-MP) Therapy

### 4.1 Introduction

Intravenously administered bone-seeking radiopharmaceuticals distribute via the circulatory system throughout the body while simultaneously accumulating in the bone. The material not taken up by the bone is efficiently cleared through the kidneys into the bladder<sup>48, 49</sup>. Using this modality all involved osseous sites can be treated simultaneously with limited associated toxicity. Selective absorption into bone and especially into diseased bony areas limits irradiation to normal tissues and increases the therapeutic ratio. Therapeutic (and diagnostic) success of a radiopharmaceutical will hinge on many interrelated factors, such as the careful choice of a radionuclide (of which its half-life and radiation emissions dictate its radiobiological effects and its diagnostic image quality), linked to a bone localizing agent of which the biochemical properties dictate its pharmacokinetics and biodistribution. The basic principle for the design of diagnostic and therapeutic radiopharmaceuticals is the incorporation of a suitable radionuclide in an appropriate chemical compound to attain the highest target-to-background concentration ratio. The important concern, especially with therapeutic radiopharmaceuticals, is to maximize the radiation dose to the lesion while minimizing that to the remainder of the body, most specifically to the critical organ in this case, the radiosensitive bone marrow.

Bisphosphonates and amino phosphonic acids (e.g., ethylenediamine tetramethylene phosphonic acid [EDTMP]) are chemically stable and are not significantly metabolized. They bind tightly to the bone matrix, and once taken up by bone are liberated only when the bone in which it was deposited is resorbed<sup>60, 61</sup>. Particle-emitting radionuclides e.g., beta-emitting <sup>153</sup>Sm, have been complexed with bisphosphonates and substituted organic amine phosphonic acid derivatives e.g., EDTMP, wherein the nitrogen and phosphorous are interconnected by an alkylene or substituted alkylene group. Certain of these complexes have been shown to be very selective for the skeletal system with very low soft-tissue uptake<sup>225</sup>. The complexes also tend to concentrate in areas of fast growing bone much more readily than in normal bone. The radionuclides used are mostly beta particle emitting, and a high radiation dose is

delivered in the area where they are deposited. Thus, therapeutic radiation doses can be delivered specifically to calcific tumours. These complexes (e.g.,  $^{153}\text{Sm-EDTMP}$ ) have been found useful in the treatment of such tumours in humans and animals as has been described in preceding chapters<sup>15, 22, 259, 260</sup>. Unfortunately the selectivity towards fast growing bone (tumour areas) is not adequate so as to avoid bone marrow suppression, which limits the radioactivity doses that can be given to a patient, and thus also the therapeutic efficacy of the agent. Any radionuclide that ends up on trabecular bone, or in the inner surface of cortical bone, will deposit energy in the radiosensitive bone marrow<sup>261</sup>.

The principal factors that lead to the accumulation of radiopharmaceuticals in bone are blood flow, extraction efficacy, and capillary permeability. The discovery that macromolecules and small particles accumulate passively in solid tumour-tissue has had enormous implications for improved design of targeted chemotherapy<sup>119, 262</sup>. This phenomenon has been called the "enhanced permeability and retention effect" (EPR-effect) and has been attributed to two main factors: tumour vasculature often displays a disrupted endothelium (i.e. becomes leaky), which allows macromolecular extravasation which are larger than seen via most other endothelial barriers, and a lack of effective lymphatic drainage, leading to macromolecular accumulation<sup>120</sup>. Generally, tumour tissues and inflammatory areas are characterized by an increased permeability of capillary endothelial layers to blood-borne macromolecules. Administration of radiolabelled macromolecules thus leads to a selective accumulation of radioactivity in these areas. Furthermore, if these tumours or inflammatory areas are calcified or associated with the bone matrix, the selective retention of the phosphonate containing macromolecule will also be enhanced by its binding to the hydroxyapatite bone matrix. At the same time, the normal bone (and especially the radiosensitive red-marrow) is protected by the normal impermeability of their capillary endothelial layers to blood-borne macromolecules (60 kDa)<sup>21</sup>. Higher and more effective therapeutic doses are thus attainable.

In a study to investigate the concept, Dormehl *et. al.*<sup>21</sup> looked at the biodistribution and pharmacokinetics of radiolabelled macromolecules of various molecular weights (MW) in the normal Chacma baboon (*Papio ursinus*). These studies were conducted by injecting the  $^{99\text{m}}\text{Tc}$  complexes of polyethyleneiminomethyl phosphonic acid (PEI-MP) MW-fractions of various molecular sizes into the experimental animals to obtain the scintigraphic images of the entire animal at various times up to four hours after injection. In this manner, an optimal molecular

size of polymeric macromolecular radioactive compounds was determined with optimal protection of normal bone, liver, and kidney. Molecular weight MW-fractions of greater than 50 kDa were excluded because of the potentially high liver exposure to radiation. Other MW-fractions that excluded were 3-10 kDa and 30-50 kDa MW because of the increased risk to kidneys. Therefore, from the results it was concluded that the optimal size molecule weight was believed to fall in the 10-30 kDa range. Since the primate model was not a cancer model, the EPR effect of PEI-MP could not be studied. Consequently, the goal of the canine study was to determine the optimal molecular weight of PEI-MP for the normal dog model and to confirm the EPR effect in the naturally occurring osteosarcoma dog model using  $^{99m}\text{Tc}$  labelled PEI-MP as a radiotracer. If the canine studies were successful, the aim was then to label the optimally sized PEI-MP with a therapeutic radionuclide such as  $^{153}\text{Sm}$  or  $^{186}\text{Re}$  for further investigation.

#### **4.2 Aims and objectives for the canine PEI-MP studies**

- 4.2.1 To determine biodistribution, pharmacokinetics, bone localization, dosimetry in normal dogs, using MW-fractions 3-10, 10-30, 20-30, 30-50, and 50-100 kDa PEI-MP labelled with  $^{99m}\text{Tc}$ . This will serve to select the size MW-fraction of PEI-MP, which will meet the criteria for optimal molecular size.
- 4.2.2 To determine biodistribution, pharmacokinetics, bone localization, dosimetry in dogs with naturally occurring osteosarcomas using  $^{99m}\text{Tc}$ -PEI-MP as determined above.
- 4.2.3 To radiolabel the optimal molecular size with therapeutic  $\beta$ -emitting radioisotope e.g.,  $^{153}\text{Sm}$  to determine the biodistribution, pharmacokinetics, bone localization, dosimetry in normal dogs.

#### **4.3 Ethical Approval**

All studies were performed after approval by the Ethics Committee of the University of Pretoria, according to the guidelines of the National Code for Animal Use in Research, Education, Diagnosis, and Testing of Drugs and Related Substances in South Africa.

#### **4.4 Materials and methods for dynamic studies in normal dogs using variously sized MW-fractions of $^{99m}\text{Tc}$ -PEI-MP**

##### **4.4.1 Preparation of polyethyleneiminomethyl phosphonic acid (PEI-MP).**

###### **4.4.1.1 Synthesis of PEI-MP.**

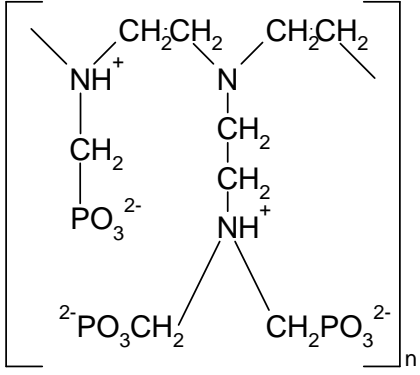
Polyethyleneiminomethyl phosphonic acid was prepared in the NECSA\* laboratories by Dr Werner Louw from the condensation of polyethyleneimine (PEI), phosphorous acid, and formaldehyde by a modified Mannich reaction in the presence of hydrochloric acid<sup>1, 21</sup>. Phosphorous acid (18.36 g), (Riedel-de Haën AG), was dissolved in 51.3 ml concentrated hydrochloric acid (32%, pro analysi, E Merck, Darmstadt), while stirring and heating to 80°C. After drop wise addition of 32% formaldehyde solution (pro analysi, E Merck, Darmstadt), the temperature was raised to 90°C (refluxing temperature) and a solution of 8.33g polyethyleneimine (Polymin<sup>R</sup>, water-free BASF) in 40 ml water, was slowly added to the reaction mixture at a rate of 0.3 ml/min. The reaction mixture was continuously purged with argon. When addition of the polyethyleneimine solution was completed, the reaction mixture was stirred under reflux for another hour, then allowed to cool slowly overnight during which the product separated as viscous oil. After decanting the mother liquid, 50 ml water was added to the oily precipitate, which formed a doughy mass upon stirring. The liquid phase was decanted and the process repeated twice where after the doughy material was dissolved in 37 ml of molar sodium carbonate solution to form the water soluble sodium salt of PEI-MP (pH 7.0). After lyophilization, 12 g of PEI-MP was obtained. See Table 4-1 for the molecular structure of PEI-MP.

---

\* NECSA – Nuclear Energy Corporation of South Africa



**Table 4-1 Molecular structure and weight of PEI-MP**

Name	Molecular weight	Molecular structure
PEI-MP polymer	0.202 per monomer unit	

#### 4.4.1.2 Purification and MW-fractionation of PEI-MP

The macromolecule PEI-MP was further purified into different macromolecular sized MW-fractions using membrane ultrafiltration (polyether sulfone membranes). An aqueous solution of sodium PEI-MP was subjected to a sequential ultrafiltration process through a sequence of 300, 100, 50, 30, 10, and 3 kDa ultrafiltration membranes (Filtron Technology Corporation, Mass., USA). The membrane retentate was washed with distilled water to a theoretically calculated purity of 99%, to yield 3 - 10, 10 - 30, 30 - 50, 50 - 100, and 100 - 300 kDa macromolecular sized MW-fractions see Table 4-2.

Typical elemental analysis gave a C:N molar ratio of 2.97:1, which on the basis of an empirical formula of a PEI-MP monomer of  $C_9H_{18}N_3O_9P_3$ , indicates a high level of methylphosphonation, in contrast to PEI with a monomer empirical formula of  $C_6H_5N_3$  and a ratio C:N of 2:1.

**Table 4-2 Percentage yield of PEI-MP molecular weight fractions obtained by membrane ultrafiltration**

Molecular weight fraction (kDa)	Percentage yield (%)
< 3	28.1
3-10	7.8
10-30	0.2
20-30	undetermined
30-50	6.4
50-100	32.4
100-300	17.7
> 300	7.8

#### 4.4.1.3 Labelling of PEI-MP with $^{99m}\text{Tc}$

The ligand PEI-MP was labelled with  $^{99m}\text{Tc}$  (as tracer) by adding sodium pertechnetate (up to 1850 MBq) to lyophilized kits of the ligand (10 mg) and a reducing agent (stannous chloride dihydrate 0.5 mg) to produce the labelled complex (pH 5.0 - 5.5). The radiolabelled complexes were analysed for radiochemical purity using instant thin-layer chromatography on silica gel impregnated glass-fibre sheets as stationary phase and acetone and 0.9% sodium chloride solutions as mobile phase. The radiochemical purity of the complexes was >95%. Two MW-fractions (50-100 kDa, 30-50 kDa) were further separated into positive and negative charged MW-fractions by CM-cellulose and DEAE-cellulose ion-exchange chromatography and subsequently labelled with  $^{99m}\text{Tc}$  (Radiochemistry department, NECSA). This was done to manipulate the distribution of the  $^{99m}\text{Tc}$ -PEI-MP in the body, especially with regard to the liver. Since after intravenous injection, cationic macromolecules were rapidly removed from plasma because of their extensive hepatic uptake, whereas anionic and neutral macromolecules were slowly removed <sup>263</sup>.

#### 4.4.2 Model System and Sample Size

Thirteen healthy German Shepherd dogs with a mean±SD weight of 29.1±3.4 kg, were used in the study. Each dog received a tracer dose of  $^{99m}\text{Tc}$ -PEI-MP of various molecular sizes as reported in Table 4-3 .

**Table 4-3 List of normal dogs used in experimental procedures using variously sized MW-fractions of <sup>99m</sup>Tc-PEI-MP molecules**

Dogs	Breed	Weight Kg	Sex	Dose MBq	MW MW-fraction kDa	Charge
1	GSD	27	M	123.21	50-100	CM(-)
2	GSD	34	M	107.3	50-100	DEAE (+)
3	GSD	27	M	236.06	30-50	CM(-)
4	GSD	28	M	238.65	10 to 30	DEAE (+)
5	GSD	26.8	M	159.1	10 to 30	neutral
6	GSD	28.5	M	215.34	10 to 30	neutral
7	GSD	33	M	235.69	8 to 30	neutral
8	GSD	30	M	252.71	3 to 10	neutral
9	GSD	31	M	143.93	30-50	DEAE (+)
10	GSD	35	M	425.87	20-30	neutral
11	GSD	26	M	323.75	20-30	neutral
12	GSD	31.5	F	302.29	20-30	neutral
13	GSD	26.5	F	275.65	20-30	neutral
14	GSD	23	F	274.54	20-30	neutral

Legend: Variously sized MW molecules of PEI-MP were used to determine the optimal sized macromolecule in dogs. Various sizes were either neutral or positively or negatively charged (Radiochemistry department, NECSA).

#### 4.4.3 Experimental Design and Experimental Procedures

The dogs underwent identical experimental procedures as previously described studies except for the mentioned differences in molecular size of the injected <sup>99m</sup>Tc-PEI-MP molecules. Five different size MW-fractions (see Table 4-3 above) of the PEI-MP macromolecule were studied, viz. in the following MW ranges: (i) 3 - 10, (ii) 10 - 30, (iii) 20 - 30, (iv) 30 – 50, and (v) 50 - 100 kDa.

Briefly, as previously described induction of anaesthesia was via an indwelling intravenous catheter\* and was performed with a combination of 0.1mg/kg medetomidine hydrochloride† and 3 mg/kg IV ketamine hydrochloride\*, and immediately followed by a

---

\* Jelco 18G

† Domitor, injectable solution 1.0 mg/ml. Novartis SA (Pty) Ltd, Animal Health, P.O.Box 92, Isando 1600

maintained controlled infusion of sodium pentobarbitone solution† initially at 30 ml/h depending on the depth of anaesthesia and decreased accordingly. The following parameters were monitored‡ on all dogs; intra-arterial blood pressure, ECG, oxygen saturation, expired CO<sub>2</sub>, and respiratory rate. The animals were placed in a supine position under the gamma camera (Siemens Orbital Camera) and were injected IV. with a bolus of 107.3 to 425.9 MBq of <sup>99m</sup>Tc-PEI-MP and data acquisition started on a countdown with a Siemens Orbiter gamma camera in 64 x 64 word mode performing a 60 min dynamic study (62 x 1 min frames) followed by static scans at hourly intervals for 3-hours.

Blood and urine samples were collected at fixed intervals for four hours, viz. every three min for the first hour, then hourly for blood samples and for urine every five min for the first hour, subsequently hourly. The activity and volume of each sample were recorded.

#### 4.4.4 Data Analysis

From the dynamic studies, regions of interest (ROI) were drawn on the images over the following organs: cardiac, lungs, kidney, liver, trabecular, cortical bone, and tumour region(s). Trabecular bone ROI was centred over the proximal humerus and cortical bone ROI over the diaphyseal (midshaft) area of the humerus. Background ROI was centred over a well-muscled area of the front limb (triceps region). See Figure 3-2 on page 117 for ROI selection.

Using Sopha Forthmacs software§ the count rate, as an average count per pixel per ROI for each time point, was recorded and exported in comma-delimited file format into an Excel spreadsheet\*\*. Because of the large volume of raw data collected for each dog, only examples of sequential calculations for a single dog receiving <sup>153</sup>Sm-EDTMP are shown in Table 8-1 (page 274) to Table 8-9 (page 282) of the Appendix. The tables illustrate how the

---

\* ANAKET-V, Injectable solution 100mg/ml. Bayer Animal Health Division, P.O.Box 143, Isando, 1600.

† Sagatal, injectable solution 60 mg/ml. Kyron Laboratories Pty Ltd, Benrose

‡ Hewlett-Packard

§ Software: Sopha Forthmacs, Version 3.01 ©, 1995. Hardware: Sophy 256, 32 bit Nuclear Medicine Computer, XT 68020/25 CPU, Sopha Medical, B-1831 Diegem Kouterveldstraat 20, BELGIUM

\*\* Microsoft ® Excel 2002 (10.4524.4219) SP-2

calculations were performed and details of the analytical processes are not reported in this section.

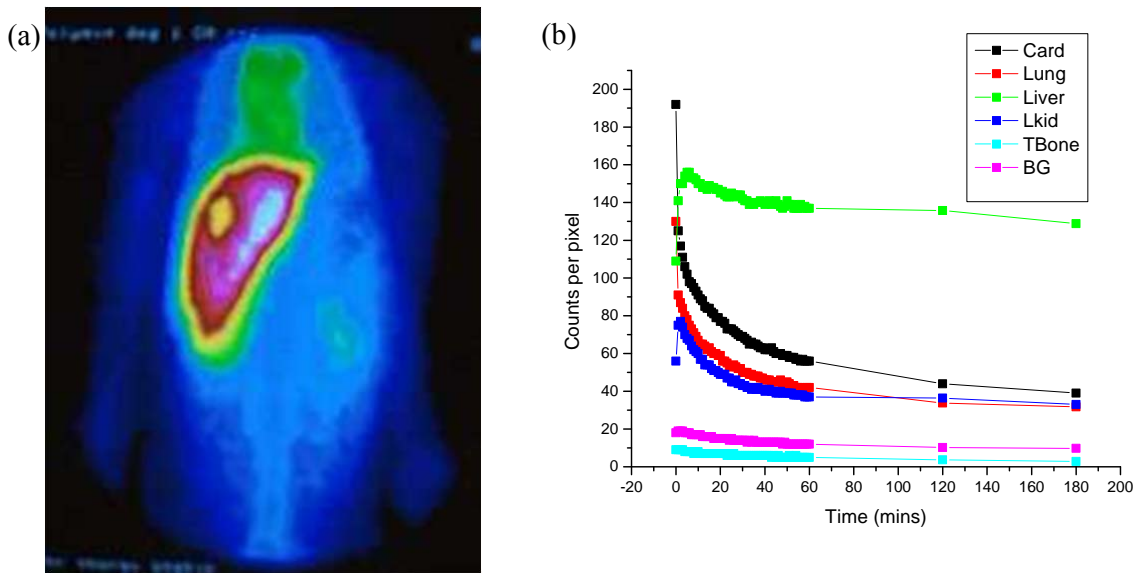
#### 4.4.5 Results from normal dogs receiving various MW-fractions of $^{99m}\text{Tc}$ -PEI-MP

In compliance with the Aim 4.2.1 on page 215, the results of normal dogs receiving  $^{99m}\text{Tc}$ -PEI-MP are reported in this section. In this section, we report on eight normal dogs (Dogs 1-8, from Table 4-3 on page 219) which received a tracer dose of  $^{99m}\text{Tc}$ -PEI-MP for dynamic scintigraphy. The results for all biodistribution and pharmacokinetic studies for individual dogs receiving various MW-fractions of  $^{99m}\text{Tc}$ -PEI-MP are reported below. Results were reported for each MW-fraction for the following compartments; cardiac, lung, left kidney, right kidney, trabecular bone, cortical bone, background and blood. For each compartment, the following pharmacokinetic parameter were reported e.g., half-life ( $T_{1/2}$  of the washout phase), time to maximum concentration ( $T_{max}$  pertaining to wash-in phase), and the percentage organ distribution for the particular compartment at 3-hours (% OD to 3-hr.'s).

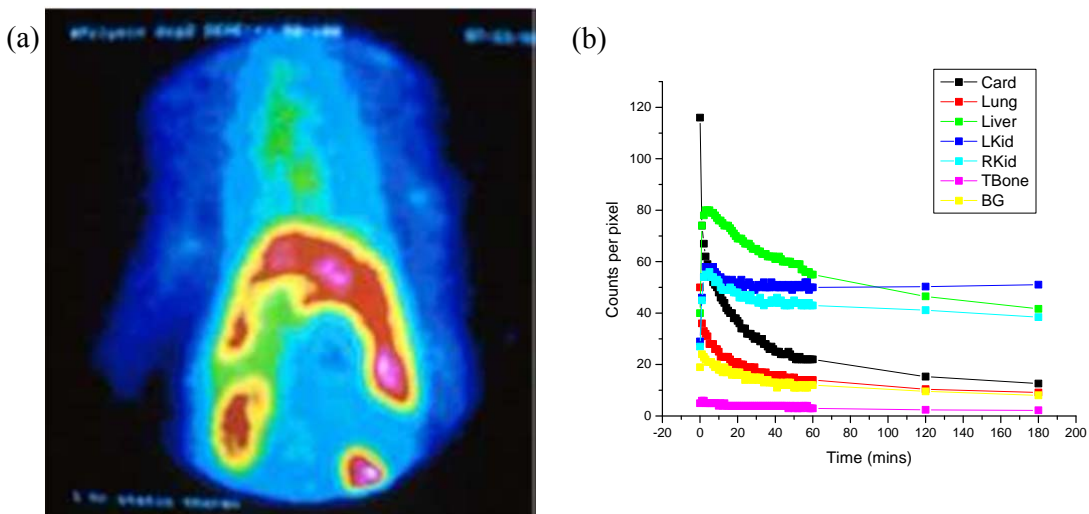
Where the pharmacokinetic and biodistribution results from dogs were in agreement with those found in the primate studies by Dormehl *et al.*, 2001<sup>21</sup>, smaller groups of dogs were studied e.g., 50-100 kDa (n=2), 30-50 kDa (n=2) and 3-10 kDa (n=1). Where a single dog was used per MW-fraction, no mean or standard deviation was reported. Molecular sizes 10-30 kDa (n=4) and 20-30 kDa (n= 5) had multiple dogs per MW-fraction for statistical comparison.

4.4.5.1 Biodistribution data from normal dogs receiving  $^{99m}\text{Tc}$ -PEI-MP MW-fractions 50-100 (-) (n=1) and (+) kDa (n=1)

**Figure 4-1 (a) Scintigraphic image and (b) time activity curves of a normal dog who received  $^{99m}\text{Tc}$ -PEI-MP 50-100 kDa (-)**



**Figure 4-2 (a) Scintigraphic image and (b) time activity curve of a normal dog who received  $^{99m}\text{Tc}$ -PEI-MP 50-100 kDa (+)**



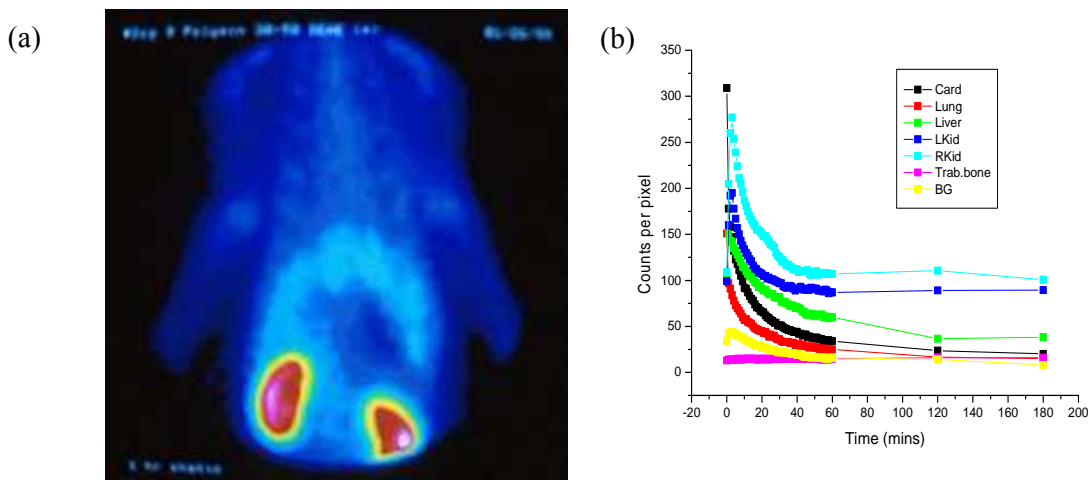
**Table 4-4 Pharmacokinetic data for various compartments for dogs receiving <sup>99m</sup>Tc-PEI-MP MW-fractions 50-100 kDa (+) and (-)**

Compartment Parameter	Cardiac	Lung	Liver	Left kidney	Right kidney	Trabecular Bone	BG	Blood
<b>50-100 kDa Negative charge MW-fraction (n=1)</b>								
T <sub>1/2</sub> (min)	7.00	11.00	>180	40.00	-	No uptake	>180	30.00
T <sub>max</sub> (min)	0.00	0.00	5.00	2.00	-	No uptake	2.00	0.00
% OD at 3 hr's	12.00	9.80	39.00	10.00	-	1.33	3.47	-
<b>50-100 kDa Positive charge MW-fraction (n=1)</b>								
T <sub>1/2</sub> (min)	3.00	10.00	>180	>180	>180	No uptake	37.00	4.00
T <sub>max</sub> (min)	0.00	0.00	4.00	3.00	5.00	No uptake	1.00	0.00
% OD at 3 hr's	7.00	5.61	25.52	31.28	23.00	1.93	4.93	-

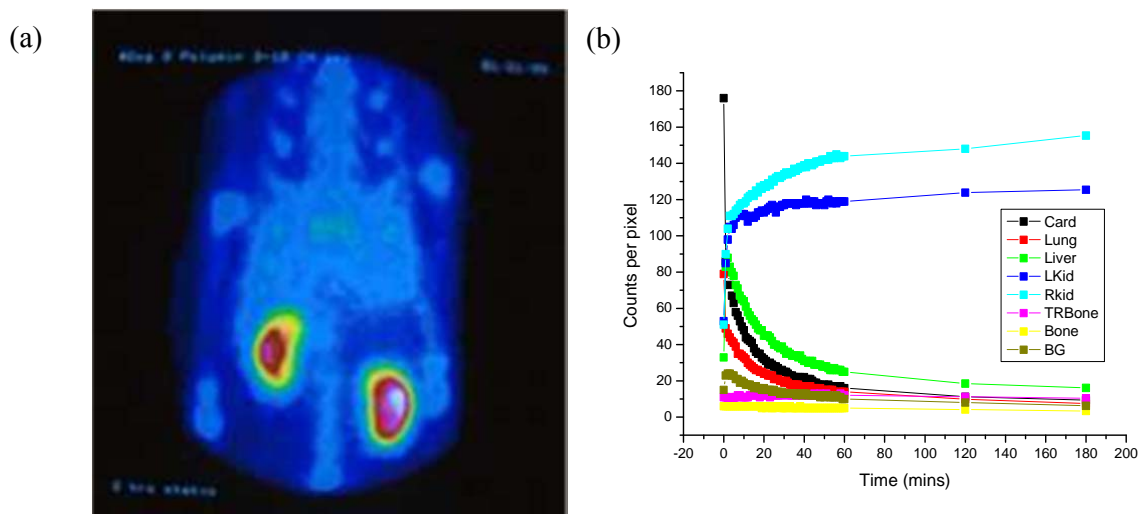
Legend: Biodistribution was significantly affected by the charge carried by <sup>99m</sup>Tc-PEI-MP 50-100 kDa. Both charged MW-fractions were taken up by the liver (green TAC in Figure 4-1 (b) and Figure 4-2 (b) above); however the positively charged MW-fractions showed higher uptake in both kidneys (Light and dark blue TAC in Figure 4-2 (b) above). In the negatively charged MW-fraction no uptake could be identified in the right kidney, this is likely due to the intense up take in the liver which may have masked the kidney ROI. Molecular weight MW-fractions greater than 50 kDa showed virtually complete exclusion of <sup>99m</sup>Tc-PEI-MP from bone.

4.4.5.2 Biodistribution data from normal dogs receiving <sup>99m</sup>Tc-PEI-MP MW-fractions kDa 30-50 (-) (n=1) and (+) kDa (n=1)

**Figure 4-3 (a) Scintigraphic image and (b) time activity curves of a normal dog who received <sup>99m</sup>Tc-PEI-MP MW-fraction 30-50 (-).**



**Figure 4-4 (a) Scintigraphic image and (b) time activity curves of a normal dog who received  $^{99m}\text{Tc}$ -PEI-MP MW-fraction 30-50 (+)**



**Table 4-5 Pharmacokinetic data for various compartments for dogs receiving  $^{99m}\text{Tc}$ -PEI-MP 30-50 kDa (+) and (-) charged**

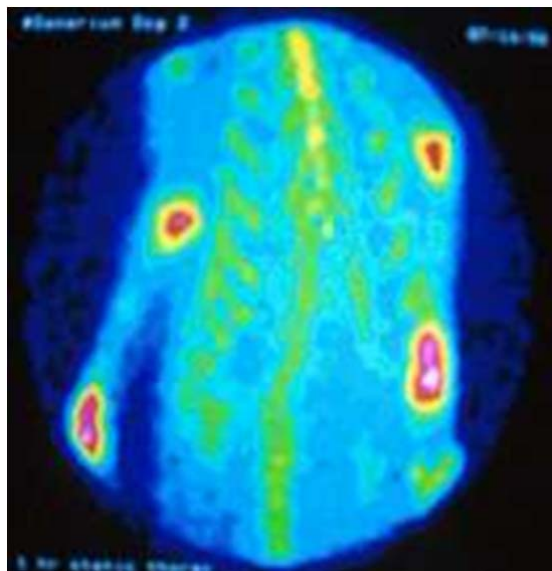
Compartment Parameter	Cardiac	Lung	Liver	Left kidney	Right kidney	Trab. bone	Cort. Bone	BG	Blood
<b>Negative charge MW-fraction 30-50 kDa (n=1)</b>									
$T_{1/2}$ (min)	3.00	5.00	31.00	25.00	34.00	>180	-	29.00	10.00
$T_{max}$ (min)	0.00	0.00	1.00	3.00	3.00	>180	-	2.00	0.00
% OD at 3 hr's	7.00	5.18	13.30	31.11	35.00	5.61	-	2.81	-
<b>Negative charge MW-fraction 30-50 kDa (n=1)</b>									
$T_{1/2}$ (min)	1.00	6.00	23.00	>180	>180	>180	>180	36.00	10.00
$T_{max}$ (min)	0.00	0.00	2.00	>180	>180	0.00	0.00	2.00	0.00
% OD at 3 hr's	3.00	2.00	5.00	37.00	46.00	3.14	1.02	1.86	-

Legend: The two dogs receiving MW-fractions  $^{99m}\text{Tc}$ -PEI-MP 30-50 kDa (+) and (-) charged macromolecule showed significant uptake in both kidneys (light and dark blue TAC curves in Figure 4-3 and Figure 4-4(b)), with the positively charged macromolecule showing the greatest accumulation. Highly polar molecules are typically not cleared well through the kidneys. Similarly to 50-100 kDa (-) MW-fraction, the negatively charged macromolecule showed the highest hepatic uptake (green TAC curve in Figure 4-3 on page 223 ). No appreciable uptake was noted for cortical bone in the negatively charged MW-fraction (see purple TAC in Figure 4-3 on page 223), although some uptake was noted in the positively charged MW-fraction (see Figure 4-4 above).

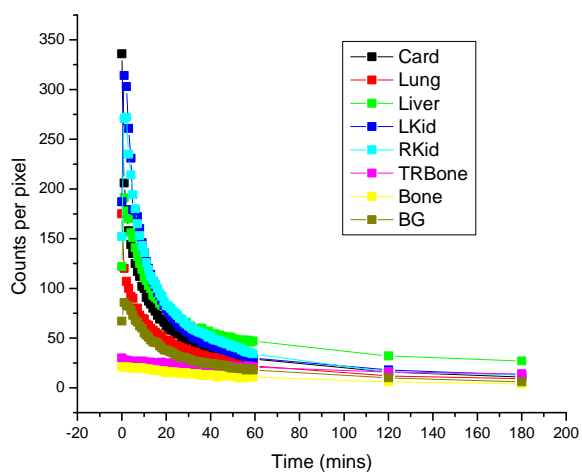


4.4.5.3 Biodistribution data from normal dogs (n=4) receiving  $^{99m}\text{Tc}$ -PEI-MP MW-fraction 20-30 kDa

**Figure 4-5 Scintigraphic image showing biodistribution data from a normal dog (n=1) receiving  $^{99m}\text{Tc}$ -PEI-MP MW-fraction 20-30 kDa**



**Figure 4-6 Time-activity curves for  $^{99m}\text{Tc}$ -PEI-MP MW-fraction 20-30 kDa (n=1)**



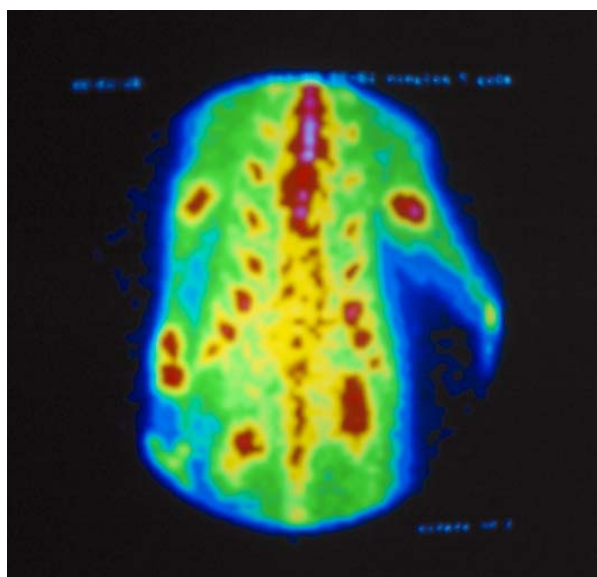
**Table 4-6 Pharmacokinetic data for various compartments for dogs receiving  $^{99m}\text{Tc}$ -PEI-MP 20-30 kDa (n=4)**

Compartment Parameter		Cardiac	Lung	Liver	Left kidney	Right kidney	Trab. Bone	Cort. Bone	BG	Blood
$T_{1/2}$ (min)	Mean±SD	3.13± 0.75	5.13±0.75	17.78±7.86	8.87±1.70	9.50±0.57	90.00±60.00	90.00±60.00	18.5±4.65	10.60±1.34
$T_{\max}$ (min)	Mean±SD	0.00	0.00	1.00	1.60±	2.00	12.75±13.09	16.66±12.85	1.50±0.57	0.00
%OD at 3hours	Mean±SD	13.47±1.66	8.58±1.24	9.13±0.29	14.50±1.91	12.87±1.21	19.93±4.75	4.61±3.73	5.35±2.14	-

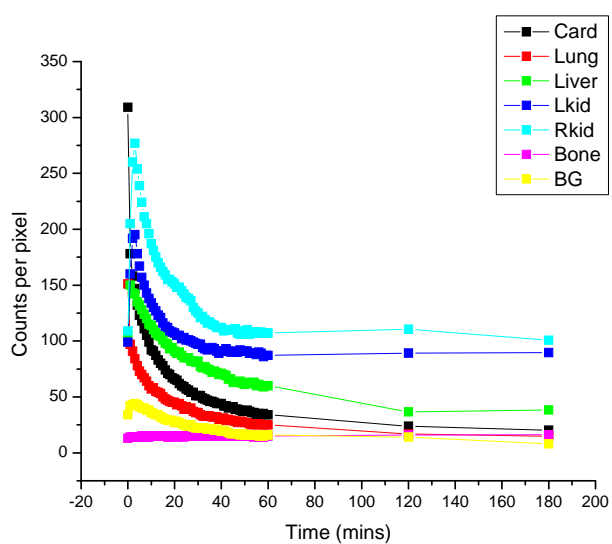
Legend: The results from MW-fraction  $^{99m}\text{Tc}$ -PEI-MP 20-30 kDa are in keeping with what was considered the ideal radiopharmaceutical i.e., a molecule that is cleared from the central compartment at a rate slightly slower than  $^{153}\text{Sm}$ -EDTMP (see pages 121 - 128 of Section 3.6) with some bone, renal and liver retention at 3-hours. This is stark in contrast to the larger MW-fractions of PEI-MP where significant liver and kidney retention was evident. In order to use this data for comparative purposes with MW-fraction 10-30 kDa, five dogs underwent dynamic scans.

4.4.5.4 Biodistribution data from normal dogs (n=4) receiving  $^{99m}\text{Tc}$ -PEI-MP MW-fraction 10-30 kDa

**Figure 4-7 Scintigraphic image showing biodistribution data from a normal (n=1) dog receiving  $^{99m}\text{Tc}$ -PEI-MP MW-fraction 10-30 kDa**



**Figure 4-8 Time-activity curve for  $^{99m}\text{Tc}$ -PEI-MP 10-30 kDa (n=1)**



**Table 4-7 Pharmacokinetic data for various compartments for dogs receiving  $^{99m}\text{Tc}$ -PEI-MP 10-30 kDa (n=4)**

Compartment Parameter		Cardiac	Lung	Liver	Lkid	Rkid	Cort. bone	Trab. bone	BG	Blood
$T_{1/2}$ (min)	Mean±SD	6.25±0.50	9.00±1.83	15.59±1.70	12.25±1.70	13.50±1.73	54.75±6.70	54.75±6.70	27.50±9.46	20±17.32
$T_{max}$ (min)	Mean±SD	0.00	0.00	1.00	2.00±00	2.00±00	4.00±4.83	4.00±4.80	3.25±3.20	0.00
%OD at 3hours	Mean±SD	13.47±4.64	11.72±5.67	10.39±5.53	19.77±7.65	18.37±13.59	8.66±1.80	11.62±6.10	4.10±3.04	-

Legend: While the results from MW-fraction  $^{99m}\text{Tc}$ -PEI-MP 10-30 kDa are in keeping with what was considered the ideal radiopharmaceutical i.e., a molecule that is cleared from the central compartment at a rate slightly slower than  $^{153}\text{Sm}$ -EDTMP (see pages 121 - 128) with some bone, renal and liver retention at 3-hours. The retention in both kidneys (see light and dark blue TAC in Figure 4-8 on page 227 ) appears higher than for the  $^{99m}\text{Tc}$ -PEI-MP 20-30 kDa MW-fraction and is the subject further investigation in Section 4.4.6 on page 231.

4.4.5.5 Biodistribution data from a normal dog receiving  $^{99m}\text{Tc}$ -PEI-MP MW-fraction 3-10 kDa (n=1)

Figure 4-9 Time-activity curves for  $^{99m}\text{Tc}$ -PEI-MP 3-10 kDa (n=1)

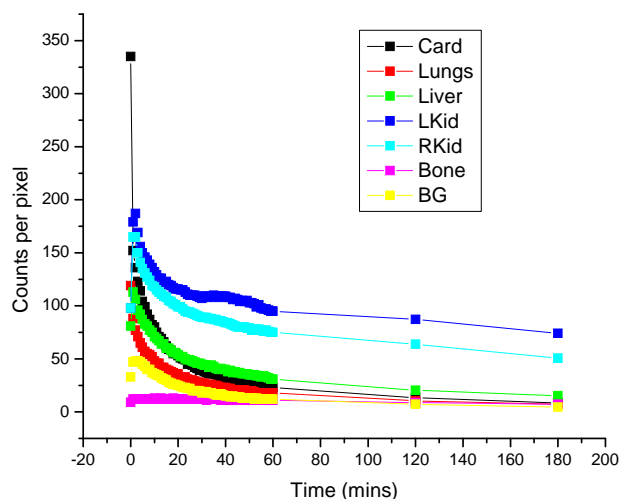


Table 4-8 Pharmacokinetic data for various compartments for a dog receiving  $^{99m}\text{Tc}$ -PEI-MP 3-10 kDa (n=1)

Compartment Parameter	Cardiac	Lung	Liver	Left kidney	Right kidney	Trabec bone	Cortical Bone	BG	Blood
$T_{1/2}$ (min)	<1.00	5.00	20.00	>180.00	60.00	-	>180.00	23.00	10.00
$T_{max}$ (min)	0.00	0.00	1.00	2.00	2.00	-	1.00	2.00	3.00
% OD at 3 hr's	5.00	4.00	9.00	44.00	30.00	-	4.36	2.70	0.00

Legend: The results from the MW-fraction  $^{99m}\text{Tc}$ -PEI-MP 3-10 kDa did not show any improvement over the MW-fractions 10-30 kDa or 20-30 kDa with regard to organ retention. Indeed the retention 44% - 30% OD in both kidneys were higher when compared to 10-30kDa (21%) or 20-30 kDa (14%).

#### 4.4.5.6 Urine activity for various MW-fractions of $^{99m}\text{Tc}$ -PEI-MP

**Table 4-9 Pharmacokinetic data for various  $^{99m}\text{Tc}$ -PEI-MP MW-fractions in urine**

MW-fraction	3-10 kDa (n=1)	10-30 kDa (mean±SD) (n=4)	20-30 kDa (mean±SD) (n=4)	30-50 kDa (n=2)	50-100 kDa (n=2)
<b>Urine parameter</b>					
% ID eliminated at 3-hours	70.56	69.75±3.45	73.91±1.80	(-)61.79 (+)45.34	(-)37.66 (+)54.68
Time to 50% elimination of ID in urine (min)	20	51±10.40	36±6.52	(-)25 (+)27	(-)20 (+)35

Legend: The % ID eliminated in urine for various  $^{99m}\text{Tc}$ -PEI-MP MW-fractions varied between fractions with the 20-30 kDa having the highest clearance of the radiopharmaceutical. This is consistent with hypothetically ideal radiopharmaceutical. The smaller MW-fractions when compared to the fractions >30 kDa the trend was for more clearance of the smaller fractions, especially when compared to the positively charged >30 kDa MW-fractions. This is consistent with the normal physiology of the kidney where large cations would be retained in the kidney.

#### 4.4.5.7 Blood activity for various MW-fractions of $^{99m}\text{Tc}$ -PEI-MP

**Table 4-10 Pharmacokinetic data for various  $^{99m}\text{Tc}$ -PEI-MP MW-fractions in blood**

MW-fraction	3-10 kDa (n=1)	10-30 kDa (mean±SD) (n=4)	20-30 kDa (mean±SD) (n=4)	30-50 kDa (n=2)	50-100 kDa (n=2)
<b>Blood parameter</b>					
$T_{1/2}$ (min)	10.00	20.00±17.32	10.60±1.34	(-)10.00 (+)10.00	(-)7.00 (+)10.00
% ID at 3 hr's	0.00	4.33±0.58	1.80±1.5	(-)3.64 (+)1.27	(-)16.10 (+)0.404

Legend: The blood  $T_{1/2}$  (min) for all MW-fractions were closely grouped, except for the 10-30 kDa MW-fraction. However, the wide SD of the 10-30 kDa makes comparison difficult between fractions. The % ID at 3-hours for the MW-fractions <50 kDa is indicative of rapid clearance of the MW-fraction from the blood into other compartments.

Based on the results from the normal dogs and comparing them with the primate studies by Dormehl *et al.*, 2001<sup>21</sup>, it was apparent that only two MW-fractions 10-30 and 20-30 kDa were potentially ideal ligands for labelling to beta-emitting radioisotopes. The other MW-fractions were excluded based on prolonged liver, kidney, and blood pool retention.

Consequently, these data were analysed further to decide on the optimal molecular weight of macromolecule, see Section 4.4.6 below.

#### 4.4.6 Statistical comparison between $^{99m}\text{Tc}$ -PEI-MP MW-fractions 10-30 and 20-30 kDa

##### 4.4.6.1 Data Analysis

The pharmacokinetic parameters (e.g.,  $T_{1/2}$ ,  $T_{max}$  and %OD at 3hours) from the  $^{99m}\text{Tc}$ -PEI-MP MW-fraction 10-30 (n=4) and 20-30 kDa (n=5) were compared using One-Way ANOVA. For nonparametric data, an ANOVA on Ranks was used. Statistical significance was set for  $P = 0.05$ . The following compartments were compared; cardiac, lung, liver, left kidney, right kidney, trabecular and cortical bone, and background (soft-tissue). Raw data for both MW-fractions used for statistical analyses were recorded and can be seen in the Appendix, Table 8-28 on page 317. Since both MW-fractions apparently display similar pharmacokinetics, the objective of this statistical comparison was to identify the MW-fraction likeliest to fulfil the criteria of an ideal ligand.

##### 4.4.6.2 Statistical results comparing $^{99m}\text{Tc}$ -PEI-MP MW-fractions 10-30 and 20-30 kDa

**Table 4-11 Statistical comparison of pharmacokinetic data from  $^{99m}\text{Tc}$ -PEI-MP MW-fractions 10-30 (n=4) and 20-30 kDa (n=4) for the cardiac compartment**

MW-fraction	10-30 kDa (mean±SD)	20-30 kDa (mean±SD)	<i>P</i> Value ( $P < 0.05$ )
Cardiac Parameter			
$T_{1/2}$ (min)	6.25±0.50	3.13± 0.75	<b><i>P</i> = 0.001</b>
$T_{max}$ (min)	0	0	-
% OD at 3-hours	13.59±4.64	13.47±1.66	<i>P</i> = 0.96

Legend: Statistical significance was found between MW-fractions for cardiac  $T_{1/2}$ . The 10-30 kDa MW-fraction had a statistically longer  $T_{1/2}$  then the 20-30 kDa fraction.

**Table 4-12 Statistical comparison of pharmacokinetic data from  $^{99m}\text{Tc}$ -PEI-MP MW-fractions 10-30 and 20-30 kDa for blood**

MW-fraction	10-30 kDa (mean±SD)	20-30 kDa (mean±SD)	<i>P</i> Value ( $P < 0.05$ )
Blood parameter			
$T_{1/2}$ (min)	20±17.321	10.6±1.34	<i>P</i> = 0.248
$T_{max}$ (min)	0	0	
% ID at 3-hours	4.33±0.58	1.8±1.5	<b><i>P</i> = 0.031</b>

Legend: Statistical significance differences was found between MW-fractions for the percentage ID at 3-hour in blood. Since the cardiac compartment is considered a reflection of the activity in blood, both parameters reflect the more prolonged cardiac washout phase ( $T_{1/2}$ ) and increased retention of the % ID at 3-hour for 10-30kDa MW-fraction compared to the 20-30kDa MW-fraction.

**Table 4-13 Statistical comparison of pharmacokinetic data from  $^{99m}\text{Tc}$ -PEI-MP MW-fractions 10-30 and 20-30 kDa for the lung compartment**

MW-fraction	10-30 kDa (mean $\pm$ SD)	20-30 kDa (mean $\pm$ SD)	<i>P</i> Value ( <i>P</i> < 0.05)
Lung Parameter			
$T_{1/2}$ (min)	9.00 $\pm$ 1.83	5.13 $\pm$ 0.75	<b><i>P</i> = 0.008</b>
$T_{\text{max}}$ (min)	0	0	-
% OD at 3-hours	11.727 $\pm$ 5.67	8.58 $\pm$ 1.24	<i>P</i> = 0.256

Legend: Statistical analysis of pharmacokinetic parameter for lungs show a longer washout phase ( $T_{1/2}$ ) in the lung for the 10-30 kDa MW-fraction. However, the percentage OD at 3-hours was not statistically different

**Table 4-14 Statistical comparison of pharmacokinetic data from  $^{99m}\text{Tc}$ -PEI-MP MW-fractions 10-30 and 20-30 kDa for the liver compartment**

MW-fraction	10-30 kDa (mean $\pm$ SD)	20-30 kDa (mean $\pm$ SD)	<i>P</i> Value ( <i>P</i> < 0.05)
Liver Parameter			
$T_{1/2}$ (min)	15.29 $\pm$ 1.70	17.78 $\pm$ 7.86	<i>P</i> = 0.60
$T_{\text{max}}$ (min)	1	1	-
% OD at 3-hours	10.39 $\pm$ 5.34	9.13 $\pm$ 0.29	<i>P</i> = 0.65

Legend: Analysis of pharmacokinetic parameters for liver did not identify statistical differences between MW-fractions.

**Table 4-15 Statistical comparison of pharmacokinetic data from  $^{99m}\text{Tc}$ -PEI-MP MW-fractions 10-30 and 20-30 kDa for the left kidney compartment**

MW-fraction	10-30 kDa (mean $\pm$ SD)	20-30 kDa (mean $\pm$ SD)	<i>P</i> Value ( <i>P</i> < 0.05)
Left Kidney Parameter			
$T_{1/2}$	12.25 $\pm$ 1.70	8.87 $\pm$ 0.85	<b><i>P</i> = 0.012</b>
$T_{\text{max}}$	2 $\pm$ 0	1.6 $\pm$ 0.5	<i>P</i> = 0.134
% OD at 3-hours	19.77 $\pm$ 7.65	14.50 $\pm$ 1.91	<i>P</i> = 0.230

Legend: Statistical analysis of the pharmacokinetic parameters for the left kidney showed a longer washout phase ( $T_{1/2}$ ) in the kidney for the 10-30 kDa MW-fraction. Although the % OD was not statistically different between MW-fractions.

**Table 4-16 Statistical comparison of pharmacokinetic data from  $^{99m}\text{Tc}$ -PEI-MP MW-fractions 10-30 and 20-30 kDa for the right kidney compartment**

MW-fraction	10-30 kDa (mean $\pm$ SD)	20-30 kDa (mean $\pm$ SD)	<i>P</i> Value ( <i>P</i> < 0.05)
Right Kidney Parameter			
$T_{1/2}$	13.50 $\pm$ 1.73	9.50 $\pm$ 0.57	<b><i>P</i> = 0.005</b>
$T_{\text{max}}$	2 $\pm$ 2	2 $\pm$ 1.75	<i>P</i> = 0.786
% OD at 3-hours	18.37 $\pm$ 13.59	12.87 $\pm$ 1.21	<i>P</i> = 0.451



Legend: Statistical analysis of the pharmacokinetic parameters for the right kidney showed a longer washout phase ( $T_{1/2}$ ) in the kidney for the 10-30 kDa MW-fraction.

**Table 4-17 Statistical comparison of pharmacokinetic data from  $^{99m}\text{Tc}$ -PEI-MP MW-fractions 10-30 and 20-30 kDa for urine**

MW-fraction	10-30 kDa (mean±SD)	20-30 kDa (mean±SD)	<i>P</i> Value ( <i>P</i> < 0.05)
Urine parameter			
% of ID eliminated at 3-hours	69.75±3.45	73.91±1.80	<b><i>P</i> = 0.01</b>
Time to 50% elimination (min)	51±10.40	36±6.52	<b><i>P</i> = 0.04</b>

Legend: Analysis of pharmacokinetic parameter for urine did identify statistical differences between MW-fractions, these were; the percentage ID at 3-hours and elimination rate (time to 50% elimination of ID). The 10-30 kDa had slower elimination rate compared to the 20-30kDa MW-fraction.

**Table 4-18 Statistical comparison of pharmacokinetic data from  $^{99m}\text{Tc}$ -PEI-MP MW-fractions 10-30 and 20-30 kDa for the cortical bone compartment**

MW-fraction	10-30 kDa (mean±SD)	20-30 kDa (mean±SD)	<i>P</i> Value ( <i>P</i> < 0.05)
Cortical bone Parameter			
$T_{1/2}$ (min)	54.75±6.70	90.00±60.00	<i>P</i> = 0.287
$T_{\text{max}}$ (min)	4.00±4.83	16.66±12.85	<i>P</i> = 0.123
% OD at 3-hours	8.66±1.80	4.61±3.73	<i>P</i> = 0.149

Legend: Analysis of pharmacokinetic parameters for cortical bone did not identify statistical differences between MW-fractions

**Table 4-19 Statistical comparison of pharmacokinetic data from  $^{99m}\text{Tc}$ -PEI-MP MW-fractions 10-30 and 20-30 kDa for the trabecular bone compartment**

MW-fraction	10-30 kDa (mean±SD)	20-30 kDa (mean±SD)	<i>P</i> Value ( <i>P</i> < 0.05)
Trab. bone Parameter			
$T_{1/2}$ (min)	54.75±6.70	90.00±60.00	<i>P</i> = 0.442
$T_{\text{max}}$ (min)	4.00±4.80	12.75±13.09	<i>P</i> = 0.257-
% OD at 3-hours	11.62±6.10	19.93±4.75	<i>P</i> = 0.075

Legend: Analysis of pharmacokinetic parameters for cortical bone did not identify statistical differences between MW-fractions. Nevertheless the 10-30 kDa MW-fraction trended towards significance (*P* = 0.075) with lower percentage OD at 3-hours than 20-30kDa MW-fraction. This could be significant when the dose of radiation to the bone marrow is calculated, see Chapter 5 on page 256.

**Table 4-20 Statistical comparison of pharmacokinetic data from  $^{99m}\text{Tc}$ -PEI-MP MW-fractions 10-30 and 20-30 kDa for the background (soft-tissue) compartment**

MW-fraction Background Parameter	10-30 kDa (mean $\pm$ SD)	20-30 kDa (mean $\pm$ SD)	<i>P</i> Value ( <i>P</i> < 0.05)
$T_{1/2}$ (min)	27.50 $\pm$ 9.46	18.50 $\pm$ 4.65	<i>P</i> = 0.139
$T_{\text{max}}$ (min)	3.25 $\pm$ 3.20	1.50 $\pm$ 0.57	<i>P</i> = 0.323
% OD at 3-hours	4.10 $\pm$ 3.04	5.35 $\pm$ 2.14	<i>P</i> = 0.528

Legend: Analysis of pharmacokinetic parameters for background did not identify statistical differences between MW-fractions.

Based on the results of the statistical evaluation between the two PEI-MP MW-fractions, the MW-fraction 20-30 kDa was considered the ideal radiopharmaceutical because of its rapid clearance from central compartment and the body (urine). Nevertheless, due to technical difficulties associated with significantly lower ultrafiltration yield (see Table 4-2, on page 218) of the 20-30kDa MW-fraction, the MW-fraction 10-30 kDa was considered acceptable because of similar pharmacokinetic results. Consequently, for further investigations the MW-fraction 10-30 kDa was used for dogs with osteosarcoma and for labelling to the therapeutic radionuclide,  $^{153}\text{Sm}$ . See sections 4.5 below and 4.6 on page 238.

#### **4.5 Materials methods for a dynamic scintigraphic $^{99m}\text{Tc}$ -PEI-MP (10-30 kDa) study in a dog with osteosarcoma**

##### 4.5.1 Experimental design

The dog, Case-14 from the earlier  $^{153}\text{Sm}$ -EDTMP study underwent a scintigraphic study using  $^{99m}\text{Tc}$ -PEI-MP (10-30 kDa) prior to receiving a therapeutic dose of  $^{153}\text{Sm}$ -EDTMP. For more detailed description of the dog, see the Section 8.5 of the Appendix, Table 8-15 on page 291. Table 4-21 on page 235 gives a summary of the dog's details. Owner's signed consent was required to conduct the experiment. The dog was subjected to identical experimental procedures as mentioned for normal dogs receiving  $^{99m}\text{Tc}$ -PEI-MP. Briefly, the animal was placed in a supine position under the gamma camera (Siemens Orbital Camera) and was injected IV. with a bolus dose of 425.9 MBq of  $^{99m}\text{Tc}$ -PEI-MP (10-30 kDa) and data acquisition started on a countdown with a Siemens Orbiter gamma camera in 64 x 64 word mode performing a 60 min dynamic study (60 x 1 min frames), followed by a static scan every hour for the next 3 hours. Blood and urine samples were collected at fixed intervals for

four hours, viz. every three min for the first hour, then hourly for blood samples and urine every five min for the first hour, subsequently hourly. The activity and volume of each sample were recorded.

**Table 4-21 The population characteristics of the osteosarcoma dog Case-14**

Case	PEI-MP fraction	Breed	Age (yrs.)	Mass (kg)	Sex	Site	T	NTC	PEI-MP T/NTC ratio
14	10 to 30	Cross Saint Bernard	10	47	F	Distal radius	32.68	7.11	4.6

Legend: Case-14 had an osteosarcoma of the distal radius with a T/NTC ratio for  $^{153}\text{Sm}$ -EDTMP of 2.04. This was an unusual finding since it would be expected that  $^{153}\text{Sm}$ -EDTMP would have a better uptake ratio compared to  $^{99\text{m}}\text{Tc}$ -PEI-MP MW-fraction 10-30 kDa.

#### 4.5.2 Data Analysis

Data was collected and analysed as previously described in the data processing and acquisition section 2.1.2.6 on page 100. Figure 3-2 on page 117 describes the ROI selection for all studies.



**Table 4-22 Pharmacokinetic results for various compartments in the osteosarcoma dog receiving  $^{99m}\text{Tc}$ -PEI-MP 10-30 kDa**

Compartment Parameter	Cardiac	Lung	Liver	Left kidney	Right kidney	Trabecular Bone	BG	Tumour
$T_{1/2}$ (min)	5	4.5	13	11	11	>180 min	22	>180 min
$T_{\max}$ (min)	0	0	1	2	2	>180 min	1	>180 min
% OD at 3 hr's	14.91	11.05	10.96	9.75	10.7	6.58	5.8	30.25

Legend: Analyses of the TAC and scintigraphy for the osteosarcoma dog receiving the 10-30 kDa MW-fraction, shows enhanced tumour uptake when compared to normal bone (see the brown and purple TAC curves in Figure 4-10 on page 236). The %OD at 3 hours for the tumour was 30.25% compared to normal bone at 6.58% resulting in a T/NTC uptake ratio of 4.6:1. The other pharmacokinetic results are similar to those found previously for the normal dog's receiving the 10-30 kDa MW-fraction. The cortical bone compartment was not recorded because very uptake, see Figure 4-11 on page 236.

**Table 4-23 Pharmacokinetic data for blood for osteosarcoma dog  $^{99m}\text{Tc}$ -PEI-MP 10-30 kDa**

Blood parameter	MW-fraction	10-30 kDa
$T_{1/2}$ (min)		10
$T_{\max}$ (min)		0
% ID at 3 hr's		1.74

Legend: The blood pharmacokinetic 10-30 kDa MW-fraction data for the osteosarcoma dog when compared to normal dogs is similar. The lower 1.74% ID at 3 hours found in the osteosarcoma dog compared to the 4.33% ID in normal dogs could be explained by the rapid and continuing uptake of the radiopharmaceutical by the tumour.

**Table 4-24 Pharmacokinetic data for cumulative urine clearance in an osteosarcoma dog receiving  $^{99m}\text{Tc}$ -PEI-MP 10-30 kDa**

Urine parameter	MW-fraction	10-30 kDa
% of ID eliminated at 3-hours		85.74
Time to 50% elimination (min)		40

Legend: The diseased dog eliminated 86% of the ID within 3-hours. This is comparable with the normal dog study for the 20-30kDa MW-fraction size. This could be explained by the variation between animals but is certainly higher than the 44% for  $^{153}\text{Sm}$ -EDTMP dogs (Table 3-19 on page 132) and the 52% for  $^{188}\text{Re}$ -HEDP percentage ID in urine at 3-hours (Table 3-30 on page 145). This characteristic combined with the 4.5:1 uptake ratio in the tumour and the low %OD in bone (compared to  $^{153}\text{Sm}$ -EDTMP) supported the use of the PEI-

MP 10-30kDa MW-fraction as a suitable radiopharmaceutical for further studies complexed to  $^{153}\text{Sm}$ .

#### 4.6 Materials and methods for MW-fraction 10-30 kDa complexed to $^{153}\text{Sm}$

##### 4.6.1 Radiolabelling of PEI-MP MW-fraction 10-30 kDa with $^{153}\text{Sm}$

$^{153}\text{Sm}$ -PEI-MP was prepared as described by Jarvis *et al*<sup>1</sup> (Radiochemistry department, NECSA). The product was further prepared for *in vivo* administration to conform with quality control standards for radiopharmaceutical preparations<sup>219</sup>.

##### 4.6.2 Model System and Sample Size

Four healthy German shepherd dogs with a mean $\pm$ SD weight of 28.95 $\pm$ 4.03 kg, were used in the study. Each dog received a tracer dose of  $^{153}\text{Sm}$ -PEI-MP 10-30 kDa as reported in Table 4-25 below.

**Table 4-25 List of normal dogs (n=4) used in experimental procedures for  $^{153}\text{Sm}$ -PEI-MP 10-30 kDa**

Dogs	Breed	Body Weight (kg)	Sex	Dose injected MBq	MW-fraction kDa	Charge
1	GSD	27	M	123.21	10 to 30	neutral
2	GSD	27	M	236.06	10 to 30	neutral
3	GSD	26.8	M	159.1	10 to 30	neutral
4	GSD	35	M	425.87	10 to 30	neutral

##### 4.6.3 Experimental Design and Experimental Procedures

The dogs underwent identical experimental procedures as described for  $^{99\text{m}}\text{Tc}$ -PEI-MP MW-fractions; see section 4.4.3 on page 219. The tracer dose of  $^{153}\text{Sm}$ -PEI-MP 10-30 kDa given to each individual dog was recorded and reported in Table 4-25 above.

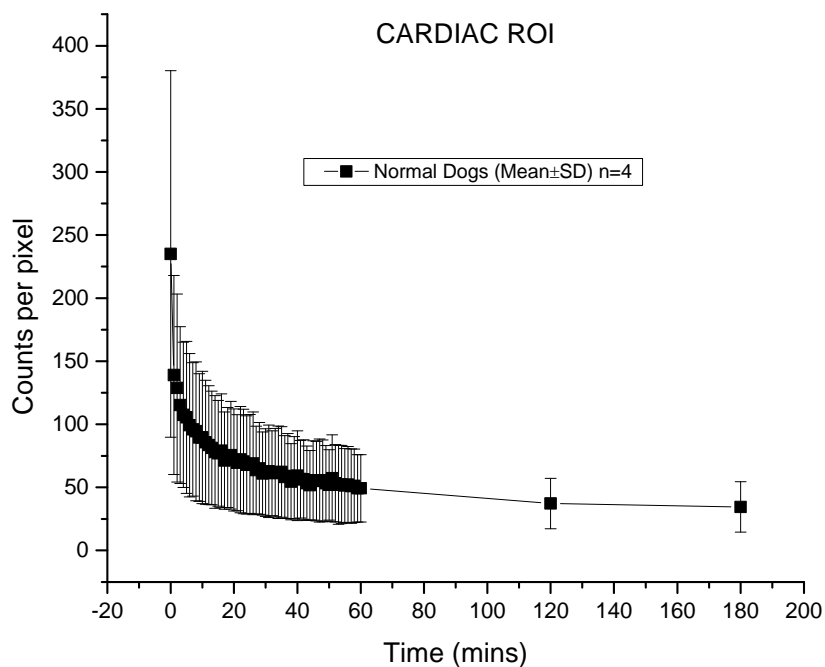
##### 4.6.4 Data Analysis

All data analysis were identical as previously described for dogs receiving  $^{99\text{m}}\text{Tc}$ -PEI-MP MW-fractions; see section 4.4.4 on page 220. Data was recorded and can be found in the Appendix; see Table 8-26 on page 315, and Table 8-27 on page 316.

4.6.5 Results from normal dogs (n=4) receiving  $^{153}\text{Sm}$ -PEI-MP 10-30 kDa MW-fraction

4.6.5.1 Biodistribution data for the cardiac blood-pool in normal dogs (n=4) receiving  $^{153}\text{Sm}$ -PEI-MP 10-30 kDa

**Figure 4-12: Time-activity curves for the cardiac ROI in normal dogs  $^{153}\text{Sm}$ -PEI-MP (10-30 kDa) (n=4)**



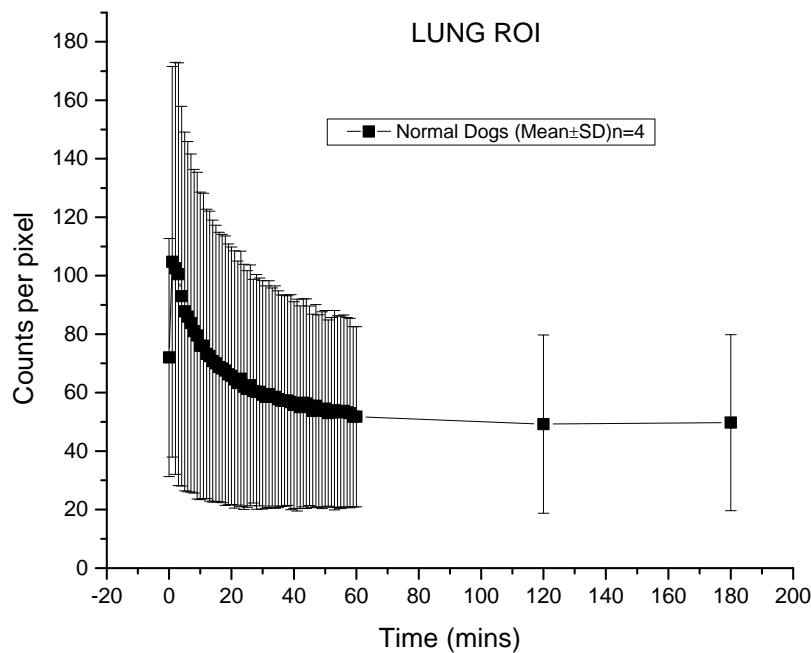
**Table 4-26: Pharmacokinetic mean±SD of the cardiac compartment in normal dogs given  $^{153}\text{Sm}$ -PEI-MP (10-30 kDa)**

Compartment	Pharmacokinetic parameter	Mean±SD
Cardiac	$T_{1/2}$ (min)	3.0±2.00
	$T_{max}$ (min)	0
	% OD at 3 hr's	15.46±0.51

Legend: Analyses of the TAC for the cardiac compartment (aka. cardiac pool) followed first-order pharmacokinetics and presented similar data as for normal dogs that received  $^{99m}\text{Tc}$ -PEI-MP MW-fraction 10-30 kDa (see Figure 4-12 above).

4.6.5.2 Biodistribution data for the lung ROI in normal (n=4) receiving  $^{153}\text{Sm}$ -PEI-MP 10-30 kDa

**Figure 4-13 Time-activity curves for the lung ROI in normal dogs receiving  $^{153}\text{Sm}$ -PEI-MP (10-30 kDa)**



**Table 4-27: Pharmacokinetic mean±SD of the lung compartment in normal dogs given  $^{153}\text{Sm}$ -PEI-MP (10-30 kDa)**

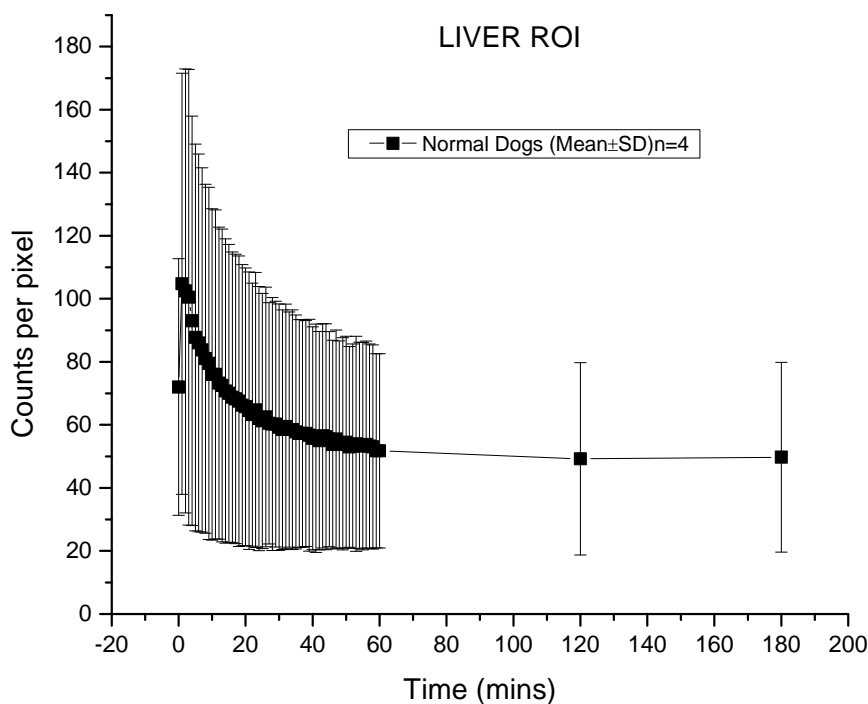
Compartment	Pharmacokinetic parameter	Mean±SD
Lungs	$T_{1/2}$ (min)	$14.5 \pm 7.41$
	$T_{max}$ (min)	0
	% OD at 3 hr's	$11.13 \pm 1.89$

Legend: Analysis of the TAC for the lung ROI found the data were similar for the data from normal dogs that received  $^{99m}\text{Tc}$ -PEI-MP 10-30 kDa



4.6.5.3 Biodistribution data for the liver ROI in normal dogs (n=4) receiving  $^{153}\text{Sm}$ -PEI-MP 10-30 kDa

**Figure 4-14 Time-activity curves for the liver ROI in normal dogs receiving  $^{153}\text{Sm}$ -PEI-MP (10-30 kDa)**



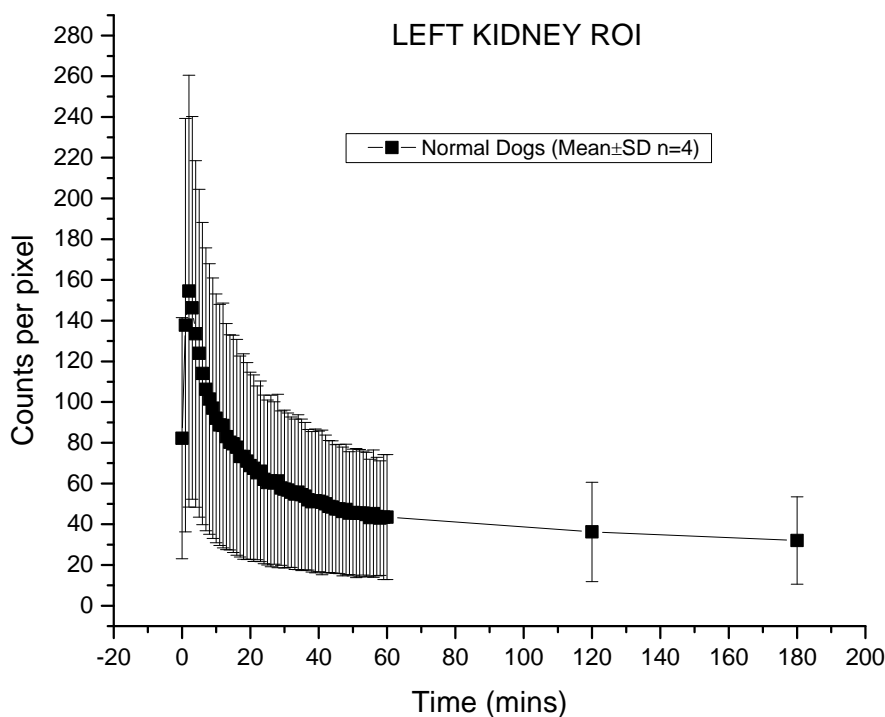
**Table 4-28: Pharmacokinetic mean±SD of the liver compartment in normal dogs given  $^{153}\text{Sm}$ -PEI-MP (10-30 kDa)**

Compartment	Pharmacokinetic parameter	Mean ±SD
Liver	Mean	
	$T_{1/2}$ (min)	43.0 ±4.58
	$T_{max}$ (min)	1.5±1.00
	% OD at 3 hr's	21.68±6.03

Legend: The polymer MW-fraction 10-30 kDa PEI-MP labelled either to  $^{99m}\text{Tc}$  or  $^{153}\text{Sm}$  shows moderate retention in the liver of normal dogs compared to the 7.79 % OD (Table 3-11 on page 124) and 14.25 % OD (Table 3-22 on page 137) at 3-hours in the liver of dogs receiving  $^{153}\text{Sm}$ -EDTMP and  $^{188}\text{Re}$ -HEDP respectively.

4.6.5.4 Biodistribution data for the left kidney ROI in normal dogs (n=4) receiving  $^{153}\text{Sm}$ -PEI-MP 10-30 kDa

**Figure 4-15 Time-activity curves for the left kidney ROI in normal dogs receiving  $^{153}\text{Sm}$ -PEI-MP (10-30 kDa)**



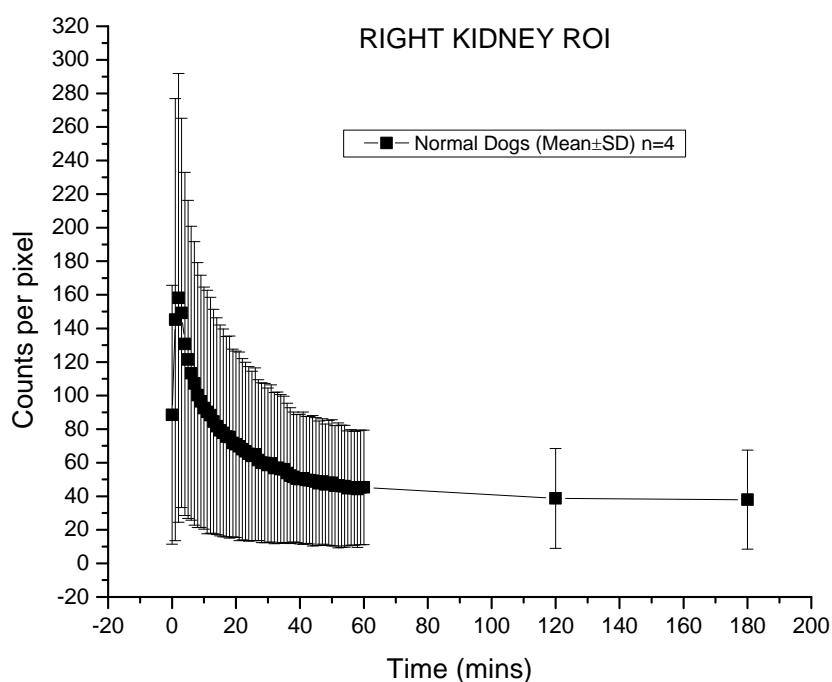
**Table 4-29: Pharmacokinetic mean±SD of the left kidney compartment in normal dogs given  $^{153}\text{Sm}$ -PEI-MP (10-30 kDa)**

Compartment	Pharmacokinetic parameter	Mean±SD
Left kidney	$T_{1/2}$ (min)	16±0.82
	$T_{max}$ (min)	2.5± 0.57
	% OD at 3 hr's	13.7±1.79

Legend: The analysis of the TAC for the left kidney  $T_{1/2}$  in dogs receiving  $^{153}\text{Sm}$ -PEI-MP (10-30 kDa) was similar to dogs receiving MW-fractions 10-30 kDa or 20-30 kDa of  $^{99m}\text{Tc}$ -PEI-MP, see Table 4-15 on page 232. The OD was also similar at 13.7% compared to 19.77% and 14.50% for  $^{99m}\text{Tc}$ -PEI-MP MW-fractions 10-30 kDa and 20-30 kDa respectively.

4.6.5.5 Biodistribution data for the right kidney ROI in normal dogs (n=4) receiving  $^{153}\text{Sm}$ -PEI-MP 10-30 kDa

**Figure 4-16 Time-activity curves for the right kidney ROI in normal dogs receiving  $^{153}\text{Sm}$ -PEI-MP (10-30 kDa)**



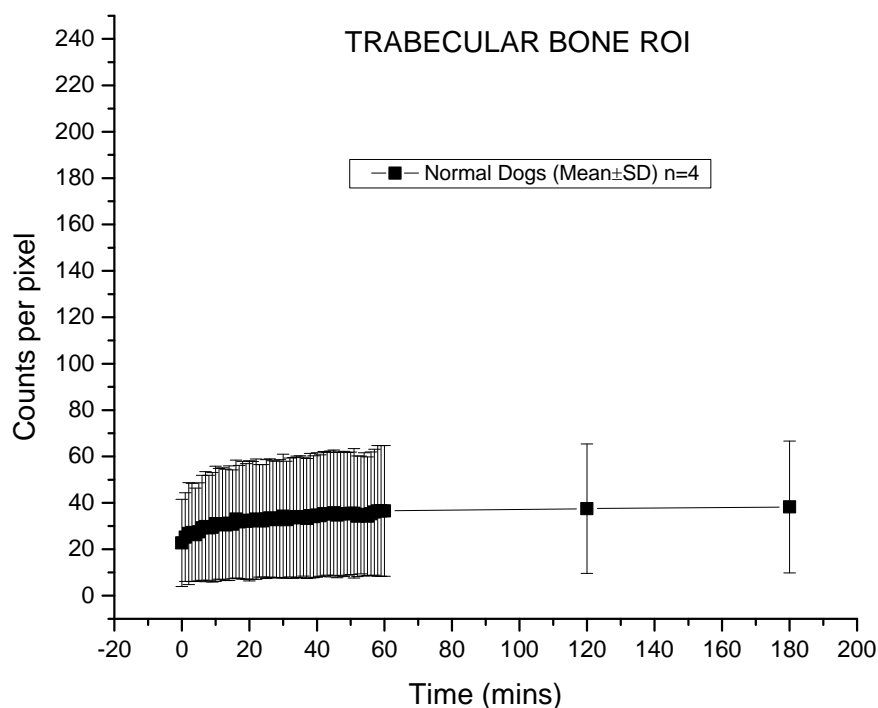
**Table 4-30: Pharmacokinetic mean±SD of the right kidney compartment in normal dogs given  $^{153}\text{Sm}$ -PEI-MP (10-30 kDa)**

Compartment	Pharmacokinetic parameter	Mean±SD
Right kidney	$T_{1/2}$ (min)	15.25 ±2.21
	$T_{max}$ (min)	2.5 ±0.57
	% OD at 3 hr's	14.55±3.31

Legend: Analogous to the left kidney, study of the TAC for the right kidney ROI found the data were similar to the data from normal dogs that received MW-fractions  $^{99m}\text{Tc}$ -PEI-MP 10-30 kDa and 20-30 kDa, see Table 4-16 on page 232.

4.6.5.6 Biodistribution data for the cardiac blood-pool in normal dogs (n=4) receiving  $^{153}\text{Sm}$ -PEI-MP 10-30 kDa

**Figure 4-17 Time-activity curves for the trabecular bone ROI in normal dogs receiving  $^{153}\text{Sm}$ -PEI-MP (10-30 kDa)**



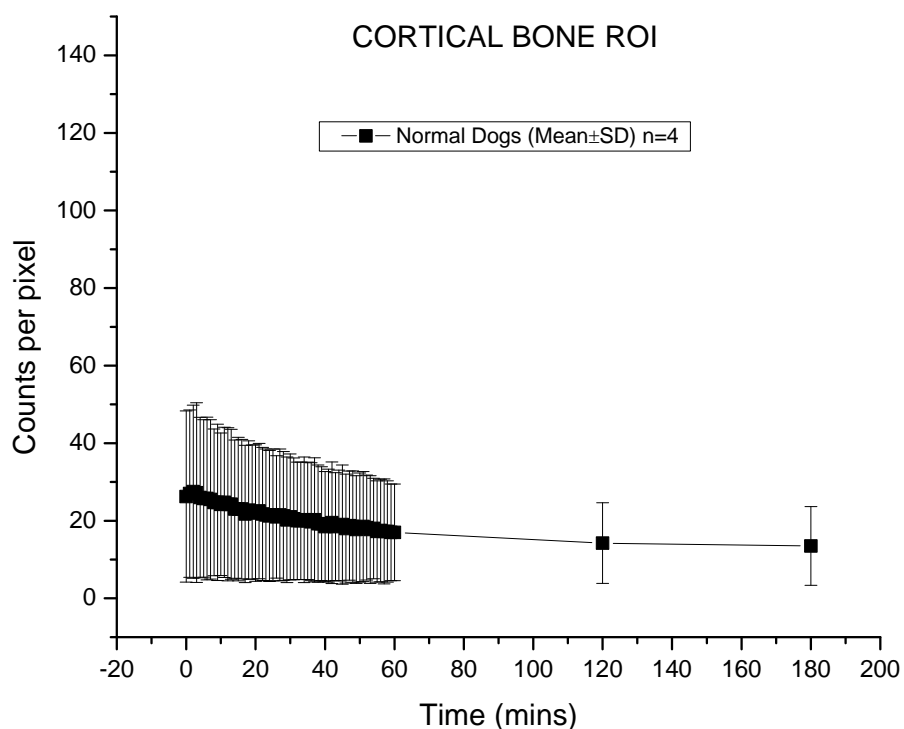
**Table 4-31: Pharmacokinetic mean±SD of the trabecular bone compartment in normal dogs given  $^{153}\text{Sm}$ -PEI-MP (10-30 kDa)**

Compartment	Pharmacokinetic parameter	Mean±SD
Trabecular Bone	$T_{1/2}$ (min)	>180
	$T_{max}$ (min)	>180
	% OD at 3 hr's	14.28 ±2.91

Legend: Analysis of the TAC for trabecular bone found the data were similar to the data from normal dogs that received MW-fractions  $^{99m}\text{Tc}$ -PEI-MP 10-30 kDa and 20-30 kDa; see Table 4-19 on page 233.

4.6.5.7 Biodistribution data for the cortical bone ROI in normal dogs (n=4) receiving  $^{153}\text{Sm}$ -PEI-MP 10-30 kDa

**Figure 4-18 Time-activity curves for the cortical bone ROI in normal dogs receiving  $^{153}\text{Sm}$ -PEI-MP (10-30 kDa)**



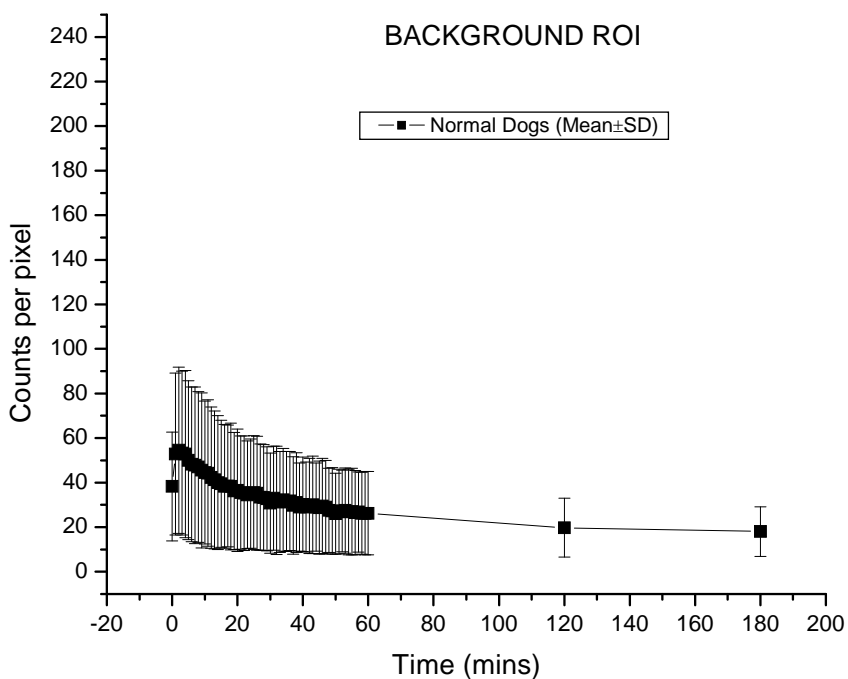
**Table 4-32: Pharmacokinetic mean±SD of the cortical compartment in normal dogs given  $^{153}\text{Sm}$ -PEI-MP (10-30 kDa)**

Compartment	Mean	Mean±SD
Cortical Bone	$T_{1/2}$ (min)	150 ±42.42
	$T_{max}$ (min)	1.5 ±1
	% OD at 3 hr's	5.29±1.29

Legend: Analysis of the TAC for cortical bone found the data were similar to the data from normal dogs that received MW-fractions  $^{99m}\text{Tc}$ -PEI-MP 10-30 kDa and 20-30 kDa; see Table 4-18 on page 233.

4.6.5.8 Biodistribution data for the background in normal dogs (n=4) receiving  $^{153}\text{Sm}$ -PEI-MP 10-30 kDa

**Figure 4-19 Time-activity curves for the background ROI in normal dogs receiving  $^{153}\text{Sm}$ -PEI-MP (10-30 kDa)**



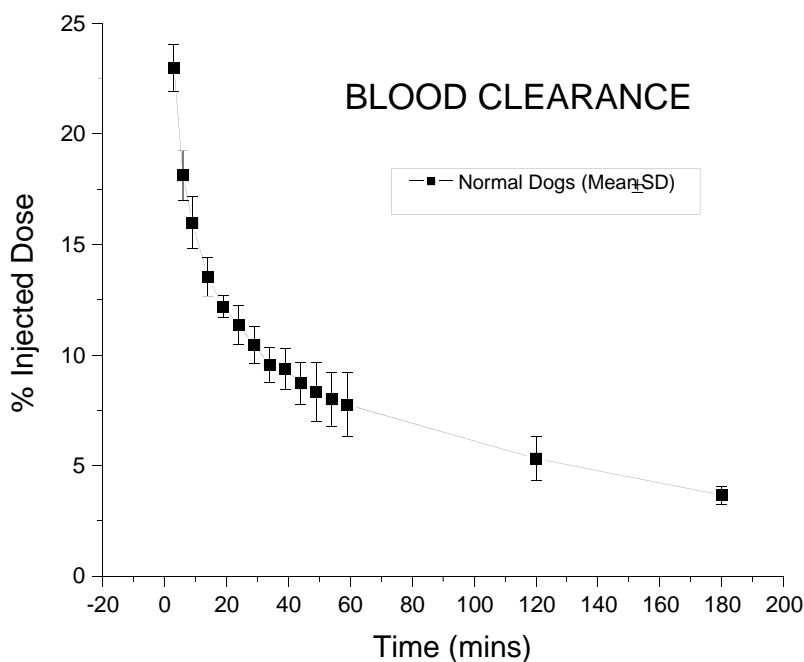
**Table 4-33: Pharmacokinetic mean±SD of the background compartment in normal dogs given  $^{153}\text{Sm}$ -PEI-MP (10-30 kDa)**

Compartment	Pharmacokinetic Parameter	Mean±SD
Background	$T_{1/2}$ (min)	76.75 ±69.48
	$T_{max}$ (min)	1.75 ±0.5
	% OD at 3 hr's	8.22 ±1.21

Legend: Analysis of the TAC for background found the data were similar to the data from normal dogs that received MW-fractions  $^{99m}\text{Tc}$ -PEI-MP 10-30 kDa and 20-30 kDa; see Table 4-20 on page 234.

4.6.5.9 Biodistribution data for the cardiac blood-pool in normal dogs (n=4) receiving  $^{153}\text{Sm}$ -PEI-MP 10-30 kDa

**Figure 4-20 Time-activity curve for blood in normal dogs receiving  $^{153}\text{Sm}$ -PEI-MP (10-30 kDa)**



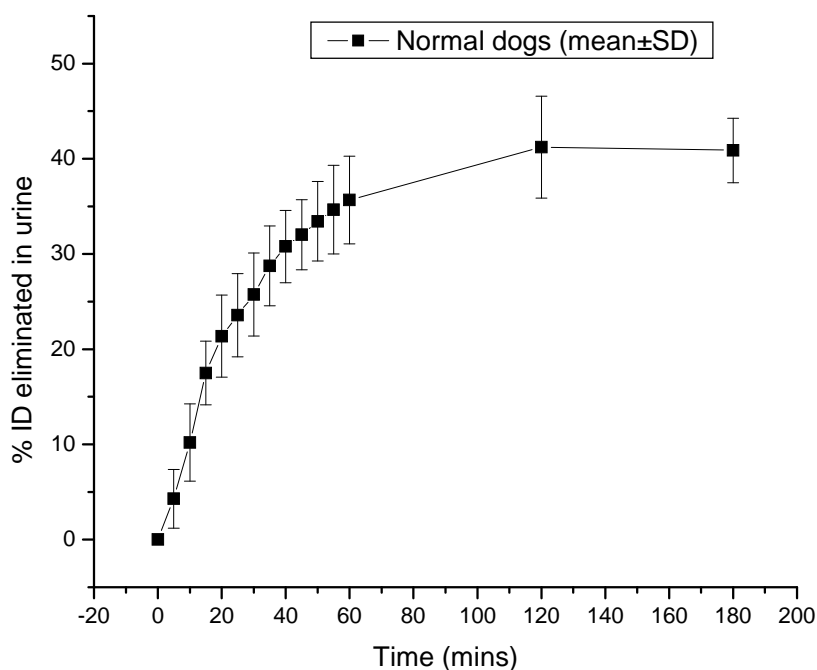
**Table 4-34 Pharmacokinetic mean±SD of the blood compartment in normal dogs given  $^{153}\text{Sm}$ -PEI-MP (10-30 kDa)**

Compartment	Pharmacokinetic Parameter	Mean±SD
Blood	$T_{1/2}$ (min)	15.25±2.5
	$T_{max}$ (min)	0
	% ID at 3 hr's	4.82±0.23

Legend: Analysis of the TAC for blood found the data were similar to the data from normal dogs that received MW-fractions  $^{99m}\text{Tc}$ -PEI-MP 10-30 kDa and 20-30 kDa; see Table 4-12 on page 231.

4.6.5.10 Biodistribution data for urine in normal dogs (n=4) receiving  $^{153}\text{Sm}$ -PEI-MP 10-30 kDa

**Figure 4-21 Cumulative time-activity curve for urine in normal dogs receiving  $^{153}\text{Sm}$ -PEI-MP (10-30 kDa)**



**Table 4-35 Cumulative urine activity for dogs receiving  $^{153}\text{Sm}$ -PEI-MP (10-30 kDa)**

Compartment	Parameter	Mean±SD
Urine	% of ID eliminated at 3-hours	42.73±4.48
	Time to 50% elimination (min)	23.75±4.78

Legend: Analysis of the accumulative TAC for urine activity found the data were similar to the data from normal dogs that received MW-fractions  $^{99m}\text{Tc}$ -PEI-MP 10-30 kDa and 20-30 kDa; see Table 4-17 on page 233.

Based on the results of the study in dogs (n=4) receiving  $^{153}\text{Sm}$ -PEI-MP MW-fraction 10-30 kDa, some differences in pharmacokinetic parameters between  $^{153}\text{Sm}$  and  $^{99m}\text{Tc}$  labelled PEI-MP were noted when comparing data e.g. liver compartment. Consequently a detailed



statistical comparison was made of the data and the results were recorded and are shown below.

#### 4.7 Statistical comparison of biodistribution and pharmacokinetic data between normal dogs receiving $^{99m}\text{Tc}$ -PEI-MP (10-30 kDa) and $^{153}\text{Sm}$ -PEI-MP (10-30 kDa)

##### 4.7.1 Statistical Analyses

The pharmacokinetic parameters e.g.  $T_{1/2}$ ,  $T_{max}$  and %OD at 3-hours, from the  $^{99m}\text{Tc}$ -PEI-MP MW-fraction 10-30 (n=4) and  $^{153}\text{Sm}$ -PEI-MP MW-fraction 10-30 kDa (n=4) were compared using One-Way ANOVA. For nonparametric data, an ANOVA on Ranks was used.

Statistical significance was set for  $P = 0.05$ . The following compartments were compared; cardiac, lung, liver, left kidney, right kidney, trabecular and cortical bone, and background (soft-tissue). Data used for the statistical comparison can be found in Table 4-7 on page 228 ( $^{99m}\text{Tc}$ -PEI-MP MW-fraction 10-30) the in Appendix; see Table 8-27 on page 316

##### 4.7.2 Results comparing normal dogs given $^{153}\text{Sm}$ -PEI-MP (10-20 kDa) (n=4) and $^{99m}\text{Tc}$ -PEI-MP (10-30 kDa) (n=4)

**Table 4-36 Pharmacokinetic data and statistical results comparing  $^{153}\text{Sm}$  and  $^{99m}\text{Tc}$  labelled 10-30 kDa PEI-MP MW-fraction**

<b>Radiopharmaceuticals</b>	$^{99m}\text{Tc}$ -PEI-MP10-30 kDa (mean±SD)	$^{153}\text{Sm}$ -PEI-MP 10-30 kDa (mean±SD)	<b>P-Value</b>
<b>Parameters</b>			
<b>Cardiac Compartment</b>			
$T_{1/2}$ (min)	6.25±0.50	3.00±2.00	<b><math>P = 0.044</math></b>
$T_{max}$ (min)	0.00	0	
% OD at 3-hours	13.47±4.64	15.46± 0.51	$P = 0.857$
<b>Lung Compartment</b>			
$T_{1/2}$ (min)	9.00±1.83	14.50±7.42	$P = 0.271$
$T_{max}$ (min)	0.00	0.00±	-
% OD at 3-hours	11.72±5.67	11.13±1.90	$P = 0.531$
<b>Liver Compartment *</b>			
$T_{1/2}$ (min)	15.59±1.70	43.00±4.58	<b><math>P &lt; 0.001</math></b>
$T_{max}$ (min)	1.00	1.50±1.00	-
% retention 3 hr's	17±2.65	50.5±14.53	<b><math>P = 0.012</math></b>
% OD at 3-hours	10.39±5.53	21.68±6.03	$P = 0.188$
<b>Left kidney Compartment</b>			
$T_{1/2}$ (min)	12.25±1.70	16.00±0.82	<b><math>P = 0.045</math></b>
$T_{max}$ (min)	2.00±00	2.50±0.58	$P = 0.203$

<b>Radiopharmaceuticals</b>	<b><sup>99m</sup>Tc-PEI-MP10-30 kDa (mean±SD)</b>	<b><sup>153</sup>Sm-PEI-MP 10-30 kDa (mean±SD)</b>	<b>P-Value</b>
<b>Parameters</b>			
% OD at 3-hours	19.77±7.65	13.71±1.79	<i>P</i> = 0.099
<b>Right kidney Compartment</b>			
T <sub>1/2</sub> (min)	13.50±1.73	15.25±2.22	<i>P</i> = 0.154
T <sub>max</sub> (min)	2.00±0.00	2.50±0.58	<i>P</i> = 0.203
% OD at 3-hours	18.37±13.59	14.55±3.32	<i>P</i> = 0.857
<b>Trabecular Bone Compartment</b>			
T <sub>1/2</sub> (min)	54.75±6.70	>180 min	<i>P</i> < 0.05
T <sub>max</sub> (min)	4.00±4.80	>180 min	<i>P</i> < 0.05
% OD at 3-hours	11.62±6.10	14.29±2.92	<i>P</i> = 0.091
<b>Cortical Bone Compartment</b>			
T <sub>1/2</sub> (min)	54.75±6.70	150.00±42.43	<i>P</i> = 0.320
T <sub>max</sub> (min)	4.00±4.83	1.50±1.00	<i>P</i> = 0.054
% OD at 3-hours	8.66±1.80	5.29±1.29	<i>P</i> = 0.160
<b>Background Compartment</b>			
T <sub>1/2</sub> (min)	27.50±9.46	76.75±69.48	<i>P</i> = 0.329
T <sub>max</sub> (min)	3.25±3.20	1.75±0.50	<i>P</i> = 0.857
% OD at 3-hours	4.10±3.04	8.23±1.22	<b><i>P</i> = 0.036</b>

Legend: While a number of parameters are statistically (bold) significant between groups, the most compelling are the liver (\*) T<sub>1/2</sub> and the % retention at 3 hours for <sup>153</sup>Sm-PEI-MP 10-30 kDa. The % retention at 3 hours was calculated as previously reported in section 2.1.2.6 on page 100. The increased liver retention and T<sub>1/2</sub> for the <sup>153</sup>Sm-PEI-MP MW-fraction are explained in the report by Jarvis *et al.*,<sup>1</sup> as being due to the interaction of <sup>153</sup>Sm with citrate, forming <sup>153</sup>Sm-citrate complex which accumulates in the liver. The left kidney parameter T<sub>1/2</sub>, also showed a statistical difference between radiopharmaceuticals. The result was not considered significant as neither the % OD for kidneys nor the % ID in urine were statistically different between groups. Other compartment parameters (cardiac and lung) are not considered clinically important since the % OD is similar for both groups. This was also borne out by the lack of differences for the blood compartment parameter, see Table 4-37 below.

**Table 4-37 Pharmacokinetic data for blood comparing <sup>153</sup>Sm and <sup>99m</sup>Tc labelled 10-30 kDa PEI-MP MW-fractions**

<b>Blood parameters</b>	<b><sup>99m</sup>Tc-PEI-MP 10-30 kDa (mean±SD)</b>	<b><sup>153</sup>Sm-PEI-MP 10-30 kDa (mean±SD)</b>	<b>P-Value</b>
T <sub>1/2</sub> (min)	20±17.321	21±2	<i>P</i> = 0.910
T <sub>max</sub> (min)	0	0	
% ID at 3 hr's	4.33±0.58	4.82±0.23	<i>P</i> = 0.40

Legend: No statistical differences for blood compartment parameters were found between radiopharmaceuticals.

**Table 4-38 Pharmacokinetic data for urine comparing  $^{153}\text{Sm}$  and  $^{99\text{m}}\text{Tc}$  labelled 10-30 kDa PEI-MP MW-fractions**

Urine parameters	$^{99\text{m}}\text{Tc}$ -PEI-MP 10-30 kDa (mean $\pm$ SD)	$^{153}\text{Sm}$ -PEI-MP 10-30 kDa (mean $\pm$ SD)	P-Value
% of ID eliminated at 3-hours	69.75 $\pm$ 3.45	42.73 $\pm$ 4.48	$P = 0.16$
Time to 50% elimination (min)	21.66 $\pm$ 3.51	23.75 $\pm$ 4.78	$P = 0.55$

Legend: No statistical differences were found for urine parameters between radiopharmaceuticals. This result show confirms similar renal clearance for both radiopharmaceuticals.

The increased liver uptake for the  $^{153}\text{Sm}$ -PEI-MP 10-30 kDa MW-fraction was concerning for two reasons; the first was the work done by Jarvis *et al.*,<sup>1</sup> that showed that this complex when in the body, was less stable than expected, secondly the higher uptake in the liver may lead to hepatic toxicity when therapeutic doses of  $^{153}\text{Sm}$ -PEI-MP are used. Consequently, this lead to another study where PEI-MP was complexed to the radionuclide  $^{186}\text{Re}$ .  $^{186}\text{Re}$  was thought desirable because of its similar chemical characteristics to  $^{99\text{m}}\text{Tc}$ , due to their juxtaposition on the periodic table. While initial work was done complexing  $^{186}\text{Re}$  to PEI-MP MW-fractions, the results were regrettably too incomplete to be including in this thesis. Part of the reason for the incomplete data was the technical difficulty associated with the low specific activity of the  $^{186}\text{Re}$  radionuclide. The low specific activity leads to low a labelling efficiency of the ligand.

#### 4.8 Section Discussion

The pharmacokinetic results of various MW-fractions of the novel ligand PEI-MP were initially studied labelled to  $^{99\text{m}}\text{Tc}$ . Various molecular weights were tested in normal dogs, and compared to previously published results in baboons. Results from the dog studies were found to be similar to the primate study for various MW-fractions<sup>21</sup>. As in the primate study, molecular weight and charge played a significant role in  $^{99\text{m}}\text{Tc}$ -PEI-MP pharmacokinetics. Increasing the size of the macromolecules and changing their charge resulted in marked changes in their pharmacokinetics and biodistribution. For PEI-MP MW-fractions larger than 50 kDa there was almost complete exclusion ( $\leq 1.93\%$  OD) of molecules from trabecular bone in the normal dog model, this included both negative and positively charged particles

(see Table 4-4 on page 222). The highest relative trabecular bone uptake of 19.93% OD at 3-hours was demonstrated by the 20 - 30 kDa MW-fraction (n=4), see Table 4-6 on page 226. Nevertheless, but this is still considerably lower than the 36.98% OD for  $^{153}\text{Sm}$ -EDTMP (n=4), see Table 3-14 on page 127. The 50-100 kDa MW-fractions experienced an excessively high uptake and prolonged retention of 39% OD by the liver. This could lead to unacceptably high radiation doses eventually from the corresponding therapeutic agents (Table 4-4 on page 222). This was somewhat attenuated in the positive charged MW-fraction (25.2% OD). However, the change in charge (+) resulted in an increased uptake by the kidneys (Figure 4-2 on page 222). Clearly, the charge of the various MW-fractions influenced liver uptake, with the negatively charged MW-fractions showing more retention for both 50-100 and 30-50 kDa MW molecules. The increased uptake by the liver with MW-fractions >50 kDa is explained by known mechanisms of extraction by the liver<sup>263</sup>. A measurable liver accumulation was present for all MW-fractions ranging from the lowest of 5% OD for the 30-50 kDa (+) fractions to 39% OD at 3-hours for the 50-100 kDa (-) fraction. Nevertheless, the retention of the MW-fractions in the liver trended towards a shorter  $T_{1/2}$  with decreasing size MW-fraction size, with the shortest  $T_{1/2}$  of 15.59 minutes for the 10-30 kDa MW-fraction (see Table 4-7 on page 228). In contrast, the MW-fractions of 50-100 kDa had the longest liver  $T_{1/2}$  of greater than 3-hours (see Table 4-4 on page 222).

Increasing MW-fraction size, as expected, also had a negative influence on renal clearance, especially with MW-fractions larger than 60 kDa e.g., 50-100 kDa. This is due to the normal kidney filtration restrictions, whereby molecules >60 kDa are not normally cleared by the glomeruli. The charge also affected glomeruli clearance with positively charged molecules showing greater retention for both 30-50 kDa and 50-100 kDa MW-fractions. The positively charged 50-100 kDa MW-fraction had an increased retention at 31% OD at 3-hours and a prolonged wash-in phase of >180 minutes (see Table 4-4 on page 222). The positively charged 30-50kDa MW-fraction had lower cleared urine activity (45.34% ID) when compared to the negatively charged 30-50 kDa (61.79% ID), indicating some retention in the kidney (see Figure 4-2 on page 222 and Table 4-9 on page 230). The MW-fraction 20-30 kDa had the highest clearance of activity in urine at 75% ID at 3-hours and one of the lowest renal retentions of 14% OD at 3-hours (see Table 4-6 on page 226 and Table 4-9 on page 230).

This study also demonstrated the required reduced normal bone uptake of  $^{99m}\text{Tc}$ -PEI-MP. The MW-fractions with the highest uptake in trabecular bone in relation to body was the 20 - 30 kDa at 19.93% OD (see Table 4-6 on page 226), which by comparison is more than double that for the other MW-fractions. While some retention in bone is good, the radiation dose could also be correspondingly higher. Other compartments such as lung and liver reflected also changes apparent in blood activity (see Table 4-10 on page 230). The negatively charged 50-100 kDa MW-fraction retained the highest activity in blood at 3-hours (16.10% ID) compared to all other MW-fractions, which were  $\leq 4.33\%$  ID. This was also reflected in the urine activity, which at 37.66% of the injected dose eliminated at 3-hours was the lowest for all MW-fractions (Table 4-9 on page 230).

The PEI-MP MW-fractions 10-30 kDa and 20-30 kDa were the most promising and fulfilled the hypothesized criteria of an ideal radiopharmaceutical. The mean blood  $t_{1/2-\alpha}$  and  $t_{1/2-\beta}$  for 10-30 kDa polymer (n=4) were  $4.76 \pm 1.5$  and  $61.78 \pm 39.08$  minutes respectively see Table 4-39 on page 255. Because of the wide standard deviation of the  $t_{1/2-\beta}$  for the 10-30 kDa polymer (n=4) we studied 20-30 kDa polymer (n=4) see Table 4-39 on page 255. The mean  $t_{1/2-\alpha}$  and  $t_{1/2-\beta}$  for 20-30 kDa polymer were  $5.50 \pm 1.38$  and  $38.55 \pm 9.46$  minutes respectively. The clearance of the % ID in urine was also significant different between MW-fractions, with the 20-30kDa molecule clearing 75% ID compared to 64.75% ID for the 10-30kDa polymer, see Table 4-39 on page 255. A single dog with osteosarcoma was given  $^{99m}\text{Tc}$ -PEI-MP 10-30 kDa polymer with similar pharmacokinetics as the normal dogs, with a renal clearance of 85.74% ID. In keeping with the aims of the study, the 20-30kDa polymer was considered more desirable because of its faster clearance. However, because of the limitations imposed by the percentage yield of the different molecular weights during ultrafiltration (see Table 4-2 on page 218), we decided to label the 10-30 kDa MW-fraction with  $^{153}\text{Sm}$ . Pharmacokinetic analyses of data for  $^{153}\text{Sm}$ -PEI-MP (10-30kDa) were similar to  $^{99m}\text{Tc}$ -PEI-MP (10-30kDa). Exceptions included, significantly longer blood  $t_{1/2-\beta}$  ( $102.85 \pm 7.40$  minutes), liver  $T_{1/2}$  and the % retention at 3-hours. Clearance of % ID in urine was the same for both groups. The prolonged blood  $t_{1/2-\beta}$ , increased liver retention and  $T_{1/2}$  for the  $^{153}\text{Sm}$ -PEI-MP MW-fraction were explained in the report by Jarvis *et al.*<sup>1</sup>. Computer modelling for blood plasma (ECCLES) was done which predicted that there would be some chemical dissociation of the  $^{153}\text{Sm}$  from the PEI-MP polymer in blood. This was due to interaction with citrate, forming  $^{153}\text{Sm}$ -citrate<sup>1</sup>. Low levels of colloidal  $^{153}\text{Sm}$ -citrate were also predicted to accumulate in the

liver. However, we also showed that uncomplexed  $^{153}\text{Sm}^{3+}$  would accumulate in the liver, possibly from dissociation of the  $^{153}\text{Sm}$  from PEI-MP (10-30kDa) which could lead to increased liver uptake. The ECCLES model for blood plasma also predicted that the anionic MW-fraction, PEI-MP (10-30kDa), would be a poor ligand complexed to  $^{166}\text{Ho}$ ,  $^{212}\text{Pb}$ ,  $^{213}\text{Pb}$ , and  $^{89}\text{Sr}$ , but was expected to be effective when complexed to  $^{186}\text{Re}$  or  $^{188}\text{Re}$ , based on its close proximity to  $^{99\text{m}}\text{Tc}$  on the periodic table <sup>1</sup>. As a preliminary study  $^{186}\text{Re}$  was labelled to 20-30 kDa (n=2) and 30-50 kDa (n=1) MW-fractions and tested in dogs. Nevertheless, these data were considered preliminary and were not reported in the thesis. Technical difficulties associated with the low specific activity of the  $^{186}\text{Re}$  radionuclide leading to low labelling efficiency of the ligand played a negative role in the study.

The parameters describing the blood pharmacokinetics of the PEI-MP MW-fractions (10-30 and 20-30 kDa) were then compared to  $^{188}\text{Re}$ -HEDP and  $^{153}\text{Sm}$ -EDTMP; see Section 8.7 of the Appendix, Table 8-29 on page 319. Interestingly, the  $t_{1/2-\alpha}$  for radiopharmaceuticals ( $^{99\text{m}}\text{Tc}$ -PEI-MP 10-30,  $^{99\text{m}}\text{Tc}$ -PEI-MP 20-30kDa,  $^{153}\text{Sm}$ -PEI-MP 10-30,  $^{188}\text{Re}$ -HEDP and  $^{153}\text{Sm}$ -EDTMP) were not found to be statistically different (see Table 3-35 on page 154 and Table 4-39 on page 255). This was also true for dogs with osteosarcoma that received  $^{188}\text{Re}$ -HEDP (n=4) and  $^{153}\text{Sm}$ -EDTMP, indicating a rapid uptake by target tissues and clearance from the central compartment with a mean $\pm$ SD of  $5.46\pm 0.63$  minutes for all isotopes (see Table 3-35 on page 154 and Table 4-39 on page 255). Therefore, while the PEI-MP MW-fractions have significantly larger MW than bisphosphonates their pharmacokinetic behaviour is similar. This is in contrast to the very prolonged  $t_{1/2-\alpha}$  found with liposomal and immunotherapy radiopharmaceuticals <sup>264</sup>. The implications for dosimetry are that there would be less radiation of non-target organs by HEDP, EDTMP and PEI-MP labelled radiopharmaceuticals. Nevertheless, it was not unexpected that the pharmacokinetic blood parameter  $t_{1/2-\beta}$  would be different between radiopharmaceuticals.  $^{153}\text{Sm}$ -EDTMP and  $^{99\text{m}}\text{Tc}$ -PEI-MP (20-30kDa) had more rapid elimination and  $^{153}\text{Sm}$ -PEI-MP (10-30 kDa), and  $^{188}\text{Re}$ -HEDP a more prolonged elimination. The differences can be explained by the prolonged washout from targets of uptake. As previously discussed, for  $^{188}\text{Re}$ -HEDP, this was bone and soft tissue. In the case of  $^{153}\text{Sm}$ -PEI-MP (10-30 kDa), this was due to prolonged hepatic retention.

**Table 4-39 Data showing pharmacokinetics, biodistribution and bone localization for PEI-MP MW-fractions and labelled radionuclides in normal dogs and dogs with osteosarcoma.**

MW-fractions Parameters	<sup>99m</sup> Tc--PEI-MP 10-30 kDa Osteosarcoma case	<sup>153</sup> Sm-PEI-MP 10-30 kDa	<sup>99m</sup> Tc-PEI-MP 20-30 kDa	<sup>99m</sup> Tc-PEI-MP 10-30 kDa	<i>P-value</i>
Number of Animals	1	4	4	4	
Tumour % ID at 3hrs	4.31	NA	NA	NA	
Trabecular Bone % ID at 3hrs	0.94	7.92±1.13**	6.08±0.94**	2.08±0.76**	<b><i>P</i>&lt;0.05</b>
Whole Body % ID at 3 hours	14.26	57.27±4.48	26.21±1.92	30.25±3.45	NA
Urine % ID eliminated at 3 hrs.	85.74	42.73±4.48**	73.91±1.80**	69.75±3.45**	<b><i>P</i>&lt;0.05</b>
Blood % ID at 3hrs	1.74	4.82±0.23**	1.80±1.50**	4.33±0.58**	<b><i>P</i>&lt;0.05</b>
Blood ( <i>t</i> <sub>1/2</sub> -α) min	5.74	5.09±1.19	5.50±1.38	4.76±1.50	NS
Blood ( <i>t</i> <sub>1/2</sub> -β) min	83.96	102.85±7.40**	38.55±9.46**	61.78±39.08**	<b><i>P</i>&lt;0.05</b>

\*The “Whole Body % ID at 3 hours” is calculated by subtracting the total % ID in urine at 3 hours from 100% e.g. 100% (Total % ID) - 85.74 % ID(urine) = 14.26 (Whole Body % ID at 3 hours).

\*\*Comparing the urine % ID at 3 hours between groups found that <sup>153</sup>Sm-PEI-MP 10-30 kDa differed from the <sup>99m</sup>Tc-PEI-MP 20-30 but not from <sup>99m</sup>Tc-PEI-MP 10-30. For the % ID in blood at 3 hours <sup>153</sup>Sm-PEI-MP 10-30 kDa differed from the <sup>99m</sup>Tc-PEI-MP 20-30 but not from <sup>99m</sup>Tc-PEI-MP 10-30. The two <sup>99m</sup>Tc MW-fractions also differed from each other a previously reported. For blood (*t*<sub>1/2</sub>-β) <sup>153</sup>Sm-PEI-MP 10-30 kDa differed from the <sup>99m</sup>Tc-PEI-MP 20-30 but not from <sup>99m</sup>Tc-PEI-MP 10-30. This interesting as it appears to indicate that <sup>153</sup>Sm did not significantly change the pharmacokinetics PEI-MP 10-30 kDa when compared to the tracer <sup>99m</sup>Tc-PEI-MP 20-30.

NA not applicable. NR not recorded

## Chapter 5. Comparative Dosimetry of Normal Dogs and Dogs with Osteosarcoma.

The OLINDA dosimetry software was used for all dosimetry calculations, in the future these results will be compared to results using the canine UF-phantom<sup>16</sup>. Briefly, the data used for dosimetry are derived from time-activity curves and the percentage organ distribution (%OD) was calculated for each region of interest, see Appendix, Table 8-4 on page 277. The activity in the body was then used to determine the percentage-injected dose (% ID) for different ROI (heart, lung, liver, kidneys, cortical bone, trabecular bone, background [soft-tissue], tumour and bladder contents [cumulative urine activity]). An example of data used in the calculations can be seen in Appendix, Table 8-4 to Table 8-9. While not needed the Excel calculations for 3-hour AUC and Residence time for each ROI were kept to compare and to verify the OLINDA results. The decay corrected pharmacokinetic data which yielded the % ID for each ROI and accumulated urine activity were entered into the OLINDA software package for exponential modeling (EXM module)<sup>213</sup>. The program allows the user to enter pharmacokinetic data (% ID) to be fitted into one or more exponential terms<sup>218</sup>. The program integrated the fitted time-activity curve to infinity (decayed data) and passed the integral back to the OLINDA pharmacokinetics input form for use in dose calculations<sup>218</sup>. In addition, we were able to compare the data from OLINDA with data derived from the UF canine phantom, which has canine specific *S*-value tables<sup>16</sup>.

The following assumptions and procedures were used for the collected data;

- The data collected as background (BG) was entered in OLINDA as “rest of the body” as the ROI was centred over soft-tissue.
- While attenuation data was collected, it was not used in the dosimetry calculations. This was considered acceptable for comparative purposes since all dogs had their dynamic studies performed in same way i.e. in the supine position.
- Data points were only collected for the first 3 to 4 hours during which the majority of the distribution (wash in) and elimination (washout) phase occurred. The OLINDA software package allowed for exponential modelling (EXM module) and data was extrapolated to infinity.



- To calculate the number of disintegrations (residence time) for the tumour region of interest the data was entered into the OLINDA software package for exponential modelling (EXM module). The integral was then entered into the nodule module (see Experimental Design Section 2.1.2.6 on page 100 for details). To calculate the radiation dose to the tumour, the mass of the tumour was derived from radiograph measurements of the tumour to calculated tumour volume, see the Appendix, Table 8-15 (on page 291) and Table 8-22 (on page 308). The mass of the tumour was then calculated based on the known density of bone. The tumour mass was entered into the nodule module to calculate the radiation dose to the tumour in mGy/MBq. The results in mGy are then multiplied by the therapeutic dose in MBq to derive the total dose in Gy to the tumour, see Appendix, Table 8-33 on page 326.

Tables were only generated for dogs receiving therapeutic radiopharmaceuticals,  $^{153}\text{Sm}$ -EDTMP,  $^{188}\text{Re}$ -HEDP,  $^{186}\text{Re}$ -HEDP, and  $^{153}\text{Sm}$ -PEI-MP 10-30 kDa, see the Appendix, Table 8-31 on page 324 and Table 8-32 on page 326. In addition, the radiation dose to tumours was also reported; see Appendix 4, Table 8-33.

**Table 5-1 Dosimetry results from various radiopharmaceuticals in normal dogs comparing radiation sensitive organs**

Radiopharmaceuticals	$^{153}\text{Sm}$ -EDTMP (n=4) Mean±SD (mGy/MBq)	$^{188}\text{Re}$ -HEDP (n=4) Mean±SD (mGy/MBq)	$^{153}\text{Sm}$ -PEI-MP 10-30 (n=4) Mean±SD (mGy/MBq)	P-value
<b>Kidney</b>	0.897±0.859	5.425±2.795	0.921±0.831	<b>P=0.013</b>
<b>Liver</b>	0.292±0.139	0.747±0.330	0.742±0.824	P=0.4
<b>Lungs</b>	0.416±0.213	1.115±1.060	0.217±0.192	P=0.348
<b>Red Marrow</b>	0.753±0.161	0.202±0.063	0.379±0.031	<b>P&lt;0.001</b>
<b>Osteogenic Cells</b>	2.514±0.484	0.365±0.111	1.278±0.331	<b>P&lt;0.001</b>
<b>Urinary Bladder Wall</b>	1.638±0.650	2.965±1.725	0.996±0.194	<b>P=0.001</b>
<b>Total Body</b>	0.086±0.010	0.068±0.053	0.089±0.046	P=0.744

Legend: Commenting on Table 5-1 above: statistical differences were found between radiopharmaceuticals for radiation dose to kidneys, red marrow, osteogenic cells, and urinary bladder wall. Dogs receiving  $^{188}\text{Re}$ -HEDP had almost a five-fold higher dose to kidneys compared to dogs receiving  $^{153}\text{Sm}$ -EDTMP and  $^{153}\text{Sm}$ -PEI-MP 10-30kDa. Interestingly, while only one dog received  $^{186}\text{Re}$ -HEDP it also had a high radiation dose to the kidney. Not

surprisingly, the radiation dose to the urinary bladder was also the highest for dogs receiving  $^{188}\text{Re}$ -HEDP. This can be explained by the prolonged blood elimination phase ( $t_{1/2\beta}=92.19\pm 9.86$  min) with clearance through the kidneys for dogs receiving  $^{188}\text{Re}$ -HEDP (see Table 3-37 on page 158). As expected this was also the case for the single normal dog receiving  $^{186}\text{Re}$ -HEDP (see Table 3-32 on page 148). The HEDP (etidronate) bisphosphonate ligand is associated with poorer binding to bone and thus released more readily from bone in comparison to the amino-bisphosphonate, EDTMP (lexidronam)<sup>61</sup>. This was also reflected in the lowest radiation dose to bone elements. The radiation doses to red marrow and osteogenic cells were statistically different for all three radiopharmaceutical with the highest recorded for  $^{153}\text{Sm}$ -EDTMP, followed by  $^{153}\text{Sm}$ -PEI-MP 10-30 kDa MW-fraction and then  $^{188}\text{Re}$ -HEDP.

Remarkably, the radiation dose to the liver for all three radiopharmaceuticals was not statistically different, even though we had previously reported increased uptake by the liver for  $^{153}\text{Sm}$ -PEI-MP 10-30 kDa MW-fraction. This was due to a dissociation of  $^{153}\text{Sm}$  from PEI-MP<sup>1</sup>.

Nevertheless, the mean uptake of  $^{153}\text{Sm}$ -PEI-MP 10-30 MW-fraction in the liver was higher compared to  $^{153}\text{Sm}$ -EDTMP but similar to  $^{188}\text{Re}$ -HEDP (see Table 4-39 on page 255 and Table 3-35 on page 154). In addition, the labelling of  $^{188}\text{Re}$ -HEDP can be complicated and an increased soft tissue uptake can occur which could explain the higher renal uptake<sup>111</sup>. Furthermore, we experienced breakthrough with scintigraphic images of the dogs receiving  $^{188}\text{Re}$ -HEDP, consequently the scintigraphic images were not as defined as for  $^{153}\text{Sm}$ -EDTMP imaging. This could be explained by either the lack of carrier<sup>232, 235</sup> or by the higher energy gamma emitted by  $^{188}\text{Re}$ , requiring a high-energy collimator.

**Table 5-2 Dosimetry data for osteosarcoma dogs receiving various radiopharmaceuticals**

<b>Radiopharmaceutical</b>	<b><sup>153</sup>Sm-EDTMP (mGy/MBq)</b>	<b><sup>188</sup>Re-HEDP (mGy/MBq)</b>	<b><sup>188</sup>Re-HEDP (mGy/MBq)</b>	<b>Tc(<sup>153</sup>Sm)-PEI-MP 10-30kDa (mGy/MBq)</b>
<b>Target Organ</b>				
<b>Osteosarcoma Cases</b>	<b>Case-13</b>	<b>Case-1</b>	<b>Case-2</b>	<b>Case-14</b>
<b>Kidney</b>	6.610	4.330	2.87	0.152
<b>Liver</b>	0.861	0.355	0.883	0.026
<b>Lungs</b>	0.242	2.010	1.71	0.049
<b>Red Marrow</b>	0.544	0.240	0.184	0.017
<b>Osteogenic Cell</b>	2.310	0.570	0.332	0.029
<b>Urinary Bladder Wall</b>	0.840	1.220	1.72	1.190
<b>Total Body</b>	0.127	0.128	0.103	0.005
<b>Tumour Self Dose</b>	25.18	44.32	30.63	26

Legend: \* Dosimetry for Case-14 was derived using OLINDA, for comparative purposes <sup>153</sup>Sm was substituted for <sup>99m</sup>Tc in OLINDA to simulate and to compare radiation dose to vital organs and the tumour between radiopharmaceuticals

Table 5-2 above, summarizes the dosimetry results for dogs with osteosarcoma. Because of the duration of the dynamic scans (3-4 hours), we were only able to perform dynamic scans on five client owned dogs, which included the tumour ROI. Case-14 (see Table 8-14) was scanned using <sup>99m</sup>Tc-PEI-MP 10-30 and the dynamic data was used in OLINDA to simulate a therapeutic dose of <sup>153</sup>Sm-PEI-MP 10-30. The radiation dose to kidneys for dogs receiving <sup>186</sup>Re-HEDP, <sup>153</sup>Sm-EDTMP, and <sup>188</sup>Re-HEDP were elevated above the simulated <sup>153</sup>Sm-PEI-MP 10-30 kDa MW-fraction dog although the osteosarcoma dogs receiving <sup>188</sup>Re-HEDP were similar to the normal <sup>188</sup>Re-HEDP dogs. The radiation doses to all organs were lower in the <sup>153</sup>Sm-PEI-MP 10-30kDa simulation compared to other radiopharmaceuticals, emphasizing its ideal radiopharmaceutical properties. The radiation dose to the tumour for all radiopharmaceuticals fall within the teletherapy dose range (26-44Gy) used to treat canine osteosarcoma<sup>265</sup>. However as reported in the autoradiography section 3.16.3.1.1, the dose is not uniform in the tumour and therefore suboptimal delivery of radiation to the tumour occurs.

## Chapter 6. Discussion

Central to our hypotheses was that naturally occurring canine osteosarcoma would serve as an investigational model for comparing the pharmacokinetics (biodistribution), dosimetry, toxicity, and therapeutic effect of  $^{153}\text{Sm}$ -EDTMP,  $^{188}\text{Re}$ -HEDP, and  $^{186}\text{Re}$ -HEDP with each other and was compared to published human pharmacokinetic data <sup>122</sup>. We also studied a novel ligand, polyethyleneiminomethyl phosphonic acid (PEI-MP). The novel ligand PEI-MP was designed to fulfil the criteria of an ideal radiopharmaceutical. Data collected from  $^{153}\text{Sm}$ -EDTMP,  $^{188}\text{Re}$ -HEDP, and  $^{186}\text{Re}$ -HEDP studies were compared to PEI-MP ligand labelled with  $^{99\text{m}}\text{Tc}$ ,  $^{153}\text{Sm}$ .

While early reports exist describing the biodistribution and some pharmacokinetic data in dogs <sup>7, 15, 102, 104, 221, 222</sup>, our study is unique as it provides time-activity curves for important radiation sensitive tissues and for blood and urine. For comparative purposes, these data enabled us to calculate radiation dose to sensitive organs using OLINDA <sup>213</sup> and in future the UF Canine Phantom <sup>16</sup>. While Corwin and Ketring <sup>222</sup> were the first investigators to describe the bony uptake of  $^{153}\text{Sm}$ -EDTMP in the dog, it was Appelbaum *et al.*, <sup>221</sup> who described for the first time the biodistribution and pharmacokinetics in the dog. They found that by 2-3-hours, 50% to 66% of the injected dose was localized in bone and 33% to 50% eliminated in the urine. In a paper by Galiano and Stradiotto <sup>266</sup> a statistical analysis of the initial biodistribution of  $^{153}\text{Sm}$ -EDTMP in a single normal dog was reported. The study describes the biodistribution and pharmacokinetics by computing the change in pixel intensity over time. They reported an increased liver uptake in the dog, which they depict as never having been described before. Indeed, this conclusion is erroneous as Goeckeller *et al.*, <sup>225</sup> reported this phenomena in rats as due to unchelated  $^{153}\text{Sm}$  stemming from poor preparation of the radiopharmaceutical. One can hypothesize that this was a possibility, as Galiano and Stradiotto <sup>266</sup> do not report using commercially produced  $^{153}\text{Sm}$ -EDTMP. We also confirmed this experimentally, when we injected uncomplexed  $^{153}\text{Sm}$  into a control dog, 47 % of the injected dose (% ID) localized in the liver (See Figure 3-3 on page 118 and Table 3-7 on page 119). We used this characteristic liver biodistribution of uncomplexed  $^{153}\text{Sm}$  as a scintigraphic control for radiochemical purity in subsequent studies using the novel ligand PEI-MP (See Figure 4-14 on page 241).

Pharmacokinetic results for canine studies using  $^{153}\text{Sm}$ -EDTMP,  $^{188}\text{Re}$ -HEDP and  $^{186}\text{Re}$ -HEDP are summarized in Table 3-35 on page 154. Statistical comparisons could only be made

between normal dogs receiving  $^{188}\text{Re}$ -HEDP (n=4) and  $^{153}\text{Sm}$ -EDTMP (n=4), and three tumour bearing dogs who received  $^{188}\text{Re}$ -HEDP. Statistical comparisons were made with published human studies from patients with bone metastases, see Table 3-36 and Table 3-37 on page 157-158<sup>122</sup>. When comparing pharmacokinetic data from the dog studies with each other, statistical differences ( $P < 0.05$ ) were found between  $^{153}\text{Sm}$ -EDTMP (n=4) and  $^{188}\text{Re}$ -HEDP (n=4) for  $t_{1/2-\beta}$  (blood elimination phase) and the % ID retained in blood at 3-hours (see Table 3-35 on page 154). The longer  $t_{1/2-\beta}$  and increased % ID in blood of  $^{188}\text{Re}$ -HEDP when compared to  $^{153}\text{Sm}$ -EDTMP are a reflection of prolonged bone and soft-tissue washout. This can be explained by the >100-fold weaker antiresorptive capability of HEDP (etidronate), a non-amino-bisphosphonate, compared to the amino-bisphosphonate ligand EDTMP (lexidronam), see bisphosphonate chemistry section 1.6.2.1.1 on page 48. For more detailed bone and soft-tissue biodistribution data from dogs receiving  $^{188}\text{Re}$ -HEDP see Figure 3-10 on page 126 and Figure 3-12 on page 128. The only statistically significant pharmacokinetic finding between dogs with osteosarcoma (n=3) and normal dogs (n=4) given  $^{188}\text{Re}$ -HEDP was % ID in blood at 3-hours, which was higher for the osteosarcoma cases (see Table 3-35 on page 154). These differences could be attributed to a number of possibilities; the most likely reasons could be due to the prolonged washout from the tumours ( $T_{1/2} = >180$  minutes [see Table 3-28 on page 143]) compared to trabecular bone ( $T_{1/2} = 135$  minutes [see Table 3-25 on page 140]) in normal dogs and/or the decreased renal clearance of  $^{188}\text{Re}$ -HEDP because of undiagnosed renal disease (Table 3-30 on page 145). Decreased renal clearance was evident by the trend in the dogs with osteosarcomas, receiving either  $^{153}\text{Sm}$ -EDTMP (29.17 % ID in urine) or  $^{188}\text{Re}$ -HEDP (30.59 % ID in urine) for greater retention of the radiopharmaceuticals in the whole body and less in the urine at 3-hours compared to normal dogs receiving  $^{153}\text{Sm}$ -EDTMP (44.34 % ID in urine) or  $^{188}\text{Re}$ -HEDP (52.31 % ID in urine). Nevertheless these data were not statistically different, see Table 3-35 on page 154.

When comparing six pharmacokinetic parameters of canine data with human metastatic bone cancer data for  $^{153}\text{Sm}$ -EDTMP no statistically differences were found between species except for blood  $t_{1/2-\beta}$  (see Table 3-36 on page 157). In human studies the average range for blood  $t_{1/2-\beta}$  for  $^{153}\text{Sm}$ -EDTMP was 65.4-690 minutes, which was longer than the 41 minutes in normal dogs (see Table 3-36 on page 157). This could possibly be explained by the tumour burden in the human research populations or by the observation that the majority of patients were aged and may have had some renal disease. Certainly, the trend in dogs with osteosarcoma was to have

increased blood  $t_{1/2-\beta}$  compared to normal dogs. When canine data was compared to human metastatic bone cancer data for  $^{188}\text{Re-HEDP}$ , only two (% ID bone, % ID urine) of the three pharmacokinetic parameters examined were found to be different between species (see Table 3-37 on page 158). However, for the % ID in bone at 3-hours the difference was between normal (43.27 % ID) dogs and tumour bearing (16.41 % ID) dogs and human metastatic bone cancers (46.1 % ID<sup>114</sup>) and tumour bearing dogs. The latter finding was unexpected, as the % ID in bone would be predicted to have similar pharmacokinetics for diseased humans and osteosarcoma dogs. Nonetheless, there are likely to be tumour and microenvironmental differences between primary bone cancer and secondary metastatic bone cancer. The statistical difference between dogs and humans for the % ID cleared in urine at 3-hours could be artificial since it was extrapolated from Figure-3 in Liepe *et al.*, 2003<sup>114</sup>. At 48-hours, the difference was no longer apparent, see Table 3-37 on page 158. Regrettably, no statistical analyses could be performed between humans and dogs for  $^{186}\text{Re-HEDP}$ . Nonetheless, a study was done in a single normal dog and when compared to three human metastatic bone cancer studies in Table 3-37 on page 158, the pharmacokinetic data was similar. For example, the % ID cleared in urine at 3-hours for humans ranged from 71 % to 65 % compared to 67% for the normal dog. Consequently, it was concluded that the findings from the various radiopharmaceutical dog studies supported the hypothesis that the biodistribution and pharmacokinetic results from dogs were similar to published human metastatic bone cancer data and thus the normal and osteosarcoma dogs could be creditable models for further radiopharmaceutical research.

Additional observational biodistribution studies were done using macro- and micro- autoradiography techniques, see section 3.16, and Figure 3-41 (on page 198) to Figure 3-51 (page 208). The purpose of these studies was to observe the macro- and micro-distribution of  $^{153}\text{Sm-EDTMP}$  within a tumour and in the surrounding bone marrow elements. Results from the studies showed a heterogeneous uptake within tumours; see Figure 3-48 on page 205. Not surprisingly, poor distribution was found in areas of poor blood supply, with also unfortunately viable tumour cells; see Table 3-60 on page 209. The heterogeneity of the uptake in cancer has implications for dosimetry to tumours, as it is obvious that part of the tumour would receive an inadequate dose of radiation, see Figure 3-49 on page 206. The studies in normal rats also confirmed the tendency of  $^{153}\text{Sm-EDTMP}$  to localize especially in red marrow areas, thus leading to high radiation dose to blood producing elements, see Figure 3-45 on page 202. In addition, high uptake was documented at the metaphyseal growth plate, confirming the

likelihood of a delay or cessation of growth if  $^{153}\text{Sm}$ -EDTMP were used in growing children, see Figure 3-43 on page 200.

To monitor myelosuppressive effects and therapeutic response of  $^{153}\text{Sm}$ -EDTMP (n=25) and  $^{188}\text{Re}$ -HEDP (n=7) a clinical trial was conducted in dogs with naturally occurring osteosarcoma; see Table 3-6 on page 112. Dogs receiving  $^{153}\text{Sm}$ -EDTMP at 37 MBq/kg (1 mCi/kg) showed only mild bone marrow toxicity (Grade 2); see Table 3-39 on page 166. There was no cessation in growth of the tumours for both radiopharmaceuticals as shown in Figure 3-38 on page 188 and Figure 3-34 on page 167. All dogs were euthanized because of progression of their tumours with an overall median survival time of 4 months (see Figure 3-39, page 191). This is significantly shorter than the standard of care, which is reported in the literature as 10-month median survival for amputation and chemotherapy  $^{188}$ . To improve the response to  $^{153}\text{Sm}$ -EDTMP, we studied the concurrent administration of a carboplatin infusion; see section 3.12 on page 170. The basis of this study was based the reports of carboplatin acting as a radiosensitizer, which improved overall survival in humans when used together with teletherapy  $^{252-255}$ . No differences in haematological toxicity were noted between the carboplatin group and dogs receiving only  $^{153}\text{Sm}$ -EDTMP (see Section 3.12.8.3.2 on page 176). Nonetheless, when the groups were combined, low grade toxicity was still present for platelets (Figure 3-35 on page 178) and WBC (Figure 3-36 on page 179), although the addition of carboplatin did not worsen the grade of toxicity. When haematological toxicity was examined in dogs receiving a single dose of  $^{188}\text{Re}$ -HEDP (n=5) had Grade-1 platelet toxicity at week-3 and -4 see Table 3-50 on page 185. Since only two cases had complete data from the multiple dose group it did not allow for further statistical analysis between groups. Nevertheless when the data were combined (n=7), platelet count remained were considered Grade-1 toxicity, see Figure 3-37 on page 186. Thus, the nature of the toxicity was only mild and would not have precluded dose escalation or continued repeated therapy with  $^{188}\text{Re}$ -HEDP.

As a group (n=21), the dogs receiving  $^{153}\text{Sm}$ -EDTMP and carboplatin had an overall mean $\pm$ SD T/NTC uptake ratio of 7.60 $\pm$ 5 with a range of 1.72-16.36. However, there was a significant difference in T/NTC uptake between the carboplatin cases (n=6) and dogs receiving only  $^{153}\text{Sm}$ -EDTMP (n=15) (see Table 3-49 on page 180). The carboplatin group had a higher T/NTC uptake ratio of 11.26 compared 5.76 for the  $^{153}\text{Sm}$ -EDTMP only group. Nevertheless, the improved T/NTC uptake of the carboplatin group did not translate into improved survival; see

Figure 3-39 (on page 191). Interestingly six dogs that had both  $^{99m}\text{Tc}$ -MDP and  $^{153}\text{Sm}$ -EDTMP scans of their tumours, had  $^{99m}\text{Tc}$ -MDP scan showing consistently lower ( $4.23\pm 2.39$ ) T/NTC uptake ratio compared to  $^{153}\text{Sm}$ -EDTMP ( $8.22\pm 4.87$ ), data not shown. This is somewhat at odds with the literature where the uptake of  $^{99m}\text{Tc}$ -MDP predicts the uptake of  $^{153}\text{Sm}$ -EDTMP<sup>7, 267</sup>. We explained the differences may be due to the poorer binding to bone (antiresorptive capacity) of MDP compared to EDTMP. The mean $\pm$ SD uptake ratio (T/NTC) for all dogs (=7) receiving  $^{188}\text{Re}$ -HEDP was  $1.69\pm 0.59$ . Uptake ratios were not recorded after the primary scan in the two dogs that received multiple-doses of  $^{188}\text{Re}$ -HEDP. Two dogs (see Case-1 and -4 in the Appendix, Table 8-21 on page 307) had a  $^{99m}\text{Tc}$ -MDP scan of their tumours a week prior to the  $^{188}\text{Re}$ -HEDP treatment. The median T/NTC uptake ratio at 3-hours for  $^{99m}\text{Tc}$ -MDP scan was 11.36 compared to 2.62 for the  $^{188}\text{Re}$ -HEDP (data not shown). Unfortunately insufficient numbers of scans of  $^{99m}\text{Tc}$ -MDP and  $^{188}\text{Re}$ -HEDP in the same dogs precluded statistical evaluation of these results. Nevertheless, this was the cases when the  $^{188}\text{Re}$ -HEDP uptake ratio (T/NTC) was observed to be statistically lower than  $^{153}\text{Sm}$ -EDTMP uptake ratios, see Table 3-59 on page 194 for details. In addition, four dogs that had T/NTC ratios for both  $^{99m}\text{Tc}$ -MDP ( $4.23\pm 2.39$ ) and  $^{153}\text{Sm}$ -EDTMP ( $8.22\pm 4.87$ ) scans, were also scanned with  $^{99m}\text{Tc}$ -PEI-MP (10-30 kDa) with a mean $\pm$ SD T/NTC ratio of  $4.67\pm 0.43$ . While only four dogs, the interesting finding is the small standard deviation of the  $^{99m}\text{Tc}$ -PEI-MP scans, while the  $^{153}\text{Sm}$ -EDTMP and  $^{99m}\text{Tc}$ -MDP had significantly more variation. The variation is significant and is best understood by looking at the coefficient of variance, which was 59.17 % for  $^{153}\text{Sm}$ -EDTMP and 54.17 %  $^{99m}\text{Tc}$ -MDP; and 9.20 % for  $^{99m}\text{Tc}$ -PEI-MP (10-30 kDa). This could be attributed to more consistent uptake ratio of the unique ligand PEI-MP and its hypothesized mechanism of action of enhanced permeability and retention (EPR) in tumour vasculature. Some tentative proof of this hypothesis is that the osteosarcoma dog (see Table 4-22 on page 237) that underwent a dynamic  $^{99m}\text{Tc}$ -PEI-MP scan had an uptake T/NTC ratio of 4.59, in contrast to a  $^{153}\text{Sm}$ -EDTMP T/NTC scan ratio of 2.04. This requires further investigation with larger groups. The significant variation of the  $^{153}\text{Sm}$ -EDTMP,  $^{188}\text{Re}$ -HEDP, and  $^{99m}\text{Tc}$ -MDP T/NTC scan ratios appear to be a function of the bisphosphonate ligand and its predilection for bony remodelling with exposure of hydroxyapatite crystals. Indeed radiographically, tumours differed significantly in their amount of lysis, reactive bone, and tumour bone formation (see Appendix; Table 8-14 on page 287 and Table 8-21 on page 307). Paradoxically, dogs with statistically higher T/NTC uptake ratios had shorter



survivals times see, Table 3-57 on page 193. In addition, when all treatment groups were combined, poor pain control was a negative predictor of survival ( $P = 0.015$ ), see Table 3-55 on page 192. As stated previously this is hardly surprising, since predictably dogs that were not controlled for pain, were more likely be euthanized. When all the treatment groups were combined, only 28% (8/29) of dogs with osteosarcoma were considered to have good pain control (see Table 3-55 on page 192).

Pharmacokinetic results for the novel ligand PEI-MP was initially studied labelled to  $^{99m}\text{Tc}$ . Various MW-fractions were tested in normal dogs, and compared to previously published results in baboons <sup>21</sup>. Results from the dog studies were found to be similar to the primate study <sup>21</sup>. As in the primate study, molecular weight and charge played a significant role in  $^{99m}\text{Tc}$ -PEI-MP pharmacokinetics. Increasing MW-fraction size, as expected, also had a negative influence on renal clearance, especially with MW-fractions larger than 60 kDa e.g., 50-100 kDa. This is due to the normal kidney filtration restrictions, whereby molecules >60 kDa are not normally cleared by the glomeruli. The charge also affected glomeruli clearance with positively charged molecules showing greater retention for both 30-50 kDa and 50-100 kDa MW-fractions. The positively charged 50-100 kDa MW-fraction had an increased retention at 31% OD at 3-hours and a prolonged wash-in phase of >180 minutes (see Table 4-4 on page 222). The positively charged 30-50kDa MW-fraction had lower cleared urine activity (45.34% ID) when compared to the negatively charged 30-50 kDa (61.79 % ID), indicating some retention in the kidney (see Figure 4-2 on page 222 and Table 4-9 on page 230). The MW-fraction 20-30 kDa had the highest clearance of activity in urine at 75% ID at 3-hours and one of the lowest renal retentions of 14% OD at 3-hours (see Table 4-6 on page 226 and Table 4-9 on page 230). This study also demonstrated the required reduced normal bone uptake of  $^{99m}\text{Tc}$ -PEI-MP. The MW-fractions with the highest uptake in trabecular bone in relation to body was the 20 - 30 kDa at 19.93% OD (see Table 4-6 on page 226), which by comparison is more than double that for the other MW-fractions. While some retention in bone is good, the radiation dose could also be correspondingly higher. Other compartments such as lung and liver reflected also changes apparent in blood activity (see Table 4-10 on page 230). The negatively charged 50-100 kDa MW-fraction retained the highest activity in blood at 3-hours (16.10 % ID) compared to all other MW-fractions, which were  $\leq 4.33$  % ID. This was also reflected in the urine activity, which at 37.66% of the injected dose eliminated at 3-hours was the lowest for all MW-fractions (Table 4-9 on page 230).

The PEI-MP MW-fractions 10-30 kDa and 20-30 kDa were the most promising and fulfilled the hypothesized criteria of an ideal radiopharmaceutical. The mean blood  $t_{1/2-\alpha}$  and  $t_{1/2-\beta}$  for MW-fraction 10-30 kDa polymer (n=4) were  $4.76 \pm 1.5$  and  $61.78 \pm 39.08$  minutes respectively (Table 4-39 on page 255). Because of the wide standard deviation of the blood  $t_{1/2-\beta}$  for the MW-fraction 10-30 kDa polymer we studied 20-30 kDa polymer (n=4). The mean  $t_{1/2-\alpha}$  and  $t_{1/2-\beta}$  for 20-30 kDa polymer were  $5.50 \pm 1.38$  and  $38.55 \pm 9.46$  minutes respectively (Table 4-39 on page 255). The clearance of the % ID in urine at 3-hours was also significantly different between  $^{99m}\text{Tc}$ -PEI-MP MW-fractions, with the 20-30kDa fraction clearing 73.91 % ID compared to 69.75 % ID for the 10-30kDa MW-fraction (Table 4-39 on page 255). A single dog with osteosarcoma was given  $^{99m}\text{Tc}$ -PEI-MP 10-30kDa MW-fraction with similar pharmacokinetics as the normal dogs, with a renal clearance of 85.74 % ID. In keeping with the aims of the study, the 20-30kDa polymer was considered more desirable because of its faster clearance from blood ( $t_{1/2-\beta} = 38.55$  min) compared to the 10-30 kDa fraction ( $t_{1/2-\beta} = 61.78$  min). However, because of the limitations imposed by the percentage yield of the different molecular weights fractions during filtration (see Table 4-2 on page 218), the 10-30 kDa MW-fraction was selected to label  $^{153}\text{Sm}$ . The pharmacokinetic data for  $^{153}\text{Sm}$ -PEI-MP 10-30kDa fraction were similar to  $^{99m}\text{Tc}$ -PEI-MP 10-30kDa fraction except for a statistically significantly (longer)  $t_{1/2-\beta}$  ( $102.85 \pm 7.40$  minutes) for the  $^{153}\text{Sm}$ -PEI-MP 10-30kDa fraction (Table 4-39 on page 255). Clearance of % ID at 3-hours in urine was not statistically different between radionuclide groups; see Table 4-38 on page 251. The prolonged blood  $t_{1/2-\beta}$  of the  $^{153}\text{Sm}$ -PEI-MP 10-30kDa fraction could be explained by the with increased liver uptake (Table 4-36 on page 249). At this stage, it was apparent that the  $^{153}\text{Sm}$ -PEI-MP MW-fraction 10-30 kDa might have been experiencing *in vivo* instability. To explain this; computer modelling for blood plasma (ECCLES) was done which predicted that there would be some chemical dissociation of the  $^{153}\text{Sm}$  from the PEI-MP polymer in blood <sup>1</sup>. This is due to interaction of  $^{153}\text{Sm}$  with citrate, forming  $^{153}\text{Sm}$ -citrate <sup>1</sup>. Low levels of colloidal  $^{153}\text{Sm}$ -citrate were also predicated to accumulate in the liver. The computer modelling predicted that uncomplexed  $^{153}\text{Sm}^{3+}$  would accumulate in the liver and that possibly some dissociation of the  $^{153}\text{Sm}$  from PEI-MP (10-30kDa) which could cause increased liver uptake. The ECCLES model for blood plasma also predicted that the anionic MW-fraction, PEI-MP (10-30kDa), would be a poor ligand complexed to  $^{166}\text{Ho}$ ,  $^{212}\text{Pb}$ ,  $^{213}\text{Pb}$ , and  $^{89}\text{Sr}$ , but was expected to be effective when complexed to  $^{186}\text{Re}$  or  $^{188}\text{Re}$ , based on its close proximity to  $^{99m}\text{Tc}$  on the periodic table <sup>1</sup>.

While initial work was done complexing  $^{186}\text{Re}$  to PEI-MP MW-fractions, the results were regrettably too incomplete to be including in this thesis. Part of the reason for the incomplete data was the technical difficulty associated with the low specific activity of the  $^{186}\text{Re}$  radionuclide. The low specific activity leads to low a labelling efficiency of the ligand.

The pharmacokinetic parameters of the PEI-MP MW-fractions (10-30kDa and 20-30 kDa) where then compared to  $^{188}\text{Re}$ -HEDP and  $^{153}\text{Sm}$ -EDTMP, see the Appendix; see Table 8-28 on page 317, Table 8-29 on page 319 and Table 8-30 on page 323 \*. Interestingly, the blood  $T_{1/2}$  for all radiopharmaceuticals ( $^{99\text{m}}\text{Tc}$ -PEI-MP 10-30kDa,  $^{99\text{m}}\text{Tc}$ -PEI-MP 20-30kDa,  $^{153}\text{Sm}$ -PEI-MP 10-30kDa,  $^{188}\text{Re}$ -HEDP and  $^{153}\text{Sm}$ -EDTMP) was not found to be statistically different (Table 8-30 on page 323). This was also true for dogs with osteosarcoma that received  $^{188}\text{Re}$ -HEDP and  $^{153}\text{Sm}$ -EDTMP. Since blood  $T_{1/2}$  is representative of the distribution phase and elimination of the radiopharmaceutical from blood to the rest of the body and it reflects the uptake by target tissues and clearance from the central compartment for all isotopes (Table 8-30 on page 323). Remarkably, even though the PEI-MP MW-fractions (ranging from 3 kDa to 30 kDa MW-fractions) have significantly larger molecular weight than bisphosphonates their pharmacokinetic behaviour is similar (see Table 1-6 on page 50 and Table 1-7 on page 65 for MW details). This is in contrast to the very prolonged blood  $T_{1/2}$  found with liposomal and immunotherapy radiopharmaceuticals <sup>264</sup>. A number of other organ compartments (cardiac, liver, kidneys, bone and background) were found to have statistically different pharmacokinetic parameters ( $T_{1/2}$ , % OD at 3-hours) between radiopharmaceuticals, see Table 8-29 on page 319. The most significant difference between radiopharmaceuticals occurred in the liver where the  $^{153}\text{Sm}$ -PEI-MP 10-30kDa fraction differed significantly from all other radiopharmaceuticals with a prolonged  $T_{1/2}$  (median = 42 min) and increased percentage OD at 3-hours (median = 21.57 %). The other significant difference between radiopharmaceuticals in bone occurred in the trabecular compartment, where  $^{153}\text{Sm}$ -EDTMP differed significantly from all other radiopharmaceuticals with a prolonged  $T_{1/2}$  (median  $\geq$  180 min) and increased percentage OD at 3-hours (median = 33.67 %). The significance of these findings has already been covered earlier in this discussion and will not be discussed again.

---

\* **Note:** Data in Table 8-29 are expressed as medians in contrast to means found in other pharmacokinetic tables in the text, and therefore may differ marginally in value when reporting the same pharmacokinetic parameters

The static image of a dog in Figure 4-10 on page 236 and the time-activity curve results in Figure 4-11 on page 236 clearly demonstrate the ability of  $^{99m}\text{Tc}$ -PEI-MP 10-30 kDa MW-fraction to localize and to be retained in the osteosarcoma in a similar way to  $^{153}\text{Sm}$ -EDTMP. In addition, the pharmacokinetic data for  $^{99m}\text{Tc}$ -PEI-MP 10-30 kDa fraction in the cardiac, lung, liver, kidneys, bone, and background compartments in the osteosarcoma dog (n=1) are similar to the normal dogs receiving  $^{99m}\text{Tc}$ -PEI-MP 10-30 kDa fraction (n=4), see Figure 4-10 on page 236 and Table 4-39 on page 255. The main difference between normal dogs and the cancer dog was in the % ID eliminated at 3-hours in the urine; see Table 4-39 on page 255. The osteosarcoma dog eliminated 85.74% of the injected dose at 3-hours in the urine compared to a mean of 69.75 % for the normal dogs. It is difficult to draw conclusion from the results for urine clearance, as there was only a single dog in the experiment. Nevertheless, the  $^{99m}\text{Tc}$ -PEI-MP MW-fractions 10-30kDa (69.75 % ID) and 20-30 kDa (73.91 % ID) do have high urine elimination rates at 3-hours compared to  $^{153}\text{Sm}$ -EDTMP (44.34 % ID), see Table 3-36 on page 157 and Table 4-39 on page 255. The eliminated % ID at 3-hours in the  $^{153}\text{Sm}$ -EDTMP osteosarcoma dog, was 29.17%.

While the ligand is responsible for the pharmacokinetics of the radiopharmaceutical, the nuclide is responsible for the radiation dose to the tumour. The effect of radiation is best expressed by the biologically effective dose (BED) and is defined by the product of the total physical dose (TD) received by a tissue and a modifying factor (RE) for that tissue<sup>131</sup>. While we can calculate the TD and rate received by the tumour, knowing the RE factor for each tissue type is crucial, as each tumour or tissue type has its own BED<sup>131, 132</sup>. The two most important radiobiological parameters required in the definition of RE are the tissue  $\alpha/\beta$  ratio and the sub-lethal damage recovery constant ( $\mu$ )<sup>132</sup>. The  $\alpha/\beta$  ratios provides a quantitative indication of the sensitivity of a given tissue, normal or cancerous, to changes in MW-fractionation or dose rate and are derived from the Linear Quadratic (LQ) formulation<sup>132</sup>. In an in-vitro study<sup>268</sup>, we found that canine osteosarcoma cell lines were relatively radio resistant, with alpha/beta ratios of 3.47, which are similar to those of normal, late-responding tissues. In addition, the survival fraction at 2-Gray (SF<sub>2</sub>) was relatively high at 0.62. Survival fraction at 2 Gray is used to compare intrinsic radiation sensitivities between cells<sup>269</sup>. We also did split-dose experiments (SLD) which showed a 2.8 to 3.9 fold increase in cell survival when the radiation doses were separated by 24 hrs. as opposed to 0 hrs. Split-dose experiments are a factor in establishing sub-lethal damage recovery constant ( $\mu$ ). In conclusion, the study found the low  $\alpha/\beta$  ratio and high SF<sub>2</sub> of the osteosarcoma

cell lines predict that canine osteosarcomas will be difficult to treat effectively with conventional fractionated radiotherapy protocols (e.g., 3.0 Gy X 19 MW-fractions) and that larger dose per fraction are needed to induce greater tumour cell kill. While these studies were done with external beam radiation, they do have implication for selection of the radionuclide therapy in targeted radiotherapy (TRT). As previously discussed in the introduction, TRT is a form of continuous low-dose radiation delivery (CLDR) i.e. highly MW-fractionated radiotherapy. Due to the pharmacokinetics and the exponential decay of radionuclide, the dose rate to the tumour is not held constant<sup>133</sup>. As with external beam radiation and CLDR, the delivery of radiation at varying dose-rates creates both lethal and sub-lethal damage<sup>133</sup>. Consequently, it is apparent that simply choosing a radionuclide based on the total physical dose (TD) is likely to lead to poor therapeutic responses especially when dealing with radiation resistant cancers e.g. osteosarcomas, which have rapid repair ability and respond better to hypo-fractionated therapy. Indeed in the case of canine osteosarcoma and potentially human osteosarcoma, the  $\beta$ -emitters such as  $^{153}\text{Sm}$  or  $^{188}\text{Re}$  or  $^{186}\text{Re}$  while having the required ability to deliver an adequate dose to the osteosarcoma, they are less likely to have a therapeutic effect. This could have been the reason why our median survival time for all osteosarcoma dogs was only 4-months compared to the 10-months plus for traditional amputation and chemotherapy.

Looking to the future there is interest in the radionuclide  $^{117\text{m}}\text{Sn}$ (Tin) which decays by emitting conversion electrons with gamma (photons) and has a half-life of 13.6 days<sup>270</sup>. In addition, work with PEI-MP 10-30kDa MW-fraction has been done in primates by Zeevaart et.al.<sup>271</sup>. The article indicates that complexing  $^{117\text{m}}\text{Sn}$  with PEI-MP is chemically feasible and may result in a new therapeutic radiopharmaceutical. While difficult to produce, new methods of production by cyclotron are being explored<sup>272</sup>.

## Chapter 7. Conclusions

This innovative and unique study allowed for the evaluation of various radiopharmaceuticals in a naturally occurring animal model of bone cancer, also documenting the pharmacokinetics, and dosimetry of a novel radiolabelled-ligand (PEI-MP). Benefits accruing from the successful completion of the study would allow more rapid transfer of rodent preclinical data into a naturally occurring canine cancer model that resembles more closely the human diseases and thus more likely to identify problems with pharmacokinetics and drug toxicities before proceeding to expensive clinical trials. The aims and expected outcomes of the study were formulated based on previously published data in dogs and primates. The study met the majority of outcomes with the exception of labelling of PEI-MP with  $^{153}\text{Sm}$ . Problems with labelling of the  $^{153}\text{Sm}$ -PEI-MP complex were first identified during scintigraphy imaging as increased liver uptake. This was subsequently predicted using computer software (ECCLES), which characterized the interaction of  $^{153}\text{Sm}$ -PEI-MP complex with citrate ions in blood. In addition, rapid deterioration of the  $^{188}\text{Re}$  generator also led to earlier than expected curtailment of the  $^{188}\text{Re}$ -HEDP therapeutic trial, although sufficient data were available to compare with other radiopharmaceuticals. This was unfortunate, as haematological toxicity data indicated that dose escalation was still possible and that the maximum tolerated dose had not yet been achieved.

Our study also highlighted the inherent limitations present in  $\beta$ -emitting radionuclides such as  $^{153}\text{Sm}$  and  $^{188}\text{Re}$  complexed with bisphosphonate ligands. The biodistribution, dosimetry and reported toxicity confirms the bone marrow as the dose limiting organ in the body, which currently limits the radiation dose to the tumour. Important, even though the radiation dose achieved by radiopharmaceuticals falls within the range reported for teletherapy, the distribution is heterogenous and therefore parts of the tumour do not receive an adequate dose due to variation in blood supply and tumour microenvironment. Even if we were able to improve distribution, the inherent radiosensitivity of the tumour is crucial to understanding which cancers are more suited to the continuous low-dose radiation delivery (CLDR) by  $\beta$ -emitting radionuclides. It is clear from our research and others that osteosarcoma appears not to be very sensitive as borne out by the 4-month median survival time. Nevertheless where tumour types are more sensitive to  $\beta$ -emitting radionuclides e.g. leukemias, a good response may be possible - as reported in preliminary trials in humans with multiple myeloma <sup>273</sup>. Multiple myeloma derived

from plasma cells is inherently more sensitive to radiation than osteosarcoma and is often diffusely spread throughout the bone marrow. Since radionuclides labelled with bisphosphonates e.g.  $^{153}\text{Sm}$ -EDTMP are characterized by their high uptake in red bone marrow areas and are delivered by blood allowing a more uniform dose delivery to bone.

As mentioned in the discussion a number other radionuclides could potentially hold promise labelled to PEI-MP, these include  $^{186}\text{Re}$  (our own experience) and  $^{117\text{m}}\text{Sn}$  <sup>271</sup>. Both have shown promising results when complexed to PEI-MP, and can be tested in the canine model. Nevertheless, research using  $^{186}\text{Re}$  is complicated by low specific activity which reduces the chance of labelling the ligand efficiently. In an encouraging report by Jansen *et. al.*, <sup>274</sup> the 10-30 kDa PEI-MP fraction showed enhanced adsorption on hydroxyapatite when complexed with  $^{117\text{m}}\text{Sn}$  in the laboratory. While preliminary, this report provided a suggestion that the  $^{117\text{m}}\text{Sn}$  - PEI-MP complex could be promising as a bone-seeking radiopharmaceutical, since the maximum adsorption capacities are comparable to other radiopharmaceuticals and PEI-MP 10-30 MW-fraction offers the opportunity of using the EPR effect for enhanced tumor accumulation and reduced red marrow uptake. The polymer PEI-MP is in its self, potentially adaptable to having multiple functional chelates bound to it. This offers the potential to make a bifunctional PEI-MP complex to carry a therapeutic radionuclide and a radiosensitizer or chemotherapy drug.

More recently significant interest has been shown in the alpha-emitter  $^{233}\text{Ra}$  <sup>5, 275-277</sup>. The  $^{233}\text{Ra}$  commercial product (Alpharadin®) has shown promise as a therapy for hormone nonresponsive prostate cancer and is the subject of a multinational phase III ALSYMPCA (Alpharadin in SYMptomatic Prostate CANcer patients) study for bone metastases. Potentially  $^{233}\text{Ra}$  may hold promise as a therapeutic agent for osteosarcoma. However there is a cautionary note as  $\alpha$ -emitters are linked to causing osteosarcoma in the beagle dog model <sup>278</sup>.

## Chapter 8. Appendices

### 8.1 Client consent form

#### Consent Form

I, \_\_\_\_\_

Herewith give permission that my dog

(Name of dog) \_\_\_\_\_

(Breed, sex, colour) \_\_\_\_\_.

May participate in the clinical study in the Department of Internal Medicine, Faculty of Medicine, and University of Pretoria.

I have read the information pamphlet and the study has been explained to me I understand that at any time I can withdraw my dog from the clinical trial. Furthermore, I understand that no costs will be incurred by me in respect of the study except for routine radiographs (X-rays) as well as haematology (blood tests), which are done once a month on routine visits to the Faculty or Private Veterinarian. I also give permission that my dog may stay overnight at the Pretoria Biomedical Research Centre

Signed at \_\_\_\_\_ (Place) on the \_\_\_\_\_ day of \_\_\_\_\_

(Signature of owner or authorized person)



## 8.2 Study information pamphlet

**Title of the Research: “Targeted radiotherapy of naturally occurring canine osteosarcomas using beta-emitting radio-isotopes with various ligands.”**

**Addendum To Above Research:**

**Title of Research: “Carboplatin radiosensitization for  $^{153}\text{Sm}$ -EDTMP limb-salvage therapy of canine osteosarcoma”.**

Bone cancer (osteosarcoma) is a relatively common condition of large breed of dogs. Currently the most successful method of treating this condition is to amputate the affected limb and to give chemotherapy every 3 weeks for 3 to 4 treatments. This treatment is not curative but controls the pain associated with this cancer as well as giving the dog a good quality of life until the cancer spreads to lungs or other organs. However there is a group of dogs that cannot undergo this treatment because of their size e.g., Great Dane. Until recently, no other form of treatment was available. We are currently investigating the efficacy of radioactive particles (radioisotopes) that have been linked to bone localizing agents. The bone cancer takes up the particle and because the cancer has rapidly dividing cells in it, it is sensitive to radiation. We have had one dog responding to the treatment but the other dogs in the group have not responded, as we would have hoped. We are currently using a radioisotope called  $^{153}\text{Sm}$ -EDTMP in combination with chemotherapy (carboplatin) infusions, which seems to exhibit promising results. Your pet will initially be x-rayed to determine if the cancer has spread, should this be the case they be excluded from the trial. If you allow us to use your dog in the study, we will require that you leave him or her with us for a 48-hour period. In this time a bone scan, chemotherapy infusion, haematology and bone biopsy will be done. Your pet will be discharged and you are requested to return to the Pretoria Biomedical Research Centre or your veterinarian on a regular basis depending on your dogs' response to treatment, for blood tests and follow-up chemotherapy.

Thank you for taking time to read the pamphlet.

Dr. R J Milner BVSc (Hons) MMedVet (Med) Dip ECVIM

Department of Internal Medicine, AEC Institute for Life Sciences

Faculty of Medicine

University of Pretoria

### 8.3 Data analysis calculations used for all radiopharmaceuticals

**Table 8-1 Manually calculated decay correction factors (DF\*) for radioisotopes used in the study**

<b>Time (hours)</b>	<b><sup>99m</sup>Tc (T<sub>1/2</sub> = 6.03-hours)</b>	<b><sup>186</sup>Re (T<sub>1/2</sub> = 89.2480 hours)</b>	<b><sup>188</sup>Re (T<sub>1/2</sub> = 17.001 hours)</b>	<b><sup>153</sup>Sm (T<sub>1/2</sub> = 46.2853-hours)</b>
<b>0</b>	1.0000	1.0000	1.0000	1.0000
<b>60</b>	0.8914	0.9923	0.9601	0.9851
<b>120</b>	0.7947	0.9846	0.9217	0.9705
<b>180</b>	0.7084	0.9770	0.8850	0.9561
<b>240</b>	0.6315	0.9694	0.8496	0.9419

Legend: Decay correction equation takes into account the exponential decrease of activity of a radioisotope with time and is given by the equation:  $A_t = A_0 e^{-0.693 \frac{t}{T}}$  where  $A_0$  is the initial activity,  $A_t$  is the activity after additional time  $t$  has elapsed and  $T$  is the half-life of the radioisotope, expressed in the same units as  $t$ . The ratio  $A_t/A_0$  is called the decay correction factor (DF\*) of the radioisotope for elapsed time  $t$ . Therefore the equation for DF can be expressed as  $DF = e^{-0.693 \frac{t}{T}}$ . For this study, decay corrected data are automatically calculated by the Sopha Forthmacs software for up to 59 minutes. For elapsed times ( $t$ ) 60, 120, 180 minutes, the manually calculated DF for <sup>99m</sup>Tc, <sup>186</sup>Re, <sup>188</sup>Re and <sup>153</sup>Sm, are shown in the table above. The table reports DF to the fourth decimal point, which is currently the accepted convention.

**Table 8-2 An example of spread sheet calculations derived from a dynamic  $^{153}\text{Sm}$ -EDTMP scintigraphy study in a normal dog**

DECAYED DATA										DECAY CORRECTED							
TIME (min)	CARD	LUNG	LIVER	LKID	RKID	CBONE	TBONE	BG	DF*	CARD	LUNG	LIVER	LKID	RKID	CBONE	TBONE	BG
0	68	22	12	19	23	11	5	5	1	68	22	12	19	23	11	5	5
1	35	23	14	28	34	10	6	6	1	35	23	14	28	34	10	6	6
2	29	20	13	32	40	10	6	6	1	29	20	13	32	40	10	6	6
3	26	18	11	28	34	10	6	6	1	26	18	11	28	34	10	6	6
↓	↓	↓	↓	↓	↓	↓	↓	↓	↓	↓	↓	↓	↓	↓	↓	↓	↓
59	8	6	4	5	7	3	11	6	0.99	8	6	4	5	7	3	11	6
60	8	6	4	5	7	3	11	6	0.98	8	6	4	5	7	3	11	6
120	7	6	3	3	5	1	11	6	0.97	8	6	4	3	5	1	11	6
180	7	6	3	2	4	1	11	5	0.95	7	6	3	2	4	1	11	6

Legend: The spreadsheet represents an example of ROI activity (average counts per pixel) over time (0 to 180 minutes) for a dynamic scintigraphy study of a normal dog using  $^{153}\text{Sm}$ -EDTMP. The table is representative of the Excel spreadsheet used to calculate decay corrected data for all time points. The decay corrected data was used in pharmacokinetic and dosimetry software calculations. In addition the decay corrected biodistribution data allowed for comparisons to be made between short half-life radioisotopes (e.g.,  $^{99\text{m}}\text{Tc}$   $T=6.9$  hrs.) and longer half-life radioisotopes (e.g.,  $^{153}\text{Sm} = 46.28$  hrs.). To determine the decay correction for the isotope ( $^{153}\text{Sm}$ ) at 60, 120 and 180 minutes, the decayed ROI activity was divided by the decay factor in the spreadsheet for that time point. For example, if the decayed activity for the cardiac ROI at 180 minutes was 7 counts per pixel then the decay corrected value was  $7/0.95 = 7.36$  counts per pixel (The table shows no decimal places, because of space constraints). For details on other radioisotopes see Table 8-1 (page 274)

**Table 8-3 An example of spreadsheet calculations derived from a 1-hour static scintigraphy study in a normal dog receiving  $^{153}\text{Sm}$ -EDTMP.**

Region of Interest	Static Counts	CF*	Converted Counts	Static Counts	DF**	Decay Corrected	CF*	Converted counts Decay Corrected
CARD	16	0.51	8.00	16	0.98	16.01	0.51	8.16
LUNG	12	0.51	6.00	12	0.98	12.00	0.51	6.12
LIVER	8	0.52	4.00	8	0.98	7.85	0.52	4.08
LKID	9	0.53	5.00	9	0.98	9.63	0.53	5.10
RKID	14	0.51	7.00	14	0.98	14.01	0.51	7.14
CBONE	6	0.50	3.00	6	0.98	6.12	0.50	3.06
TBONE	22	0.50	11.00	22	0.98	22.45	0.50	11.22
BG	13	0.48	6.00	12.50	0.98	12.76	0.48	6.12

Legend: The conversion factor (CF\*) was calculated by taking the last count recorded for each ROI in the dynamic study (59 min) and dividing it by the static count (60 min) for the same ROI. This calculation gives a CF for each static ROI, which is used to convert the counts recorded at 2, 3 and 4 hours. The same CF is used for both decayed and decay corrected counts. As previously described in Table 8-1, the ROI decayed counts are divided by the calculated decay factor (DF\*\*) to give a decay corrected count. Following calculations for time points at 120 and 180 minutes the converted counts were then added to the appropriate rows in the example shown in Table 8-2 (page 275).

**Table 8-4 An example of the percentage organ distribution calculations derived from a scintigraphy study in a normal dog receiving  $^{153}\text{Sm}$ -EDTMP.**

TIME (min)	Average Counts per ROI									TIME (min)	Percentage organ distribution (%OD)* per ROI								
	CARD	LUNG	LIVER	LKID	RKID	CBONE	TBONE	BG	Total**		CARD	LUNG	LIVER	LKID	RKID	CBONE	TBONE	BG	
0	68	22	12	19	23	11	5	5	165	0	41.21	13.33	7.27	11.52	13.94	6.67	3.03	3.03	
1	35	23	14	28	34	10	6	6	156	1	22.44	14.74	8.97	17.95	21.79	6.41	3.85	3.85	
2	29	20	13	32	40	10	6	6	156	2	18.59	12.82	8.33	20.51	25.64	6.41	3.85	3.85	
3	26	18	11	28	34	10	6	6	139	3	18.71	12.95	7.91	20.14	24.46	7.19	4.32	4.32	
↓	↓	↓	↓	↓	↓	↓	↓	↓	↓	↓	↓	↓	↓	↓	↓	↓	↓	↓	
59	8	6	4	5	7	3	11	6	51	59	16.12	12.09	8.06	10.08	14.11	5.88	21.57	12.09	
60	8	6	4	5	7	3	11	6	51	60	16.12	12.09	8.06	10.08	14.11	5.88	21.57	12.09	
120	8	6	4	3	5	1	11	6	43	120	17.44	13.78	8.15	7.02	11.36	3.00	25.70	13.56	
180	7	6	3	2	4	1	11	6	40	180	18.24	14.99	7.28	5.69	10.40	2.66	26.83	13.91	

Legend: The spreadsheet was used to calculate the percentage organ distribution (%OD)\* for each ROI time point. The %OD was derived (decayed or decayed corrected) by summing the data (Total\*\*) for each ROI time point and then expressing each ROI time point as a percentage of the total for that time point (e.g., at 0 min the cardiac ROI= 68 counts, which when expressed as %OD =  $68/165 \times 100 = 41.21\%$ ). The %OD per ROI was then used in further calculations to determine, for example, the percentage injected dose (% ID) for each ROI time point, see Table 8-5 on page 278 and Table 8-8 on page 281 for further calculations.

**Table 8-5 An example of calculations used to derive urine time-activity curves and body retention curves expressed as a percentage injected dose for a dog receiving  $^{153}\text{Sm}$ -EDTMP.**

URINE SAMPLES					Injected Dose = 4.89mCi					
TIME (min)	VOL (ml)	Counts / ml	Total counts	DF	D.corr.cts	CF (EQP)	IDu mCi	Cum. Amt. IDu mCi	% IDu	ID Body mCi
0	0	0.00E+00	0.00E+00	0.2442	0.00E+00	1.76E-06	0.0000	0.00	0.00	4.89
5	24	1.99E+06	4.78E+07	0.2442	8.15E+06	1.76E-06	0.1434	0.14	2.93	4.75
10	4	2.58E+06	1.03E+07	0.2442	1.06E+07	1.76E-06	0.1866	0.33	6.75	4.56
15	6	2.87E+06	1.72E+07	0.2442	1.17E+07	1.76E-06	0.2059	0.54	10.96	4.35
20	12	2.48E+06	2.98E+07	0.2442	1.02E+07	1.76E-06	0.1795	0.72	14.63	4.17
25	7	2.07E+06	1.45E+07	0.2442	8.47E+06	1.76E-06	0.1491	0.86	17.68	4.03
30	2	2.05E+06	4.10E+06	0.2442	8.41E+06	1.76E-06	0.1480	1.01	20.71	3.88
35	3	2.84E+06	8.52E+06	0.2442	1.16E+07	1.76E-06	0.2042	1.22	24.88	3.67
40	6.5	2.44E+06	1.59E+07	0.2442	9.98E+06	1.76E-06	0.1756	1.39	28.47	3.50
45	6	2.87E+06	1.72E+07	0.2442	1.18E+07	1.76E-06	0.2077	1.60	32.72	3.29
50	2	2.82E+06	5.64E+06	0.2442	1.15E+07	1.76E-06	0.2024	1.80	36.86	3.09
55	1.5	2.75E+06	4.13E+06	0.2442	1.12E+07	1.76E-06	0.1971	2.00	40.89	2.89
60	4	2.52E+06	1.01E+07	0.2442	1.03E+07	1.76E-06	0.1813	2.18	44.60	2.71
120	34	1.45E+06	4.93E+07	0.2442	5.95E+06	1.76E-06	0.1047	2.29	46.74	2.60
180	37	4.77E+05	1.76E+07	0.2442	1.95E+06	1.76E-06	0.0343	2.32	47.44	2.57

Legend: The spreadsheet above shows the calculations used to derive the injected dose excreted in urine (IDu) or the inverse, which is the dose retained in the body. To calculate the eliminated activity in urine, the counts per ml of urine (for each time point) were multiplied by the urine volume (VOL) produced to give a total urine activity (Total Counts) for that time point. Since the urine activity was counted 94 hours after sampling, a decay factor (DF=0.2442) was necessary to correct for  $^{153}\text{Sm}$  radionuclide decay. In addition a correction factor (CF [EQP] =  $1.76 \times 10^{-6}$  for  $^{153}\text{Sm}$ ) was required for the well counter to convert the urine counts to millicuries (mCi). Thus, IDu = [(Total counts / DF) x CF]/100. The cumulative amount (Cum. Amt. IDu) was calculated by adding the cumulative activity (mCi) from previous time point to the next time point to arrive at a total urine activity at 3-hours. The % IDu = (Cum. Amt. IDu mCi) / (ID mCi) x 100. The dose in the body is the inverse of the eliminated amount found in urine (Cum. Amt. IDu mCi).

**Table 8-6 An example of calculations used to derive blood time-activity curves for a dog receiving  $^{153}\text{Sm}$ -EDTMP**

BLOOD SAMPLES				Body weight (BW) = 27 kg. Blood volume (BV) = 87ml/kg. ID = 4.89 mCi			
Time (min)	Total BV (ml)	Counts / ml	CF (EQP)	Total Activity (mCi)	DF	IDb mCi	% IDb
0	2349	0	1.76E-06	0.00E+00	0.2442	0.00	0.00
3	2349	75553	1.76E-06	3.12E-01	0.2442	1.28	26.16
6	2349	58573	1.76E-06	2.42E-01	0.2442	0.99	20.28
9	2349	57567	1.76E-06	2.38E-01	0.2442	0.97	19.93
14	2349	25005	1.76E-06	1.03E-01	0.2442	0.42	8.66
19	2349	20734	1.76E-06	8.57E-02	0.2442	0.35	7.18
24	2349	20998	1.76E-06	8.68E-02	0.2442	0.36	7.27
29	2349	19458	1.76E-06	8.04E-02	0.2442	0.33	6.74
34	2349	16010	1.76E-06	6.62E-02	0.2442	0.27	5.54
39	2349	14680	1.76E-06	6.07E-02	0.2442	0.25	5.08
44	2349	12869	1.76E-06	5.32E-02	0.2442	0.22	4.46
49	2349	11477	1.76E-06	4.74E-02	0.2442	0.19	3.97
54	2349	10372	1.76E-06	4.29E-02	0.2442	0.18	3.59
59	2349	5818	1.76E-06	2.41E-02	0.2442	0.10	2.01
120	2349	3045	1.76E-06	1.26E-02	0.2442	0.05	1.05
180	2349	1344	1.76E-06	5.56E-03	0.2442	0.02	0.47

Legend: The spreadsheet above shows the calculations used to derive the pharmacokinetics of the injected dose in blood (IDb). To calculate the activity in blood, the counts per ml of blood (for each time point) were multiplied by the total blood volume (BV = 87ml/kg)<sup>279</sup>. Since the blood activity was counted sometime after sampling, a decay factor (DF) was used to correct for radionuclide decay for  $^{153}\text{Sm}$ , in this case DF=0.2442. In addition a correction factor (CF [EQP] =  $1.76 \times 10^{-6}$  for  $^{153}\text{Sm}$ ) was required for the well counter to convert the blood counts to millicuries (mCi). Thus, IDb = (Total counts x CF) / DF. The % IDb = (IDb mCi) / (ID mCi) x 100. The data points for blood were then imported into pharmacokinetic software (PK Solutions). The software resolves a curve into a series of exponential terms (first-order rate processes) corresponding to the distribution ( $t_{1/2\alpha}$ ), and elimination ( $t_{1/2\beta}$ ) phases occurring during the time course of the drug in the blood.

**Table 8-7 An example of calculations used to derive organ activity (mCi) from %OD for a dog receiving  $^{153}\text{Sm}$ -EDTMP**

Time (min)	%OD								ID BODY	Time (min)	ID mCi							
	CARD	LUNG	LIVER	LKID	RKID	TRAB	BONE	BG			CARD	LUNG	LIVER	LKID	RKID	TRAB	BONE	BG
0	41.21	13.33	7.27	11.52	13.94	3.03	6.67	3.03	4.89	0	2.02	0.65	0.36	0.56	0.68	0.15	0.33	0.15
5	19.47	13.27	7.96	18.58	22.12	6.19	7.08	5.31	4.75	5	0.92	0.63	0.38	0.88	1.05	0.29	0.34	0.25
10	17.98	12.36	7.87	16.85	20.22	10.11	7.87	6.74	4.56	10	0.82	0.56	0.36	0.77	0.92	0.46	0.36	0.31
15	17.95	12.82	8.97	15.38	19.23	11.54	6.41	7.69	4.35	15	0.78	0.56	0.39	0.67	0.84	0.50	0.28	0.33
20	17.39	13.04	7.25	14.49	18.84	13.04	7.25	8.70	4.18	20	0.73	0.54	0.30	0.61	0.79	0.54	0.30	0.36
25	17.46	12.70	7.94	14.29	17.46	14.29	6.35	9.52	4.03	25	0.70	0.51	0.32	0.58	0.70	0.58	0.26	0.38
30	15.94	12.75	7.97	14.34	17.53	15.63	4.69	11.16	3.88	30	0.62	0.49	0.31	0.56	0.68	0.61	0.18	0.43
35	16.74	11.72	8.37	15.07	16.74	16.40	4.92	10.04	3.67	35	0.61	0.43	0.31	0.55	0.61	0.60	0.18	0.37
40	18.27	10.96	7.31	12.79	16.44	17.90	5.37	10.96	3.50	40	0.64	0.38	0.26	0.45	0.58	0.63	0.19	0.38
45	18.09	12.06	10.05	12.06	14.07	19.69	3.94	10.05	3.29	45	0.60	0.40	0.33	0.40	0.46	0.65	0.13	0.33
50	18.10	12.06	8.04	10.05	14.07	19.70	5.91	12.06	3.09	50	0.56	0.37	0.25	0.31	0.43	0.61	0.18	0.37
55	16.42	12.31	8.21	10.26	14.36	22.11	4.02	12.31	2.89	55	0.47	0.36	0.24	0.30	0.42	0.64	0.12	0.36
60	16.12	12.09	8.06	10.08	14.11	21.57	5.88	12.09	2.71	60	0.44	0.33	0.22	0.27	0.38	0.58	0.16	0.33
120	17.44	13.78	8.15	7.02	11.36	25.70	3.00	13.56	2.60	120	0.45	0.36	0.21	0.18	0.30	0.67	0.08	0.35
180	18.24	14.99	7.28	5.69	10.40	26.83	2.66	13.91	2.57	180	0.47	0.39	0.19	0.15	0.27	0.69	0.07	0.36

Legend: The organ activity in mCi was calculated from the %OD (see Table 8-4 on page 277) multiplied by injected dose (ID) retained in the body e.g. cardiac (CARD) activity at 0 hour = (41.21% x 4.89mCi = 2.02 mCi)



**Table 8-8 An example of calculations used to derive the percentage injected dose (% ID) for a dog receiving  $^{153}\text{Sm-EDTMP}$**

% ID: Organ Distribution									Total % ID
Time (min)	CARDIAC	LUNG	LIVER	LKID	RKID	TRAB	BONE	BG	Retained in the body
0	41.21	13.33	7.27	11.52	13.94	3.03	6.67	3.03	100.00
5	18.90	12.88	7.73	18.04	21.47	6.01	6.87	5.15	97.07
10	16.77	11.53	7.34	15.72	18.86	9.43	7.34	6.29	93.27
15	15.98	11.42	7.99	13.70	17.12	10.27	5.71	6.85	89.04
20	14.85	11.14	6.19	12.37	16.09	11.14	6.19	7.42	85.38
25	14.38	10.46	6.53	11.76	14.38	11.76	5.23	7.84	82.34
30	12.64	10.11	6.32	11.38	13.90	12.40	3.72	8.85	79.31
35	12.58	8.80	6.29	11.32	12.58	12.32	3.70	7.55	75.13
40	13.07	7.84	5.23	9.15	11.76	12.80	3.84	7.84	71.54
45	12.17	8.12	6.76	8.12	9.47	13.25	2.65	6.76	67.31
50	11.43	7.62	5.08	6.35	8.89	12.44	3.73	7.62	63.15
55	9.70	7.28	4.85	6.06	8.49	13.07	2.38	7.28	59.10
60	8.93	6.70	4.47	5.58	7.81	11.95	3.26	6.70	55.39
120	9.29	7.34	4.34	3.74	6.05	13.69	1.60	7.22	53.25
180	9.58	7.88	3.83	2.99	5.47	14.10	1.40	7.31	52.55

Legend: The percentage injected dose (% ID) was calculated from the ID (ROI) divided by the ID (Body) expressed a percentage; see Table 8-5 on page 278. Thus the % ID at 1 hour for the cardiac ROI was  $(0.44 \text{ mCi} / 4.89 \text{ mCi}) \times 100 = 8.93\%$ . These decay corrected data of % ID were used imported into OLINDA software which was used for dosimetry calculations.

**Table 8-9 An example of manual calculations used to derive AUC and residence time curves for a dog receiving  $^{153}\text{Sm-EDTMP}$** 

AUC AND RESIDENCE TIME (Trapezoid method)								
Time (hr's)	CARD	LUNG	LIVER	LKID	RKID	BONE	BG	TRBONE
0	0.1078	0.0470	0.0269	0.0530	0.0635	0.0243	0.0147	0.0162
5	0.0727	0.0497	0.0307	0.0688	0.0822	0.0289	0.0233	0.0315
10	0.0667	0.0467	0.0312	0.0599	0.0733	0.0266	0.0268	0.0402
15	0.0628	0.0460	0.0289	0.0531	0.0677	0.0242	0.0291	0.0436
20	0.0595	0.0440	0.0259	0.0492	0.0621	0.0233	0.0311	0.0467
25	0.0550	0.0419	0.0262	0.0471	0.0576	0.0182	0.0340	0.0492
30	0.0514	0.0385	0.0257	0.0462	0.0540	0.0151	0.0334	0.0504
35	0.0523	0.0339	0.0235	0.0417	0.0496	0.0154	0.0314	0.0512
40	0.0514	0.0325	0.0244	0.0352	0.0433	0.0132	0.0298	0.0531
45	0.0481	0.0321	0.0241	0.0295	0.0374	0.0130	0.0293	0.0523
50	0.0431	0.0303	0.0202	0.0253	0.0354	0.0124	0.0303	0.0520
55	0.0380	0.0285	0.0190	0.0237	0.0332	0.0115	0.0285	0.0510
60	0.4455	0.3431	0.2152	0.2279	0.3389	0.1187	0.3403	0.6268
120	0.4614	0.3719	0.1996	0.1644	0.2815	0.0733	0.3553	0.6794
180	0.4679	0.4118	0.1962	0.1432	0.1585	0.0733	0.3738	0.7409
<b>AUC (mCi-hours)</b>	2.0835	1.5980	0.9179	1.0683	1.4382	0.4914	1.4111	2.5843
<b>RES TIME (hrs.)</b>	0.4261	0.3268	0.1877	0.2185	0.2941	0.1005	0.2886	0.5285

Legend: Definition of AUC trapezoid method:  $A_x = (0.5 \times [\text{base1} + \text{base 2}]) \times \text{height}$ . The sum of all the  $A_x$  from 0-3-hours gives the AUC. RES TIME (3-hour Residence time). The residence time is the area under a source organ's time-activity curve divided by the administered activity<sup>211</sup>. For example, if the area under the time-activity curve is 2.08 millicurie-hours, and the activity administered was 4.89 millicuries, the residence time is  $2.08/4.89 = 0.43$  hours.

## 8.4 Biodistribution and pharmacokinetic tables for dogs receiving various radiopharmaceuticals

**Table 8-10 Biodistribution and pharmacokinetic data for individual dogs undergoing dynamic scintigraphy receiving  $^{153}\text{Sm}$ -EDTMP**

Radiopharmaceutical	$^{153}\text{Sm}$ -EDTMP				
	Dog 1	Dog 2	Dog 3	Dog 4	Mean $\pm$ SD
Region of Interest					
$T_{1/2}$ Cardiac (min)	1.00	2.00	2.00	1.00	1.50 $\pm$ 0.58
$T_{\max}$ Cardiac (min)	0.00	0.00	0.00	0.00	0.00
Cardiac % OD at 3-hours	18.80	11.17	17.02	14.58	15.39 $\pm$ 3.30
$T_{1/2}$ Lungs (min)	2.00	10.00	6.00	1.00	4.75 $\pm$ 4.11
$T_{\max}$ Lungs (min)	1.00	1.00	0.00	2.00	1.00 $\pm$ 0.82
Lungs %OD at 3-hours	15.00	9.60	8.50	8.33	10.36 $\pm$ 3.15
$T_{1/2}$ Liver (min)	10.00	14.00	8.00	2.00	8.50 $\pm$ 5.00
$T_{\max}$ Liver (min)	1.00	1.00	1.00	0.00	0.75 $\pm$ 0.50
Liver %OD at 3-hours	7.45	4.77	8.51	10.42	7.79 $\pm$ 2.36
$T_{1/2}$ LKID (min)	8.00	8.00	7.00	8.00	7.75 $\pm$ 0.50
$T_{\max}$ LKID (min)	2.00	2.00	1.00	1.00	1.50 $\pm$ 0.58
LKID %OD at 3-hours	5.83	6.18	8.51	8.33	7.21 $\pm$ 1.40
$T_{1/2}$ RKID (min)	8.00	9.00	8.00	8.00	8.25 $\pm$ 0.50
$T_{\max}$ RKID (min)	2.00	2.00	1.00	1.00	1.50 $\pm$ 0.58
RKID %OD at 3-hours	9.11	7.19	6.38	6.25	7.23 $\pm$ 1.32
$T_{1/2}$ Trabecular Bone (min)	Accumulate	Accumulate	Accumulate	Accumulate	Accumulate
$T_{\max}$ Trabecular Bone (min)	Accumulate	Accumulate	Accumulate	Accumulate	Accumulate
Trabecular Bone %OD at 3-hours	30.56	50.00	34.04	33.30	36.98 $\pm$ 8.81
$T_{1/2}$ Cortical Bone (min)	Accumulate	Accumulate	Accumulate	Accumulate	Accumulate
$T_{\max}$ Cortical Bone (min)	Accumulate	Accumulate	Accumulate	Accumulate	Accumulate
Bone %OD at 3-hours	11.90	8.77	12.77	10.42	10.97 $\pm$ 1.76
$T_{1/2}$ Background (min)	15.00	16.00	20.00	11.00	15.50 $\pm$ 3.70
$T_{\max}$ Background (min)	0.00	1.00	1.00	1.00	0.75 $\pm$ 0.50
Background %OD at 3-hours	3.01	3.02	4.26	8.33	7.68 $\pm$ 5.54
Blood $T_{1/2}$ (min)	13.10	16.29	16.18	16.86	15.61 $\pm$ 1.70
Blood $t_{1/2-\alpha}$ (min)	4.74	6.26	5.36	6.25	5.59 $\pm$ 0.66
Blood $t_{1/2-\beta}$ (min)	44.34	38.39	40.69	41.82	41.19 $\pm$ 31.86
Blood % ID at 3-hours	0.47	0.81	1.32	0.51	0.78 $\pm$ 0.39
Urine % ID at 3-hours	32.77	39.56	51.47	53.56	44.34 $\pm$ 9.8
Urine: Time to 50% elimination of ID% (min)	16.65	25.13	32.61	23.70	24.52 $\pm$ 6.54

Legend: For the trabecular bone compartment shows the term “accumulate”, this term means the parameter was > 180 min

**Table 8-11 Biodistribution and pharmacokinetic data for individual dogs undergoing dynamic scintigraphy receiving <sup>188</sup>Re-HEDP.**

Radiopharmaceutical	<sup>188</sup> Re-HEDP								
	Dog 6	Dog 7	Dog 8	Dog 9	Mean±SD	Case-1	Case-2	Case-3	Mean±SD
Region of Interest									
T <sub>½</sub> Cardiac (min)	8	23	19	12	15.61±6.91	22	22	5	16.38±10.13
T <sub>max</sub> Cardiac (min)	0	0	0	0	0	0	0	0	0
Cardiac % OD at 3-hours	14	16	15	15	15.00±0.82	15	16	13	14.67±1.53
T <sub>½</sub> Lungs (min)	14	24	32	17	21.73±8.04	38	34	CND	36.27±2.69
T <sub>max</sub> Lungs (min)	0	0	0	1	0.25±0.50	0	0	0	0
Lungs %OD at 3-hours	13	14	15	14	14.00±0.82	14	14	13	13.67±.58
T <sub>½</sub> Liver (min)	26	32	27	15	24.86±6.95	98	30	17	48.41±43.43
T <sub>max</sub> Liver (min)	1	0	1	1	0.75±0.50	2	1	2	1.67±.58
Liver %OD at 3-hours	14	14	14	15	14.25±0.50	12	15	14	13.67±1.53
T <sub>½</sub> LKID (min)	25	25	36	26	27.97±5.12	20	44	CND	32.37±17.04
T <sub>max</sub> LKID (min)	3	3	2	2	2.50±0.58	3	3	3	3.00±
LKID %OD at 3-hours	13	12	12	12	12.25±0.50	14	11	14	13.00±1.73
T <sub>½</sub> RKID (min)	27	35	24	17	25.70±7.73	18	39	66	40.93±24.13
T <sub>max</sub> RKID (min)	2	3	2	2	2.25±0.50	3	3	1	2.33±1.53
RKID %OD at 3-hours	14	14	12	13	13.25±0.96	15	12	14	13.67±1.53
T <sub>½</sub> Trabecular Bone (min)	68	73	77	61	69.71±7.11	60	66	CND	63.02±4.27
T <sub>max</sub> Trabecular Bone (min)	0	0	0	0	0	0	0	0	0
Trabecular Bone %OD at 3-hours	13	12	11	11	11.75±0.96	12	12	12	12.00±
T <sub>½</sub> Cortical Bone (min)	44	61	59	74	59.48±12.30	52	120	120	97.33±39.26
T <sub>max</sub> Cortical Bone (min)	1	3	0	0	1.00±1.41	0	0	0	0
Bone %OD at 3-hours	10	10	14	8	10.50±2.52	10	12	10	10.67±1.16
T <sub>½</sub> Background (min)	49	64	59	58	57.51±6.44	50	55	CND	52.50±3.54
T <sub>max</sub> Background (min)	1	1	2	2	1.50±0.58	0	0	1	0.33±0.58
Background %OD at 3-hours	10	7	8	12	9.25±2.22	8	8	10	8.67±1.16
Blood T <sub>½</sub> (min)	14	19	14	14	15.25±2.50	15	15	15	15.00±0.00
Blood t <sub>½-α</sub> (min)	6	7	6	7	6.59±0.61	4	6	5	5.26±0.97
Blood t <sub>½-β</sub> (min)	91	103	80	95	92.19±9.87	92	84	138	104.92±29.16
Blood % ID at 3-hours	5	5	4	5	4.83±0.23	9	5	9	7.77±2.22
Urine % ID at 3-hours	67	43	57	42	52.31±12.02	29	45	18	30.59±13.32
Urine: Time to 50% elimination of ID% (min)	25	40	43	30	34.50±8.43	45	30	60	45±15.00
Whole body retention % ID at 3-hours	33	57	43	58	47.69±12.02	71	55	82	69.41±13.32
T <sub>½</sub> Tumour (min)	NA	NA	NA	NA	NA	>180	NR	NR	>180
T <sub>max</sub> Tumour (min)	NA	NA	NA	NA	NA	3	NR	NR	3
Tumour %OD at 3-hours	NA	NA	NA	NA	NA	13.29	NR	NR	13.29

Legend: CND = Could not be determined in Case-3 because of prolonged uptake in the ROI. NR = not recorded NA = not applicable

**Table 8-12 Biodistribution and pharmacokinetic data for individual dogs undergoing dynamic scintigraphy receiving uncomplexed  $^{186}\text{Re}$  and  $^{186}\text{Re}$  -HEDP**

Radiopharmaceutical	Uncomplexed $^{186}\text{Re}$	$^{186}\text{Re}$ -HEDP
	Dog 10	Dog 11
<b>Region of Interest</b>		
<b><math>T_{1/2}</math> Cardiac (min)</b>	1.00	8.28
<b><math>T_{\max}</math> Cardiac (min)</b>	0.00	0.00
<b>Cardiac % OD at 3-hours</b>	4.35	14.00
<b><math>T_{1/2}</math> Lungs (min)</b>	60.00	13.54
<b><math>T_{\max}</math> Lungs (min)</b>	0.00	0.00
<b>Lungs %OD at 3-hours</b>	3.73	13.00
<b><math>T_{1/2}</math> Liver (min)</b>	120.00	26.14
<b><math>T_{\max}</math> Liver (min)</b>	1.00	1.00
<b>Liver %OD at 3-hours</b>	4.97	14.00
<b><math>T_{1/2}</math> Stomach (min)</b>	Accumulating	NA
<b><math>T_{\max}</math> Stomach (min)</b>	Accumulating	NA
<b>Stomach %OD at 3-hours</b>	82.00	NA
<b><math>T_{1/2}</math> LKID (min)</b>	NA	24.00
<b><math>T_{\max}</math> LKID (min)</b>	NA	3.00
<b>LKID %OD at 3-hours</b>	NA	13.00
<b><math>T_{1/2}</math> RKID (min)</b>	NA	24.81
<b><math>T_{\max}</math> RKID (min)</b>	NA	3.00
<b>RKID %OD at 3-hours</b>	NA	13.00
<b><math>T_{1/2}</math> Trabecular Bone (min)</b>	NA	68.00
<b><math>T_{\max}</math> Trabecular Bone (min)</b>	NA	0.00
<b>Trabecular Bone %OD at 3-hours</b>	NA	14.00
<b><math>T_{1/2}</math> Cortical Bone (min)</b>	NA	44.00
<b><math>T_{\max}</math> Cortical Bone (min)</b>	NA	1.00
<b>Bone %OD at 3-hours</b>	NA	10.00
<b><math>T_{1/2}</math> Background (min)</b>	26.00	41.00
<b><math>T_{\max}</math> Background (min)</b>	1.00	1.00
<b>Background %OD at 3-hours</b>	10.00	9.00
<b>Blood <math>T_{1/2}</math> (min)</b>	2.00	2.27
<b>Blood <math>t_{1/2-\alpha}</math> (min)</b>	9.56	5.83
<b>Blood <math>t_{1/2-\beta}</math> (min)</b>	80.22	88.12
<b>Blood % ID at 3-hours</b>	5.23	4.88
<b>Urine % ID at 3-hours</b>	29.19	67.02
<b>Urine: Time to 50% elimination of ID% (min)</b>	60.00	60.00

Legend: For the stomach compartment shows the term “accumulate”, this term means the parameter was > 180 min. No kidney ROI were recorded because of the intense uptake in the stomach which masked activity in both kidneys ROI.

**Table 8-13 Whole body effective half-life ( $T_e$ ) for various radiopharmaceuticals**

Radiopharmaceutical	$T_e$ (hrs.)	$T_p$ (hrs.)	$T_b$ (hrs.)
<sup>186</sup> Re- HEDP	12.29	89.23	14.25
<sup>188</sup> Re - HEDP Normal Dog1	7.80	17.00	14.41
<sup>188</sup> Re -HEDP Normal Dog2	10.64	17.00	28.42
<sup>188</sup> Re -HEDP Normal Dog3	9.50	17.00	21.51
<sup>188</sup> Re -HEDP Normal Dog4	11.98	17.00	40.60
<sup>188</sup> Re -HEDP OSA Dog1	13.09	17.00	56.90
<sup>188</sup> Re - HEDP OSA Dog2	12.39	17.00	45.63
<sup>188</sup> Re - HEDP OSA Dog3	14.73	17.00	110.44
<sup>153</sup> Sm EDTMP Normal Dog1	32.27	46.29	106.53
<sup>153</sup> Sm EDTMP Normal Dog2	30.15	46.29	86.46
<sup>153</sup> Sm EDTMP Normal Dog3	32.81	46.29	112.64
<sup>153</sup> Sm EDTMP Normal Dog4	27.42	46.29	67.24
<sup>153</sup> Sm -EDTMP OSA Dog13	41.83	46.29	433.63
<sup>153</sup> Sm- PEI-MP 10-30 kDa Dog1	34.28	46.29	132.12
<sup>153</sup> Sm- PEI-MP 10-30 kDa Dog2	18.52	46.29	30.87
<sup>153</sup> Sm- PEI-MP 10-30 kDa Dog3	35.88	46.29	159.63
<sup>153</sup> Sm- PEI-MP 10-30 kDa Dog4	29.99	46.29	85.13
<sup>99m</sup> Tc- PEI-MP 10-30 kDa Dog1	4.76	6.02	22.83
<sup>99m</sup> Tc- PEI-MP 10-30 kDa Dog2	4.81	6.02	23.96
<sup>99m</sup> Tc-PEI-MP 10-30 kDa Dog3	4.55	6.02	18.59
<sup>99m</sup> Tc- PEI-MP 10-30 kDa Dog4	4.63	6.02	20.00
<sup>99m</sup> Tc-PEI-MP 10-30 kDa OSADog	3.78	6.02	10.15
<sup>99m</sup> Tc-PEI-MP 20-30 kDa Dog1	5.23	6.02	39.90
<sup>99m</sup> Tc-PEI-MP 20-30 kDa Dog2	4.66	6.02	20.58
<sup>99m</sup> Tc-PEI-MP 20-30 kDa Dog3	4.80	6.02	23.65
<sup>99m</sup> Tc-PEI-MP 20-30 kDa Dog4	5.07	6.02	32.22

Legend: The Effective half-life ( $T_e$ ), is derived from the equation  $T_e = \frac{T_p \times T_b}{T_p + T_b}$ . Where  $T_p$  is the physical half-life of the radionuclide and  $T_b$  is the biological half-life of the radionuclide plus ligand (i.e. the radiopharmaceutical). The biological half-life is derived from pharmacokinetic calculations for whole body (excluding urine activity) - AUC $_{\infty}$  (area under the curve to infinity)/hrs.

### 8.5 Clinical cases receiving $^{153}\text{Sm-EDTMP}$ and $^{188}\text{Re-HEDP}$

**Table 8-14 Profile of osteosarcoma and multilobular osteosarcoma dogs receiving  $^{153}\text{Sm-EDTMP}$**

Case	Breed	Age (yrs.)	Mass (kg)	Sex	Site	TNM*	Histopathology	T	NTC	T/NTC**	Pain control response	Survival (Months)	Legend
1	Rottweiler	8	44.4	F	Left proximal humerus	T2N0M0	NR (see Table 8-15, below)	484	62	7.80	Poor	1m.	Flare reaction. Tumour progression. Euthanized.
2	Great Dane	7	57	F	Right distal radius	T2N0M0	NR (see Table 8-15, below)	2911	222	13.10	Poor	1m.	Flare reaction. Tumour progression. Euthanized.
3	Cross Breed	8	34	F	Right proximal humerus	T2N0M0	Fibroblastic	NR	NR	NR	Poor	3m	Tumour progression. Pathological fracture evident. Euthanized
4	Rottweiler	6	51.55	M	Left distal radius	T2N0M0	Fibroblastic	564	83	6.80	Poor	4m	Tumour progression. Euthanized. Necropsy - multiple lung and spleen metastases
5	Ridgeback	5	42	F	Left distal radius	T2N0M0	NR (see Table 8-15, below)	648	221	2.93	Moderate	4m.	Tumour progression. Euthanized.
6	Bullmastiff	5	42	F	Left proximal humerus	T2N0M0	Fibroblastic osteosarcoma	593	177	3.35	Poor	3m	Tumour progression. Euthanized. Necropsy - no evidence of metastases micro and macroscopically
7	Rottweiler cross	2	38.3	F	Right distal femur	T2N0M0	Osteoblastic osteosarcoma	$^{153}$	89	1.72	Moderate	6m	Amputation at 4 months due to tumour progression. Euthanized. Necropsy at 6 months multiple metastases present in lungs, heart, liver, kidneys, GIT, neck muscles
8	Boxer	7.5	41	M	Right proximal humerus	T1M0	NR (see Table 8-15, below)	618	219	2.82	Moderate	7m	Tumour progression. Euthanized. Necropsy metastasis was evident in lungs and other body parts.

Case	Breed	Age (yrs.)	Mass (kg)	Sex	Site	TNM*	Histopathology	T	NTC	T/NTC**	Pain control response	Survival (Months)	Legend
9	Dalmatian	1.5	22.4	M	Right scapula	T2N0M0	NR (see Table 8-15, below)	1852	124	14.90	Good	48m	Died from unrelated causes, no evidence of metastases
10	Rottweiler	13	53	M	Scapula	T2N0M0	Osteosarcoma	2087	624	3.34	Moderate	4m	Tumour progression. Euthanized. Radiographic evidence of metastases to rib and distal radius. <u>Urine activity collected repeated scapula and distal radius scans</u>
11	Mixed Breed	11	30	F	Pelvis	T2N0M0	Mixed osteosarcoma	NR	NR	NR	NR	NR	Unknown. Lost to follow-up. <u>Urine collected for activity</u>
12	Rottweiler	9	30	F	Zygomatic arch	T2N0M0	Osteoblastic osteosarcoma	Not done (dog aggressive)	NR	NR	Poor	2m	Flare reaction. Tumour progression. Euthanized. Necropsy - no metastases present in lungs at necropsy. <u>Haematology done.</u>
13	Rottweiler	5	37	F	Distal femur	T2N0M0	Osteoblastic osteosarcoma	118	61	1.94	NA	NA	Euthanized immediately as amputation could not be done. Necropsy - no metastases evident on necropsy. Dynamic study and autoradiography done.
14	Cross Saint Bernard	10	47	F	Distal radius	T2N0M0	Mixed osteosarcoma	13.85	6.80	2.04	NA	4m	Underwent amputation at 2 weeks due to size of tumour. Given isotope before surgery, <b>second dose</b> <sup>153</sup> Sm-EDTMP at 3 months. Tumour progression. Radiographs show metastases from 2 months. Necropsy - identified multiple pulmonary metastasis and a large mass, hypertrophic osteodystrophy present at necropsy. <sup>99m</sup> Tc-PEI-MP 10-30 kDa




Case	Breed	Age (yrs.)	Mass (kg)	Sex	Site	TNM*	Histopathology	T	NTC	T/NTC**	Pain control response	Survival (Months)	Legend
15	Mixed Breed	10	29	F	Distal tibia	T2N0M0	Telangiectic osteosarcoma	1914	117	16.36	Poor	2m	Tumour progression. Necropsy - no metastases evident necropsy. <i>(Some haematology. Dynamic study done with <sup>186</sup>Re-polymin.)</i>
16	Labrador	8	33	F	Caudal skull, right of midline invading caudal fossa	T2N0M0	Multilobular osteosarcoma	694	173	4.01	Good	6m	Static disease. No increase in size of MLO over time. Increase in radiodensity of mass. <b>Second dose</b> <sup>153</sup> Sm-EDTMP given at 3 months. Euthanized. Necropsy - compression of brain in caudal fossa led to progression of neurological signs.
17	Small Mixed Breed	10	7	F	Right Orbit	T2N0M0	Multilobular osteosarcoma	995	173	5.75	NR	NR	Lost to follow-up, Tumour progression. Euthanized.
18	German Shepherd	8	34	F	Hard palate, cranial to cribriform plate, midline	T2N0M0	Multilobular osteosarcoma	758	168	4.51	Moderate	5m	Debulking surgery was done prior to <sup>153</sup> Sm-EDTMP. Moderate pain control. Tumour progression. <b>Second dose</b> <sup>153</sup> Sm-EDTMP given at 3 months. <i>Haematology done and repeated image and collection of urine 17 hours.</i>
19	Bouvier	8	57kg	F	Distal radius	T1M0	Osteoblastic osteosarcoma	3427	1441	2.38	Moderate	4m	Tumour progression. Euthanized. Necropsy – metastasis (single) evident in lung at post-mortem. Necropsy results indicate necrosis and haemorrhage in the tumour. <i>Haematology done</i>
20	German Shepherd	9	20	M	Distal radius	T2N0M0	Osteosarcoma	3476	251	13.85	Moderate	3m	3m. Moderate pain control. Tumour progression. Euthanized. <i>Some haematology, urine activity recorded</i>
<b>Radiosensitization (Carboplatin infusion)</b>													

Case	Breed	Age (yrs.)	Mass (kg)	Sex	Site	TNM*	Histopathology	T	NTC	T/NTC**	Pain control response	Survival (Months)	Legend
21	Doberman	10	42	M	Left distal radius	T2N0M0	Osteoblastic osteosarcoma	3172	227	13.97	Good	2.4m	Tumour progression. Euthanized. Necropsy - not done.
22	Rottweiler	7	51	F	Distal radius	T2N0M0	Osteoblastic osteosarcoma	1203	208	5.78	Good	16.4m	Received 2 doses carboplatin 300mg/m <sup>2</sup> . Tumour progression. Amputation at 7 months. Euthanized. Necropsy (private veterinarian) showed abdominal metastasis in the spleen.
23	Rottweiler	10	65	M	Distal radius	T2N0M0	Osteoblastic osteosarcoma	3873	334	11.60	Good	3m	Progressive disease. Euthanized <i>Haematology available</i>
24	Crossbreed	8	47	M	Distal radius	T2N0M0	Osteoblastic osteosarcoma	2447	228	10.73	Good	7.5m	Progressive disease. Euthanized
25	Labrador Cross	12	45	M	Distal Femur	T2N0M0	Osteoblastic osteosarcoma	2625	208	12.62	Moderate	3.25m	Progressive disease. Metastases at one month enlarged lymph node. Euthanized
26	Doberman	11	42	M	Distal radius ulna (bilateral)	T2N0M0	Osteoblastic osteosarcoma	2303	182	12.65	Good	6.5m	Progressive disease. Died acute metastases




\* TNM Staging: T0 (No evidence of primary tumour) T1 (Tumour confined to within bone medulla/cortex) T2 (Tumour extending beyond periosteum), N0 (tumor cells absent from regional lymph nodes), M0 (No evidence of distant metastases) M1 (Distant metastases present).




\*\* T/NTC. . Counts per pixel were recorded for the tumour (T) and contra-lateral ROI (NTC=non-tumour counts) and calculated as a ratio (T/NTC).



**Table 8-15 Radiographic description, tumour size, volume and mass in naturally occurring canine osteosarcomas following treatment with <sup>153</sup>Sm-EDTMP cases**



Case	Site	Radiological description on admission	Size* of primary tumour at day 0.	Ellipsoid Volume** (cm <sup>3</sup> )	Tumour Mass g (density for bone 1.40 g/cm <sup>3</sup> )	Radiographs
1	Left proximal humerus	Limited to proximal metaphyseal region, increased opacity with mottled appearance, caudal thin brush-like periosteal reaction.	5x4x4cm	41.89	58.65	


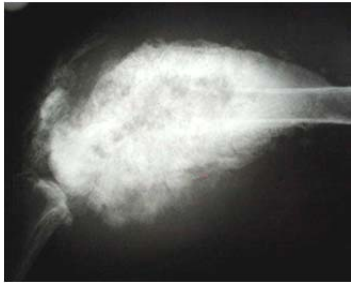

\* The sizes of primary tumour were taken from radiographs [(length)x(width)x(height)] with the first measurement being the length of the tumour along the long axis of the bone followed at the maximum measurement in a cranio-caudal orientation followed by the lateral to medial (maximum) measurement (always at 90 degrees to each other). \*\*The tumour volume was calculated from the equation for the volume of an ellipsoid (Volume =  $\pi/6$ (length)x(width)x(height)), the ellipsoid is considered a more applicable representation of the tumour volume than a rectangle<sup>245</sup>.

Case	Site	Radiological description on admission	Size* of primary tumour at day 0.	Ellipsoid Volume** (cm <sup>3</sup> )	Tumour Mass g (density for bone 1.40 g/cm <sup>3</sup> )	Radiographs
2	Right distal radius	Metaphyseal region moth-eaten to permeative lysis, endosteal scalloping, destruction of cranial cortex, Codman's triangle.	7x4x4.5cm	65.98	92.37	
3	Right proximal humerus	Destruction of cranial and caudal cortices metaphyseal region, proximal area sclerotic, distal area permeative lysis, periosteal reaction.	5x3.5x3cm	27.49	38.49	
4	Left distal radius	metaphysis geographic and moth-eaten lysis, Codman's triangle, endosteal scalloping, cortical destruction	5x3x3cm	23.57	32.99	



Case	Site	Radiological description on admission	Size* of primary tumour at day 0.	Ellipsoid Volume** (cm <sup>3</sup> )	Tumour Mass g (density for bone 1.40 g/cm <sup>3</sup> )	Radiographs
5	Left distal radius	metaphysis geographic and moth-eaten lysis, Codman's triangle, endosteal scalloping, cortical destruction	5x2.5x2.5cm	16.36	22.91	
6	Left proximal humerus	Sclerotic changes in medullary cavity, destruction of proximal cortices, palisade periosteal reaction	7x5x4cm	73.31	102.64	
7	Right distal femur	metaphyseal region sclerotic changes, destruction of caudal cortices, solid periosteal reaction	7x3x3.5cm	38.49	53.89	



Case	Site	Radiological description on admission	Size* of primary tumour at day 0.	Ellipsoid Volume** (cm <sup>3</sup> )	Tumour Mass g (density for bone 1.40 g/cm <sup>3</sup> )	Radiographs
8	Right proximal humerus	Sclerosis in metaphysis with small areas of moth-eaten lysis	7x3x3cm	32.99	46.19	
9	Right scapula	Diffuse permeative lysis of the right scapula. Significant periosteal reaction	95% scapula involvement)	95	133	



Case	Site	Radiological description on admission	Size* of primary tumour at day 0.	Ellipsoid Volume** (cm <sup>3</sup> )	Tumour Mass g (density for bone 1.40 g/cm <sup>3</sup> )	Radiographs
10	Scapula	Check with owner for histopathology. Marked soft-tissue swelling, moth eaten to geographic lysis. Some new bone formation, loss of scapula morphology	405	405.00	567.00	
11	Pelvis	Soft-tissue swelling, destructive lysis of tabula and ramus of the left ischium	5x3x4	31.42	43.99	



Case	Site	Radiological description on admission	Size* of primary tumour at day 0.	Ellipsoid Volume** (cm <sup>3</sup> )	Tumour Mass g (density for bone 1.40 g/cm <sup>3</sup> )	Radiographs
12	Zygomatic arch	Mineralized mass with thick palisade periosteal reaction. Permeative lysis of the zygomatic arch.	3.2x6.5x2	21.78	30.50	
13	Distal femur	Extensive periosteal reaction (Codman's triangle) Diaphysis and distal metaphysis and epiphysis replaced by neoplastic bone.	15x15x7	824.78	1154.69	
14	Distal radius	Metaphysis geographic and moth-eaten lysis, Codman's triangle, endosteal scalloping, cortical destruction	8x4x3	50.27	70.38	




Case	Site	Radiological description on admission	Size* of primary tumour at day 0.	Ellipsoid Volume** (cm <sup>3</sup> )	Tumour Mass g (density for bone 1.40 g/cm <sup>3</sup> )	Radiographs
15	Distal tibia	Distal metaphysis geographic and moth-eaten lysis, Codman's triangle, endosteal scalloping, cortical destruction	5x2x3.5	18.33	25.66	
16	Caudal skull, right of midline invading caudal fossa	Solid reaction	4cm diameter	33.52	46.93	
17	Right Orbit	Solid reaction	Not available	NA	NA	Not available

Case	Site	Radiological description on admission	Size* of primary tumour at day 0.	Ellipsoid Volume** (cm <sup>3</sup> )	Tumour Mass g (density for bone 1.40 g/cm <sup>3</sup> )	Radiographs
18	Hard palate, cranial to cribriform plate, midline	Solid reaction	5x2x4	20.95	29.33	
19	Distal radius	(fibroblastic on biopsy)/ metaphyseal region / endosteal sclerosis, destruction of both cortices with loss trabeculation, no periosteal reaction.	3x1.6x2.5	6.28	8.80	
20	Distal radius	NA	NA	NA	NA	Unavailable

Case	Site	Radiological description on admission	Size* of primary tumour at day 0.	Ellipsoid Volume** (cm <sup>3</sup> )	Tumour Mass g (density for bone 1.40 g/cm <sup>3</sup> )	Radiographs
21	Left distal radius	. Permeative lysis of distal radius cortices, loss of both medial and lateral cortices. Endosteal sclerosis. Codman's triangle medial aspect.	5x3x3.5	27.49	38.49	
22	Right distal radius	Metaphysis geographic and moth-eaten lysis, Codman's triangle, endosteal scalloping, cortical destruction. Significant destruction of the distal radius	5x3x3.5	27.49	38.49	

Case	Site	Radiological description on admission	Size* of primary tumour at day 0.	Ellipsoid Volume** (cm <sup>3</sup> )	Tumour Mass g (density for bone 1.40 g/cm <sup>3</sup> )	Radiographs
23	Distal radius	Sunburst medial periosteal reaction over metaphysis. Endosteal scalloping and permeative lysis of medial cortex. Codman's triangle present proximally	5x2x3.5	18.33	25.66	
24	Distal radius	Metaphysis geographic and moth-eaten lysis, Codman's triangle, endosteal scalloping, cortical destruction. Significant destruction of the distal radius	6x3.5X3	32.99	46.19	

Case	Site	Radiological description on admission	Size* of primary tumour at day 0.	Ellipsoid Volume** (cm <sup>3</sup> )	Tumour Mass g (density for bone 1.40 g/cm <sup>3</sup> )	Radiographs
25	Distal Femur	Metaphysis geographic and moth-eaten lysis, Codman's triangle, endosteal scalloping, cortical destruction. Significant destruction of the distal femur with a solid periosteal reaction on the cranial surface of the femur.	9x4.5x4	84.83	118.77	
26	Distal radius	Not recorded	Not recorded	NA	NA	Not available

**Table 8-16 Descriptive statistics showing increasing tumour volume ratio from baseline over a 4 month period for dogs (n=9) receiving <sup>153</sup>Sm-EDTMP**

	Month 1	Month 2	Month 3	Month 4
<b>Number of Subjects*</b>	9.00	8.00	7.00	2.00
<b>Mean tumour volume ratio</b>	1.00	2.35	4.15	3.33
<b>SD</b>	0.00	0.96	1.57	0.25
<b>SE</b>	0.00	0.34	0.60	0.18
<b>95% Confidence interval</b>	0.00	0.80	1.46	2.11
<b>Min</b>	1.00	1.50	2.33	3.15
<b>Max</b>	1.00	4.51	6.48	3.50

Legend: The data for calculating the change in the volume of the tumours over time was based on the volumes of primary tumours reported in the Appendix Table 8-15 (on page 291). To make a comparison from base line, the tumour volume was divided by itself to give a starting value of 1; all subsequent measurements (monthly) were recorded and divided by the initial value to give a ratio of increase in size by the tumour. These data were then compared to each other using descriptive statistics and a linear regression analysis; see Figure 3-34 on page 167. \*With time a numbers of subjects were lost from the study due to owner compliance and death due to disease progression.

**Table 8-17 Raw data for haematology results for dogs receiving  $^{153}\text{Sm-EDTMP}$  and  $^{153}\text{Sm-EDTMP}$  plus carboplatin**

Case number*		$^{153}\text{Sm-EDTMP}$					$^{153}\text{Sm-EDTMP}$ plus carboplatin				
		8	12	14	15	16	21	22	23	24	25
Haemoglobin (g/dl)	Week-0	13.80	9.80	16.70	16.60	14.70	16.60	15.40	17.40	19.20	13.00
	Week-1	18.30	4.60	16.20	14.80	15.40	16.60	14.40	17.40	19.20	13.00
	Week-2	17.50	5.90	16.30	14.10	13.60	17.40	14.50	19.20	18.00	12.40
	Week-3	17.30	4.13	--	15.70	--	16.30	13.50	17.40	--	10.60
	Week-4	13.00	8.10	--	--	--	16.30	12.60	17.80	--	--
WBC ( $\times 10^3 \mu\text{l}$ )	Week-0	10.60	8.30	4.40	10.30	4.70	4.66	12.10	8.46	8.49	13.68
	Week-1	5.20	4.70	4.00	8.50	5.20	4.66	7.67	8.46	8.49	13.68
	Week-2	4.80	8.90	6.70	10.60	4.90	4.09	5.25	7.14	4.19	6.09
	Week-3	4.40	13.00	--	3.90	--	4.53	5.86	10.00	--	8.64
	Week-4	6.60	33.00	--	--	--	7.67	16.70	16.45	--	--
Haematocrit (%)	Week-0	39.00	28.00	47.00	45.00	40.00	49.60	44.00	50.00	54.00	37.50
	Week-1	61.00	14.00	46.00	42.00	43.00	49.60	40.00	50.00	54.00	37.50
	Week-2	51.00	17.00	47.00	40.70	38.00	50.80	40.00	47.40	52.00	36.50
	Week-3	51.00	13.00	--	50.00	--	47.40	39.00	50.10	--	31.30
	Week-4	40.00	25.00	--	--	--	48.30	35.00	51.80	--	--
Platelet count ( $\times 10^3 \mu\text{l}$ )	Week-0	222.00	97.00	291.00	649.00	319.00	22.00	479.00	204.00	243.00	575.00
	Week-1	152.00	104.00	375.00	574.00	137.00	22.00	329.00	204.00	243.00	575.00
	Week-2	77.00	80.00	263.00	545.00	70.00	38.00	65.00	48.00	48.00	259.00
	Week-3	61.00	2.84	--	100.00	--	65.00	76.00	148.00	--	492.00
	Week-4	155.00	9.20	--	--	--	30.00	183.00	306.00	--	--

Legend: The normal range for dog haemoglobin is 12-18 g/dl, for WBC is 6 - 17  $\times 10^3 \mu\text{l}$ , for haematocrit 37% – 55% , and the lower range for platelet count in normal dogs is 200  $\times 10^3 \mu\text{l}$ .

**Table 8-18 Descriptive statistics for haematology results for the  $^{153}\text{Sm}$ -EDTMP and  $^{153}\text{Sm}$ -EDTMP plus carboplatin group**

Radiopharmaceutical		$^{153}\text{Sm}$ -EDTMP	$^{153}\text{Sm}$ -EDTMP plus carboplatin
Haematology Parameters		Mean±SEM	Mean±SEM
Haemoglobin (g/dl)	Week-0	14.32±1.26	16.32±1.03
	Week-1	13.86±2.39	16.12±1.10
	Week-2	13.48±2.02	16.30±1.24
	Week-3	12.38±4.15	14.45±1.52
	Week-4	10.55±2.45	15.57±1.55
WBC ( $\times 10^3 \mu\text{l}$ )	Week-0	7.66±1.33	9.48±1.58
	Week-1	5.52±0.78	8.59±1.45
	Week-2	7.18±1.13	5.35±0.58
	Week-3	7.10±2.95	7.26±1.25
	Week-4	19.80±13.20	13.61±2.97
Haematocrit (%)	Week-0	39.80±3.31	47.02±2.86
	Week-1	41.20±7.61	46.22±3.17
	Week-2	38.74±5.90	45.34±3.04
	Week-3	38.00±12.50	41.95±4.26
	Week-4	32.50±7.50	45.03±5.12
Platelet count ( $\times 10^3 \mu\text{l}$ )	Week-0	315.60±91.74	304.60±99.33
	Week-1	268.40±90.17	274.60±90.27
	Week-2	207.00±91.97	91.60±42.07
	Week-3	54.61±28.23	195.25±100.61
	Week-4	82.10±72.90	173.00±79.83

Legend: The normal range for dog haemoglobin is 12-18 g/dl, for WBC is 6 - 17  $\times 10^3 \mu\text{l}$ , for haematocrit 37% – 55% , and the lower range for platelet count in normal dogs is 200  $\times 10^3 \mu\text{l}$ .



**Table 8-19 Raw data for histopathological scores from osteosarcoma sections**

Sample	Capillary Density	Osteoblast Density	Osteoclast Density	Pyknotic nuclei density	Legend
<b>Section 1 (negative for uptake)</b>					
<b>1 HPF</b>	0	1	0	4	4+ osteoid, 1+ mineralized bone
<b>2 HPF</b>	0	1	0	3	
<b>3 HPF</b>	0	1	0	2	
<b>4 HPF</b>	0	1	0	3	
<b>5 HPF</b>	0	1	0	4	
<b>Section 1 (Moderate uptake)</b>					
<b>1 HPF</b>	1	4	1	2	1+ osteoid, 3+ mineralized bone
<b>2 HPF</b>	1	4	0	2	
<b>3 HPF</b>	1	3	0	3	
<b>4 HPF</b>	3	4	1	3	
<b>5 HPF</b>	1	3	0	2	
<b>Section 2 (High uptake)</b>					
<b>1 HPF</b>	4	3	4	1	4+ mineralized bone
<b>2 HPF</b>	4	3	4	1	
<b>3 HPF</b>	4	3	4	1	
<b>4 HPF</b>	4	3	4	1	
<b>5 HPF</b>	4	3	4	1	

Legend: Scoring for capillary, osteoblast, osteoclast and pyknotic nuclei density was based on a score of 0 to 4. Five areas examined under high powered field (HPF = x 400 magnification)

0 = no evidence of capillaries or cells

1 = structure or cell found in only 1/5 areas

2 = structure or cell found in only 2/5 areas

3 = structure or cell found in only 3/5 areas

4 = structure or cell found in only 5/5 areas

**Table 8-20 Statistical Analysis of scores from osteosarcoma histological sections using ANOVA on Ranks**


<b>Capillary Density</b>	N	Median	25%	75%	Comparison	ANOVA on Ranks <i>P</i> <0.05
Moderate	5	1.000	1.000	1.500	High vs. None	Yes
None	5	0.000	0.000	0.000	High vs. Moderate	No
High	5	4.000	4.000	4.000	Moderate vs. None	No
<b>Osteoblast Density</b>	N	Median	25%	75%		
Moderate	5	4.000	3.000	4.000	Moderate vs. None	Yes
None	5	1.000	1.000	1.000	Moderate vs. High	No
High	5	3.000	3.000	3.000	High vs. None	No
<b>Osteoclast Density</b>	N	Median	25%	75%		
Moderate	5	0.000	0.000	1.000	High vs. None	Yes
None	5	0.000	0.000	0.000	High vs. Moderate	No
High	5	4.000	4.000	4.000	Moderate vs. None	No
<b>Pyknotic Nuclei Density</b>	N	Median	25%	75%		
Moderate	5	2.000	2.000	3.000	None vs. High	Yes
None	5	3.000	2.750	4.000	None vs. Moderate	No
High	5	1.000	1.000	1.000	Moderate vs. High	No

**Table 8-21 Summary of cases with naturally occurring canine osteosarcomas following treatment with <sup>188</sup>Re-HEDP**

Case	Breed	Age (yrs.)	Mass (kg)	Sex	Site	TNM staging*	Histopathology	T	NTC	T/NTC	Pain Response	Survival (Months)	Outcome
1	Pyrenean Mt Dog	10	59.9	F	Right distal radius	T2N0M0	Osteoblastic osteosarcoma	102	81	1.25	Good	7	Euthanized. At 4 months amputation with cisplatin chemotherapy (no mets evident in lungs regional lymph node positive. Extensive metastases at euthanasia.
2	Rottweiler	7	45	F	Left proximal humerus	T2N0M0	Chondroblastic osteosarcoma	393	196	2.00	Good	6	Euthanized, Slow growing tumour. No evidence of metastases at necropsy. At 5 months received repeated doses of isotope (x4).
3	Rottweiler	8	56	M	Left proximal humerus	T2N0M0	Osteoblastic osteosarcoma /	196	145	1.35	Moderate	3	Euthanized, tumour progression, with possible early lung metastases. Underlying renal disease.
4	Irish Wolf Hound	5.5	65	F	Right distal radius	T2N0M0	Telangiectatic osteosarcoma	219	79	2.77	Good	6	Euthanized, At 1.5 months amputation with cisplatin (due to pathological fracture). Metastases not evident till 5 months, extensive at euthanasia
5	Rottweiler	12	35	F	Left proximal humerus	T2N0M0	Osteoblastic osteosarcoma	NR	NR	NR	Poor	2	Euthanized, tumour progression. No metastases evident at necropsy
6	Whippet	13	11.3	M	Rib (Right)	T2N0M0	Osteosarcoma	225	164	1.37	Poor	2	Euthanized, tumour progression
7	Labrador	10	25.2	M	Nose (Right side)	T2N0M0	Telangiectic osteosarcoma	162	116	1.39	Moderate	3	Progression, euthanized. Metastases to stomach



\* T0 (No evidence of primary tumour) T1 (Tumour confined to within bone medulla/cortex) T2 (Tumour extending beyond periosteum), N0 (tumor cells absent from regional lymph nodes), M0 (No evidence of distant metastases) M1 (Distant metastases present).



**Table 8-22 Radiographic description, tumour size, volume and mass in naturally occurring canine osteosarcomas following treatment with <sup>188</sup>Re-HEDP**


Case	Site	Radiological description on admission	Size* of primary tumour at day 0	**Ellipsoid Volume (cm <sup>3</sup> )	Tumour Mass g (density for bone 1.40 g/cm <sup>3</sup> )	Radiographs
1	Right distal radius	Extensive soft-tissue swelling, sunburst periosteal reaction with amorphous bone production. Cortical destruction extensive	7x5.5x6.5cm	131.05	183.47	

---

\* The sizes of primary tumour were taken from radiographs with the first measurement being the length of the tumour along the long axis of the bone followed at the maximum measurement in a cranio-caudal orientation followed by the lateral to medial (maximum) measurement (always at 90 degrees to each other). \*\*The tumour volume was calculated from the equation for the volume of an ellipsoid (Volume =  $\pi/6$ (length)x(width)x(height)), the ellipsoid is considered a more applicable representation of the tumour volume than a rectangle<sup>245</sup>.

Case	Site	Radiological description on admission	Size* of primary tumour at day 0	**Ellipsoid Volume (cm3)	Tumour Mass g (density for bone 1.40 g/cm3)	Radiographs
2	Left proximal humerus	Metaphyseal region and head moth-eaten to permeative lysis, irregular periosteal reaction	6.5x4.5x4cm	61.27	85.78	
3	Left proximal humerus	Permeative lysis and adjacent areas of sclerosis, thick brush-like periosteal reaction.	6.5x3.5x3.5cm	41.70	58.38	

Case	Site	Radiological description on admission	Size* of primary tumour at day 0	**Ellipsoid Volume (cm3)	Tumour Mass g (density for bone 1.40 g/cm3)	Radiographs
4	Right distal radius	Extensive soft-tissue swelling with amorphous bone. Codman's triangle proximal with thin to thick periosteal reaction. Tumour may have arisen sub-periosteally.	8.5x5x3cm	66.77	93.47	
5	Left proximal humerus	Permeative lysis of the cortex with solid thick brush like periosteal reaction.	10x6x5.5cm	172.81	241.93	

Case	Site	Radiological description on admission	Size* of primary tumour at day 0	**Ellipsoid Volume (cm3)	Tumour Mass g (density for bone 1.40 g/cm3)	Radiographs
6	Rib (Right)	Rib (9) has an area of moth-eaten lysis and irregular periosteal reaction. This is surrounded soft-tissue mass	Bone 2cm in diameter Soft-tissue 6cm in diameter	4.19	5.87	
7	Nose (right side)	Marked soft-tissue opacification of the right caudal half of nasal passage with turbinate destruction.	NR	NR	NR	NR

**Table 8-23 Raw data for haematology results for  $^{188}\text{Re}$ -HEDP (single dose) and  $^{188}\text{Re}$ -HEDP (multiple dose)**

		$^{188}\text{Re}$ -HEDP (single dose)					$^{188}\text{Re}$ -HEDP (multiple dose)	
	Case	Dog 4	Dog 1	Dog 3	Dog 2	Dog 6	Dog 2	Dog 5
Hb (g/dl)	Week-0	14.6	12.2	11.3	16.8	17.8	15.7	12.9
	Week-1	15.7	13.4	10.2	16.1	17.3	14.6	14.7
	Week-2	17.4	11	10.8	18.4	16.5	15	14.4
	Week-3	15.6	7.96	9	17	16	15.1	14.1
	Week-4	15.7	7.5	9.5	15.7	15	15.3	14
WBC x $10^3 \mu\text{l}$	Week-0	6.3	7.4	9.9	10.8	10.8	7.74	8.2
	Week-1	10.5	12.6	13.9	6.9	16.8	12	9.7
	Week-2	6.28	5.7	11.7	8.2	17	10.1	4.8
	Week-3	10.5	4.69	18.7	8	16.8	8.4	7.8
	Week-4	11	4.7	19	7.74	15	11.4	8
Hct %	Week-0	42	35	32	48	49	45	37
	Week-1	45	39	30	44	50	42	45
	Week-2	48	32	30	44	47	41	43
	Week-3	45	23.1	26	44	45	43	43
	Week-4	44	22	27	45	43	43	42
PLT x $10^3 \mu\text{l}$	Week-0	444	288	330	443	395	398	128
	Week-0	460	437	95	329	371	362	240
	Week-1	341	307	360	343	200	359	173
	Week-2	229	111	60	353	175	283	173
	Week-4	235	115	75	398	150	324	<sup>153</sup>

Legend: The normal range for dog haemoglobin is 12-18 g/dl, for WBC is 6 - 17 x  $10^3 \mu\text{l}$ , for haematocrit 37% – 55% , and the lower range for platelet count in normal dogs is 200 x  $10^3 \mu\text{l}$ .



**Table 8-24 Descriptive statistics for haematology results for the  $^{188}\text{Re}$ -HEDP (single dose) and  $^{188}\text{Re}$ -HEDP (multiple dose)**

Parameter and Units		Group-1	Group-2
		$^{188}\text{Re}$ -HEDP (Single-dose)	$^{188}\text{Re}$ -HEDP (Multiple-dose)
		Mean $\pm$ SEM	Mean $\pm$ SEM
<b>Haemoglobin g/dl</b>	<b>Week-0</b>	14.54 $\pm$ 1.26	14.30 $\pm$ 1.40
	<b>Week-1</b>	14.54 $\pm$ 1.26	14.65 $\pm$ 0.05
	<b>Week-2</b>	14.82 $\pm$ 1.63	14.70 $\pm$ 0.30
	<b>Week-3</b>	13.11 $\pm$ 1.91	14.60 $\pm$ 0.50
	<b>Week-4</b>	12.68 $\pm$ 1.74	14.65 $\pm$ 0.65
<b>White blood cell count x 10<sup>3</sup> <math>\mu</math>l</b>	<b>Week-0</b>	9.04 $\pm$ 0.93	7.97 $\pm$ 0.23
	<b>Week-1</b>	12.14 $\pm$ 1.66	10.85 $\pm$ 1.15
	<b>Week-2</b>	9.78 $\pm$ 2.09	7.45 $\pm$ 2.65
	<b>Week-3</b>	11.74 $\pm$ 2.64	8.10 $\pm$ 0.30
	<b>Week-4</b>	11.49 $\pm$ 2.54	9.70 $\pm$ 1.70
<b>Haematocrit %</b>	<b>Week-0</b>	41.20 $\pm$ 3.40	41.00 $\pm$ 4.00
	<b>Week-1</b>	41.60 $\pm$ 3.39	43.50 $\pm$ 1.50
	<b>Week-2</b>	40.20 $\pm$ 3.83	42.00 $\pm$ 1.00
	<b>Week-3</b>	36.62 $\pm$ 4.95	43.00 $\pm$ 0.00
	<b>Week-4</b>	36.20 $\pm$ 4.85	42.50 $\pm$ 0.50
<b>Platelet count x 10<sup>3</sup> <math>\mu</math>l</b>	<b>Week-0</b>	380.00 $\pm$ 31.03	263.00 $\pm$ 135.00
	<b>Week-1</b>	338.40 $\pm$ 65.15	301.00 $\pm$ 61.00
	<b>Week-2</b>	310.20 $\pm$ 28.86	266.00 $\pm$ 93.00
	<b>Week-3</b>	185.60 $\pm$ 50.68	228.00 $\pm$ 55.00
	<b>Week-4</b>	194.60 $\pm$ 57.29	238.50 $\pm$ 85.50

Legend: The normal range for dog haemoglobin is 12-18 g/dl, for WBC is 6 - 17 x 10<sup>3</sup>  $\mu$ l, for haematocrit 37% – 55% , and the lower range for platelet count in normal dogs is 200 x 10<sup>3</sup>  $\mu$ l.

**Table 8-25 Data corrected for baseline (1) showing increasing tumour volume over time for dogs receiving a single dose of <sup>188</sup>Re-HEDP**

Case \ Time	1 month	2 month	3 month	4 month*	6 month*
1	1.00	NR	3.68	NR	NR
2	1.00	1.38	2.41	1.88	2.15
3	1.00	2.62	6.48	NR	NR
4	1.00	1.44	1.98	NR	NR
5	1.00	4.51	6.06	NR	NR

Legend: The data for calculating the change in the volume of the tumours over time was based on the volumes of primary tumours reported in the Appendix, Table 8-22 on page 308. To make a comparison from base line, the tumour volume was divided by itself to give a starting value of 1; all subsequent measurements (monthly) were recorded and divided by the initial value to give a ratio of increase in size by the tumour. These data were then compared to each other using descriptive statistics and a linear regression analysis; see Figure 3-38 on page 188. \*With time a numbers of subjects were lost from the study due to owner compliance and death due to disease progression. NR – not recorded, radiographs unavailable.

### 8.6 Biodistribution and pharmacokinetic tables for dogs receiving $^{153}\text{Sm-PEI-MP MW-fraction10-30 kDa}$

**Table 8-26 Raw data from dogs receiving a tracer dose of  $^{153}\text{Sm-PEI-MP MW-fraction10-30 kDa}$**

Compartment Animal	Parameter	Cardiac	Lung	Liver	Left kidney	Right kidney	Trabec. bone	Cortical Bone	BG
Dog 1	$T_{1/2}$ (min)	2	23	39	15	16	Accm	>180 min	50
	$T_{\max}$ (min)	0	0	1	3	3	Accm	1	2
	% retention 3 hrs.	13	27	35	17	25	Accm	50	30
	% OD at 3 hrs.	15.56	11.9	15.16	14.5	17.69	18.52	6.69	7.76
Dog 2	$T_{1/2}$ (min)	2	15	45	14	13	Accm	>1hr	44
	$T_{\max}$ (min)	0	0	2	2	2	Accm	0	2
	% retention 3 hrs.	20	32	47	29	25	Accm	60	90
	% OD at 3 hrs.	12.62	7.77	19.4	15	16	12	5.8	9.71
Dog 3	$T_{1/2}$ (min)	3	11	>180 min	15	15	Accm	2hrs	>180 min
	$T_{\max}$ (min)	0	0	1	3	3	accm	1	2
	% retention 3 hrs.	14	21	70	20	23	Accm	40	64
	% OD at 3 hrs.	14.7	8.82	28.2	11.76	10.78	12.7	3.9	8.82
Dog 4	$T_{1/2}$ (min)	6	8	42	17	18	Accm	>180 min	29
	$T_{\max}$ (min)	0	0	1	2	2	Accm	2	1
	% retention 3 hrs.	17	21	50	23	26	Accm	66	25
	% OD at 3 hrs.	15.79	10.5	24.81	12.78	12.78	12	4.5	6.77

**Table 8-27: The mean±SD values for compartments derived from raw data in normal dogs (n=4) given <sup>153</sup>Sm-PEI-MP (MW 10-30 kDa)**

Compartment	Pharmacokinetic Parameter	Number of dogs	Mean± SD
Cardiac	T <sub>½</sub> (min)	4	3.00±2.00
	Tmax(min)	4	0.00
	% OD at 3 hrs.	4	15.46±0.51
Lungs	T <sub>½</sub> (min)	4	14.50±7.42
	Tmax(min)	4	0.00±
	% OD at 3 hrs.	4	11.13±1.90
Liver	T <sub>½</sub> (min)	3	43.00±4.58
	Tmax(min)	4	1.50±1.00
	% OD at 3 hrs.	4	21.68±6.03
Left kidney	T <sub>½</sub> (min)	4	16.00±0.82
	Tmax(min)	4	2.50±0.58
	% OD at 3 hrs.	4	13.71±1.79
Right kidney	T <sub>½</sub> (min)	4	15.25±2.22
	Tmax(min)	4	2.50±0.58
	% OD at 3 hrs.	4	14.55±3.32
Cortical Bone	T <sub>½</sub> (min)	2	150.00±42.43
	Tmax(min)	4	1.50±1.00
	% OD at 3 hrs.	4	5.29±1.29
Trabecular Bone	T <sub>½</sub> (min)	0	--
	Tmax(min)	0	--
	% OD at 3 hrs.	4	14.29±2.92
Background	T <sub>½</sub> (min)	4	76.75±69.48
	Tmax(min)	4	1.75±0.50
	% OD at 3 hrs.	4	8.23±1.22

### 8.7 Combined pharmacokinetic data for dogs receiving PEI-MP and other radiopharmaceuticals

**Table 8-28 Raw pharmacokinetic data for various radiopharmaceuticals**

Organ Parameter	Cardiac			Lung			Liver			Left kidney			Right Kidney			Bone			Trabec B			BG		
	T <sub>½</sub>	T <sub>max</sub>	%OD	T <sub>½</sub>	T <sub>max</sub>	%OD	T <sub>½</sub>	T <sub>max</sub>	%OD	T <sub>½</sub>	T <sub>max</sub>	%OD	T <sub>½</sub>	T <sub>max</sub>	%OD	T <sub>½</sub>	T <sub>max</sub>	%OD	T <sub>½</sub>	T <sub>max</sub>	%OD	T <sub>½</sub>	T <sub>max</sub>	%OD
<sup>153</sup> Sm-PEI-MP 10-30kDa	2	0	16	25	0	13	39	1	18	16	3	16	16	3	17	180	1	6	180	180	14	48	2	10
<sup>153</sup> Sm-PEI-MP 10-30kDa	2	0	16	14	0	12	48	3	15	16	2	15	13	2	18	--	3	7	180	180	19	50	2	8
<sup>153</sup> Sm-PEI-MP 10-30kDa	2	0	15	11	0	9	42	1	28	15	3	12	14	3	11	120	1	4	180	180	13	180	2	9
<sup>153</sup> Sm-PEI-MP 10-30kDa	6	0	16	8	0	11	42	1	25	17	2	13	18	2	13	--	1	5	180	180	12	29	1	7
<sup>99m</sup> Tc-PEI-MP 10-30kDa	7	0	7	10	0	5	14	1	13	10	2	31	11	2	35	46	2	7	46	2	7	40	2	2
<sup>99m</sup> Tc-PEI-MP 10-30kDa	6	0	14	11	0	15	15	1	20	14	2	18	14	2	2	53	11	9	53	11	9	29	1	1
<sup>99m</sup> Tc-PEI-MP 10-30kDa	6	0	17	7	0	15	18	1	15	12	2	16	14	2	16	60	3	10	60	3	10	23	8	7
<sup>99m</sup> Tc-PEI-MP 10-30kDa	6	0	17	8	0	6	15	1	15	13	2	14	15	2	21	60	0		60	0	21	18	2	6
<sup>99m</sup> Tc-PEI-MP 20-30kDa	3	0	11	6	0	9	28	1	28	9	1	13	10	2	14	60	22	4	60	22	15	17	1	6
<sup>99m</sup> Tc-PEI-MP 20-30kDa	3	0	14	4	0	9	20	1	20	8	2	15	9	2	12	60	26	5	60	26	18	20	2	7
<sup>99m</sup> Tc-PEI-MP 20-30kDa	4	0	15	6	0	9	10	1	10	9	1	17	9	1	14	180	2	0	180	2	21	13	2	5
<sup>99m</sup> Tc-PEI-MP 20-30kDa	4	0	14	6	0	9	13	1	13	10	2	13	10	2	12	60		9	60	1	26	24	1	3

Organ Parameter	Cardiac			Lung			Liver			Left kidney			Right Kidney			Bone			Trabec B			BG		
	T <sub>½</sub>	T <sub>max</sub>	%OD	T <sub>½</sub>	T <sub>max</sub>	%OD	T <sub>½</sub>	T <sub>max</sub>	%OD	T <sub>½</sub>	T <sub>max</sub>	%OD	T <sub>½</sub>	T <sub>max</sub>	%OD	T <sub>½</sub>	T <sub>max</sub>	%OD	T <sub>½</sub>	T <sub>max</sub>	%OD	T <sub>½</sub>	T <sub>max</sub>	%OD
<sup>188</sup> Re-HEDP OSA	22	0	15	38	0	14	98	2	12	20	3	14	18	3	15	52	0	12	60	0	10	50	0	8
<sup>188</sup> Re-HEDP OSA	22	0	16	34	0	14	30	1	15	44	3	11	39	3	12	120	0	12	66	0	12	55	0	8
<sup>188</sup> Re-HEDP OSA	5	0	13	CND	0	13	17	2	14	CND	3	14	66	1	14	120	0	12	CND	0	10	CND	1	10
<sup>188</sup> Re-HEDP	8	0	14	14	0	13	26	1	14	25	3	13	27	2	14	44	0	13	68	1	10	49	1	10
<sup>188</sup> Re-HEDP	23	0	16	24	0	14	32	0	14	25	3	12	35	3	14	61	0	12	73	3	10	64	1	7
<sup>188</sup> Re-HEDP	19	0	15	32	0	15	27	1	14	36	2	12	24	2	12	59	0	11	77	0	14	59	2	8
<sup>188</sup> Re-HEDP	12	0	15	17	1	14	15	1	15	26	2	12	17	2	13	74	0	11	61	0	8	58	2	12
<sup>153</sup> Sm-EDTMP	1	0	19	2	1	15	10	1	7	8	2	6	8	2	9	180	180	31	180	180	12	15	0	3
<sup>153</sup> Sm-EDTMP	2	0	11	10	1	10	14	1	5	8	2	6	9	2	7	180	180	50	180	9	9	16	1	3
<sup>153</sup> Sm-EDTMP	2	0	17	6	0	9	8	1	9	7	1	9	8	1	6	180	180	34	180	180	13	20	1	4
<sup>153</sup> Sm-EDTMP	1	0	15	1	2	8	2	0	10	8	1	8	8	1	6	180	180	33	120	180	10	11	1	8

Legend: Data were collated from Table 8-10 on page 283, Table 8-11 on page 284 and Table 8-26 on page 315. These raw data were used to compare all the radiopharmaceuticals with each other for differences in biodistribution, pharmacokinetics and dosimetry. Where ROI activity from tables was recorded as >180 min, the assumption was made to use 180 min for statistical comparisons. CND = T<sub>½</sub> could not be determined for the lung and left kidney compartment in the dog receiving <sup>188</sup>Re-HEDP (see Case-3 in Table 8-11 on page 284) because of prolonged uptake in the ROI.

**Table 8-29 Descriptive statistics and ANOVA on Ranks of organ compartments from various radiopharmaceuticals used for comparative purposes in the discussion sections.**

Pharmacokinetic parameter	Group	N	Missing	Median	25 <sup>th</sup> percentile	75 <sup>th</sup> percentile	P value
<b>Cardiac T<sub>1/2</sub> (min)</b>	<sup>153</sup> Sm-PEI-MP10-30 kDa	4	0	2.00	2.00	4.00	
	<sup>99m</sup> Tc-PEI-MP 10-30 kDa	4	0	6.00	6.00	6.75	
	<sup>99m</sup> Tc-PEI-MP 20-30 kDa	4	0	3.50	2.50	4.50	
	<sup>188</sup> Re-HEDP OSA	3	0	22.20	4.68	22.26	
	<sup>188</sup> Re-HEDP	4	0	15.42	9.10	22.32	<b>P&lt;0.05</b>
	<sup>153</sup> Sm-EDTMP	4	0	1.50	1.00	2.00	<b>P&lt;0.05</b>
<b>Cardiac %OD at3hrs</b>	<sup>153</sup> Sm-PEI-MP10-30 kDa	4	0	15.68	15.14	15.79	
	<sup>99m</sup> Tc-PEI-MP 10-30 kDa	4	0	13.70	8.68	16.18	
	<sup>99m</sup> Tc-PEI-MP 20-30 kDa	4	0	13.91	13.20	15.39	
	<sup>188</sup> Re-HEDP OSA	3	0	15.00	13.00	16.00	
	<sup>188</sup> Re-HEDP	4	0	15.00	14.25	15.75	
	<sup>153</sup> Sm-EDTMP	4	0	15.80	12.88	17.91	
<b>Lung T<sub>1/2</sub> (min)</b>	<sup>153</sup> Sm-PEI-MP10-30 kDa	4	0	12.50	9.50	19.50	
	<sup>99m</sup> Tc-PEI-MP 10-30 kDa	4	0	10.00	7.75	10.75	
	<sup>99m</sup> Tc-PEI-MP 20-30 kDa	4	0	5.50	5.13	6.13	
	<sup>188</sup> Re-HEDP OSA	3	1*	36.27	34.36	38.17	
	<sup>188</sup> Re-HEDP	4	0	20.75	14.52	29.93	
	<sup>153</sup> Sm-EDTMP	4	0	4.00	1.50	8.00	
<b>Lung %ODat3hrs</b>	<sup>153</sup> Sm-PEI-MP10-30 kDa	4	0	11.13	1.90	0.95	
	<sup>99m</sup> Tc-PEI-MP 10-30 kDa	4	0	11.73	5.67	3.27	
	<sup>99m</sup> Tc-PEI-MP 20-30 kDa	4	0	8.58	1.24	0.56	
	<sup>188</sup> Re-HEDP OSA	3	0	14.00	13.00	14.00	
	<sup>188</sup> Re-HEDP	4	0	14.00	13.25	14.75	
	<sup>153</sup> Sm-EDTMP	4	0	10.36	3.15	1.57	
<b>Liver T<sub>1/2</sub> (min)</b>	<sup>153</sup> Sm-PEI-MP10-30 kDa	4	0	42.00	40.50	45.00	<b>P&lt;0.05</b>
	<sup>99m</sup> Tc-PEI-MP 10-30 kDa	4	0	15.00	14.25	17.25	
	<sup>99m</sup> Tc-PEI-MP 20-30 kDa	4	0	15.38	12.31	22.05	
	<sup>188</sup> Re-HEDP OSA	3	0	30.49	16.80	97.94	
	<sup>188</sup> Re-HEDP	4	0	26.39	17.87	30.32	

Pharmacokinetic parameter	Group	N	Missing	Median	25 <sup>th</sup> percentile	75 <sup>th</sup> percentile	P value
	<sup>153</sup> Sm-EDTMP	4	0	9.00	5.00	12.00	<b>P&lt;0.05</b>
<b>Liver %ODat3hrs</b>	<sup>153</sup> Sm-PEI-MP10-30 kDa	4	0	21.57	16.74	26.62	<b>P&lt;0.05</b>
	<sup>99m</sup> Tc-PEI-MP 10-30 kDa	4	0	15.00	13.73	18.75	
	<sup>99m</sup> Tc-PEI-MP 20-30 kDa	4	0	15.38	12.31	22.05	
	<sup>188</sup> Re-HEDP OSA	3	0	14.00	12.00	15.00	
	<sup>188</sup> Re-HEDP	4	0	14.00	14.00	14.75	
	<sup>153</sup> Sm-EDTMP	4	0	7.98	6.11	9.47	<b>P&lt;0.05</b>
<b>Left Kidney T<sub>½</sub> (min)</b>	<sup>153</sup> Sm-PEI-MP10-30 kDa	4	0	16.00	15.50	16.50	
	<sup>99m</sup> Tc-PEI-MP 10-30 kDa	4	0	12.00	10.50	13.50	
	<sup>99m</sup> Tc-PEI-MP 20-30 kDa	4	0	9.00	8.38	10.75	
	<sup>188</sup> Re-HEDP OSA	3	1*	32.37	20.32	44.41	<b>P&lt;0.05</b>
	<sup>188</sup> Re-HEDP	4	0	25.58	25.14	33.19	
	<sup>153</sup> Sm-EDTMP	4	0	8.00	7.50	8.00	<b>P&lt;0.05</b>
<b>Left Kidney T<sub>max</sub> (min)</b>	<sup>153</sup> Sm-PEI-MP10-30 kDa	4	0	2.50	2.00	3.00	
	<sup>99m</sup> Tc-PEI-MP 10-30 kDa	4	0	2.00	2.00	2.00	
	<sup>99m</sup> Tc-PEI-MP 20-30 kDa	4	0	2.00	1.00	2.00	
	<sup>188</sup> Re-HEDP OSA	3	0	3.00	3.00	3.00	
	<sup>188</sup> Re-HEDP	4	0	2.50	2.00	3.00	
	<sup>153</sup> Sm-EDTMP	4	0	1.50	1.00	2.00	
<b>Left Kidney %ODat3hrs</b>	<sup>153</sup> Sm-PEI-MP10-30 kDa	4	0	13.64	12.27	15.15	
	<sup>99m</sup> Tc-PEI-MP 10-30 kDa	4	0	18.00	16.50	27.75	<b>P&lt;0.05</b>
	<sup>99m</sup> Tc-PEI-MP 20-30 kDa	4	0	14.10	12.99	15.57	
	<sup>188</sup> Re-HEDP OSA	3	0	14.00	11.00	14.00	
	<sup>188</sup> Re-HEDP	4	0	12.00	12.00	12.75	
	<sup>153</sup> Sm-EDTMP	4	0	7.26	6.01	8.42	<b>P&lt;0.05</b>
<b>Right Kidney T<sub>½</sub> (min)</b>	<sup>153</sup> Sm-PEI-MP10-30 kDa	4	0	15.00	13.25	17.50	
	<sup>99m</sup> Tc-PEI-MP 10-30 kDa	4	0	14.00	11.00	14.00	
	<sup>99m</sup> Tc-PEI-MP 20-30 kDa	4	0	10.00	9.00	12.50	
	<sup>188</sup> Re-HEDP OSA	3	1*	38.90	17.87	66.00	<b>P&lt;0.05</b>
	<sup>188</sup> Re-HEDP	4	0	25.52	18.36	33.22	
	<sup>153</sup> Sm-EDTMP	4	0	8.00	8.00	8.75	<b>P&lt;0.05</b>
<b>Right Kidney T<sub>max</sub> (min)</b>	<sup>153</sup> Sm-PEI-MP10-30 kDa	4	0	2.50	2.00	3.00	
	<sup>99m</sup> Tc-PEI-MP 10-30 kDa	4	0	2.00	2.00	2.00	



Pharmacokinetic parameter	Group	N	Missing	Median	25 <sup>th</sup> percentile	75 <sup>th</sup> percentile	P value
	<sup>99m</sup> Tc-PEI-MP 20-30 kDa	4	0	2.00	1.00	2.00	
	<sup>188</sup> Re-HEDP OSA	3	0	3.00	3.00	3.00	
	<sup>188</sup> Re-HEDP	4	0	2.50	2.00	3.00	
	<sup>153</sup> Sm-EDTMP	4	0	1.50	1.00	2.00	
<b>Right Kidney %ODat3hrs</b>	<sup>153</sup> Sm-PEI-MP10-30 kDa	4	0	14.87	11.28	17.51	
	<sup>99m</sup> Tc-PEI-MP 10-30 kDa	4	0	16.00	2.00	35.00	<b>P&lt;0.05</b>
	<sup>99m</sup> Tc-PEI-MP 20-30 kDa	4	0	13.89	11.83	17.24	
	<sup>188</sup> Re-HEDP OSA	3	0	14.00	12.00	15.00	
	<sup>188</sup> Re-HEDP	4	0	13.50	12.25	14.00	
	<sup>153</sup> Sm-EDTMP	4	0	6.79	6.28	8.63	
<b>Trabecular Bone T<sub>½</sub> (min)</b>	<sup>153</sup> Sm-PEI-MP10-30 kDa	4	2*	150.00	120.00	180.00	
	<sup>99m</sup> Tc-PEI-MP 10-30 kDa	4	0	53.00	46.00	60.00	<b>P&lt;0.05</b>
	<sup>99m</sup> Tc-PEI-MP 20-30 kDa	4	0	60.00	60.00	120.00	
	<sup>188</sup> Re-HEDP OSA	3	0	63.02	60.00	66.05	
	<sup>188</sup> Re-HEDP	4	0	70.66	62.44	76.04	
	<sup>153</sup> Sm-EDTMP	4	0	180.00	180.00	180.00	<b>P&lt;0.05</b>
<b>Trabecular Bone T<sub>max</sub> (min)</b>	<sup>153</sup> Sm-PEI-MP10-30 kDa	4	0	180.00	180.00	180.00	
	<sup>99m</sup> Tc-PEI-MP 10-30 kDa	4	0	3.00	2.25	9.00	
	<sup>99m</sup> Tc-PEI-MP 20-30 kDa	4	0	2.00	0.75	23.00	
	<sup>188</sup> Re-HEDP OSA	3	0	0.00	0.00	0.00	
	<sup>188</sup> Re-HEDP	4	0	0.50	0.00	2.00	
	<sup>153</sup> Sm-EDTMP	4	0	180.00	94.50	180.00	
<b>Trabecular Bone %OD at 3hrs</b>	<sup>153</sup> Sm-PEI-MP10-30 kDa	4		5.28	4.07	6.53	<b>P&lt;0.05</b>
	<sup>99m</sup> Tc-PEI-MP 10-30 kDa	4	0	9.39	6.61	10.00	
	<sup>99m</sup> Tc-PEI-MP 20-30 kDa	4	1	4.25	1.29	8.32	<b>P&lt;0.05</b>
	<sup>188</sup> Re-HEDP OSA	3	0	12.00	12.00	12.00	
	<sup>188</sup> Re-HEDP	4	0	11.50	11.00	12.75	
	<sup>153</sup> Sm-EDTMP	4	0	33.67	31.25	46.01	<b>P&lt;0.05</b>
<b>Cortical Bone T<sub>½</sub> (min)</b>	<sup>153</sup> Sm-PEI-MP10-30 kDa	4	2*	180.00	180.00	180.00	
	<sup>99m</sup> Tc-PEI-MP 10-30 kDa	4	0	53.00	47.75	58.25	
	<sup>99m</sup> Tc-PEI-MP 20-30 kDa	4	0	60.00	60.00	90.00	
	<sup>188</sup> Re-HEDP OSA	3	0	120.00	52.00	120.00	
	<sup>188</sup> Re-HEDP	4	0	59.86	47.81	70.87	

Pharmacokinetic parameter	Group	N	Missing	Median	25 <sup>th</sup> percentile	75 <sup>th</sup> percentile	P value
	<sup>153</sup> Sm-EDTMP	4	0	180.00	150.00	180.00	
<b>Cortical Bone T<sub>max</sub>(min)</b>	<sup>153</sup> Sm-PEI-MP10-30 kDa	4	0	180.00	180.00	180.00	
	<sup>99m</sup> Tc-PEI-MP 10-30 kDa	4	0	3.00	2.25	9.00	
	<sup>99m</sup> Tc-PEI-MP 20-30 kDa	4	0	2.00	0.75	23.00	
	<sup>188</sup> Re-HEDP OSA	3	0	0.00	0.00	0.00	
	<sup>188</sup> Re-HEDP	4	0	0.50	0.00	2.00	
	<sup>153</sup> Sm-EDTMP	4	0	180.00	94.50	180.00	
<b>Cortical Bone %OD at 3hrs</b>	<sup>153</sup> Sm-PEI-MP10-30 kDa	4	0	13.30	12.21	17.35	
	<sup>99m</sup> Tc-PEI-MP 10-30 kDa	4	0	9.39	6.61	10.00	<b>P&lt;0.05</b>
	<sup>99m</sup> Tc-PEI-MP 20-30 kDa	4	1	20.51	16.40	23.48	<b>P&lt;0.05</b>
	<sup>188</sup> Re-HEDP OSA	3	0	10.00	10.00	12.00	
	<sup>188</sup> Re-HEDP	4	0	10.00	8.50	13.00	
	<sup>153</sup> Sm-EDTMP	4	0	11.16	9.18	12.55	
<b>BG T<sub>½</sub>(min)</b>	<sup>153</sup> Sm-PEI-MP10-30 kDa	4	0	48.00	29.00	50.00	
	<sup>99m</sup> Tc-PEI-MP 10-30 kDa	4	0	29.00	23.00	40.00	<b>P&lt;0.05</b>
	<sup>99m</sup> Tc-PEI-MP 20-30 kDa	4	0	18.00	15.00	22.00	
	<sup>188</sup> Re-HEDP OSA	3	0	52.50	50.00	55.00	
	<sup>188</sup> Re-HEDP	4	0	58.44	51.16	62.94	<b>P&lt;0.05</b>
	<sup>153</sup> Sm-EDTMP	4	0	15.50	12.00	19.00	<b>P&lt;0.05</b>
<b>BG % 3hrs</b>	<sup>153</sup> Sm-PEI-MP10-30 kDa	4	0	8.23	1.22	0.61	
	<sup>99m</sup> Tc-PEI-MP 10-30 kDa	4	0	3.33	3.22	1.86	<b>P&lt;0.05</b>
	<sup>99m</sup> Tc-PEI-MP 20-30 kDa	4	0	5.56	1.92	0.86	
	<sup>188</sup> Re-HEDP OSA	3	0	8.67	1.16	0.67	
	<sup>188</sup> Re-HEDP	4	0	9.25	2.22	1.11	<b>P&lt;0.05</b>
	<sup>153</sup> Sm-EDTMP	4	0	4.66	2.52	1.26	

Legend: These descriptive data were used to compare all the radiopharmaceuticals with each other for differences in biodistribution, pharmacokinetics and dosimetry. The results are expressed in medians and IQR (interquartile range 25<sup>th</sup> and 75<sup>th</sup> percentile). The data were collated from Table 8-28 on page 317.

**Table 8-30 Descriptive statistics blood and urine for various radiopharmaceuticals**

Pharmacokinetic Parameter	Group Name	N	Mean±SD
<b>Blood T<sub>½</sub> (TIME)</b>	<sup>153</sup> Sm-PEI-MP 10-30 kDa	4	15.25±2.50
	<sup>99m</sup> Tc-PEI-MP 10-30 kDa	4	20.00±17.32
	<sup>99m</sup> Tc-PEI-MP 20-30 kDa	4	10.60±1.34
	<sup>188</sup> Re-HEDP OSA	3	15.00±0.00
	<sup>188</sup> Re-HEDP	4	15.25±2.50
	<sup>153</sup> Sm-EDTMP	4	16.84±5.00
<b>Blood % ID at 3hrs</b>	<sup>153</sup> Sm-PEI-MP 10-30 kDa	4	4.82±0.23
	<sup>99m</sup> Tc-PEI-MP 10-30 kDa	4	4.33±0.58
	<sup>99m</sup> Tc-PEI-MP 20-30 kDa	4	1.80±1.50
	<sup>188</sup> Re-HEDP OSA	3	7.76±2.22
	<sup>188</sup> Re-HEDP	4	4.82±0.23
	<sup>153</sup> Sm-EDTMP	4	0.78±0.23
<b>Urine Accumulated % ID at 3hrs</b>	<sup>153</sup> Sm-PEI-MP 10-30 kDa	4	42.73±4.48
	<sup>99m</sup> Tc-PEI-MP 10-30 kDa	4	69.75±3.45
	<sup>99m</sup> Tc-PEI-MP 20-30 kDa	4	73.91±1.80
	<sup>188</sup> Re-HEDP OSA	3	30.59±13.31
	<sup>188</sup> Re-HEDP	4	52.31±12.02
	<sup>153</sup> Sm-EDTMP	4	44.34±9.80

Legend: These descriptive data were used to compare all the radiopharmaceuticals with each other for differences in biodistribution, pharmacokinetics and dosimetry.

## 8.8 Dosimetry results for various radiopharmaceuticals

**Table 8-31 Dosimetry results (mGy/MBq) for various organs derived from OLINDA software from normal dogs**

Radiopharmaceutical	Dogs				Descriptive statistics
	Normal Dog1	Normal Dog2	Normal Dog3	Normal Dog4	
<b><sup>153</sup>Sm-EDTMP (mGy/MBq)</b>					<b>Mean±SD</b>
Kidney	0.342	1.930	1.260	0.057	0.897±0.859
Liver	0.228	0.145	0.325	0.469	0.292±0.139
Lungs	0.614	0.529	0.394	0.127	0.416±0.213
Red Marrow	0.741	0.980	0.685	0.606	0.753±0.161
Osteogenic Cells	2.007	3.150	2.580	2.320	2.514±0.484
Urinary Bladder Wall	1.32	1.360	1.260	2.610	1.638±0.650
Total Body	0.0849	0.096	0.092	0.072	0.086±0.010
<b><sup>188</sup>Re-HEDP (mGy/MBq)</b>					<b>Mean±SD</b>
Kidney	4.100	7.880	2.120	7.600	5.425±2.795
Liver	0.312	0.860	0.715	1.100	0.747±0.330
Lungs	0.310	2.060	0.091	2.000	1.115±1.060
Red Marrow	0.161	0.222	0.143	0.281	0.202±0.063
Osteogenic Cells	0.264	0.414	0.283	0.499	0.365±0.111
Urinary Bladder Wall	5.430	1.570	2.020	2.840	2.965±1.725
Total Body	0.059	0.013	0.060	0.141	0.068±0.053
<b><sup>153</sup>Sm-PEI-MP10-30 kDa</b>					<b>Mean±SD</b>
Kidney	1.100	2.020	0.198	0.365	0.921±0.831

<b>Radiopharmaceutical</b>	<b>Dogs</b>				<b>Descriptive statistics</b>
Liver	0.161	0.186	1.920	0.701	0.742±0.824
Lungs	0.019	0.090	0.414	0.344	0.217±0.192
Red Marrow	0.414	0.355	0.395	0.350	0.379±0.031
Osteogenic Cells	1.710	0.990	1.360	1.050	1.278±0.331
Urinary Bladder Wall	0.765	1.240	0.991	0.988	0.996±0.194
Total Body	0.142	0.046	0.112	0.056	0.089±0.046
<b><sup>186</sup>Re (mGy/MBq)</b>	<b><sup>186</sup>Re-HEDP Normal Dog 1</b>	<b><sup>186</sup>Re -PEI-MP 20-30 kDa</b>			
Kidney	3.480	1.900			
Liver	0.814	4.350			
Lungs	0.141	1,51			
Red Marrow	0.363	0.046			
Osteogenic Cells	0.560	0.066			
Urinary Bladder Wall	1.990	1.880			
Total Body	0.069	0.145			

Legend: The tissue listed in the dosimetry table derived from pharmacokinetic organ compartment data entered into the OLINDA software. The tissue is reported because of its radiation sensitivity, for example the radiation dose to the red marrow is one of the most significance determinant of the therapeutic dose of a radiopharmaceutical because of dose limiting myelosuppression. The dose is calculate by multiplying the inject dose in MBq by the value for that tissue in mGy.

**Table 8-32 Dosimetry results derived using OLINDA software for dogs with osteosarcoma**

Osteosarcoma Dogs	<sup>153</sup> Sm-EDTMP (Case-13)	<sup>188</sup> Re-HEDP (Case-1)	<sup>188</sup> Re-HEDP (Case-2)	Tc( <sup>153</sup> Sm)-PEI-MP 10-30 kDa (Case-14)*	Tc( <sup>186</sup> Re)-PEI-MP 10-30 kDa (Case-14)	<sup>186</sup> Re -PEI-MP 20-30 kDa (Case-12)
Kidney (mGy/MBq)	6.610	4.330	2.87	0.152	0.186	0.224
Liver	0.861	0.355	0.883	0.026	0.031	0.020
Lungs	0.242	2.010	1.71	0.049	0.059	0.024
Red Marrow	0.544	0.240	0.184	0.017	0.015	0.123
Osteogenic Cells	2.310	0.570	0.332	0.029	0.019	0.153
Urinary Bladder Wall	0.840	1.220	1.72	1.190	1.460	2.000
Total Body	0.127	0.128	0.103	0.005	0.010	0.010
Tumour Self Dose (Gy)	25.18 Gy	44.32 Gy	30.63 Gy	26 Gy	26 Gy	NR

**Table 8-33 Self dose calculations for tumours**

Tumour self-dose calculations	Tc( <sup>153</sup> Sm)-PEI-MP 10-30 kDa (Case-14)	Tc( <sup>186</sup> Re)-PEI-MP 10-30 kDa (Case-14)	<sup>188</sup> Re-HEDP (Case-1)	<sup>188</sup> Re-HEDP (Case-2)	<sup>153</sup> Sm-EDTMP (Case-13)
Number disintegrations	0.62	0.62	0.94	0.34	1.13
Tumour size (g)	70.00	70.00	183.47	85.78	1154.69
mGy/MBq	1.50	1.50	2	1.84	1.84
BW (kg)	47.00	47.00	59.9	45	37
Total dose (BWx37 MBq)	1739.00	1739.00	2216.30	1665.00	1369.00
Self-dose (Total dose x mGy/MBq) Gy	26.09	26.09	44.33	30.64	25.19

\* Dosimetry for Case-14 was derived using OLINDA, two radionuclides were simulated (<sup>153</sup>Sm and <sup>186</sup>Re) to compare radiation dose to vital organs and the tumour.

## Chapter 9. References

### Reference List

- (1) Jarvis NV, Zeevaart JR, Wagener JM et al. Metal-ion speciation in blood plasma incorporating the water-soluble polymer, polyethyleneimine functionalised with methylenephosphate groups, in therapeutic radiopharmaceuticals. *Radiochimica Acta* 2002;90:237-246.
- (2) Lam MG, de Klerk JM, van Rijk PP, Zonnenberg BA. Bone seeking radiopharmaceuticals for palliation of pain in cancer patients with osseous metastases. *Anticancer Agents Med Chem* 2007;7(4):381-397.
- (3) Louw WK, Dormehl IC, van Rensburg AJ et al. Evaluation of samarium-153 and holmium-166-EDTMP in the normal baboon model. *Nucl Med Biol* 1996;23(8):935-40.
- (4) Chakraborty S, Das T, Banerjee S et al. <sup>177</sup>Lu-EDTMP: a viable bone pain palliative in skeletal metastasis. *Cancer Biother Radiopharm* 2008;23(2):202-213.
- (5) Liepe K. Alpharadin, a <sup>223</sup>Ra-based alpha-particle-emitting pharmaceutical for the treatment of bone metastases in patients with cancer. *Curr Opin Investig Drugs* 2009;10(12):1346-1358.
- (6) Nilsson S, Larsen RH, Fossa SD et al. First clinical experience with alpha-emitting radium-223 in the treatment of skeletal metastases. *Clin Cancer Res* 2005;11(12):4451-4459.
- (7) Lattimer JC, Corwin LA, Jr., Stapleton J et al. Clinical and clinicopathologic response of canine bone tumor patients to treatment with samarium-153-EDTMP. *J Nucl Med* 1990;31(8):1316-25.
- (8) Franzius C, Bielack S, Flege S et al. High-activity samarium-153-EDTMP therapy followed by autologous peripheral blood stem cell support in unresectable osteosarcoma. *Nuklearmedizin* 2001;40(6):215-20.
- (9) Franzius C, Bielack S, Sciuk J, Vollet B, Jurgens H, Schober O. High-activity samarium-153-EDTMP therapy in unresectable osteosarcoma. *Nuklearmedizin* 1999;38(8):337-40.
- (10) Anderson PM, Wiseman GA, Dispenzieri A et al. High-dose samarium-153 ethylene diamine tetramethylene phosphonate: low toxicity of skeletal irradiation in patients with osteosarcoma and bone metastases. *J Clin Oncol* 2002;20(1):189-96.
- (11) Anderson PM, Wiseman GA, Erlandson L et al. Gemcitabine radiosensitization after high-dose samarium for osteoblastic osteosarcoma. *Clin Cancer Res* 2005;11(19 Pt 1):6895-6900.

- (12) Anderson P, Nunez R. Samarium leixidronam (153Sm-EDTMP): skeletal radiation for osteoblastic bone metastases and osteosarcoma. *Expert Rev Anticancer Ther* 2007;7(11):1517-1527.
- (13) Loeb DM, Garrett-Mayer E, Hobbs RF et al. Dose-finding study of 153Sm-EDTMP in patients with poor-prognosis osteosarcoma. *Cancer* 2009;115(11):2514-2522.
- (14) Franzius C, Schuck A, Bielack SS. High-dose samarium-153 ethylene diamine tetramethylene phosphonate: low toxicity of skeletal irradiation in patients with osteosarcoma and bone metastases. *J Clin Oncol* 2002;20(7):1953-4.
- (15) Lattimer JC, Corwin LA, Jr., Stapleton J et al. Clinical and clinicopathologic effects of Samarium-153-EDTMP administered intravenously to normal Beagle dogs. *J Nucl Med* 1990;31:586-593.
- (16) Padilla L, Lee C, Milner R, Shahlaee A, Bolch WE. Canine Anatomic Phantom for Preclinical Dosimetry in Internal Emitter Therapy. *J Nucl Med* 2008.
- (17) Mueller F, Fuchs B, Kaser-Hotz B. Comparative biology of human and canine osteosarcoma. *Anticancer Res* 2007;27(1A):155-164.
- (18) Khanna C, Lindblad-Toh K, Vail D et al. The dog as a cancer model. *Nat Biotechnol* 2006;24(9):1065-1066.
- (19) Thomas R, Wang HJ, Tsai PC et al. Influence of genetic background on tumor karyotypes: evidence for breed-associated cytogenetic aberrations in canine appendicular osteosarcoma. *Chromosome Res* 2009;17(3):365-377.
- (20) Dernell WS, Straw RC, Withrow SJ. Tumors of the Skeletal System. In: Withrow SJ, MacEwen EG, editors. *Small Animal Clinical Oncology*. 3rd ed. Philadelphia: W. B. Saunders Company; 2001. 378-417.
- (21) Dormehl IC, Louw WK, Milner RJ, Kilian E, Schneeweiss FH. Biodistribution and pharmacokinetics of variously sized molecular radiolabelled polyethyleneiminomethyl phosphonic acid as a selective bone seeker for therapy in the normal primate model. *Arzneimittelforschung* 2001;51(3):258-63.
- (22) Milner RJ, Dormehl I, Louw WK, Croft S. Targeted radiotherapy with Sm-153-EDTMP in nine cases of canine primary bone tumours. *J S Afr Vet Assoc* 1998;69(1):12-7.
- (23) Clarke B. Normal bone anatomy and physiology. *Clin J Am Soc Nephrol* 2008;3 Suppl 3:S131-S139.
- (24) Hadjidakis DJ, Androulakis II. Bone remodeling. *Ann N Y Acad Sci* 2006;1092:385-396.
- (25) Barger AM, Fan TM, de Lorimier LP, Sprandel IT, O'Dell-Anderson K. Expression of receptor activator of nuclear factor kappa-B ligand (RANKL) in neoplasms of dogs and cats. *J Vet Intern Med* 2007;21(1):133-140.



- (26) Mori K, Le GB, Berreur M et al. Human osteosarcoma cells express functional receptor activator of nuclear factor-kappa B. *J Pathol* 2007;211(5):555-562.
- (27) Shen L, Xie X, Su Y, Luo C, Zhang C, Zeng B. Parathyroid Hormone versus Bisphosphonate Treatment on Bone Mineral Density in Osteoporosis Therapy: A Meta-Analysis of Randomized Controlled Trials. *PLoS ONE* 2011;6(10):e26267.
- (28) Lasota J, Fanburg-Smith JC. Genetics for the diagnosis and treatment of mesenchymal tumors. *Semin Musculoskelet Radiol* 2007;11(3):215-230.
- (29) Kansara M, Thomas DM. Molecular pathogenesis of osteosarcoma. *DNA Cell Biol* 2007;26(1):1-18.
- (30) Wang LL. Biology of osteogenic sarcoma. *Cancer J* 2005;11(4):294-305.
- (31) Sandberg AA, Bridge JA. Updates on the cytogenetics and molecular genetics of bone and soft tissue tumors: osteosarcoma and related tumors. *Cancer Genet Cytogenet* 2003;145(1):1-30.
- (32) Hayden JB, Hoang BH. Osteosarcoma: basic science and clinical implications. *Orthop Clin North Am* 2006;37(1):1-7.
- (33) Marcellin-Little DJ, DeYoung DJ, Thrall DE, Merrill CL. Osteosarcoma at the site of bone infarction associated with total hip arthroplasty in a dog. *Vet Surg* 1999;28(1):54-60.
- (34) Ragland BD, Bell WC, Lopez RR, Siegal GP. Cytogenetics and molecular biology of osteosarcoma. *Lab Invest* 2002;82(4):365-73.
- (35) Fuchs B, Pritchard DJ. Etiology of osteosarcoma. *Clin Orthop* 2002;(397):40-52.
- (36) Levine RA, Fleischli MA. Inactivation of p53 and retinoblastoma family pathways in canine osteosarcoma cell lines. *Vet Pathol* 2000;37(1):54-61.
- (37) Mendoza S, Konishi T, Dernell WS, Withrow SJ, Miller CW. Status of the p53, Rb and MDM2 genes in canine osteosarcoma. *Anticancer Res* 1998;18(6A):4449-53.
- (38) Yasko AW, Patel SR, Pollack A, Pollock RE. Sarcomas of soft tissue and bone. In: Lenhard RE, Osteen RT, Gansler T, editors. *The American Cancer Society's Clinical Oncology*. Atlanta: The American Cancer Society, Inc.; 2001. 611-631.
- (39) Brodey RS. The use of naturally occurring cancer in domestic animals for research into human cancer: general considerations and a review of canine skeletal osteosarcoma. *Yale J Biol Med* 1979;52(4):345-61.
- (40) Kadosawa T, Nozaki K, Sasaki N, Takeuchi A. Establishment and characterization of a new cell line from a canine osteosarcoma. *J Vet Med Sci* 1994;56(6):1167-9.

- (41) Saifuddin A. The accuracy of imaging in the local staging of appendicular osteosarcoma. *Skeletal Radiol* 2002;31(4):191-201.
- (42) Saifuddin A, Burnett SJ, Mitchell R. Pictorial review: ultrasonography of primary bone tumours. *Clin Radiol* 1998;53(4):239-46.
- (43) Picci P, Vanel D, Briccoli A et al. Computed tomography of pulmonary metastases from osteosarcoma: the less poor technique. A study of 51 patients with histological correlation. *Ann Oncol* 2001;12(11):1601-4.
- (44) Bacci G, Lari S. Current treatment of high grade osteosarcoma of the extremity: review. *J Chemother* 2001;13(3):235-43.
- (45) Bruland OS, Skretting A, Aas M. Targeted radiotherapy of osteosarcoma using <sup>153</sup>Sm-EDTMP. A promising approach. *Acta Oncol* 1996;35:381-384.
- (46) Sawyer EJ, Cassoni AM, Waddington W, Bomanji JB, Briggs TW. Rhenium-186 HEDP as a boost to external beam irradiation in osteosarcoma. *Br J Radiol* 1999;72(864):1225-9.
- (47) Mundy GR. Metastasis to bone: causes, consequences and therapeutic opportunities. *Nat Rev Cancer* 2002;2(8):584-93.
- (48) Atkins HL. Overview of Nuclides for Bone Pain Palliation. *Appl Radiat Isot* 1998;49(4):277-283.
- (49) Lewington VJ. Cancer therapy using bone-seeking isotopes. *Phys Med Biol* 1996;41(10):2027-42.
- (50) Serafini AN. Therapy of metastatic bone pain. *J Nucl Med* 2001;42(6):895-906.
- (51) Bouchet LG, Bolch WE, Goddu SM, Howell RW, Rao DV. Considerations in the selection of radiopharmaceuticals for palliation of bone pain from metastatic osseous lesions. *J Nucl Med* 2000;41(4):682-7.
- (52) Chakraborty S, Das T, Sarma HD, Venkatesh M, Banerjee S. Comparative studies of <sup>177</sup>Lu-EDTMP and <sup>177</sup>Lu-DOTMP as potential agents for palliative radiotherapy of bone metastasis. *Appl Radiat Isot* 2008;66(9):1196-1205.
- (53) Das T, Chakraborty S, Unni PR et al. <sup>177</sup>Lu-labeled cyclic polyaminophosphonates as potential agents for bone pain palliation. *Appl Radiat Isot* 2002;57(2):177-184.
- (54) Nilsson S, Strang P, Aksnes AK et al. A randomized, dose-response, multicenter phase II study of radium-223 chloride for the palliation of painful bone metastases in patients with castration-resistant prostate cancer. *Eur J Cancer* 2012;48(5):678-686.

- (55) Saha GB. Instrumentation for Radiation Detection and Measurement. In: Saha GB, editor. *Fundamentals of Nuclear Pharmacy*. Fourth ed. New York: Springer-Verlag; 1998. 31-64.
- (56) Saha GB. Radioactive Decay. In: Saha GB, editor. *Fundamentals of Nuclear Pharmacy*. 4th ed. New York: Springer-Verlag; 1998. 11-30.
- (57) Andrews HL. Charged Particle Emission and Radioactive decay. In: Andrews HL, editor. *Radiation Biophysics*. New Jersey: Prentice-Hall, Inc.; 1974. 83-99.
- (58) Berger JS, Coursey JS, Zucker MA, Chang J. Stopping-Power and Range Tables for Electrons, Protons, and Helium Ions. *National Institute of Standards and Technology* 2005; Available at: URL: <http://physics.nist.gov>.
- (59) Unterweger MP, Hoppes DD, Schima FJ, Coursey JS. Radionuclide Half-Life Measurements. *National Institute of Standards and Technology, Physics Laboratory, Ionizing Radiation* 2003; Available at: URL: <http://physics.nist.gov>. Accessed August 8, 2007.
- (60) Kimmel DB. Mechanism of action, pharmacokinetic and pharmacodynamic profile, and clinical applications of nitrogen-containing bisphosphonates. *J Dent Res* 2007;86(11):1022-1033.
- (61) Milner RJ, Farese J, Henry CJ, Selting K, Fan TM, de Lorimier LP. Bisphosphonates and cancer. *J Vet Intern Med* 2004;18(5):597-604.
- (62) Russell RG, Watts NB, Ebtino FH, Rogers MJ. Mechanisms of action of bisphosphonates: similarities and differences and their potential influence on clinical efficacy. *Osteoporos Int* 2008;19(6):733-759.
- (63) Lin JH. Bisphosphonates: a review of their pharmacokinetic properties. *Bone* 1996;18(2):75-85.
- (64) Mercadante S. Malignant bone pain: pathophysiology and treatment. *Pain* 1997;69(1-2):1-18.
- (65) Aapro M, Abrahamsson PA, Body JJ et al. Guidance on the use of bisphosphonates in solid tumours: recommendations of an international expert panel. *Ann Oncol* 2008;19(3):420-432.
- (66) Clezardin P, Benzaid I, Croucher PI. Bisphosphonates in preclinical bone oncology. *Bone* 2011;49(1):66-70.
- (67) Fleisch H. Development of bisphosphonates. *Breast Cancer Res* 2002;4(1):30-34.
- (68) Rogers MJ, Gordon S, Benford HL et al. Cellular and molecular mechanisms of action of bisphosphonates. *Cancer* 2000;88(12 Suppl):2961-78.

- (69) Neves M, Gano L, Pereira N et al. Synthesis, characterization and biodistribution of bisphosphonates Sm-153 complexes: correlation with molecular modeling interaction studies. *Nucl Med Biol* 2002;29(3):329-338.
- (70) Neville-Webbe HL, Holen I, Coleman RE. The anti-tumour activity of bisphosphonates. *Cancer Treat Rev* 2002;28(6):305-319.
- (71) Ebetino FH, Hogan AM, Sun S et al. The relationship between the chemistry and biological activity of the bisphosphonates. *Bone* 2011;49(1):20-33.
- (72) Russell RG. Bisphosphonates: mode of action and pharmacology. *Pediatrics* 2007;119 Suppl 2:S150-S162.
- (73) Ito M, Amizuka N, Nakajima T, Ozawa H. Ultrastructural and cytochemical studies on cell death of osteoclasts induced by bisphosphonate treatment. *Bone* 1999;25(4):447-52.
- (74) Dormehl IC, Louw WK, Schneeweiss FH et al. Uptake of ethylenediamine tetramethylene phosphonic acid in normal bone after multiple applications. A non-human primate study. *Arzneimittelforschung* 1998;48(4):408-14.
- (75) Adami S, Zamberlan N. Adverse effects of bisphosphonates. A comparative review. *Drug Saf* 1996;14(3):158-170.
- (76) Mashiba T, Hirano T, Turner CH, Forwood MR, Johnston CC, Burr DB. Suppressed bone turnover by bisphosphonates increases microdamage accumulation and reduces some biomechanical properties in dog rib. *J Bone Miner Res* 2000;15(4):613-20.
- (77) Mashiba T, Turner CH, Hirano T et al. Effects of high-dose etidronate treatment on microdamage accumulation and biomechanical properties in beagle bone before occurrence of spontaneous fractures. *Bone* 2001;29(3):271-8.
- (78) Peter CP, Guy J, Shea M, Bagdon W, Kline WF, Hayes WC. Long-term safety of the aminobisphosphonate alendronate in adult dogs. I. General safety and biomechanical properties of bone. *J Pharmacol Exp Ther* 1996;276(1):271-6.
- (79) Green JR, Seltenmeyer Y, Jaeggi KA, Widler L. Renal tolerability profile of novel, potent bisphosphonates in two short-term rat models. *Pharmacol Toxicol* 1997;80(5):225-230.
- (80) O'Sullivan TL, Akbari A, Cadnapaphornchai P. Acute renal failure associated with the administration of parenteral etidronate. *Ren Fail* 1994;16(6):767-773.
- (81) Berenson JR, Rosen L, Vescio R et al. Pharmacokinetics of pamidronate disodium in patients with cancer with normal or impaired renal function. *J Clin Pharmacol* 1997;37(4):285-290.
- (82) Body JJ. The risk of cumulative renal effects of intravenous bisphosphonates. *Support Cancer Ther* 2006;3(2):77-83.

- (83) Tyrrell CJ, Collinson M, Madsen EL, Ford JM, Coleman T. Intravenous pamidronate: infusion rate and safety. *Ann Oncol* 1994;5 Suppl 7:S27-S29.
- (84) Rumberiha WK, Fitzgerald SD, Kruger JM et al. Use of pamidronate disodium to reduce cholecalciferol-induced toxicosis in dogs. *Am J Vet Res* 2000;61(1):9-13.
- (85) Rumberiha WK, Kruger JM, Fitzgerald SF et al. Use of pamidronate to reverse vitamin D3-induced toxicosis in dogs. *Am J Vet Res* 1999;60(9):1092-7.
- (86) Body JJ, Mancini I. Bisphosphonates for cancer patients: why, how, and when? *Support Care Cancer* 2002;10(5):399-407.
- (87) Sonnemann J, Eckervogt V, Truckenbrod B, Boos J, Winkelmann W, van Valen F. The bisphosphonate pamidronate is a potent inhibitor of human osteosarcoma cell growth in vitro. *Anticancer Drugs* 2001;12(5):459-65.
- (88) Mackie PS, Fisher JL, Zhou H, Choong PF. Bisphosphonates regulate cell growth and gene expression in the UMR 106-01 clonal rat osteosarcoma cell line. *Br J Cancer* 2001;84(7):951-8.
- (89) Giuliani N, Pedrazzoni M, Passeri G, Girasole G. Bisphosphonates inhibit IL-6 production by human osteoblast-like cells. *Scand J Rheumatol* 1998;27(1):38-41.
- (90) Frith JC, Monkkonen J, Blackburn GM, Russell RG, Rogers MJ. Clodronate and liposome-encapsulated clodronate are metabolized to a toxic ATP analog, adenosine 5'-(beta, gamma-dichloromethylene) triphosphate, by mammalian cells in vitro. *J Bone Miner Res* 1997;12(9):1358-67.
- (91) Endo N, Rutledge SJ, Opas EE, Vogel R, Rodan GA, Schmidt A. Human protein tyrosine phosphatase-sigma: alternative splicing and inhibition by bisphosphonates. *J Bone Miner Res* 1996;11(4):535-43.
- (92) Klenner T, Wingen F, Keppler BK, Krempien B, Schmahl D. Anticancer-agent-linked phosphonates with antiosteolytic and antineoplastic properties: a promising perspective in the treatment of bone-related malignancies? *J Cancer Res Clin Oncol* 1990;116(4):341-50.
- (93) Pool BL, Berger M, Schlehofer JR, Wingen F. In vivo and in vitro investigations on biological effects of aromatic bis-(2-chloroethyl)amino-bisphosphonic acids, new agents proposed for chemotherapy of bone tumors: cytostatic activity in rat osteosarcoma; toxicity and genotoxicity in liver and bone marrow; mutagenicity in *S. typhimurium*. *Invest New Drugs* 1988;6(2):67-78.
- (94) Tomlin JL, Sturgeon C, Pead MJ, Muir P. Use of the bisphosphonate drug alendronate for palliative management of osteosarcoma in two dogs. *Vet Rec* 2000;147(5):129-32.

- (95) Fan TM, de Lorimier LP, O'Dell-Anderson K, Lacoste HI, Charney SC. Single-agent pamidronate for palliative therapy of canine appendicular osteosarcoma bone pain. *J Vet Intern Med* 2007;21(3):431-439.
- (96) Diel IJ. Antitumour effects of bisphosphonates: first evidence and possible mechanisms. *Drugs* 2000;59(3):391-9.
- (97) Farese JP, Ashton J, Milner R, Ambrose LL, Van Gilder J. The effect of the bisphosphonate alendronate on viability of canine osteosarcoma cells in vitro. *In Vitro Cell Dev Biol Anim* 2004;40(3-4):113-117.
- (98) Body JJ, Bartl R, Burckhardt P et al. Current use of bisphosphonates in oncology. International Bone and Cancer Study Group. *J Clin Oncol* 1998;16(12):3890-9.
- (99) Polascik TJ. Bisphosphonates in oncology: evidence for the prevention of skeletal events in patients with bone metastases. *Drug Des Devel Ther* 2009;3:27-40.
- (100) Saad F, Gleason DM, Murray R et al. Long-term efficacy of zoledronic acid for the prevention of skeletal complications in patients with metastatic hormone-refractory prostate cancer. *J Natl Cancer Inst* 2004;96(11):879-882.
- (101) Small EJ, Smith MR, Seaman JJ, Petrone S, Kowalski MO. Combined analysis of two multicenter, randomized, placebo-controlled studies of pamidronate disodium for the palliation of bone pain in men with metastatic prostate cancer. *J Clin Oncol* 2003;21(23):4277-4284.
- (102) Moe L, Boysen M, Aas M, Lonaas L, Gamlem H, Bruland OS. Maxillectomy and targeted radionuclide therapy with <sup>153</sup>Sm-EDTMP in a recurrent canine osteosarcoma. *J Small Anim Pract* 1996;37(5):241-6.
- (103) Straw RC, Powers BE, Klausner J et al. Canine mandibular osteosarcoma: 51 cases (1980-1992). *J Am Anim Hosp Assoc* 1996;32(3):257-62.
- (104) Aas M, Moe L, Gamlem H, Skretting A, Ottesen N, Bruland OS. Internal radionuclide therapy of primary osteosarcoma in dogs, using <sup>153</sup>Sm-ethylene-diamino-tetramethylene-phosphonate (EDTMP). *Clin Cancer Res* 1999;5(10 Suppl):3148s-3152s.
- (105) Kvinnsland Y, Bruland O, Moe L, Skretting A. A method for measurement of the uptake patterns of two beta-emitting radionuclides in the same tissue section with a digital silicon detector: application to a study of <sup>89</sup>SrCl<sub>2</sub> and <sup>153</sup>Sm-EDTMP in a dog with spontaneous osteosarcoma. *Eur J Nucl Med Mol Imaging* 2002;29(2):191-7.
- (106) Barnard SM, Zuber RM, Moore AS. Samarium Sm 153 lexidronam for the palliative treatment of dogs with primary bone tumors: 35 cases (1999-2005). *J Am Vet Med Assoc* 2007;230(12):1877-1881.
- (107) Lam MG, de Klerk JM, Zonnenberg BA. Treatment of painful bone metastases in hormone-refractory prostate cancer with zoledronic acid and samarium-153-

- ethylenediaminetetramethylphosphonic acid combined. *J Palliat Med* 2009;12(7):649-651.
- (108) Lam MG, Dahmane A, Stevens WH, van Rijk PP, de Klerk JM, Zonnenberg BA. Combined use of zoledronic acid and <sup>153</sup>Sm-EDTMP in hormone-refractory prostate cancer patients with bone metastases. *Eur J Nucl Med Mol Imaging* 2008;35(4):756-765.
- (109) Knapp FF, Jr., Beets AL, Guhlke S et al. Availability of rhenium-188 from the alumina-based tungsten-188/rhenium-188 generator for preparation of rhenium-188-labeled radiopharmaceuticals for cancer treatment. *Anticancer Res* 1997;17(3B):1783-95.
- (110) Liepe K, Franke WG, Kropp J, Koch R, Runge R, Hliscs R. [Comparison of rhenium-188, rhenium-186-HEDP and strontium-89 in palliation of painful bone metastases]. *Nuklearmedizin* 2000;39(6):146-51.
- (111) Palmedo H, Guhlke S, Bender H et al. Dose escalation study with rhenium-188 hydroxyethylidene diphosphonate in prostate cancer patients with osseous metastases. *Eur J Nucl Med* 2000;27(2):123-30.
- (112) Palmedo H, Manka-Waluch A, Albers P et al. Repeated bone-targeted therapy for hormone-refractory prostate carcinoma: randomized phase II trial with the new, high-energy radiopharmaceutical rhenium-188 hydroxyethylidenediphosphonate. *J Clin Oncol* 2003;21(15):2869-2875.
- (113) Li S, Liu J, Zhang H, Tian M, Wang J, Zheng X. Rhenium-188 HEDP to treat painful bone metastases. *Clin Nucl Med* 2001;26(11):919-22.
- (114) Liepe K, Kropp J, Runge R, Kotzerke J. Therapeutic efficiency of rhenium-188-HEDP in human prostate cancer skeletal metastases. *Br J Cancer* 2003;89(4):625-629.
- (115) Liepe K, Kotzerke J. A comparative study of <sup>188</sup>Re-HEDP, <sup>186</sup>Re-HEDP, <sup>153</sup>Sm-EDTMP and <sup>89</sup>Sr in the treatment of painful skeletal metastases. *Nucl Med Commun* 2007;28(8):623-630.
- (116) Maxon HR, III, Thomas SR, Hertzberg VS et al. Rhenium-186 hydroxyethylidene diphosphonate for the treatment of painful osseous metastases. *Semin Nucl Med* 1992;22(1):33-40.
- (117) de Klerk JM, Zonnenberg BA, Blijham GH et al. Treatment of metastatic bone pain using the bone seeking radiopharmaceutical Re-186-HEDP. *Anticancer Res* 1997;17(3B):1773-1777.
- (118) Jain RK. Determinants of tumor blood flow: a review. *Cancer Res* 1988;48(10):2641-58.
- (119) Seymour LW. Passive tumor targeting of soluble macromolecules and drug conjugates. *Crit Rev Ther Drug Carrier Syst* 1992;9(2):135-87.

- (120) Maeda H, Bharate GY, Daruwalla J. Polymeric drugs for efficient tumor-targeted drug delivery based on EPR-effect. *Eur J Pharm Biopharm* 2009;71(3):409-419.
- (121) Verma N, Singh-Wadhwa S, Chan WL. Bony metastases seen on scintigraphy with samarium-153. *Clin Nucl Med* 2002;27(3):207.
- (122) Bayouth JE, Macey DJ, Kasi LP, Fossella FV. Dosimetry and toxicity of samarium-153-EDTMP administered for bone pain due to skeletal metastases. *J Nucl Med* 1994;35(1):63-9.
- (123) Madrazo A, Schwarz G, Churg J. Radiation nephritis: A review. *Journal of Urology* 1975;114:822-827.
- (124) Gudkov AV, Komarova EA. The role of p53 in determining sensitivity to radiotherapy. *Nat Rev Cancer* 2003;3(2):117-129.
- (125) Vit JP, Rosselli F. Role of the ceramide-signaling pathways in ionizing radiation-induced apoptosis. *Oncogene* 2003;22(54):8645-8652.
- (126) DeRegis CJ, Moore AS, Rand WM, Berg J. Cisplatin and doxorubicin toxicosis in dogs with osteosarcoma. *J Vet Intern Med* 2003;17(5):668-673.
- (127) Prasad KN. Antioxidants in cancer care: when and how to use them as an adjunct to standard and experimental therapies. *Expert Rev Anticancer Ther* 2003;3(6):903-915.
- (128) Thrall DE. Biologic Principles of Radiation Therapy. In: Morrison WB, editor. *Cancer in Dogs and Cats. Medical and Surgical Management*. Maryland: Williams & Wilkins; 1998. 399-413.
- (129) Thrall DE. Biologic basis of radiation therapy. *Vet Clin North Am [Small Anim Pract]* 1997;27:21-36.
- (130) Gillette-EL. Radiation oncology. *Semin Vet Med Surg (Small Anim)* 1995;10:127-213.
- (131) Dale RG. The use of the linear-quadratic radiobiological model for quantifying kidney response in targeted radiotherapy. *Cancer Biother Radiopharm* 2004;19(3):363-370.
- (132) Dale RG. Dose-rate effects in targeted radiotherapy. *Phys Med Biol* 1996;41:1871-1884.
- (133) Dale RG, Carabe-Fernandez A. The radiobiology of conventional radiotherapy and its application to radionuclide therapy. *Cancer Biother Radiopharm* 2005;20(1):47-51.
- (134) Brown SA. Pharmacokinetics: Disposition and fate of drugs in the body. In: Adams HR, editor. *Veterinary Pharmacology and Therapeutics*. 8th ed. Ames: Iowa State University Press; 2001. 15-56.
- (135) Greish K. Enhanced permeability and retention of macromolecular drugs in solid tumors: a royal gate for targeted anticancer nanomedicines. *J Drug Target* 2007;15(7-8):457-464.



- (136) Jain RK. Delivery of molecular and cellular medicine to solid tumors. *Adv Drug Deliv Rev* 2001;46(1-3):149-68.
- (137) Jain RK. Transport of molecules, particles, and cells in solid tumors. *Annu Rev Biomed Eng* 1999;1:241-63.
- (138) Coomber BL, Denton J, Sylvestre A, Kruth S. Blood vessel density in canine osteosarcoma. *Can J Vet Res* 1998;62(3):199-204.
- (139) Robert C, Montemont G, Rebuffel V, Verger L, Buvat I. Optimization of a parallel hole collimator/CdZnTe gamma-camera architecture for scintimammography. *Med Phys* 2011;38(4):1806-1819.
- (140) Zeng GL, Gagnon D, Matthews CG, Kolthammer JA, Radachy JD, Hawkins WG. Image reconstruction algorithm for a rotating slat collimator. *Med Phys* 2002;29(7):1406-1412.
- (141) Daniel GB, Poteet B, Kowalsky RD. Image artifacts and quality control. In: Berry CR, Daniel GB, editors. *Handbook of veterinary nuclear medicine*. 1997. 36-44.
- (142) Doherty J, Graham D. Radiopharmacy. In: Sharp PF, Gemmell HG, Murray AD, editors. *Practical Nuclear Medicine*. Third Edition ed. London: Springer-Verlag; 2005. 113-142.
- (143) Silberstein EB, Ryan J. Prevalence of adverse reactions in nuclear medicine. Pharmacopeia Committee of the Society of Nuclear Medicine. *J Nucl Med* 1996;37(1):185-192.
- (144) Hesselwood SR, Keeling DH. Frequency of adverse reactions to radiopharmaceuticals in Europe. *Eur J Nucl Med* 1997;24(9):1179-1182.
- (145) Vail DM, MacEwen EG. Spontaneously occurring tumors of companion animals as models for human cancer. *Cancer Invest* 2000;18(8):781-92.
- (146) Knapp DW, Waters DJ. Naturally occurring cancer in pet dogs: important models for developing improved cancer therapy for humans. *Mol Med Today* 1997;3(1):8-11.
- (147) Hahn KA, Bravo L, Adams WH, Frazier DL. Naturally occurring tumors in dogs as comparative models for cancer therapy research. *In Vivo* 1994;8(1):133-43.
- (148) Withrow SJ, Powers BE, Straw RC, Wilkins RM. Comparative aspects of osteosarcoma. Dog versus man. *Clin Orthop* 1991;(270):159-68.
- (149) MacEwen EG. Spontaneous tumors in dogs and cats: models for the study of cancer biology and treatment. *Cancer Metastasis Rev* 1990;9(2):125-36.
- (150) Selvarajah GT, Kirpensteijn J, van Wolferen ME, Rao NA, Fieten H, Mol JA. Gene expression profiling of canine osteosarcoma reveals genes associated with short and long survival times. *Mol Cancer* 2009;8:72.

- (151) Inoue M, Shiramizu K. Immunohistochemical detection of p53 and c-myc proteins in canine mammary tumours. *J Comp Pathol* 1999;120(2):169-75.
- (152) Haga S, Nakayama M, Tatsumi K et al. Overexpression of the p53 gene product in canine mammary tumors. *Oncol Rep* 2001;8(6):1215-9.
- (153) Setoguchi A, Sakai T, Okuda M et al. Aberrations of the p53 tumor suppressor gene in various tumors in dogs. *Am J Vet Res* 2001;62(3):433-9.
- (154) Albaric O, Bret L, Amardeihl M, Delverdier M. Immunohistochemical expression of p53 in animal tumors: a methodological study using four anti-human p53 antibodies. *Histol Histopathol* 2001;16(1):113-21.
- (155) Johnson AS, Couto CG, Weghorst CM. Mutation of the p53 tumor suppressor gene in spontaneously occurring osteosarcomas of the dog. *Carcinogenesis* 1998;19(1):213-7.
- (156) van Leeuwen IS, Cornelisse CJ, Misdorp W, Goedegebuure SA, Kirpensteijn J, Rutteman GR. P53 gene mutations in osteosarcomas in the dog. *Cancer Lett* 1997;111(1-2):173-8.
- (157) Sagartz JE, Bodley WL, Gamblin RM, Couto CG, Tierney LA, Capen CC. p53 tumor suppressor protein overexpression in osteogenic tumors of dogs. *Vet Pathol* 1996;33(2):213-21.
- (158) Pirkey-Ehrhart N, Withrow SJ, Straw RC et al. Primary rib tumors in 54 dogs. *J Am Anim Hosp Assoc* 1995;31(1):65-9.
- (159) Ru G, Terracini B, Glickman LT. Host related risk factors for canine osteosarcoma. *Vet J* 1998;156(1):31-9.
- (160) Cooley DM, Waters DJ. Skeletal neoplasms of small dogs: a retrospective study and literature review. *J Am Anim Hosp Assoc* 1997;33(1):11-23.
- (161) Mehl ML, Withrow SJ, Seguin B et al. Spontaneous regression of osteosarcoma in four dogs. *J Am Vet Med Assoc* 2001;219(5):614-7.
- (162) Withrow SJ. Osteosarcoma. *Vet Q* 1998;20 Suppl 1:19-21.
- (163) Lucroy MD, Peck JN, Berry CR. Osteosarcoma of the patella with pulmonary metastases in a dog. *Vet Radiol Ultrasound* 2001;42(3):218-20.
- (164) Gamblin RM, Straw RC, Powers BE, Park RD, Bunge MM, Withrow SJ. Primary osteosarcoma distal to the antebrachio-carpal and tarsocrural joints in nine dogs (1980-1992). *J Am Anim Hosp Assoc* 1995;31(1):86-91.
- (165) Dickerson ME, Page RL, LaDue TA et al. Retrospective analysis of axial skeleton osteosarcoma in 22 large-breed dogs. *J Vet Intern Med* 2001;15(2):120-4.

- (166) Heyman SJ, Diefenderfer DL, Goldschmidt MH, Newton CD. Canine axial skeletal osteosarcoma. A retrospective study of 116 cases (1986 to 1989). *Vet Surg* 1992;21(4):304-10.
- (167) Thomas WB, Daniel GB, McGavin MD. Parosteal osteosarcoma of the cervical vertebra in a dog. *Vet Radiol Ultrasound* 1997;38(2):120-3.
- (168) Moore GE, Mathey WS, Eggers JS, Estep JS. Osteosarcoma in adjacent lumbar vertebrae in a dog. *J Am Vet Med Assoc* 2000;217(7):1038-40.
- (169) Dickinson PJ, McEntee MC, Lipsitz D, Keel K, LeCouteur RA. Radiation induced vertebral osteosarcoma following treatment of an intradural extramedullary spinal cord tumor in a dog. *Vet Radiol Ultrasound* 2001;42(5):463-70.
- (170) Thamm DH, Mauldin EA, Edinger DT, Lustgarten C. Primary osteosarcoma of the synovium in a dog. *J Am Anim Hosp Assoc* 2000;36(4):326-31.
- (171) Thomsen BV, Myers RK. Extraskelatal osteosarcoma of the mandibular salivary gland in a dog. *Vet Pathol* 1999;36(1):71-3.
- (172) Kuntz CA, Dernell WS, Powers BE, Withrow S. Extraskelatal osteosarcomas in dogs: 14 cases. *J Am Anim Hosp Assoc* 1998;34(1):26-30.
- (173) Langenbach A, Anderson MA, Dambach DM, Sorenmo KU, Shofer FD. Extraskelatal osteosarcomas in dogs: a retrospective study of 169 cases (1986-1996). *J Am Anim Hosp Assoc* 1998;34(2):113-20.
- (174) Slayter MV, Boosinger TR, Pool RR, Dämmrich K, Misdorp W, Larsen S. Histopathological Classification of Bone and Joint Tumors of Domestic Animals. *WHO Organization* 1994.
- (175) Kirpensteijn J, Kik M, Rutteman GR, Teske E. Prognostic significance of a new histologic grading system for canine osteosarcoma. *Vet Pathol* 2002;39(2):240-6.
- (176) Konde LJ. Aggressive Versus Nonaggressive Bone lesions. In: Thrall DE, editor. *Textbook of Veterinary Diagnostic Radiology*. 2nd ed. Philadelphia: W.B. Saunders Company; 1994. 15-23.
- (177) Waters DJ, Coakley FV, Cohen MD et al. The detection of pulmonary metastases by helical CT: a clinicopathologic study in dogs. *J Comput Assist Tomogr* 1998;22(2):235-40.
- (178) Davis GJ, Kapatkin AS, Craig LE, Heins GS, Wortman JA. Comparison of radiography, computed tomography, and magnetic resonance imaging for evaluation of appendicular osteosarcoma in dogs. *J Am Vet Med Assoc* 2002;220(8):1171-6.

- (179) Wallack ST, Wisner ER, Werner JA et al. Accuracy of magnetic resonance imaging for estimating intramedullary osteosarcoma extent in pre-operative planning of canine limb-salvage procedures. *Vet Radiol Ultrasound* 2002;43(5):432-441.
- (180) Leibman NF, Kuntz CA, Steyn PF et al. Accuracy of radiography, nuclear scintigraphy, and histopathology for determining the proximal extent of distal radius osteosarcoma in dogs. *Vet Surg* 2001;30(3):240-5.
- (181) Forrest LJ, Dodge RK, Page RL et al. Relationship between quantitative tumor scintigraphy and time to metastasis in dogs with osteosarcoma. *J Nucl Med* 1992;33(8):1542-7.
- (182) Hahn KA, Hurd C, Cantwell HD. Single-phase methylene diphosphate bone scintigraphy in the diagnostic evaluation of dogs with osteosarcoma. *J Am Vet Med Assoc* 1990;196(9):1483-6.
- (183) Lamb CR, Berg J, Bengston AE. Preoperative measurement of canine primary bone tumors, using radiography and bone scintigraphy. *J Am Vet Med Assoc* 1990;196:1474-1478.
- (184) Berg J, Lamb CR, O'Callaghan MW. Bone scintigraphy in the initial evaluation of dogs with primary bone tumours. *J Am Vet Med Assoc* 1990;196:917-920.
- (185) Hahn KA, Richardson RC. *Cancer chemotherapy: a veterinary handbook*. Malvern, PA 19355; USA: Williams & Wilkins 200 Chester Field Parkway; 1995.
- (186) Garzotto CK, Berg J, Hoffmann WE, Rand WM. Prognostic significance of serum alkaline phosphatase activity in canine appendicular osteosarcoma. *J Vet Intern Med* 2000;14(6):587-92.
- (187) Ehrhart N, Dernell WS, Hoffmann WE, Weigel RM, Powers BE, Withrow SJ. Prognostic importance of alkaline phosphatase activity in serum from dogs with appendicular osteosarcoma: 75 cases (1990-1996). *J Am Vet Med Assoc* 1998;213(7):1002-6.
- (188) Mauldin GN, Matus RE, Withrow SJ, Patnaik AK. Canine osteosarcoma. Treatment by amputation versus amputation and adjuvant chemotherapy using doxorubicin and cisplatin. *J Vet Intern Med* 1988;2(4):177-80.
- (189) Spodnick GJ, Berg J, Rand WM et al. Prognosis for dogs with appendicular osteosarcoma treated by amputation alone: 162 cases (1978-1988). *J Am Vet Med Assoc* 1992;200:995-999.
- (190) Thompson JP, Fugent MJ. Evaluation of survival times after limb amputation, with and without subsequent administration of cisplatin, for treatment of appendicular osteosarcoma in dogs: 30 cases (1979-1990). *J Am Vet Med Assoc* 1992;200(4):531-3.
- (191) Berg J. Canine osteosarcoma: amputation and chemotherapy. *Vet Clin North Am Small Anim Pract* 1996;26(1):111-21.

- (192) Berg J, Weinstein MJ, Schelling SH, Rand WM. Treatment of dogs with osteosarcoma by administration of cisplatin after amputation or limb-sparing surgery: 22 cases (1987-1990). *J Am Vet Med Assoc* 1992;200(12):2005-8.
- (193) Straw RC, Withrow SJ, Richter SL et al. Amputation and cisplatin for treatment of canine osteosarcoma. *Journal of Veterinary Internal Medicine* 1991;5(4):205-210.
- (194) Chun R, Kurzman ID, Couto CG, Klausner J, Henry C, MacEwen EG. Cisplatin and doxorubicin combination chemotherapy for the treatment of canine osteosarcoma: a pilot study. *J Vet Intern Med* 2000;14(5):495-8.
- (195) Kurzman ID, MacEwen EG, Rosenthal RC et al. Adjuvant therapy for osteosarcoma in dogs: results of randomized clinical trials using combined liposome-encapsulated muramyl tripeptide and cisplatin. *Clin Cancer Res* 1995;1(12):1595-601.
- (196) Kleinerman ES, Jaffe N. Liposomal MTP-PE for the adjuvant therapy of osteosarcoma. *Prog Clin Biol Res* 1990;343:263-79.
- (197) MacEwen EG, Kurzman ID, Rosenthal RC et al. Therapy for osteosarcoma in dogs with intravenous injection of liposome-encapsulated muramyl tripeptide. *J Natl Cancer Inst* 1989;81(12):935-8.
- (198) Berg J, Gebhardt MC, Rand WM. Effect of timing of postoperative chemotherapy on survival of dogs with osteosarcoma. *Cancer* 1997;79(7):1343-50.
- (199) Khanna C, Prehn J, Hayden D et al. A randomized controlled trial of octreotide pamoate long-acting release and carboplatin versus carboplatin alone in dogs with naturally occurring osteosarcoma: evaluation of insulin-like growth factor suppression and chemotherapy. *Clin Cancer Res* 2002;8(7):2406-12.
- (200) Bergman PJ, MacEwen EG, Kurzman ID et al. Amputation and carboplatin for treatment of dogs with osteosarcoma: 48 cases (1991 to 1993). *J Vet Intern Med* 1996;10(2):76-81.
- (201) Bacon NJ, Ehrhart NP, Dernell WS, Lafferty M, Withrow SJ. Use of alternating administration of carboplatin and doxorubicin in dogs with microscopic metastases after amputation for appendicular osteosarcoma: 50 cases (1999-2006). *J Am Vet Med Assoc* 2008;232(10):1504-1510.
- (202) Heidner GL, Page RL, McEntee MC, Dodge RK, Thrall DE. Treatment of canine appendicular osteosarcoma using cobalt 60 radiation and intraarterial cisplatin. *J Vet Intern Med* 1991;5(6):313-6.
- (203) Straw RC, Withrow SJ. Limb-sparing surgery versus amputation for dogs with bone tumors. *Vet Clin North Am Small Anim Pract* 1996;26(1):135-43.
- (204) Withrow SJ, Thrall DE, Straw RC et al. Intra-arterial cisplatin with or without radiation in limb-sparing for canine osteosarcoma. *Cancer* 1993;71(8):2484-90.

- (205) Thrall DE, Withrow SJ, Powers BE et al. Radiotherapy prior to cortical allograft limb sparing in dogs with osteosarcoma: a dose response assay. *Int J Radiat Oncol Biol Phys* 1990;18(6):1351-7.
- (206) LaRue SM, Withrow SJ, Powers BE et al. Limb-sparing treatment for osteosarcoma in dogs. *J Am Vet Med Assoc* 1989;195(12):1734-44.
- (207) Ramirez O, Dodge RK, Page RL et al. Palliative radiotherapy of appendicular osteosarcoma in 95 dogs. *Vet Radiol Ultrasound* 1999;40(5):517-522.
- (208) Straw RC, Withrow SJ, Powers BE. Management of canine appendicular osteosarcoma. *Vet Clin North Am Small Anim Pract* 1990;20(4):1141-61.
- (209) Dernell WS, Straw RC, Cooper MF, Powers BE, LaRue SM, Withrow SJ. Multilobular osteochondrosarcoma in 39 dogs: 1979-1993. *J Am Anim Hosp Assoc* 1998;34(1):11-8.
- (210) Siegel JA, Thomas SR, Stubbs JB et al. MIRD pamphlet no. 16: Techniques for quantitative radiopharmaceutical biodistribution data acquisition and analysis for use in human radiation dose estimates. *J Nucl Med* 1999;40(2):37S-61S.
- (211) Stabin MG. MIRDOSE: personal computer software for internal dose assessment in nuclear medicine. *J Nucl Med* 1996;37(3):538-46.
- (212) Stabin MG, Tagesson M, Thomas SR, Ljungberg M, Strand SE. Radiation dosimetry in nuclear medicine. *Appl Radiat Isot* 1999;50(1):73-87.
- (213) Stabin MG, Sparks RB, Crowe E. OLINDA/EXM: the second-generation personal computer software for internal dose assessment in nuclear medicine. *J Nucl Med* 2005;46(6):1023-1027.
- (214) Lombardi MH. Radioisotopic blood volume and cardiac output in dogs. *Am J Vet Res* 1972;33(9):1825-1834.
- (215) Stabin MG, Siegel JA, Sparks RB, Eckerman KF, Breitz HB. Contribution to red marrow absorbed dose from total body activity: a correction to the MIRD method. *J Nucl Med* 2001;42(3):492-8.
- (216) McKinstry P, Schnitzer JE, Light TR, Ogden JA, Hoffer P. Relationship of <sup>99m</sup>Tc-MDP uptake to regional osseous circulation in skeletally immature and mature dogs. *Skeletal Radiol* 1982;8(2):115-21.
- (217) Polig E, Jee WS. Bone structural parameters, dosimetry, and relative radiation risk in the beagle skeleton. *Radiat Res* 1989;120(1):83-101.
- (218) OLINDA/EXM [computer program]. Version 1 Vanderbilt University, Nashville, Tennessee; 2008.

- (219) Saha GB. Radiopharmaceuticals and methods of radiolabeling. In: Saha GB, editor. *Fundamentals of Nuclear Pharmacy*. 4th ed. New York: Springer; 1997. 80-111.
- (220) Pichardo JC, Milner RJ, Bolch WE. MRI measurement of bone marrow cellularity for radiation dosimetry. *J Nucl Med* 2011;52(9):1482-1489.
- (221) Appelbaum FR, Sandmaier BM, Brown P et al. Myelosuppression and mechanism of recovery following administration of <sup>153</sup>Sm-EDTMP. *Antibody Immunoconj Radiopharmacol* 1988;1:263-270.
- (222) Ketring AR. <sup>153</sup>Sm-EDTMP and <sup>186</sup>Re-HEDP as bone therapeutic radiopharmaceuticals. *Int J Rad Appl Instrum B* 1987;14(3):223-32.
- (223) Weininger J, Ketring AR, Deutsch EA. <sup>186</sup>Re-HEDP: a potential therapeutic bone agent. *Nuklearmedizin* 1984;23(2):81-2.
- (224) Maxon HR3, Schroder LE, Washburn LC et al. Rhenium-188(Sn)HEDP for treatment of osseous metastases. *J Nucl Med* 1998;39(4):659-63.
- (225) Goeckeler WF, Edwards B, Volkert WA, Holmes RA, Simon J, Wilson D. Skeletal localization of Samarium-153 chelates: Potential therapeutic bone agents. *J Nucl Med* 1987;28:495-504.
- (226) Farhanghi M, Holmes RA, Volkert WA, Logan KW, Singh A. Samarium-153-EDTMP: pharmacokinetic, toxicity and pain response using an escalating dose schedule in treatment of metastatic bone cancer. *J Nucl Med* 1992;33(8):1451-8.
- (227) Brenner W, Kampen WU, Kampen AM, Henze E. Skeletal uptake and soft-tissue retention of <sup>186</sup>Re-HEDP and <sup>153</sup>Sm-EDTMP in patients with metastatic bone disease. *J Nucl Med* 2001;42(2):230-6.
- (228) Maxon HR, Deutsch EA, Thomas SR et al. Re-186(Sn) HEDP for treatment of multiple metastatic foci in bone: human biodistribution and dosimetric studies [published erratum appears in Radiology 1988 May;167(2):582]. *Radiology* 1988;166(2):501-507.
- (229) de Klerk JM, van DA, van het Schip AD, Zonnenberg BA, van Rijk PP. Pharmacokinetics of rhenium-186 after administration of rhenium-186-HEDP to patients with bone metastases. *J Nucl Med* 1992;33(5):646-651.
- (230) Brenner W, Kampen WU, Brummer C et al. Bone uptake studies in rabbits before and after high-dose treatment with <sup>153</sup>Sm-EDTMP or <sup>186</sup>Re-HEDP. *J Nucl Med* 2003;44(2):247-251.
- (231) Liepe K, Hliscs R, Kropp J, Runge R, Knapp FF, Jr., Franke WG. Dosimetry of <sup>188</sup>Re-hydroxyethylidene diphosphonate in human prostate cancer skeletal metastases. *J Nucl Med* 2003;44(6):953-960.

- (232) Lin WY, Lin CP, Yeh SJ et al. Rhenium-188 hydroxyethylidene diphosphonate: a new generator-produced radiotherapeutic drug of potential value for the treatment of bone metastases. *Eur J Nucl Med* 1997;24(6):590-5.
- (233) Holmes RA. [153Sm]EDTMP: a potential therapy for bone cancer pain. *Semin Nucl Med* 1992;22(1):41-5.
- (234) Lin WY, Hsieh JF, Lin CP et al. Effect of reaction conditions on preparations of rhenium-188 hydroxyethylidene diphosphonate complexes. *Nucl Med Biol* 1999;26(4):455-9.
- (235) Hsieh BT, Hsieh JF, Tsai SC, Lin WY, Wang SJ, Ting G. Comparison of various rhenium-188-labeled diphosphonates for the treatment of bone metastases. *Nucl Med Biol* 1999;26(8):973-6.
- (236) Scheffler J, Derejko M, Bandurski T, Romanowicz G. Application of rhenium-188 HEDP in bone metastases therapy. *Nucl Med Rev Cent East Eur* 2003;6(1):55-57.
- (237) Vucina J, Han R. [Production and therapeutic use of rhenium-186, 188--the future of radionuclides]. *Med Pregl* 2003;56(7-8):362-365.
- (238) Gentili A, Miron SD, Bellon EM. Nonosseous accumulation of bone-seeking radiopharmaceuticals. *Radiographics* 1990;10(5):871-881.
- (239) Flynn BM, Treves ST. Diffuse hepatic uptake of technetium-99m methylene diphosphonate in a patient receiving high dose methotrexate. *J Nucl Med* 1987;28(4):532-534.
- (240) Powers CI, Lin DS, Lin CM. Liver localization of [99mTc]MDP in a case of metastatic malignant melanoma. *Int J Nucl Med Biol* 1984;11(1):73-6.
- (241) Lyons KP, Kuperus J, Green HW. Localization of Tc-99m-pyrophosphate in the liver due to massive liver necrosis: case report. *J Nucl Med* 1977;18(6):550-552.
- (242) Zachos TA, Aiken SW, DiResta GR, Healey JH. Interstitial fluid pressure and blood flow in canine osteosarcoma and other tumors. *Clin Orthop* 2001;(385):230-6.
- (243) Pelfrene AF. A search for a suitable animal model for bone tumors: a review. *Drug Chem Toxicol* 1985;8(1-2):83-99.
- (244) Parodi AL. [Canine osteosarcoma as a model in comparative oncology]. *Sem Hop* 1982;58(30-31):1731-5.
- (245) Feldman JP, Goldwasser R, Shlomo M, Schwartz J, Orion I. A mathematical model for tumor volume evaluation using two-dimensions. *Journal of Applied Quantitative Methods* 2009;4(4):455-462.



- (246) Henderson RA, Brawner WRJ, Brewer WGJ, Henry CJ. Clinical staging. In: Hahn KA, Richardson RC, editors. *Cancer chemotherapy: A veterinary handbook*. Baltimore: Williams & Wilkins; 1995. 23-44.
- (247) Clamon G, Herndon J, Cooper R, Chang AY, Rosenman J, Green MR. Radiosensitization with carboplatin for patients with unresectable stage III non-small-cell lung cancer: a phase III trial of the Cancer and Leukemia Group B and the Eastern Cooperative Oncology Group. *J Clin Oncol* 1999;17(1):4-11.
- (248) Coleman CN, Mitchell JB. Clinical radiosensitization: why it does and does not work. *J Clin Oncol* 1999;17(1):1-3.
- (249) Koukourakis MI, Stefanaki I, Giatromanolaki A et al. Fractionated carboplatin radiosensitization: a phase I dose-escalation study. *Am J Clin Oncol* 1998;21(6):595-601.
- (250) Beck JA, Strizek AA. Full-thickness resection of the hard palate for treatment of osteosarcoma in a dog. *Aust Vet J* 1999;77(3):163-5.
- (251) Sciuto R, Maini CL, Tofani A, Fiumara C, Scelsa MG, Broccatelli M. Radiosensitization with low-dose carboplatin enhances pain palliation in radioisotope therapy with strontium-89. *Nucl Med Commun* 1996;17(9):799-804.
- (252) Douple EB, Richmond RC, O'Hara JA, Coughlin CT. Carboplatin as a potentiator of radiation therapy. *Cancer Treat Rev* 1985;12 Suppl A:111-124.
- (253) Yang LX, Douple E, Wang HJ. Irradiation-enhanced binding of carboplatin to DNA. *Int J Radiat Biol* 1995;68(6):609-614.
- (254) Yang LX, Douple EB, O'Hara JA, Wang HJ. Production of DNA double-strand breaks by interactions between carboplatin and radiation: a potential mechanism for radiopotential. *Radiat Res* 1995;143(3):309-315.
- (255) Yang LX, Douple EB, Wang HJ. Irradiation enhances cellular uptake of carboplatin. *Int J Radiat Oncol Biol Phys* 1995;33(3):641-646.
- (256) Cameron PJ, Klemp PF, Martindale AA, Turner JH. Prospective <sup>153</sup>Sm-EDTMP therapy dosimetry by whole-body scintigraphy. *Nucl Med Commun* 1999;20(7):609-15.
- (257) Collins C, Eary JF, Donaldson G et al. Samarium-153-EDTMP in bone metastases of hormone refractory prostate carcinoma: a phase I/II trial. *J Nucl Med* 1993;34:1839-1844.
- (258) Milner RJ, Henry CJ, Dormehl IC, Louw WK, Kilian E. Samarium-153-EDTMP targeted radiotherapy and carboplatin radiosensitization in naturally occurring canine osteosarcoma. *J Vet Intern Med* 16[3], 367. 2002.

Ref Type: Abstract

- (259) Turner JH, Martindale AA, Sorby P et al. Samarium-153 EDTMP therapy of disseminated skeletal metastasis. *Eur J Nucl Med* 1989;15(12):784-95.

- (260) Alberts AS, Smit BJ, Louw WK et al. Dose response relationship and multiple dose efficacy and toxicity of samarium-153-EDTMP in metastatic cancer to bone. *Radiother Oncol* 1997;43(2):175-9.
- (261) van Rensburg AJ, Alberts AS, Louw WK. Quantifying the radiation dosage to individual skeletal lesions treated with samarium-153-EDTMP. *J Nucl Med* 1998;39(12):2110-5.
- (262) Duncan R. Polymer conjugates for tumour targeting and intracytoplasmic delivery. The EPR effect as a common gateway? 1999;2(11):441-449.
- (263) Nishida K, Mihara K, Takino T et al. Hepatic disposition characteristics of electrically charged macromolecules in rat in vivo and in the perfused liver. *Pharm Res* 1991;8(4):437-44.
- (264) Emmanouilides C. Radioimmunotherapy for non-hodgkin lymphoma : historical perspective and current status. *J Clin Exp Hematop* 2007;47(2):43-60.
- (265) Coomer A, Farese J, Milner R, Liptak J, Bacon N, Lurie D. Radiation therapy for canine appendicular osteosarcoma. *Vet Comp Oncol* 2009;7(1):15-27.
- (266) Galiano E, Stradiotto M. A statistical analysis of the initial biodistribution of 153Sm-EDTMP in a canine. *Appl Radiat Isot* 2005;63(1):79-85.
- (267) Bianchi L, Baroli A, Marzoli L, Verusio C, Chiesa C, Pozzi L. Prospective dosimetry with 99mTc-MDP in metabolic radiotherapy of bone metastases with 153Sm-EDTMP. *Eur J Nucl Med Mol Imaging* 2009;36(1):122-129.
- (268) Fitzpatrick L, Farese JP, Milner RJ et al. Intrinsic radiosensitivity and repair of sublethal damage in canine osteosarcoma cell lines. *Am J Vet Res*. In press 2007.
- (269) Fertil B, Malaise EP. Inherent cellular radiosensitivity as a basic concept for human tumor radiotherapy. *Int J Radiat Oncol Biol Phys* 1981;7(5):621-629.
- (270) Bishayee A, Rao DV, Srivastava SC, Bouchet LG, Bolch WE, Howell RW. Marrow-sparing effects of 117mSn(4+)diethylenetriaminepentaacetic acid for radionuclide therapy of bone cancer. *J Nucl Med* 2000;41(12):2043-50.
- (271) Zeevaart JR, Louw WK, Kolar ZI, Kilian E, van Rensburg FE, Dormehl IC. Biodistribution and pharmacokinetics of variously molecular sized 117mSn(II)-polyethyleneiminomethyl phosphonate complexes in the normal primate model as potential selective therapeutic bone agents. *Arzneimittelforschung* 2004;54(6):340-347.
- (272) Maslov OD, Starodub GY, Vostokin GK et al. Production of (117m)Sn with high specific activity by cyclotron. *Appl Radiat Isot* 2011;69(7):965-968.
- (273) Dispenzieri A, Wiseman GA, Lacy MQ et al. A phase I study of 153Sm-EDTMP with fixed high-dose melphalan as a peripheral blood stem cell conditioning regimen in patients with multiple myeloma. *Leukemia* 2005;19(1):118-125.

- (274) Jansen DR, Zeevaart JR, Denkova A, Kolar ZI, Krijger GC. Hydroxyapatite chemisorption of N,N',N'-trimethylenephosphonate-poly(ethyleneimine) (PEI-MP) combined with Sn<sup>2+</sup> or Sn<sup>4+</sup>. *Langmuir* 2009;25(5):2790-2796.
- (275) Bruland OS, Nilsson S, Fisher DR, Larsen RH. High-linear energy transfer irradiation targeted to skeletal metastases by the alpha-emitter <sup>223</sup>Ra: adjuvant or alternative to conventional modalities? *Clin Cancer Res* 2006;12(20 Pt 2):6250s-6257s.
- (276) Cheetham PJ, Petrylak DP. Alpha particles as radiopharmaceuticals in the treatment of bone metastases: mechanism of action of radium-223 chloride (Alpharadin) and radiation protection. *Oncology (Williston Park)* 2012;26(4):330-7, 341.
- (277) Hindorf C, Chittenden S, Aksnes AK, Parker C, Flux GD. Quantitative imaging of <sup>223</sup>Ra-chloride (Alpharadin) for targeted alpha-emitting radionuclide therapy of bone metastases. *Nucl Med Commun* 2012;33(7):726-732.
- (278) White RG, Raabe OG, Culbertson MR, Parks NJ, Samuels SJ, Rosenblatt LS. Bone sarcoma characteristics and distribution in beagles injected with radium-226. *Radiat Res* 1994;137(3):361-70.
- (279) Kunugiyama I, Ito N, Furukawa Y. Determination of blood volume in dogs using an enriched stable isotope <sup>50</sup>Cr. *Nippon Juigaku Zasshi* 1989;51(5):855-860.